# AN EXPERIMENTAL AND NUMERICAL STUDY ON HEAT AND MASS TRANSFER IN ADSORBENT BED OF AN ADSORPTION HEAT PUMP

**A Thesis Submitted to**
**the Graduate School of Engineering and Sciences of**
**İzmir Institute of Technology**
**in Partial Fulfillment of the Requirements for the Degree of**

**DOCTOR OF PHILOSOPHY**

**in Mechanical Engineering**

**by**
**Gamze GEDİZ İLİŞ**

**May 2012**
**İZMİR**

We approve the thesis of **Gamze GEDİZ İLİŞ**

_____
**Assoc. Prof. Dr. Moghtada MOBEDİ**
Supervisor

_____
**Prof. Dr. Sacide ALSOY ALTINKAYA**
Committee Member

_____
**Prof. Dr. Ali GÜNGÖR**
Committee Member

_____
**Assoc. Prof. Dr. Aytunç EREK**
Committee Member

_____
**Assist. Prof. Dr. Ünver ÖZKOL**
Committee Member

**15 May 2012**

_____
**Prof. Dr. Metin TANOĞLU**
Head of the Department of Mechanical Engineering

_____
**Prof. Dr. R. Tuğrul SENGER**
Dean of the Graduate School of Engineering and Sciences

# ACKNOWLEDGEMENTS

This thesis would not have been possible without the support of my advisor who was abundantly helpful and offered invaluable support and guidance. I owe my deepest gratitude to Assoc. Prof. Dr. Moghtada MOBEDI. I would like to thank to my co-advisor, Prof. Dr. Semra ÜLKÜ for her supervision and encouragement during my PhD studies. I am also thankful to Prof. Dr. Sacide ALSOY ALTINKAYA and Assist. Prof. Dr. Ünver ÖZKOL for their valuable recommendations and contributions.

I would like to show my gratitude to Ersin YAZGAN and his co-workers for the construction of the experimental setup. My special thanks are to the staff of Sesa Elektronik. I am particularly thankful for the assistance and friendship given by Assist. Prof. Dr. Hasan DEMİR. I would like to appreciate deeply to my friend Zeynep Elvan YILDIRIM.

Finally, I am deeply grateful to my husband Emin Ö. İLİŞ for his great encouragement, helpfulness and patience during my PhD graduate. I wishes to express my love and gratitude to my beloved family; my brother Murat GEDİZ, my great mother Sevim GEDİZ, my dad Ahmet GEDİZ, for their understanding and endless love, through the duration of my life.

This thesis is dedicated to my lovely daughter Lara İLİŞ who is my reason of living.

To my daughter, Lara İLİŞ

# ABSTRACT


## AN EXPERIMENTAL AND NUMERICAL STUDY ON HEAT AND MASS TRANSFER IN ADSORBENT BED OF AN ADSORPTION HEAT PUMP

Because of the limited conventional energy sources, the improvement of thermal heat pumps has gained attentions of researchers in recent years. Adsorption heat pump, which is a kind of thermal heat pump, can be directly operated with the low temperature heat sources such as waste heat, geothermal and solar energy. Although, adsorption heat pump has many advantages compared to the conventional heat pump, there are still many difficulties for its practical application. Adsorbent bed is one the most important component of adsorption heat pump. Heat and mass transfer in the adsorbent bed should be accelerated in order to attain a small sized, high powered adsorption heat pump.

In this thesis, a theoretical and experimental study is performed on heat and mass transfer in an adsorbent bed. A detailed literature survey on the design of adsorbent bed is done. The designed adsorbent beds are classified, and their advantages and disadvantages are discussed. In order to analyze heat and mass transfer in an adsorbent bed, transport of adsorptive in an adsorbent particle should be well known. A theoretical study on heat and mass transfer in a single adsorbent particle located in an infinite adsorptive medium is performed to understand the effects of internal and external heat and mass transfer resistances. Heat and mass transfer equations for an annular adsorbent bed are derived for uniform and non-uniform pressure approaches and numerically solved to determine temperature and concentration profiles in the bed. These equations are also non-dimensionalized to reduce number of governing parameters. The non-dimensionalization of the equations yields important dimensionless parameters that can be used not only to describe heat and mass transfer in an adsorbent bed but also employ them during design of the bed. Furthermore, an experimental setup was designed and constructed to validate the obtained numerical results. The experimental results were compared with the solution of the numerical results and a good agreement was obtained between them.

# ÖZET

## ADSORPSİYONLU BİR ISI POMPASININ ADSORBENT YATAĞINDA ISI VE KÜTLE TRANSFERİNİN DENEYSEL VE SAYISAL ÇALIŞMASI

Enerji kaynaklarının sınırlı olması nedeni ile son yıllarda termal ısı pompalarının geliştirilmesi araştırmacıların dikkatini çekmektedir. Bir çeşit termal ısı pompası olan adsorpsiyonlu ısı pompaları atık ısı, jeotermal ve güneş enerjisi gibi düşük sıcaklık kaynaklarını doğrudan kullanabilmektedir. Ancak, adsorpsiyonlu ısı pompalarının geleneksel ısı pompalarına göre çok sayıda avantajı olmasına rağmen halen birçok pratik kullanımda sorunu bulunmaktadır. Adsorpsiyonlu ısı pompasının en önemli ekipmanlarından biri adsorbent yataktır. Daha küçük boyutta ve yüksek güçte adsorpsiyonlu ısı pompası elde edilebilmesi için adsorbent yatağındaki ısı ve kütle transferi hızlandırılmalıdır.

Bu tezde, adsorbent yatağındaki ısı ve kütle transferi üzerine teorik ve deneysel çalışmalar yapılmıştır. Adsorbent yatak dizaynı üzerine detaylı bir yayın taraması yapılmıştır. Adsorbent yatağındaki ısı ve kütle transferinin analizinin yapılabilmesi için adsorbent taneciğindeki adsorptive transferi iyi bilinmelidir. İç ve dış ısı ve kütle transferi dirençlerinin etkisini anlayabilmek için sonsuz adsorptive ortama konulan bir adsorbent taneciğindeki ısı ve kütle transferi teorik olarak incelenmiştir. Sabit ve sabit olmayan basınç yaklaşımı kullanılarak silindirik bir adsorbent yataktakı ısı ve kütle transferi denklemleri çıkarılmış, yataktaki sıcaklık ve konsantrasyon profilleri hesaplanmıştır. Bu denklemler parametre sayısını azaltmak amacı ile boyutsuzlaştırılmıştır. Denklemlerin boyutsuzlaştırılması, yataktaki ısı ve kütle transferinin anlatılmasının yanında, yatak dizaynında kullanılabilecek önemli boyutsuz parametrelerin elde edilmesini sağlamıştır. Ayrıca, elde edilen sayısal sonuçları doğrulamak için bir deney düzeneği geliştirilmiş ve kurulmuştur. Elde edilen deneysel sonuçlar sayısal sonuçlarla karşılaştırılmış ve birbirleri arasında iyi bir uyum olduğu görülmüştür.

# TABLE OF CONTENT

# LIST OF FIGURES

**Figure** **Page**

# LIST OF TABLES

**Table** **Page**

# LIST OF SYMBOLS

| | |
|---|---|
| $Bi_h$ | Heat transfer Biot number |
| $Bi_m$ | Mass transfer Biot number |
| $Bi_m^{'}$ | Modified mass transfer Biot number |
| c | concentration, mole $m^{-3}$ |
| $C_p$ | specific heat, kJ $kg^{-1}$ $K^{-1}$ |
| COP | coefficient of performance |
| D | diffusivity, $m^2$ $s^{-1}$ |
| $D_{bed}$ | effective diffusivity of adsorptive in adsorbent bed, $m^2$ $s^{-1}$ |
| $D_{eff}$ | effective diffusivity, $m^2$ $s^{-1}$ |
| $D_K$ | Knudsen diffusivity, $m^2$ $s^{-1}$ |
| $D_m$ | molecular diffusivity, $m^2$ $s^{-1}$ |
| $D_0$ | reference diffusivity, $m^2$ $s^{-1}$ |
| E | diffusional activation energy, J $mol^{-1}$ |
| G | dimensionless parameter group (Chapter 5), slope of isotherm (Chapter 6) |
| h | heat transfer coefficient, W $m^{-2}$ $K^{-1}$ |
| J | Diffusive flux, mole $m^{-2}sec^{-1}$ |
| k | Boltzman constant, $JK^{-1}$ $molecule^{-1}$ |
| K | Dimensionless parameter |
| $K_{app}$ | apparent permeability of adsorbent bed, $m^2$ |
| $K_{inh}$ | inherent permeability of adsorbent bed, $m^2$ |
| Ku | Kutateladze number |
| Le | Lewis number |
| M | molecular weight of adsorptive, kg $mol^{-1}$ |
| m | mass, kg |
| n | time step, a constant |
| Nu | Nusselt number |

| | |
|---|---|
| P | pressure, kPa |
| q | uncertainty function |
| Q | heat transferred, W $kg_s^{-1}$ |
| $Q_{ab}$ | heat of isosteric heating process, kJ $kg_s^{-1}$ |
| $Q_{bc}$ | heat of isobaric desorption process, kJ $kg_s^{-1}$ |
| $Q_{cd}$ | heat of isosteric cooling process, kJ $kg_s^{-1}$ |
| $Q_{da}$ | heat of isobaric adsorption process, kJ $kg_s^{-1}$ |
| r | particle radius variable, m |
| $r_p$ | radius of adsorbent granule, m |
| $r_{pore}$ | radius of pore, m |
| R | radius of bed, m; ideal gas constant, J $mol^{-1}$ $K^{-1}$ |
| $R_i$ | inner radius of bed, m |
| $R_o$ | outer radius of bed, m |
| Re | Reynolds number |
| Sh | Sherwood number |
| Sc | Schmidt number |
| SCP | specific cooling power, W $kg^{-1}$ |
| SHP | specific heating power, W $kg^{-1}$ |
| t | time, s |
| T | temperature, K |
| $V$ | Darcy velocity, m $s^{-1}$ |
| V | volume of system, $m^3$ |
| $W$ | adsorbate concentration, $kg_l$ $kg_S^{-1}$ |
| $\overline{W}$ | average adsorbate concentration, $kg_l$ $kg_S^{-1}$ |

**Greek letters**

| | |
|---|---|
| α | thermal diffusivity, $m^2$ $s^{-1}$ |
| $\alpha^*$ | dimensionless parameter |
| $\Delta H_{ads}$ | heat of adsorption, kJ $kg_l^{-1}$ |
| $\Delta H_{va}$ | heat of vaporization, kJ $kg_v^{-1}$ |
| φ | porosity |
| λ | thermal conductivity , W $m^{-1}$ $K^{-1}$ |
| μ | adsorptive viscosity, $Nsm^{-2}$ |
| Ω | collision integral |

| | |
|---|---|
| $\rho$ | density, kg $m^{-3}$ |
| $\sigma$ | collision diameter for Lennard-Jones potential, $A^0$ |
| $\theta$ | dimensionless temperature variable |
| $\tau$ | dimensionless time variable |
| $\tau$ | tortuosity |
| $\tau_{total}$ | total period |
| $\Gamma$ | dimensionless parameter |
| $\Pi$ | dimensionless parameter |
| $\Lambda$ | dimensionless parameter |
| $\phi$ | annular direction |
| $\delta$ | fin thickness, m |
| $\gamma$ | dependent variable |
| $\xi$ | dependent variable |
| * | dimensionless |

**Subscripts**

| | |
|---|---|
| ads | adsorption |
| bed | adsorbent bed |
| bedos | adsorbent bed outer surface |
| bs | bottom surface |
| cond | condenser |
| const | constant |
| cyc | cycle |
| eff | effective |
| eva | evaporator |
| f | fluid |
| fin | fin |
| i | initial |
| *l* | adsorbed phase |
| lo | lower surface |
| o | outer |
| r | radial direction |
| reg | regeneration |
| s | adsorbent or solid phase |

| | |
|---|---|
| sat | saturation |
| up | upper surface |
| *v* | vapor phase |
| ∞ | equilibrium |

# CHAPTER 1

# INTRODUCTION

In recent years, energy consumption has drawn both researchers' and governments' attention. Due to the demand of higher comfort conditions and industrial development, energy consumption has increased; therefore, energy plants have gained importance. Most of the world energy need is met from fossil fuels and non-renewable energy resources. However, renewable energy sources can play a remarkable role in producing energy without devastating the environment. Compared to renewable energy sources, energy plants working with fossil fuels cause the depletion of ozone layer. Latest investigations' main aim is to reduce losses associated with energy transformation minimizing the costs and the environmental impact. Regarding these reasons, researchers have focused on the development of energy systems that are environmentally friendly, based on innovative technologies that use renewable energy sources. Using energy sources that are easily replaced, named as renewable energy, have many advantages over fossil fuels such as not causing global environmental problems and sustainability of human life. Consequently, many researchers have worked on the improvement of thermal heat pumps working with renewable energy sources.

Thermal heat pumps can operate with sustainable thermal sources such as geothermal energy, solar energy, and waste heat. These kinds of pumps are more environmental friendly novel systems. They have high primary energy efficiencies. Besides the traditional definitions of the efficiency or performance of devices, the primary energy efficiency has gained critical importance. Since the mechanical heat pumps work with electrical power, their primary energy efficiency is less than their COP. For example, the primary energy efficiency of traditional heat pumps is about 90-100%, while the primary energy efficiency of thermal driven heat pumps was determined around 130-180% (Ülkü 1987).

There are three kinds of thermal driven heat pumps as absorption, adsorption, and chemical heat pumps. The absorption heat pump is produced by many manufacturers and used in the market whereas the adsorption and chemical heat pumps

are still under investigation. However, the commercial use of adsorption heat pump in industry is a new concern. Adsorption heat pump can directly operate with any kind of thermal energy sources such as solar and geothermal energy. The low level temperature thermal energy source can be utilized by adsorption heat pump for heating and cooling purposes. Compared to the absorption or the mechanical heat pumps, the adsorption heat pump has some significant advantages. They can work with a low level temperature heat reservoir. Thanks to the lack of moving components, it is a noiseless system and has a long life time. What's more, it has also simple principle of working.

A basic adsorption heat pump consists of four main components: an adsorbent bed, a condenser, an evaporator, and an expansion valve. Adsorption and desorption in the adsorbent bed provide circulation of working fluid (adsorbate) without requirement for mechanical energy. The selection of appropriate adsorbent–adsorbate pair is an important factor for design of an adsorption heat pump. Adsorbate should have high latent heat, non-corrosive, non-toxic and good thermal and chemical stability within the working conditions (temperature and pressure ranges). Adsorbents should have the features of high adsorption capacity, high thermal conductivity, low cost and also high thermal stability. Besides its many advantages, adsorption heat pump has some disadvantages such as requirements of advanced manufacturing technology and special designs to maintain vacuum for a long period of time. One of the important drawbacks of an adsorption heat pump is its relatively low specific cooling and heating powers (SCP/SHP) and coefficient of performance (COP) compared to the mechanical heat pumps. However, it should be mentioned that the primary energy efficiency value of adsorption heat pump is comparable with the traditional heat pump.

Adsorbent bed is the most important component of an adsorption heat pump. The evaporated adsorbate is adsorbed by adsorbent particles in the adsorbent bed and then it is desorbed to the condenser. The enhancement of heat and mass transfer reduces the period of cycle and consequently increases the power of adsorption heat pump. In order to improve heat and mass transfer in a granular adsorbent bed, the mechanism of heat and mass transport in the bed should be recognized well.

Adsorption phenomena have broad range of applications in nature as well as in industry. It plays an important role in the catalytic reaction and separation/purification processes such as recovery of the chemical compounds, water purification, separation, and purification of air, drying, medical treatments, and recently thermally driven energy systems. The period of an adsorption process and adsorption capacity are two

significant criteria that should be considered in the design of an adsorption system. For instance, a high adsorption capacity in a short adsorption period is required in order to have high values of specific cooling or heating performance for an adsorption heat pump. The adsorption rate in an adsorbent particle or an adsorbent layer is highly influenced from temperature. Determination of adsorption capacity and adsorption period of a process is not easy, since heat and mass transports are highly coupled. The solution of heat and mass transport equations for an adsorption process provides useful information that can be used for an adsorbent bed design.

This thesis focused on the heat and mass transfer in an adsorbent bed of adsorption heat pump. The experimental and numerical investigations on heat and mass transfer in a granular adsorbent bed are performed. The heat and mass transfer mechanism in an annular granular adsorbent bed is analyzed numerically by using uniform and non-uniform pressure approaches. The governing equations, initial and boundary conditions are written in both dimensional and non-dimensional forms and solutions on the adsorption period are obtained. By non-dimensionalization of the governing equations, dimensionless parameters which can help designers to predict the effects of different parameters on the adsorbent bed design are found. The effect of the fin inside of an adsorbent bed, used for acceleration of heat and mass transfer, is also theoretically analyzed. The theoretical studies are performed mainly for silica gel-water pair; however, different adsorbent-adsorbate pairs such as zeolite-water, active carbon-methanol etc. are taken into consideration to indicate the application of dimensionless parameters on different adsorbent-adsorbate pairs.

An experimental set up, filled with silica gel granules, for validation of the obtained numerical solutions was designed and constructed. The experiments were performed for adsorption process and the obtained experimental results were compared with the solution of the numerical results. The adsorbent bed has annular shape and thermocouples were located inside the bed to observe the change of temperature of silica gel-water pair during adsorption period. Most of the experiments were performed for pressure range below 10 kPa for which water can evaporate in room condition. The temperature of the outer surface of the bed was maintained at required value by using an electrical heater. The measured temperature and pressure values were transferred to the computer and saved by using set of data loggers. The results of numerical solutions showed good agreement with the experimental data, indicating the correctness of the theoretical results.

The thesis consists of twelve chapters. Porous media and adsorption phenomena concepts and their relevant equations are reviewed in Chapter 2. In Chapter 3, working principle of an adsorption heat pump, performance analysis, definition of parameters such as COP and SCP/SHP, advantages and disadvantages of adsorption heat pump, comparison of heat pumps, the developed advanced adsorption heat pump, comparison of common adsorbent-adsorbate pairs are explained. Furthermore, the designs of adsorbent bed are classified and reported designs in literature are reviewed. The equations solved by researchers to analyze heat and mass transfer in an adsorbent bed are classified in Chapter 4. The details of studies such as aims and employed assumptions for each study are also given. The additional required equations for solution of heat and mass transfer equations such as adsorption equilibria, effective mass diffusivity, and thermal diffusivity are reviewed and classified. The available studies on heat and mass transfer in a single adsorbent particle are also reviewed in Chapter 4. In order to understand the heat and mass transfer mechanism in an adsorbent bed, heat and mass transfer in a single adsorbent particle should be well known. Accordingly Chapter 5 is presented to show the effects of heat and mass transfer resistances on adsorption process for a single particle. The heat and mass transfer equations are solved numerically for isothermal and non-isothermal conditions. There are two approaches for simulation of an adsorption process in an adsorbent bed as uniform and non-uniform pressure approaches. The related heat and mass transfer equations for uniform and non-uniform approaches are presented in Chapter 6. These equations are non-dimensionalized and dimensionless form of the governing equations and boundary conditions are also given. Furthermore, heat transfer equation for a fin located in an annular adsorbent bed is presented. The experimental setup constructed for validation of the numerical solutions is explained in details in Chapter 7. The components of the setup, measuring devices and other equipment are mentioned and the experimental procedure is explained. Finite difference method is used to solve heat and mass transfer equations for adsorbent particle and adsorbent bed. The numerical methods used in the theoretical studies are given in Chapter 8. The discritization of the domain, the finite difference forms of the governing equations, and the solution procedure are explained. The obtained theoretical results of the studied cases and achieved experimental results are given in Chapter 9 and 10, respectively. The obtained results are presented via graphics and discussions are performed. The validation of the numerical results is given in Chapter 10. As mentioned, the dimensionless parameters

found during the theoretical studies can play an important role in design of an adsorbent bed. Chapter 11 is presented to provide hints on design of an adsorbent bed based on the dimensionless parameters found. Finally, the results of the performed theoretical and experimental studies in this thesis are concluded in Chapter 12.

# CHAPTER 2

# POROUS MEDIA AND ADSORPTION PHENOMENA

In this chapter, the information on porous media and adsorption phenomena is given. The definitions related with porous media such as porosity, Darcy Law, effective thermal capacity and thermal capacitance are presented. Physical and chemical adsorption, adsorbents, adsorption equilibria, and heat of adsorption are explained, briefly. Also the mechanism of heat and mass transfer in an adsorbent bed is explained and the terms such as diffusivity and permeability are described.

## 2.1. What is Porous Media

A material containing pores or voids is called as porous medium. This solid material can be either rigid or undergoes small deformation. Many natural substances such as rocks, bones, human lungs, and manmade materials such as cements, foams, and ceramics can be considered as porous media (Figure 2.1). The pores in porous media can be open or closed. The open pores inside the porous media allow fluid flow through the material. In a natural porous medium, the pores may have different distributions with respect to pore size and its shape that might be irregular. The concept of porous media is used in many areas of applied science and engineering such as mechanics (acoustics, geomechanics, soil mechanics, rock mechanics), engineering (petroleum engineering, construction engineering), geosciences (hydrogeology, petroleum geology, geophysics), biology and biophysics, material science, etc.

There might be two or three phases in a porous material: solid (adsorbent), fluid (adsorptive), and if there is adsorption, the adsorbed phase in the solid (adsorbate) (Figure 2.2). The thermophysical properties of these phases are different.

(a) (b) (c)

Figure 2.1. Examples of natural porous materials, a) normal human lung tissue, b) beach sand), c) crashed limestone (Source: iiarjournals 2011, panoramio 2011, nashvillenaturalstone 2011)

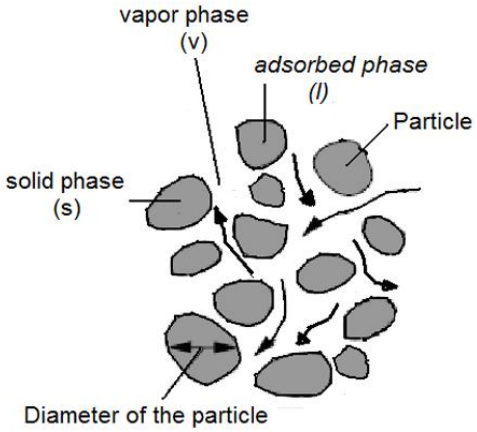


Figure 2.2. Three phases in a porous material

### 2.1.1. Porosity

Porosity can be defined as the ratio of the void volume to the total volume. In Figure 2.3, the particles and voids in a porous medium are illustrated. For an isotropic medium, the porosity can be written as:

$$\varphi = \frac{V_{voids}}{V_{total}} \tag{2.1}$$

In many natural porous medium, the porosity cannot be greater than 0.6 (Nield and Bejan 2006).

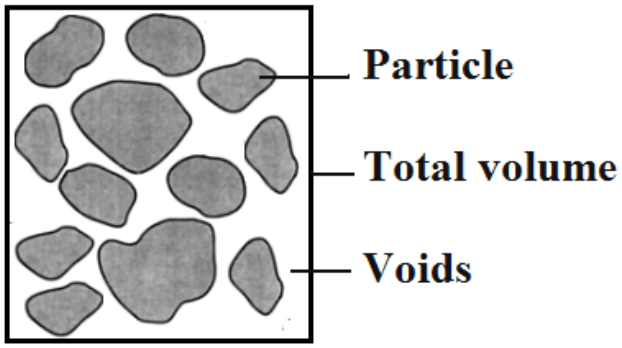


Figure 2.3. The void and pore volumes in a porous medium

### 2.1.2. Darcy Law

Darcy's law describes the flow of a fluid through a porous medium. The law was formulated by Henry Darcy and based on the flow of water through a bed of sand. Darcy velocity is proportional with the permeability and pressure drop over a given distance where a reverse relation exists between the velocity and fluid viscosity. The negative sign is needed because of the fluid flow from high to low pressure. The change in pressure is negative (in the *x*-direction) while flow will be in positive direction (in the *x*-direction) (Figure 2.4).

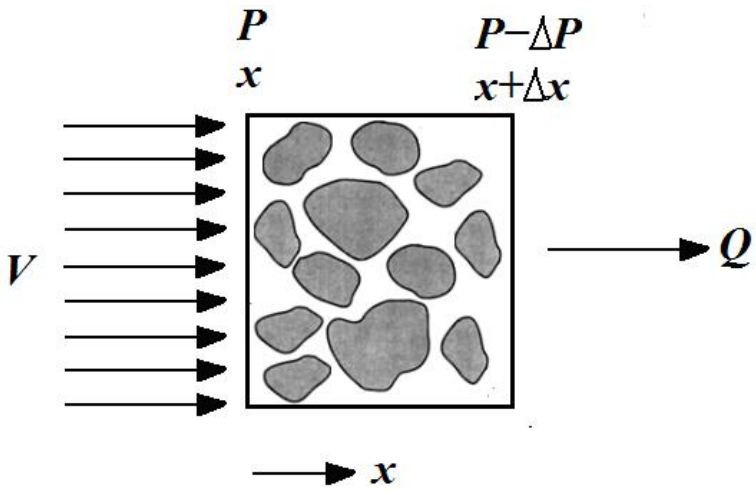


Figure 2.4. Fluid flow in a porous medium

Based on the Figure (2.4), Darcy law mathematically can be described as:

$$V = \frac{K_{app}}{\mu}(-\frac{\partial P}{\partial x}) \tag{2.2}$$

where $V$ is the Darcy velocity of the fluid ($ms^{-1}$), $K_{app}$ is the apparent permeability ($m^2$), and $\mu$ is the viscosity of fluid ($Nsm^{-2}$).

Darcy's law summarizes that:

- no flow occurs if there is no pressure gradient over a distance
- flow will occur from high pressure towards low pressure if there is a pressure gradient (opposite the direction of increasing gradient – hence the negative sign in Darcy's law)
- the greater the discharge rate the greater the pressure gradient (through the same formation material)
- the flow rate of fluid will often be different — through different formation materials (or even through the same material, in a different direction) — even if the same pressure gradient exists in both cases.

### 2.1.3. Effective Thermal Conductivity and Thermal Capacitance of a Porous Medium

For a porous medium, the overall thermal conductivity should be defined including different phases in a porous medium (Solid, fluid and adsorbed phase - Figure 2.2). There are many relations proposed for determination of effective thermal conductivity in literature, however one of the most used relation is:

$$\lambda_{eff} = (1-\varphi)\lambda_S + \varphi\lambda_V \tag{2.3}$$

$\lambda_S$ includes the thermal conductivity of both the adsorbent and adsorbate. Effective thermal capacitance should be defined for porous medium. Effective thermal capacitance contains the phases of solid, vapor, and the liquid phases. The liquid phase also affected from the average adsorbate concentration. In adsorption process, the

adsorbed vapor is not in liquid phase, however many researchers determine adsorbate properties from the liquid phase state. The effective thermal capacity can be defined in porous medium as:

$$(\rho C_p)_{eff} = (1-\varphi)\left[(\rho C_p)_s + \rho_s C_{pl}\overline{W}\right] + \varphi(\rho C_p)_v \qquad (2.4)$$

where indice *s*, *l* and *v* represent the adsorbent, adsorbate and adsorptive, respectively. $\overline{W}$ represents the average adsorbate concentration.

## 2.2. What is Gas Adsorption

A porous solid (adsorbent) can take up large volumes of vapors. Adsorbent is allowed to come to equilibrium with vapor which means that the solid cannot take up no more vapor after. This exothermic phenomenon is named as adsorption.

Two types of interactions occur between adsorbent surface and vapor; physical and chemical adsorptions: Physical adsorption (physisorption) involves relatively weak intermolecular interaction forces (H-bonds, Van der Waals, dipole-dipole interactions etc). Chemical adsorption (chemisorptions) results from chemical bond formation (strong interaction) between the adsorbent and the adsorbate in a monolayer on the surface. Chemical and physical adsorption can be distinguished by following properties (Rouquerol et al. 1999):

- Physisorption is generally reversible but chemisorption is irreversible process involves higher heat of adsorption,
- Physisorption generally occurs in multilayer, chemisorption takes place in a monolayer,
- Physisorption occurs with polarization of adsorptive molecules. In chemisorption, there is bond formation between adsorptive and surface of adsorbent,
- Physisorption is always exothermic and involved energy is equal or larger than the energy of condensation of adsorptive. The energy of chemisorption is the same as the energy change in chemical reaction.

## 2.2.1. Adsorbents

Adsorbents are used usually in the form of spherical pellets or rods. They have high thermal stability and small pore diameters, which results in higher exposed surface area and consequently they have high surface capacity for adsorption. The adsorbents also have distinct pores structure which enables fast transport of the gaseous vapors. There are many pore structures with different shape and size. Figure 2.5 shows the structure of porous adsorbents having different pore sizes. These pores are classified based on their effective width (Sing et al. 1985):

- Macropores : having effective width > 50 nm
- Mesopores : having effective width ≈ 2 - 50 nm
- Micropores : having effective width < 2 nm

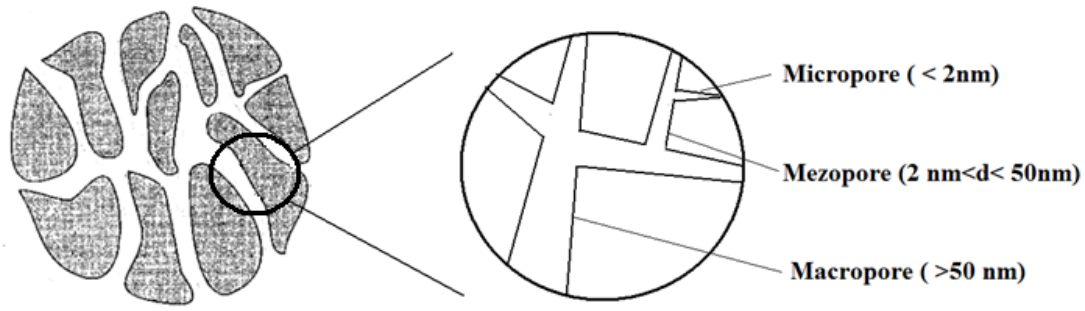


Figure 2.5. Structure of porous adsorbent

Many type of adsorbents such as zeolite, silica gel, active carbon are used in industry. Literature survey shows that silica gel was widely used in adsorption heat pump studies due to high adsorption capacity of water and low regeneration temperature. Silica gel is a matrix of hydrated silicon dioxide. (Ülkü and Mobedi 1989). Brief information on silica gel structure is given in next subsection since the present thesis is performed on silica gel –water pair.

## 2.2.2. Silica gel

Silica gel is one of the most common used adsorbents in adsorption heat pump. The application of silica gel is due to its large water adsorption capacity (~40% by weight). Silica gel has low regeneration temperature (~150$^{o}$C) compared with synthetic zeolites (~350$^{o}$C). Hydroxyl group on surface of silica gel is shown in Figure 2.6 (Suzuki 1990).

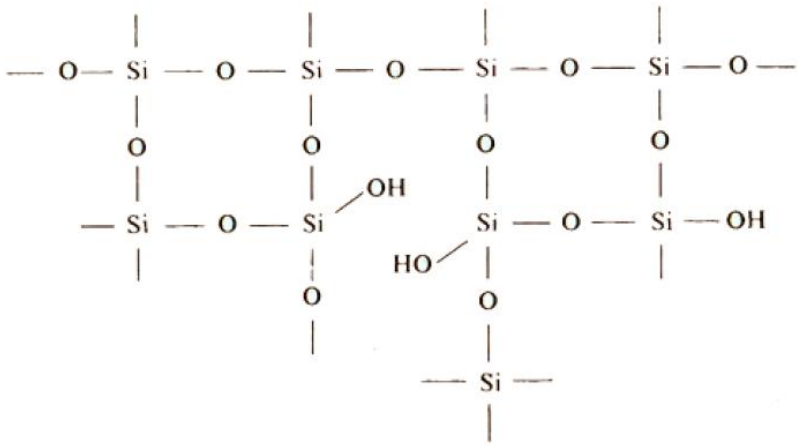


Figure 2.6. Hydroxyl group on surface of silica gel
(Source: Suzuki 1990)

In common types of silica gels, there are many different pore size distributions; Silica gels can be classified into four groups as Type A, Type B, Type 3A, and Type RD based on the pore size distributions. The approximate pore size distribution of Type A silica gels is around 0.8-3.0 nm and for Type B pore size is about 0.7-5 nm, and 0.8-7.5 nm is for Type RD. The specific surface areas are about 650 $m^2 g^{-1}$ for Type A, 550 $m^2 g^{-1}$ for Type B, 606 $m^2 g^{-1}$ for Type 3A, and 720 $m^2 g^{-1}$ for Type RD (Ng et al. 2001, Chua et al. 2002).

## 2.2.3. Adsorption Equilibria

Adsorption equilibria relationship gives the amount adsorbed taken up by unit mass of the adsorbent at specified pressure and temperature. The amount of adsorbate adsorbed by the adsorbent depends on the adsorbate concentration, temperature of adsorbent and adsorptive, and adsorptive pressure as well as the thermophysical properties of adsorbent particle.

In order to solve heat and mass transfer equations for an adsorbent bed, the adsorbate equilibrium concentration at any temperature and pressure is required. The adsorption equilibria model provides relations between equilibrium concentration, adsorptive pressure and temperature.

The adsorption process occurs until adsorbent particles reach equilibrium. Based on adsorbent structure and adsorptive, many models have been developed to represent equilibrium condition for an adsorbent-adsorbate pair. Literature survey shows that following models have been proposed for adsorption equilibria of silica gel-water pair.

1) The Freundlich equation

$$W^* = k\left(\frac{P(T_v)}{P_{sat}(T_s)}\right)^{\frac{1}{n}} \tag{2.5}$$

where $W^*$ is water uptake of the silica gel and is defined as the mass of the water adsorbed to the mass of silica gel; *k* and *n* are constants and determined by a fitting process, where P is the adsorptive pressure and $P_{sat}$ is the saturation pressure, and $T_v$ and $T_s$ are the temperatures of water vapor and silica gel, respectively.

2) The Dubinin – Astakhov (DA) equation

$$W^* = a * \exp\left(-k\left(\ln\frac{P_{sat}(T_s)}{P_{sat}(T_v)}\right)^n\right) \tag{2.6}$$

where a, k and *n* are constants, $P_{sat}(T)$ represents the saturation vapor pressure, and $T_v$ and $T_s$ are the temperatures of water vapor and silica gel, respectively.

3) The modified Freundlich equation

$$W^* = A(T_s)\left(\frac{P(T_v)}{P_{sat}(T_s)}\right)^{B(T_s)} \tag{2.7}$$

where $W^*$ is the amount adsorbed in equilibrium, $P_{sat}$ is the saturation pressure $T_s$ is the temperature of the silicagel, $T_v$ is the refrigerant temperature. The A and B are the polynomial functions, as (Xia et al. 2008):

$$A(T_S) = A_0 + A_1 T_S + A_2 T_S^2 + A_3 T_S^3 \tag{2.8}$$

$$B(T_S) = B_0 + B_1 T_S + B_2 T_S^2 + B_3 T_S^3 \tag{2.9}$$

4) The Henry's Equation

$$W^* = K_o \exp\left(\frac{\Delta H_{ads}}{RT}\right) P \tag{2.10}$$

where $K_o$ is constant in $Pa^{-1}$, P is adsorptive pressure in Pa, R is gas constant in kJ/kgK, $\Delta H_{ads}$ is isosteric heat of adsorption in kJ/kg.

5) The Toth's Equation

$$W^* = \frac{K_o \exp\left(\frac{\Delta H_{ads}}{RT}\right) P}{\left[1 + \left(\frac{K_o}{q_\infty}\left(\frac{\exp \Delta H_{ads}}{(RT)P}\right)\right)^t\right]^{\frac{1}{t}}} \tag{2.11}$$

where $K_o$ is constant in $Pa^{-1}$, P is the adsorptive pressure in Pa.

6) The Clapeyron Equation-Isoster Equation

$$\ln(p) = A(w) + \frac{B(w)}{T} \tag{2.12}$$

where A(w) and B(w) are polynomial functions.

### 2.2.4. Heat of Adsorption

The heat of adsorption is the heat generated during the adsorption process. The heat of adsorption depends on temperature, pressure, and coverage. There are three different definitions for heat of adsorption:

- Differential heat of adsorption
- Integral heat of adsorption
- Isosteric heat of adsorption

Differential heat of adsorption can be defined as the heat evaluation when unit quantity of adsorbate adsorbed in an isolated system. The heat of adsorption depends on the change of the state from adsorptive to adsorbate. The differential molar enthalpy of adsorption can be expressed by differential of enthalpy of adsorptive and adsorbate.

The integral heat of adsorption is obtained by integrating the differential heat of adsorption against amount of adsorbate from initial adsorbate to the required taking value. The integral heat of adsorption equation is valid at constant temperature.

The isosteric heat of adsorption is defined from isotherms at different temperatures and can be calculated by the means of Clausius-Clapeyron type relationship at a constant adsorbate loading.

## 2.3. Mechanism of Heat and Mass Transfer in Adsorbent Bed

Mass transfer within the adsorbent particle (intraparticle mass transfer) and mass transfer in voids between adsorbent particles (interparticle mass transfer) are the mass transfer mechanisms in a closed type granular adsorbent bed. Heat and mass transfer mechanism in the adsorbent bed of adsorption heat pump depends on many parameters such as particle size, adsorbent diffusivity, porosity, thermal conductivity of the adsorbent and adsorbate, and adsorption equilibria of adsorbent-adsorbate pair.

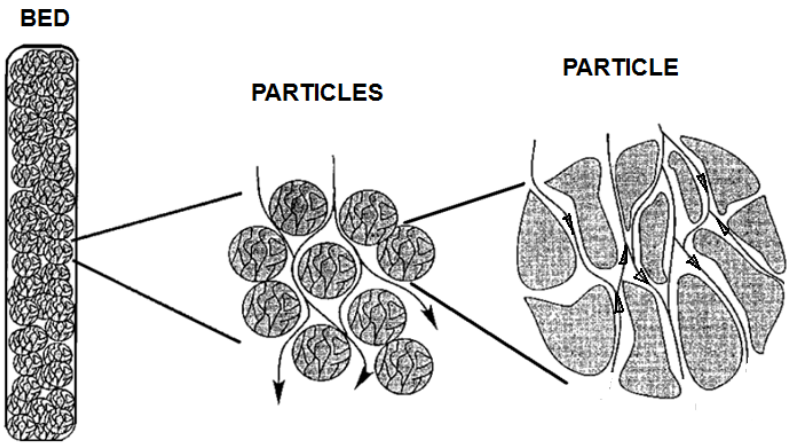


Figure 2.7. Schematic representation of inter-particle and intra-particle flow

A granular adsorbent bed is schematically shown in Figure 2.7. It contains of adsorbent granules which have porous structure. The interparticle mass transfer mainly occurs because of the pressure difference of adsorptive in the adsorbent bed. That's why most of studies employ Darcy Law to represent the adsorptive flow between the adsorbent particles. However, some researchers (e.g. Leong and Liu 2004a) include Knudsen and molecular diffusions in representing of adsorptive transfer in the adsorbent bed. The intraparticle mass transfer mechanism can be described as the adsorptive transfer in an adsorbent particle. The intraparticle mass transfer is generally formed by diffusion mode of transport in the adsorbent particle. The intraparticle mass transfer takes place in the pores of adsorbent having internal surface areas much greater than external surface area. The convective flow through the pores inside the adsorbent particle is negligible and that is why intraparticle adsorptive transfer can be considered as a diffusion process. Hence, Fick's Law with proper concentration gradient and mass diffusivity are used to describe the adsorptive transfer in the particle. Mass diffusion in a particle is controlled by some mechanisms such as micropore, macropore, and surface diffusion etc. Pore structure of the particle, temperature-pressure-concentration range of the process condition and the adsorbent-adsorbate properties control the mass transfer mechanism in a single adsorbent particle. In the present study, the surface diffusion is considered to describe the diffusion of water vapor in silica gel.

## 2.4. Diffusivity

The adsorbate concentration of the adsorbent particle is directly affected from the intraparticle diffusivity. The effective mass diffusivity of the adsorbent varies with adsorbent temperature and activation energy. For the silica gel particle in which surface diffusion occurs, the effective intraparticle diffusivity can be calculated from the Arrhenius equation (Suzuki 1990):

$$D_{eff} = D_o e^{-E/RT} \tag{2.13}$$

where $D_o$ is the reference diffusivity ($m^2s^{-1}$) and E is the activation energy (J $mol^{-1}$) and they are calculated from the experimental data. Activation energy can be defined as the minimum energy required for starting a chemical reaction.

In addition to flow due to adsorptive pressure difference described by Darcy law, the diffusion flow through the bed is also considered for determination of flow in the bed. This diffusion mechanism is significant particularly for small size of voids between particles for which convective transport is negligible or convective transport is in the order of diffusion transport. The diffusion mechanism in voids between particles (interparticle diffusion) can be described by Knudsen and molecular diffusion mechanisms. When the average distance between molecular collisions is greater than pore diameter and collisions between a molecule and the pore walls occur more frequently than a collision between two diffusing molecules, the flow occurs by Knudsen diffusion. The Knudsen diffusivity can be found from Equation (2.14). When, the pore diameter is larger than the average distance between molecular collisions and the collisions between diffusing molecules occur more frequently than collisions between molecules and pore walls, the flow occurs by molecular diffusion. The molecular diffusivity can be obtained from Equation (2.15) (Karger and Ruthven 1992).

$$D_k = 97 r_{pore} \sqrt{T/M} \tag{2.14}$$

$$D_m = 0.02628 \frac{\sqrt{T^3/M}}{P\sigma^2\Omega} \tag{2.15}$$

Then, combination of Knudsen and molecular diffusivity for a bed called as bed diffusivity $D_{bed}$, can be predicted by the following relations:

$$\frac{1}{D_{bed}} = \frac{1}{D_m} + \frac{1}{D_k} \tag{2.16}$$

## 2.5. Permeability

Permeability is the ability of a porous material to allow fluids to pass through the porous solid. The values of permeability for natural porous materials vary widely. Typical values for soils, in terms of the unit $m^2$, are: clean gravel $10^{-7}$–$10^{-9}$, clean sand $10^{-9}$–$10^{-12}$, peat $10^{-11}$–$10^{-13}$, stratified clay $10^{-13}$–$10^{-16}$, and unweathered clay $10^{-16}$–$10^{-20}$ (Nield and Bejan 2006). The permeability is independent of the nature of the fluid but related with the geometry of the medium. In order to use Darcy law and determine velocity field in a porous medium, permeability of porous medium should be known. The permeability depends on porosity, particle radius and structure, and dimension of pores. Blake-Kozeny equation is widely used to determine the inherent permeability which is valid for void fractions less than φ=0.5 (Bird et al. 2002):

$$K_{inh} = \frac{r_p^2 \varphi^3}{37.5(1-\varphi)^2} \tag{2.17}$$

where φ is porosity of the bed, $r_p$ is the particle diameter (m). In this study, the above correlation is used to determine the inherent permeability.

The apparent permeability of the adsorbent bed, $K_{app}$, can be calculated by the following relation (Leong and Liu 2004):

$$K_{app} = K_{inh} + \frac{\varphi\mu}{\tau P} D_{bed} \tag{2.18}$$

The apparent permeability includes two terms which are inherent permeability and $\frac{\varphi\mu}{\tau P} D_{bed} \cdot D_{bed}$ is the mass diffusivity of the bed as given in previous subsection

(Karger and Ruthven 1992). $\tau$ is the tortuosity which defines the property of curve being twisted or having many turns in porous media. The tortuosity is evaluated for diffusion and for flow in a clear channel (without porous media); the tortuosity equals to 1. $\mu$ is the viscosity of water vapor in the above equation.

# CHAPTER 3

# ADSORPTION HEAT PUMP

Nowadays, due to energy shortage and depletion of ozone layer, improvement of thermal heat pumps has gained attentions of many researchers. Adsorption heat pump which is a kind of thermal heat pump can be operated with the thermal energy sources. The main drawback of an adsorption heat pump is its relatively low specific cooling and heating powers (SCP/SHP) and coefficient of performance (COP), while its primary energy efficiency value is in the same order of magnitude with traditional heat pumps.

In this chapter, working principle of an adsorption heat pump, the terms of COP, SHP/SCP, advantages and disadvantages of an adsorption heat pump, comparison of heat pumps, advanced heat pumps, adsorbent-adsorbate pairs used in the adsorption heat pumps, and adsorbent bed designs are handled.

## 3.1. Working Principle of an Adsorption Heat Pump

A basic adsorption heat pump consists of four main components: an adsorber, a condenser, an evaporator, and an expansion valve (Figure 3.1) (Ülkü 1986, Ülkü 1991, Demir et al. 2008). A cycle can be schematically represented on the Clapeyron diagram (ln(P) vs. -1/T) as shown in Figure 3.2.

At the beginning of adsorption process (point d), both valves (V1 and V2) are closed. The adsorbent bed and evaporator are both at the evaporator pressure, $P_{eva}$. By opening the valve V1, the evaporator starts to get heat from the space required to be cooled. The evaporated adsorbate in the evaporator is adsorbed by the adsorbent granules in the adsorbent bed. The process continues until the concentration of adsorbate in granules attains to $W_2$ level. The process (d-a) is known as the isobaric adsorption process. During the adsorption process, heat of adsorption is released in the adsorbent bed.

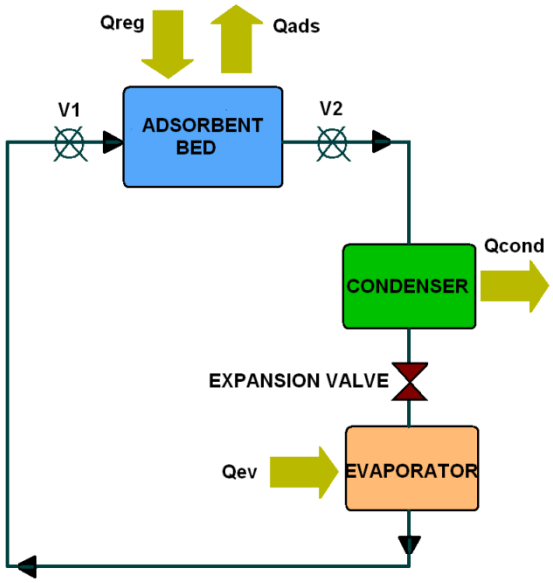


Figure 3.1. A schematic view of an adsorption heat pump

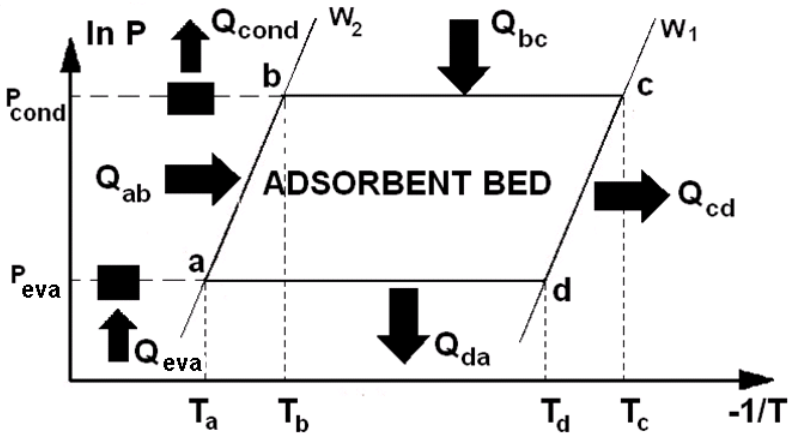


Figure 3.2. A cycle of an adsorption heat pump on Clapeyron diagram

After isobaric adsorption process, the valve V1 is closed and then isosteric heating process starts (a-b). During this process, the adsorbent bed is heated and the temperature of the adsorbent bed rises from $T_a$ to $T_b$ while the adsorbate concentration in the bed remains constant at $W_2$. The pressure of the adsorbent bed is increased from $P_{eva}$ to $P_{cond}$ during the isosteric heating process. The next process is desorption process (b-c) which starts by opening of valve V2 placed between the adsorber and the condenser. During the desorption process, the temperature of adsorbent bed is increased from $T_b$ to $T_c$ while its pressure remains at $P_{cond}$. The desorbed adsorbate leaves the adsorber, and it is condensed in the condenser and as a result the adsorbate concentration falls from $W_2$ to $W_1$. Finally, both valves V1 and V2 are closed and the adsorbent bed is cooled to reduce

its pressure from $P_{cond}$ to $P_{eva}$. During this process, which is known as isosteric cooling process, the temperature of adsorbent bed falls from $T_c$ to $T_d$.

The adsorption heat pump cycle operates under vacuum. This system requires high vacuum technology, special materials and gaskets which increase the cost of adsorption heat pump. However, some studies have been performed to obtain systems that can operate with high vacuum technology (Wang and Zhu 2002). Although, this improvement may solve one of the main problems of the adsorption heat pumps, the corrosion problem can be faced in the system (Wang and Zhu 2002).

## 3.2. Performance Analysis

Despite the many advantages of adsorption heat pumps, the applications of adsorption systems have been limited because of their low specific cooling power (SCP) and low coefficient of performance (COP). The definitions and relations for determination of these effectiveness terms are presented in the following chapters.

### 3.2.1. Coefficient of Performance

The amount of heat from isosteric heating process ($Q_{ab}$), isobaric desorpiton process ($Q_{bc}$), isosteric cooling process ($Q_{cd}$), isobaric adsorption process ($Q_{da}$) can be defined and written as:

- the amount of heat ($Q_{ab}$) which should be transferred to the adsorbent bed to increase temperature of the bed from $T_a$ to $T_b$,
- the portion of the heat ($Q_{bc}$) which is transferred to the adsorbent bed increases the temperature of adsorbate-adsorbent pair and adsorbent bed while the other portion causes the desorption process,
- the heat loss ($Q_{cd}$) when the valve between the condenser and adsorbent bed is closed, the temperature of adsorbent bed ($T_c$) is decreased to $T_d$,
- the heat loss ($Q_{da}$) due to heat of adsorption when the valve between the adsorbent bed and evaporator is opened and vaporization of the adsorbate in the evaporator is started (Figure 3.2).

$$Q_{ab} = \int_{T_a}^{T_b} \left[ m_s (C_{p_s} + WC_{p_v}) + m_{bed} C_{p_{bed}} \right] dT \tag{3.1}$$

$$Q_{bc} = \int_{T_b}^{T_c} \left[ m_s (C_{p_s} + WC_{p_v}) + m_{bed} C_{p_{bed}} \right] dT + \int_{b}^{c} m_s \Delta H_{ads} dW \tag{3.2}$$

$$Q_{cd} = \int_{T_c}^{T_d} \left[ m_s (C_{p_s} + WC_{p_v}) + m_{bed} C_{p_{bed}} \right] dT \tag{3.3}$$

$$Q_{da} = \int_{T_d}^{T_a} \left[ m_s (C_{p_s} + WC_{p_v}) + m_{bed} C_{p_{bed}} \right] dT + \int_{d}^{a} m_s \Delta H_{ads} dW \tag{3.4}$$

The heat of evaporation which causes cooling effect and heat of condensation which can be employed for heating purposes can be determined by the following relations:

$$Q_{ev} = m_s \Delta W \Delta H_{va} + \int_{T_{cond}}^{T_{ev}} m_s \Delta W C_{p_v} dT \tag{3.5}$$

$$Q_{cond} = m_s \Delta W \Delta H_{va} \tag{3.6}$$

The cooling and heating COP of an intermittent adsorption heat pump can be determined by (Ülkü 1986, Pons et al.1999, Pons and Kodama 2000):

$$COP_{cooling} = \frac{Q_{eva}}{Q_{ab} + Q_{bc}} \tag{3.7}$$

$$COP_{heating} = \frac{Q_{cond} + Q_{cd} + Q_{da}}{Q_{ab} + Q_{bc}} \tag{3.8}$$

### 3.2.2. Specific Cooling and Heating Powers

Specific cooling or heating power (SCP/SHP) is the ratio of cooling/heating power per mass of adsorbent per cycle time. The definition of SCP/SHP involves the period of cycle and has important role to compare the various adsorption heat pump designs (Demir et al. 2008).

$$SCP = \frac{Q_{eva}}{m\tau_{cyc}} \tag{3.9}$$

$$SHP = \frac{Q_{cond} + Q_{cd} + Q_{da}}{m\tau_{cyc}} \tag{3.10}$$

## 3.3. Advantages and Disadvantages of an Adsorption Heat Pump

The important advantages of the adsorption heat pumps can be described as follows:

- Adsorption heat pump which is a kind of thermal heat pump can be operated with the thermal energy sources such as waste heat, geothermal and solar energies,
- They can work with a low level temperature heat reservoir,
- It is a noiseless system due to the lack of moving components,
- They have long life time and do not require frequent maintenance,
- They have simple principle of working,
- They are environmental friendly since they do not contain any hazardous materials for environment.

Adsorption heat pump requires high technology and special designs to maintain high vacuum. They have large volume and weight compared to traditional mechanical heat pump system. One of important drawbacks of an adsorption heat pump is its relatively low specific cooling and heating powers (SCP/SHP) and coefficient of performance (COP) due to weak thermal conductivity of the bed, while its primary energy efficiency value is comparable with the traditional heat pumps. The enhancement of heat and mass transfer reduces the period of cycle and consequently increases the power of adsorption heat pump. The heat and mass transfer mechanism in the adsorbent bed should be recognized very well in order to reduce the period of the cycle. The solution of relevant governing equations for an adsorbent bed can provide valuable details and help researchers in the design of the adsorbent bed. The slow heat and mass transfer in the adsorbent bed is the main drawback of the adsorption heat pump. The enhancement of heat and mass transfer rate reduces the period of cycle and consequently increases the power.

## 3.4. Comparison of Heat Pumps

The future of adsorption heat pumps can be clearly visualized by the comparison of the adsorption heat pump with the conventional heat pumps. Table 3.1 illustrates the COP values of adsorption, absorption, and mechanical heat pump systems. As known, the COP value of the vapor compression heat pumps is higher than thermal driven pumps.

The waste heat or any heat source which is thrown away is used as a driving energy in the adsorption heat pump. This waste heat has no operational cost. The vapor compression heat pumps operate with electrical power that is produced by the heat of fossil fuels. In conclusion, the primary energy efficiency of mechanical heat pumps will be less than their COP values.

## 3.5. Methods for Improvement of Adsorption Heat Pump

To improve the adsorption heat pump systems, the performed studies can be categorized in three groups:

1. advanced adsorption cycles which can operate with low temperature heat sources, increase COP and provide continious operation,
2. new or improved adsorbent–adsorbate pairs (ex. SWS-1L) (Saha et al. 2009) in order to increase adsorption rate,
3. new designs of an adsorbent bed for improving the heat and mass transfer.

These three main categories are explained in the following chapters.

Table 3.1. Coefficients of performance of heat pump systems for cooling
(Source: Demir et al. 2008)

| **Types of Heat Pumps and Working Pairs** | **Coefficient of Performance ($COP_{cooling}$)** | |
|---|---|---|
| Adsorption | Carbon-Methanol | 0.43 |
| | Zeolite-Water | 0.8 |
| | Silica gel-Water | 0.3-0.6 |
| Absorption | Methanol-Water | 0.7-1.1 |
| | Lithium Bromide-Water | |
| Vapor compression | | 3-4 |

## 3.5.1. Advanced Adsorption Cycles

One of the disadvantages of the adsorption heat pumps are their intermittent working. Many studies on adsorption heat pump have been providing a continuous cooling or heating process to increase the COP values. The developed systems have been called as advanced adsorption heat pump cycles. The increase the number of the adsorbent beds of the heat pump provides continuity of cooling and heating processes. The increase of COP is obtained by recovering and utilizing heat which is transferred during isosteric cooling and isobaric adsorption of another adsorption cycle.

The advanced cycles can be categorized into two groups as; uniform temperature adsorber process and thermal wave process (Douss and Meunier 1989, Meunier 2002). The uniform temperature adsorber process systems consist of two or more adsorbent beds, operating with the same refrigerant, an evaporator, and a condenser. In this system, one of the adsorbent bed is preheated by the heat of another adsorber which is under the cooling process. The heat transfer fluid is used to transfer heat between the adsorbent beds (Chahbani et al. 2002). This type of advanced cycle improves the COP up to 50% (Meunier 2002, Dous and Meunier 1989, Szarzynski et al. 1997).

The thermal wave process systems are consists of two or more beds, a condenser, and an evaporator. Between the two adsorbent beds, heat transfer fluid is circulated. One bed works under cooling while the other one is under heating process. The heating of fluid is continued to desorption temperature by a heating system and then it is fed to adsorbent bed in heating period for the isobaric desorption process.

After leaving of heat transfer fluid from adsorber in heating period, it is cooled by a cooler in cooling period. Then, the heat transfer fluid completes a cycle in the system. To change flow direction of heat transfer fluid for the reverse process, a reversible pump is used (Meunier 2002, Dous and Meunier 1989, Szarzynski et al. 1997, Pons and Szarzynski 2000, Chahbani et al. 2004).

### 3.5.2. Improved Adsorbent-Adsorbate Pairs

The adsorbent-adsorbate pair is one of the main parts of adsorption heat pump system. The adsorbate should be non-corrosive, non-toxicity and should have high latent heat and good thermal and chemical stability. Moreover, adsorbents should have high adsorption capacity, high thermal conductivity, and stability, and should be cheap. Detailed information on the adsorbents was given in Chapter 2. Zeolite-water, active carbon-methanol, silica gel-water, activated alumina-water and carbon-ammonia are some of the common adsorbent-adsorbate pairs used in adsorption heat pump systems (Ülkü and Mobedi 1989, Cerkvenik et al. 2001). Another important criterion for the selection of suitable adsorbent-adsorbate pair is the type of interaction between solid adsorbent and vapor adsorbate (physisorption and chemisorption) as mentioned in Chapter 2. Comparisons of adsorbent-adsorbate pairs are given in Table 3.2 (Ülkü and Mobedi 1989). As can be seen from the table, the maximum adsorption capacity among all pairs is achieved by active carbon-water pair. Zeolite-water pairs have high quantity of heat of adsorption. The lowest working temperature range is seen for silica gel-water pairs. The adsorbent of different manufacturers can have the different structures and as seen from the table, silica gel-water and zeolite 13X-water pairs are presented with different thermophysical properties.

### 3.5.3. Innovative Design of Adsorbent Bed

There are lots of numerical and theoretical studies on the importance of the adsorbent bed design of adsorption heat pump in the literature. To improve the SCP/SHP values of an adsorption heat pump, the design of the adsorbent bed has an important role. The heat and mass transfer mechanisms should be improved and for this purpose, many researchers study on the adsorbent bed design. In this section, the studies

reported in the literature are handled. The designed adsorbent beds can be classified in three groups as: a) unconsolidated adsorbent beds, b) coated adsorbent beds, c) consolidated adsorbent beds. Three different investigated adsorbent bed designs with related examples are explained below.

### 3.5.3.1. Unconsolidated Adsorbent Beds

Adsorbents in this kind of adsorbent beds are used without any special process such as chemical process. Adsorbents used in this kind of adsorbent beds can be pellets, granules, or fibers in shape.

During the adsorption process, adsorptive, which is evaporated from evaporator, flows between the adsorbents and it is adsorbed. During the desorption process, the adsorbate separates from the adsorbent granules and fills the voids between the adsorbent granules. It flows to the condenser and then it is condensed while heat is released to the environment. An example for an adsorbent bed filled with adsorbent granules is illustrated in Figure 3.3. As seen, there are two types of voids for the unconsolidated adsorbent bed; a) voids between adsorbent granules, b) voids in the adsorbent granule. For this reason, interparticle mass transfer and intraparticle mass transfer mechanism are mentioned in this kind of adsorbent beds. As given in Chapter 2, the interparticle mass transfer refers to mass transfer between particles in the adsorbent bed and intraparticle mass transfer takes place within the absorbent particle.

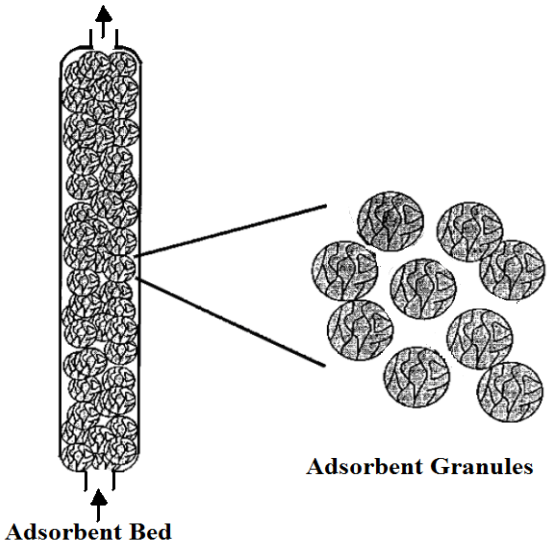


Figure 3.3. Adsorbent bed and adsorbent granules

Table 3.2. Comparisons of adsorbent-adsorbate pairs
(Source: Ülkü and Mobedi 1989)

| Adsorbate-Adsorbent | Max. Adsorbate Capacity (kg/kg)* | Avg. Heat of Adsorption ($kJ/kg_s$)* | Adsorbent Sp. Heat (kJ/kg)* | Energy density ($kJ/kg_s$) | Temperature Range ($^oC$) |
|---|---|---|---|---|---|
| Water-Zeolite 4A | 0.22 | 4400 | 1.05 | 1250 | 30-350 |
| Water-Zeolite 5A | 0.22 | 4180 | 1.05 | 1200 | 30-350 |
| Water-Zeolite MgA | 0.29 | 3400 | 1.06 | 800 | 60-250 |
| Water-Zeolite 13X | 0.30 | 4400 | 0.92 | 1290 | 30-350 |
| Water-Zeolite 13X | 0.27 | | 0.84 | 930 | 20-300 |
| Water-Zeolite 10A | 0.20 | 4000 | | 897 | 50-250 |
| Water-Zeolite 13X | 0.27 | 3400 | 1.06 | 1200 | 30-350 |
| Water-Clinoptilolite | 0.12 | 3000 | 1.11 | 480 | 20-240 |
| Water-Mordenite | 0.11 | 4000 | | 419 | 30-350 |
| Water-Chabazite | 0.17 | 3000 | 1.08 | 700 | 30-250 |
| Water-Charcoal | 0.40 | 2320 | 1.09 | 1200 | 30-250 |
| Water-Ac. Alumina | 0.19 | 2480 | 1.00 | 660 | 30-250 |
| Water-Silica gel | 0.37 | 2560 | 0.88 | 1000 | 30-150 |
| Water-Silica gel | 0.20 | 2500 | 1.045 | 600 | 20-130 |
| Methanol-Zeolite 13 | 0.20 | 2400 | 1.07 | | |
| Methanol-Zeolite 4A | 0.16 | 2300 | 1.07 | | |
| Methanol-Zeolite 5A | 0.17 | 2300 | 1.07 | | |
| Methanol-Zeolite 5A | 0.17 | 2300 | 1.07 | | |
| Methanol-Ac. Carbon | 0.32 | 1400 | 0.9 | 590 | 20-140 |

* Energy densities were calculated using the data given in the reference for possible max. load

The size of the adsorbent granules has an important effect on the mass transfer mechanism. The interparticle mass transfer can be increased by using big size adsorbent granules. Although the increase of particle size increases permeability in the bed, it also increases the intraparticle mass transfer resistance. The intraparticle mass transfer

resistance can be decreased by using small size granules. However, very small adsorbent granules may cause the increase of the interparticle mass transfer resistance.

One of the earliest studies on adsorbent bed design was performed by Kivrak and Mobedi (Kivrak 1987, Mobedi 1987). The bed was filled with 24.9 kg zeolite and the water vapor was chosen as an adsorptive. The details of adsorbent bed is given in Figure 3.4.

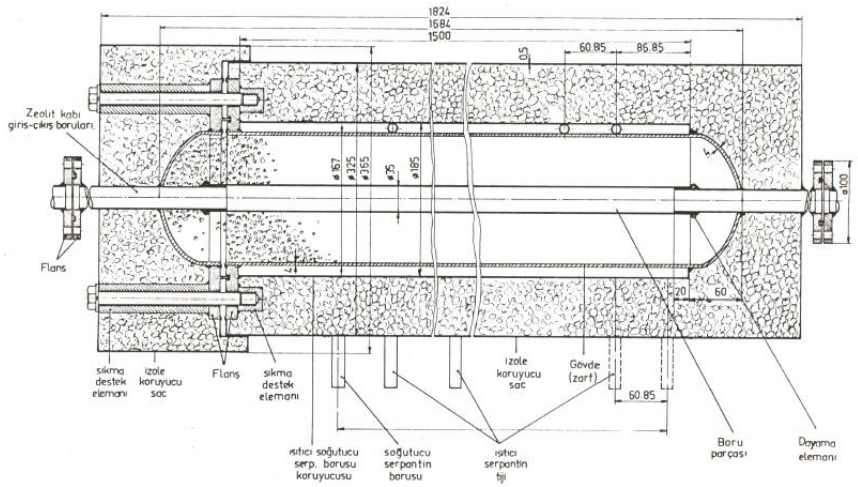


Figure 3.4. One of the earliest adsorbent bed design example (Source: Kivrak 1987, Mobedi 1987)

To increase heat transfer rate in an adsorbent bed is to increase the heat transfer area. That's why, in many unconsolidated adsorbent beds, fins are placed into the adsorbent bed to increase the heat transfer rate. The adsorbent granules are placed between these fins. There are many experimental and numerical studies on the use of fins in adsorbent bed for enhancement of heat transfer. The experimental examples of unconsolidated adsorbent bed designs are shown in Figure 3.5. Figure 3.5(a) shows the slim thin wall shell tube adsorber designed for improving heat transfer rate studied by Gui et al. (2002). The activated carbon was used as an adsorbent. The fins mounted on tubes were used to increase heat transfer rate from the tubes to the activated carbon in order to increase the heat transfer surface area. Saha et al. (2006) used activated carbon fiber/ethanol pair. The oxygen-free copper fins were used and the activated carbon fibers were packed tightly inside these fins as illustrated in Figure 3.5(b). Critoph et al. (2000) (Figure 3.5(c)) studied on a prototype of a fast cycle adsorption refrigerator that is composed of laminate of monolithic carbon discs and aluminum fins. Demir et al. (2008) studied with the silica gel-water pair and the silica gel particles were placed between fins to increase the heat transfer area (Figure 3.5 (d)). Zhang (2000) placed

twelve radial fins that are symmetrically distributed in the adsorbent and welded to the inner tube as shown in Figure 3.5(e). These fins were used to intensify heat conduction in the bed.

It should be mentioned that Ilis et al. (2011) performed a numerical study on a cylindrical adsorbent bed assisted by fins and they concluded that the use of fin in the adsorbent bed is meaningless when the ratio of the adsorbate diffusion in the adsorbent particle to the transport of heat transfer throughout the adsorbent bed is low. The details of this study are explained in the Chapter 8.

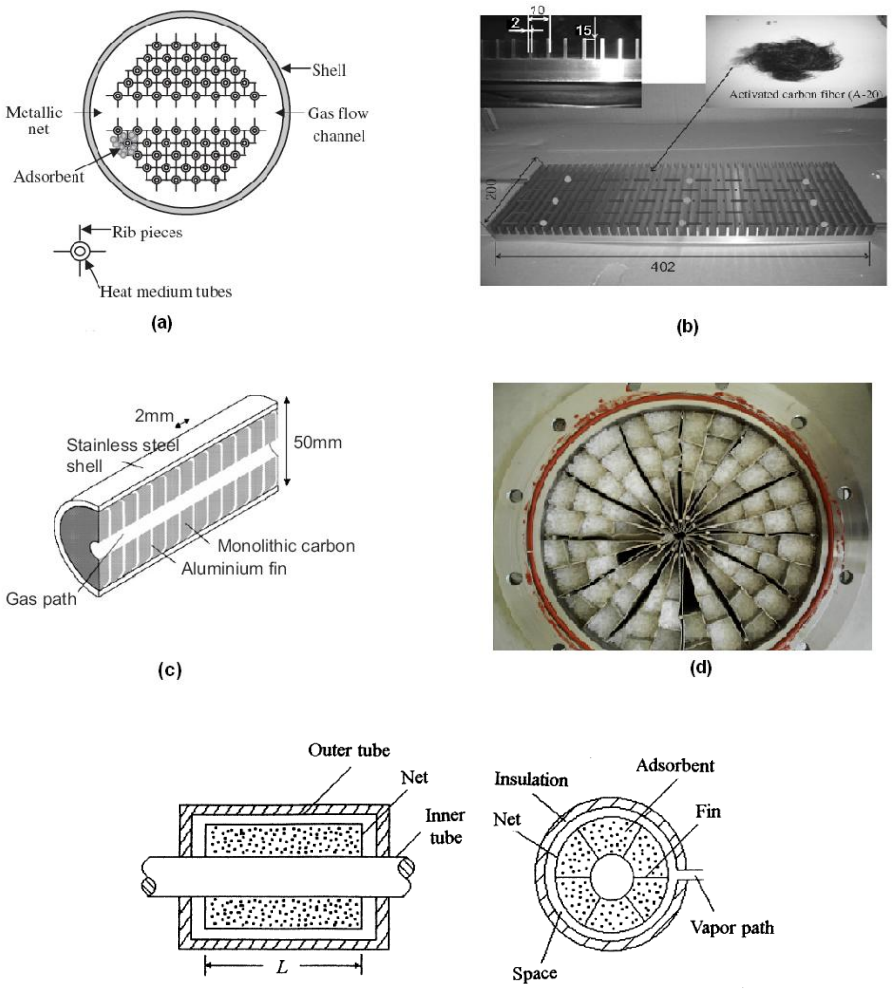


Figure 3.5. Unconsolidated adsorbent bed designs-experimental studies on the use of fins (Source: Gui et al. 2002, Saha et al. 2006, Critoph et al. 2000, Demir et al. 2008, Zhang 2000)

Besides the studies performed on the use of the fins for acceleration of heat and mass transfer in the adsorbent bed, other methods have been also studied. For example, the use of metal net inside the adsorbent bed (Lang et al. 1999) and the use of composite

adsorbents (Dellero et al. 1999) for heat transfer enhancement can be found in literature. In the study of Lang et al. (1999), the adsorber/desorber was designed as a gilled heat exchanger. The zeolite pellets were placed on the horizontal heat exchanger surface in unilayer. The complete heat exchanger was covered with a metal mesh to prevent a loss of zeolite. Dellero et al. (1999) proposed the use of carbon fibers as additive in a chemical heat pump. Three mixtures of carbon fibers with the reagent compounds were analyzed. By adding carbon fibers, the thermal conductivity of the reagent bed was enhanced and using the different mixtures, the performances of a chemical heat pump were compared.

Many numerical studies have beed done by researchers to simulate and understand the heat and mass transfer mechanism in the adsorbent bed. As shown in Figure 3.6, different bed designs are investigated by researchers. Ben Amar et al. (1996) solved the heat and mass transfer equations for the shell and tube type adsorber and the adsorbent was placed outside the tubes (Figure 3.6(a)). The adsorbent bed was heated or cooled by a thermal fluid circulating in the center of the adsorber. The adsorbent-adsorbate pair was zeolite NaX/water and activated carbon AX21/ammonia. Chahbani et al. (2004) studied performance of adsorptive heat pump systems with carbon/ammonia pair. The adsorber which is illustrated in Figure 3.6(b) was cylindrical and heat transfer fluid circulated around the adsorbent. In Figure 3.6(c), the adsorber is a cylinder, which encloses a metal tube for the purpose of heat exchange between the solid adsorbent, and heating or cooling fluid within the tube. Fins were located around the tube to increase the heat transfer rate to the adsorbents. The fin thickness and the spacing between the fins were declared very small (Chua et al. 2004). Leong and Liu (Leong and Liu 2004a) analyzed adsorbent beds with zeolite NaX and 13X /water pairs. The analyzed adsorbent bed in their studies is a hollow cylinder, which encloses a metal tube for the purpose of heat exchange between the solid adsorbent, and heating or cooling fluid within the tube as shown in Figure 3.6(d).

In conclusion, the design of the adsorbent bed has a significant effect on the power of the adsorption heat pumps. The heat and mass transfer rate should be increased in the adsorbent bed and this thesis focuses on this purpose.

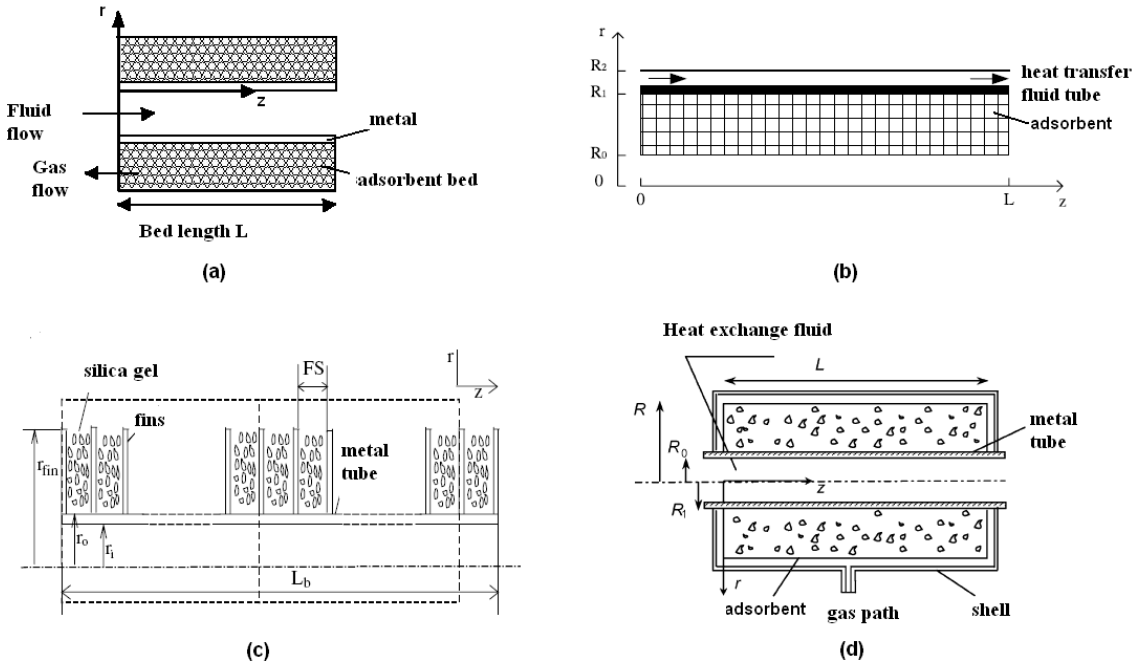


Figure 3.6. Unconsolidated adsorbent bed designs-numerical studies (Source: Ben Amar et al. 1996, Chahbani et al. 2004, Chua et al. 2004, Leong and Liu 2004a)

### 3.5.3.2. Coated Adsorbent Beds

In the coated adsorbent bed design, the adsorbent is coated around a metal fins or a tube. For this kind of adsorbent bed, the adsorbent layer is very thin and this causes the increase of the heat and mass transfer rate in the adsorbent bed. Heat transfer area is also increased due to the coating around a tube or plate. On the contrary, mass transfer resistance may increase for the thick coated adsorbent layers. As shown in Figure 3.7 (a), a tube was coated with an adsorbent to increase the heat and mass transfer rate. The heating or cooling fluid flows inside of the metal tube, and the adsorptive flows over the adsorbent tube (Restruccia et al. 2002). As illustrated in Figure 3.7(b), the adsorbent was coated on finned tubes, and then the heat transfer area was increased by the fins (Restuccia et al. 2005). In recent years, metal foam production technology has been developed and the porous metal foam (Cu, Al etc.) production gets common. Some researchers use metal foams coated by adsorbent to increase the heat transfer rate in the adsorbent bed. The open cell metal foam was prepared by Bonaccorsi et al. (2006) is shown in Figure 3.7(c). Seeding the metal substrate before the hydrothermal synthesis is a widely used methodology to improve the coating accretion on the surface. This application is seen in Figure 3.7(d).

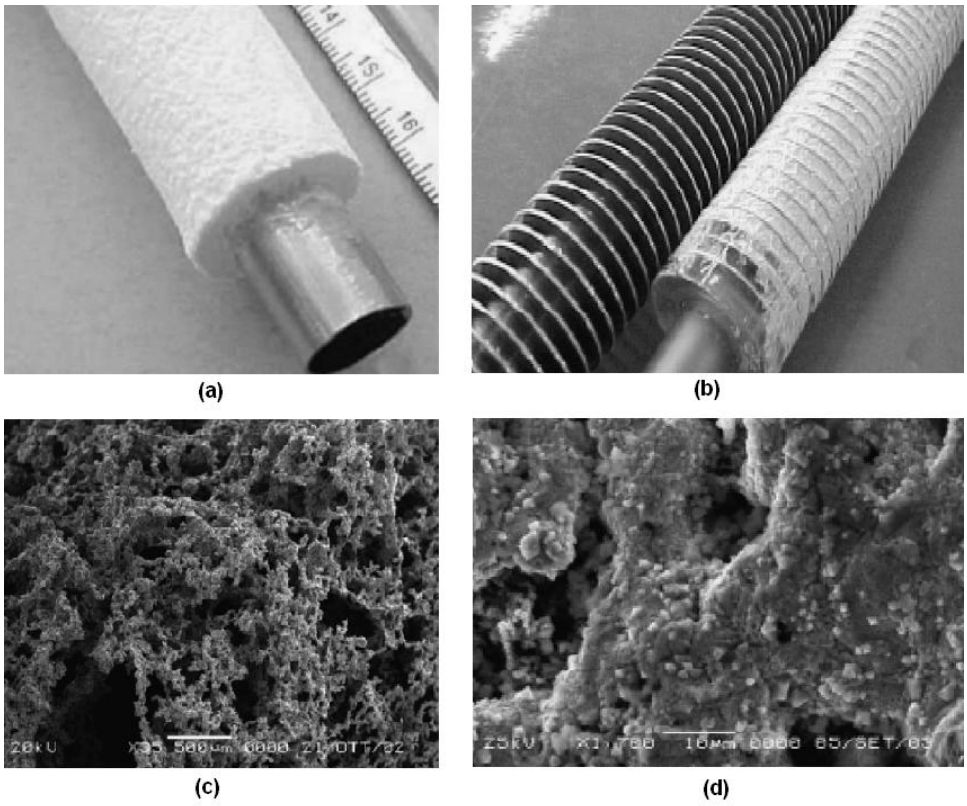


Figure 3.7. Coated adsorbent beds (Source: Restruccia et al. 2002, Restuccia et al. 2005, Bonaccorsi et al. 2006)

### 3.5.3.3. Consolidated Adsorbent Beds

Heat transfer rate through an adsorbent particle can be increased by the use of special processes (chemical and thermal). The performed studies show that some special processes increase the heat transfer rate noteworthy in the adsorbent bed (Wang et al. 2006, Wang et al. 2004). A composite adsorbent is obtained by using a material which has high heat transfer coefficient (Graphite, Al etc.) under thermal and chemical processes. It should be mentioned that the increase of the heat transfer rate in an adsorbent may affect the mass transfer rate. The manufacturing procedure of a consolidated composite adsorbent performed by Wang et al. (2006) is shown in Figure 3.8. As seen, the graphite powders are expanded and heated. Then, the calcium chloride powders (thermal conductivity of $CaCl_2$ is about 0.4 $Wm^{-1}K^{-1}$) are added to the slurry of expanded graphite and water. The mixture is molded by compression. Finally, the consolidated composite adsorbent is obtained after completely removing the water. Thermal conductivity of composite adsorbent becomes about 9.2 $Wm^{-1}K^{-1}$.

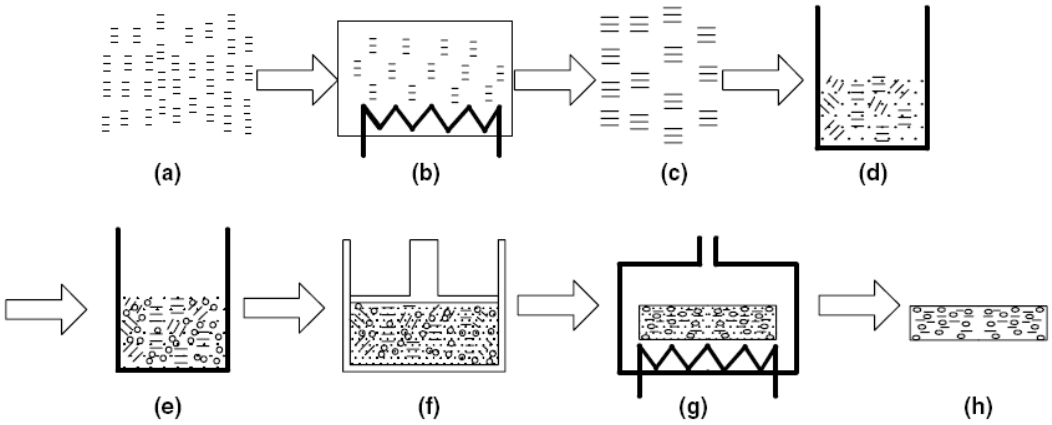


Figure 3.8. Manufacturing procedure of the prepared composite adsorbent; a) expandable graphite powders, b) heat treatment for expansion, c) expanded graphite powders, d) slurry of expanded graphite and water, e) mixture of the slurry and $CaCl_2$, f) pressing, g) vacuum drying, h) consolidated composite adsorbent (Source: Wang et al. 2006)

# CHAPTER 4

# LITERATURE SURVEY

In this chapter, a detailed review on simulation studies of the heat and mass transfer in the adsorbent bed of adsorption heat pump is presented. The aim of the studies and the made assumptions by researchers are summarized. The heat and mass transfer equations of each reported study are given and classified according to resistance of heat and mass transfer in the adsorbent bed. Moreover, the employed adsorption equilibria relations, mass balance equation for the adsorbent particle, permeability equation, thermal conductivity, and mass transfer diffusivity equations are also reviewed and classified. Two main tables are presented to summarize the performed studies. The first table covers the name of researchers, considered adsorbent-adsorbate pair, made assumptions, aim, and results of the study, the figure of the analyzed bed and an indicating equation number which refers to the set of equation solved by researchers. Based on the given indicating equation number of Table 4.1, the set of governing equations solved by researchers are presented in Table 4.2. The definitions of important parameters used in each study with their units can also be found in Table 4.2.

The classification of heat and mass transfer equations for an adsorbent bed is performed according to the resistances of heat and mass transfer through the bed. The heat and mass transfer equations are classified into three groups as uniform temperature and pressure models, non uniform temperature and pressure models, and uniform pressure-non uniform temperature models. The mass balance equations solved by researchers for an adsorbent particle are classified into three groups as equilibrium model, LDF model, and solid diffusion model. Moreover, the models used to determine adsorptive velocity in the bed are classified into four groups as Darcy law model, Darcy and Fick’s laws model, Ergun’s model and Ergun’s and Fick’s laws model. The equations for determination of effective thermal conductivity and equations of adsorption equilibria are also presented in Table 4.1 and necessary discussions are performed.

In this chapter, besides the literature survey on the design and simulation of the adsorbent bed, literature survey on a single adsorbent particle is done. In order to

understand the heat and mass transfer mechanism in the adsorbent bed, the heat and mass transfer mechanism in a single adsorbent particle should be known well.

## 4.1. Literature Survey on Adsorption Heat Pump and Adsorbent Bed

In this section, simulation of heat and mass transfer in the adsorbent bed are given, and the analyzed systems by researchers are summarized. The studies are detailly classified by the governing equations according to heat and mass transfer resistance of adsorbent bed and mass balance equations for the adsorbent particle, permeability and diffusivity models, equivalent thermal conductivity and adsorption equilibria relationships.

### 4.1.1. Simulation of Heat and Mass Flow in the Adsorbent Bed

Studies on heat and mass transfer in the adsorbent bed of an adsorption heat pump can be performed experimentally and/or theoretically. The experimental study on adsorbent bed is not easy and requires special measuring devices and technologies. One of difficulties in experimental works is low operation pressure of adsorption heat pump which causes leakage problem in the system and consequently failure of the experiment. The measuring of temperature and adsorbate concentration in different locations of an adsorbent bed under low pressure is difficult. The determination of temperature and particularly adsorbate concentration in the adsorbent bed may not be achieved experimentally.

Number of simulation studies on heat and mass transfer in the adsorbent bed is higher than experimental ones due to difficulties on prediction of temperature and adsorbate concentration profiles in the adsorbent bed by experimental methods. The variation of temperature, pressure, and adsorbate concentration profiles during the four processes of adsorption heat pump can be obtained and COP, SCP, and SHP of system can be predicted if simulation study is performed. The changes of COP, SCP, and SHP with operation temperature and pressures for different adsorbent-adsorbate pairs can also be investigated by using simulation methods. The theoretical studies can be performed for a single bed or multiple adsorbent beds. However, it should be mentioned that to be sure from the results of simulation studies, the results of experimental works

are required. The simulation and experimental studies complete each other and both investigation approaches should be performed.

#### 4.1.1.1. Governing Equations for Heat and Mass Flow through the Adsorbent Bed

In general, the following equations are required to be solved to find temperature and concentration profiles in an adsorbent bed of adsorption heat pump;

- a continuity equation refers the conservation of mass in the adsorbent bed,
- a relation for determination of adsorptive flow in the adsorbent bed, (such as Darcy law, Fick's law, Ergun's equation)
- an energy balance equation includes both adsorptive and adsorbent particles,
- a mass balance equation for adsorbent particle.

The solutions of the above equations provide temperature, adsorptive pressure, adsorptive velocity, and adsorbate concentration in the adsorbent bed at any instant of the cycle. In addition to the above mentioned equations, further equations are required to solve the governing equations:

- a state relation between adsorptive pressure, temperature and adsorptive density. Most of researchers assumed adsorptive as an ideal gas,
- an adsorption equilibria relationship for adsorbent-adsorbate pair to determine equilibrium adsorbate concentration at a specified temperature and pressure,
- a relation for determination of the effective mass diffusivity which highly depends on adsorbent – adsorptive temperature.

The above governing equations are non-linear and coupled. Practically, the simultaneous solution of these governing equations requires some assumptions. In this review, the made assumptions by researchers are presented and reviewed.

### 4.1.2. A Summary on the Analyzed Systems

Heat and mass transfer in an adsorbent bed was simulated by many researchers. Table 4.1 (page 62) presents a brief review on the performed studies. The name of researchers, the adsorbent-adsorbate pair, aims and results of their study, assumptions

taken into consideration and the figure of the analyzed adsorbent bed are presented in Table 4.1. Moreover, a key number is given in below of adsorbent bed figure which refers the set of equation solved by researchers. The set of governing equations numbered in Table 4.1 are presented in Table 4.2. By using the key number, the set of governing equations solved by a researcher can be easily found from Table 4.2. The related governing equations numbered in Table 4.1 which are adsorption equilibria, mass transfer equation for particle, heat and mass transfer equation for the adsorbent bed, equation for equivalent thermal conductivity, mass diffusivity and permeability relations, and the definition of important symbols used in the equations are given in Table 4.2. In this section brief information about studies presented in Table 4.1 is given.

As seen from Table 4.1, Leong and Liu (Leong and Liu 2004a, 2004b, 2006, 2008, Liu and Leong 2005) analyzed adsorbent beds with zeolite NaX and 13X /water pairs. The analyzed adsorbent bed in their studies is a hollow cylinder, which encloses a metal tube for the purpose of heat exchange between the solid adsorbent, and heating or cooling fluid within the tube. The adsorptive which transfers heat to the condenser or takes heat from the evaporator passes through the gas path in the adsorbent bed. Moreover, Liu and Leong (Liu and Leong 2006) investigated a cascading system, which consists of two zeolite/water adsorbers and one silica gel/water adsorber. They solved the heat and mass transfer equations for the three adsorbers.

Chua et al. (Chua et al. 1999, 2001, 2004), Saha et al. (Saha et al. 2003), and Wang and Chua (Wang and Chua 2007a, 2007b) simulated the heat and mass transfer in the adsorbent beds with silica gel/water pair. A detailed schematic view of the analyzed adsorbent bed is given in Ref (Chua et al. 2004). In that figure, the adsorber is a cylinder, which encloses a metal tube for the purpose of heat exchange between the solid adsorbent, and heating or cooling fluid within the tube. Fins are located around the tube to increase the heat transfer rate to the adsorbents. The fin thickness and the spacing between the fins were declared very small. All of those simulation studies (Chua et al. 1999, 2001, 2004, Saha et al. 2003, Wang and Chua 2007a, 2007b) were performed on two-bed or multi-bed adsorption chiller. A comparison between simulated results of Ref (Wang and Chua 2007a) and experimental data was also performed and it was found that the difference in performance prediction from lumped parameter model and distributed parameter model is 10%.

Sun et al. numerically studied on zeolite 13X/water and zeolite 13X/ammonia pairs (Sun et al. 1995). The adsorbent bed heated or cooled by a fluid inside a tube

which can be located either in the center or on the external side of the cylindrical bed. The system was a long adsorbent bed which was heated by heat transfer fluid through a tube and connected only to the surroundings at the two ends. Ben Amar et al. (Ben Amar et al. 1996) solved the heat and mass transfer equations for the shell and tube type adsorber and the adsorbent was placed outside the tubes. The adsorbent bed was heated or cooled by a thermal fluid circulating in the center of the adsorber. The adsorbent-adsorbate pair was zeolite NaX/water and activated carbon AX21/ammonia.

Cacciola et al. (Cacciola et al. 1993) studied the dynamic behavior of a two-reactor adsorption heat pump with zeolite 4A/water pair. The operating principle of the system was described and the governing equations were derived for the adsorbent bed. The dynamic model of heat and mass transfer in compact adsorbent bed with zeolite/water pair was studied by Marletta et al. (Marletta et al. 2002). A stainless steel tube (type AISI 304, internal diameter 9 mm, thickness 0.5 mm) was coated with 5 mm of zeolite. The heating or cooling fluid flows inside of the metal tube, and the adsorptive flows over the adsorbent bed. A similar study was performed by Restuccia et al. (Restuccia et al. 2002). In their study the adsorber design was same with the study of the Marletta et al. (Marletta et al.2002), except the dimensions of the stainless steel tube whose internal diameter is 14 mm and thickness is 0.4 mm. Restuccia et al. (Restuccia et al. 2004) solved the heat transfer equation for an adsorber with SWS-1L (mesoporous silica gel impregnated with $CaCl_2$)/water pair. The sorbent material consists of 1.1 kg of dry SWS-1L granules with 0.8–1.6 mm sizes. The adsorbent bed was placed in a cylindrical vacuum chamber and an external circuit allows the heating/cooling of the adsorbent bed. A good agreement between the model and experimental measurements was declared. The pair was zeolite 4A/water in the study of Maggio et al. (Maggio et al. 2006) who used a two-dimensional numerical model to describe a double-bed adsorption machine, with internal heat recovery, using two heat exchangers coated with a consolidated layer of zeolite 4A. In their study, a bed thickness as 2-3 mm was recommended to obtain high performance. They declared that their developed model is very useful for analyzing of adsorbent beds with internal heat recovery. Vasta et al. (Vasta et al. 2008) and Freni et al. (Freni et al. 2008) studied the dynamic simulation of an adsorptive solar ice-maker with active carbon/methanol. In both studies, the simulation was performed based on climatic data measured at CNR-TAE institute in Messina, Italy. The results of Vasta et al. (Vasta et al. 2008) were performed for a whole year of 2005 and detailed results of a week of June and December 2005 were

shown. The results of Freni et al. (Freni et al. 2008) were presented in detail for a period of twenty days of May 2005. In the study of Maggio et al. (Maggio et al. 2009), a novel composite sorbent lithium chloride in silica gel pores was proposed for application in solar-powered adsorptive ice makers. As mentioned before, lithium chloride in silica gel pores can be used to design highly efficient solar powered adsorptive ice makers.

$CaCl_2$ confined to KSK silica gel with average pore size of 15 nm, SWS-1L and water pair was taken account in the study of Saha et al. (Saha et al. 2009). The adsorbent bed is cylindrical and bended in a closed container. In their study, both the steady state and dynamic behaviors of SWS-1L in a two bed solid sorption cooling system was presented. The results showed that the SWS-1L adsorbents are more powerful than the other commercial available silica gel adsorbents.

Chahbani et al. (Chahbani et al. 2002, 2004) studied performance of adsorptive heat pump systems with carbon/ammonia pair. The adsorber was cylindrical and heat transfer fluid circulated around the adsorbent. The refrigerant was either evacuated to the condenser or transferred from the evaporator through the empty central part of the bed. They declared that the heat and mass transfer limitations affects the performance of adsorption heat pump systems. Three mass transfer equations for adsorbent as equilibria model, linear driving force model and solid diffusion model were studied in their work and results of these models were compared with each others.

Sakoda and Suzuki (Sakoda and Suzuki 1984, 1986) worked on solar powered adsorption cooling systems with silica gel/water pair. In their study (Sakoda and Suzuki 1984), the adsorber consists of five T tubes. A copper-constantan thermocouple was inserted into a narrow glass tube which was inserted into the bed to reach the center of it. The silica gel which was used in this study is a type of silica gel that changes its color from blue to pink when its moisture adsorption amount reaches about 10 weight percent. A simple model taking into accounts both the adsorption properties and apparatus characteristics were proposed and the experimental results were successfully interpreted by the model. The adsorbent bed of their other study (Sakoda and Suzuki 1986) was a steel box of 500 mm x 500 mm in width and 50 mm in depth. The box was divided into four blocks in which ten heat transfer fins of 50 mm x 50 mm square and 0.5 mm thick were welded. After 10 kg of silica gel between 10 and 20 mesh size were packed in each block, the lid of the container was hermetically welded. A cooling pipe of 15 mm outer diameter was welded on the upside of the container. Suzuki (Suzuki 1993) also performed a study on adsorption cooling system by zeolite NaX and water

pair and the technological limits for the application of adsorption system to passenger car air conditioning were theoretically investigated. It is declared that the application of adsorption cooling system to automobiles could be possible if appropriate design of adsorbent beds used to improve heat transfer characteristics.

Silica gel/water pair was used in the study of Demir et al. (Demir et al. 2009). The bed was cylindrical and the adsorptive flow was only in radial direction. The adsorptive could flow easily in the center of the annulus and enter with a uniform velocity to the portion filled with granules. It was found that, the distributions of temperature and adsorbate concentration are considerably influenced from the bed porosity. The adsorption period increases with the increase of the porosity value.

Yong and Sumathy (Yong and Sumathy 2004) worked with monolith activated carbon/ammonia and activated carbon/methanol pairs. The system that was taken under consideration is cylindrical. The study showed that there is a possibility to design a fast adsorption cycle by either increasing the permeability of the adsorbent or reducing the thickness of the adsorbent bed.

Zeolite 13X and water vapor pair was used by Zhang and Wang (Zhang and Wang 1999a, 1999b). The adsorber in these studies was considered as cylindrical double-tubes and the heating and cooling fluid flows through the inner tube to supply or extract heat from the adsorber. The results showed that, the fin numbers in the adsorber, the adsorbent thickness, and the heat transfer coefficient of the bed influences the adsorber performance (Zhang and Wang 1999a). Also for the isosteric phase, the heat pipe effect plays an important role in heat and mass transfer in the adsorber (Zhang and Wang 1999b). Zhang (Zhang 2000) also studied with zeolite 13X-water pair. The adsorber model of this study is same with the previous studies of Zhang and Wang (Zhang and Wang 1999a, 1999b). It was found that if the internal and external mass transfer resistances among the adsorbent particles are taking into account, it can be utilized to study the effects of adsorption kinetics and the bed consolidation on the system performance.

The pair used in the study of Alam et al. (Alam et al. 2000) is silica gel and water. The adsorber was designed as a heat exchanger. The adsorber was divided into two parts. One is adsorbent side which is filled with granules; the other is the heat transfer fluid side. The results showed that the changes of frequency, bed NTU, Ar and Bi numbers have strong effects on the system performance.

In the study of Ilis et al. (Ilis et al. 2010) the adsorbent bed is annular type and filled with adsorbent granules. The pair is silica gel-water. The adsorptive assumed to be flow only in radial direction. In this study, heat and mass transfer in a granular adsorbent bed for an isobaric adsorption process is investigated numerically. The governing equations were non-dimensionalized two dimensionless parameter were found. The effects of G and Γ parameters on local and average temperatures and adsorbate concentration in the adsorbent bed for the adsorption process are studied.

In another study of Ilis et al. (Ilis et al. 2011), the analyzed adsorbent bed is an annular bed with inner fins in radial direction. The silica gel-water pair was taken as a pair. The flow assumed to be only in radial direction. The non-dimensionalization of heat transfer equation for the adsorbent bed and mass balance equation for the adsorbent particle yield two dimensionless parameters as Kutateladze number and a dimensionless parameter denoted by Γ which compared the rates of mass diffusion within the adsorbent particle and heat diffusion in the adsorbent bed. Moreover, the non-dimensionalization of conduction heat transfer equation of radial fin yield two dimensionless parameters as dimensionless fin coefficient parameter and thermal diffusivity ratio. The effect of these dimensionless parameters on heat and mass transfer were analyzed in this study.

### 4.1.3. Classification of Governing Equations According to Heat and Mass Transfer Resistance of Adsorbent Bed

As seen from Table 4.1, simulation studies were performed to predict temperature, adsorptive concentration, and adsorptive pressure in the adsorbent bed as well as to determine dynamic behavior of mass transfer in an adsorbent particle. In order to solve the heat and mass transfer equations for an adsorbent bed, assumptions and approximations were made by researchers and high nonlinear and coupled heat and mass transfer equations were simplified. The models used to solve heat and mass transfer equations for a bed can be classified into three categories as Uniform Pressure-Uniform Temperature, Uniform Pressure-Non Uniform Temperature and Non Uniform Pressure - Non Uniform Temperature. It should be mentioned that Non Uniform Temperature – Non Uniform Pressure is the main model and other models are simplified from this model. The base of this kind of the classification of the heat and

mass transfer equations is the assumptions that made on heat and mass transfer resistances. A negligible heat or mass transfer resistance in an adsorbent bed provides almost a uniform distribution of temperature or concentration and this allows the use of uniform models. There is no doubt that solving of uniform model equations is easier than the equations of non uniform models since in uniform models temperature and/or concentration only depends on time.

Parameters such as bed porosity, effective thermal capacitance and thermal conductivity, bed thickness, shape of adsorbent particles and rate of adsorption heat transfer affect heat transfer resistance in an adsorbent bed. Some parameters such as mass transfer diffusivity in the adsorbent particle, size of adsorbent particle, bed porosity, and bed thickness influence mass transfer resistance. Unfortunately, detailed studies on determination of heat and mass transfer resistances in the adsorbent bed of adsorption heat pump could not be found in the literature. Our literature survey shows that conditions for application of the uniform models are not well known and researchers decided on the use of uniform models based on their experimental observations.

Some assumptions such as constant porosity, constant thermal properties of adsorptive and adsorbate are commonly employed in the studies. Most of studies used thermal equilibrium condition for heat transfer equations which means that the adsorbent, adsorbate and adsorptive are at the same temperature in any location in the adsorbent bed and hence the solution of only one heat transfer equation can yield variation of temperature with time.

Generally finite difference and finite volume methods are used to solve the coupled heat and mass transfer equations for the bed. As it was mentioned before, the uniform temperature and pressure models makes solution of the problem easier since the temperature or the adsorbate concentrations based on time only which can be solved by the methods such as Euler or Runge-Kutta methods.

Boundary condition is another important issue which should be taken into account during literature survey. There is no need to write the boundary condition when uniform models are employed since dependent variables which are temperature and adsorbate concentration depends on time. However for the non-uniform model, boundary conditions should be well defined. A convective heat transfer between casing of the adsorbent bed and working fluid, used to heat or cool the adsorbent, were widely employed as boundary conditions. Based on the design of adsorbent bed, for some

studies as constant heat flux or constant temperature, boundary conditions are imposed to the surface of adsorbent bed.

It is clear that an adsorbent bed involves a casing in which adsorbent particles are placed. The thermal capacitance of the adsorbent casing was involved in some studies in order to obtain more realistic results while some works concentrated on theoretical results and neglected the thermal capacitance of casing material. A working fluid may be used to heat the adsorbent bed during desorption or cool it throughout the adsorption process. Heat transfer equation for working fluid was also derived and solved in some studies to consider the simultaneous interaction between the working fluid and the adsorbent bed.

A cycle of an adsorption heat pump is an intermittent process. This disadvantage of adsorption heat pump generally is overcome by using double or multiple adsorbent beds. The heat released from a cycle can be transferred to another cycle or even mass transfer between cycles is possible. These technologies not only provide continuity of heating or cooling of an adsorption heat pump, but also promote COP of the cycle. The simulation of heat and mass transfer for double and multiple adsorbent beds was also performed and simulation studies on these kinds of systems can be found in literature. The heat and mass transfer equations for each adsorbent bed are linked to others and the continuity of simulated cycle was performed by adjusting different initial and/or boundary conditions. In this section, the simulation studies presented in Table 4.2 are classified based on the mentioned categories and the employed heat and mass transfer equations for each study are briefly explained.

### 4.1.3.1. Uniform Temperature – Uniform Pressure Models

The distributions of temperature, adsorptive pressure, and adsorbate concentration in an adsorbent bed depend on both time and space. The governing equations that should be solved are highly non linear coupled partial differential equations. The solutions of these equations are difficult and require special numerical methods. That's why, spatial heat and mass transfer resistances in the bed were assumed negligible in some studies. In those studies, time is the only independent parameter in the heat and mass transfer equations. The dependent variables which are density and pressure of adsorptive, temperature of adsorbent (or adsorptive), and concentration of adsorbate

vary only with time. In addition to time dependence heat and mass transfer equations for the adsorbent bed, further equations are also required to obtain temperature and adsorbate concentration in the bed. Mass balance equation for adsorbent particle should be solved and adsorption equilibria must be well known. Adsorption equilibria establish a relation between adsorbate concentration with pressure and temperature at equilibrium condition. Brief information about the studies neglected heat and mass transfer resistances of the adsorbent bed are presented in this section.

The set of equation (2) presented in Table 4.2 (page 96) was considered by Liu and Leong (Liu and Leong 2006). Two zeolite adsorbent beds and a silica gel adsorbent bed were analyzed in their study. Heat and mass recovery carried out between the two zeolite adsorbent beds were taken into account. The pressure of the adsorbent bed was assumed at condensing or evaporating pressure so mass transfer resistance in the bed was neglected during the adsorption and desorption processes. The efficiency of heat exchanger in which working fluid is circulated was also considered in their calculation. Heat losses from the system to the external environmental were neglected. Thermal capacitance of heat exchanger in the bed and adsorbent container were also neglected in the heat transfer equation.

Chua et al. (Chua et al. 1999) and Wang and Chua (Wang and Chua 2007a) solved the set of equation (3) and (7), respectively, to model the performance of two beds silica gel/water adsorption chiller. During the adsorption and desorption processes, the adsorbent bed is at evaporator and condenser pressures, respectively therefore interparticle mass transfer resistance was neglected. In these studies, the thermal capacitance of the heat exchanger in the adsorbent bed was taken into consideration. They used constant values for the overall heat transfer coefficient of heat exchanger in the adsorber for the heating and cooling processes. The heat transfer between adsorptive and adsorbent particles which are at different temperatures during the adsorption and desorption processes was also taken into account in the heat transfer equation. The tubes of the heat exchanger were divided into finite elements and the summation of heat transfer between tubes and working fluid yielded total heat transfer between them.

The set of equation (4) was considered in the study of Chua et al. (Chua et al. 2001) to find the temperature variation in a multi bed regenerative adsorption chiller. The governing equations were non-dimensionalized in their study and then solved. The thermal capacitance of heat exchanger was taken into account in the heat transfer equation. The enthalpy difference between adsorptive and adsorbent particles during

adsorption and desorption processes was considered. In order to determine heat transfer between tube and adsorber, the heat exchanger in the bed was divided into finite pieces. The mass transfer resistance in the bed was neglected in their study and condenser and adsorber were always maintained at the saturated vapor pressure.

Saha et al. (Saha et al. 2003) solved the set of equation (5) and investigated the performance of a dual mode, three stages non-regenerative, and six-bed regenerative silica gel-water chiller. The thermal capacitance of the Cu tubes and Al fins were considered in heat transfer equation. The heat transfer between saturated vapor from evaporator and adsorbent particles was included in the energy equation. The mass transfer resistance through the bed was neglected and refrigerant was assumed to reach simultaneously to all silica gel particles in the adsorber.

Cacciola et al. (Cacciola et al. 1993) performed a study on dynamic simulation of recuperative adsorption heat pump. They made the governing equations (set of equation (11)) dimensionless to show that the influences of the important parameters on the performance of the system. Restuccia et al. (Restuccia et al. 2004) solved the energy and mass transfer equations shown in set of equations (14) to determine the variation of temperature of adsorbent bed with time. The thermal capacitance of heat exchanger in the adsorber was also considered in the heat transfer equation and mass transfer resistance in the bed was neglected.

The set of equation (16) was used by Vasta et al. (Vasta et al. 2008), Freni et al. (Freni et al. 2008), and Maggio et al. (Maggio et al. 2009). The most important point of these studies is that heat of adsorption was not constant and determined as a function of adsorbate concentration. Mass transfer resistance was neglected for all of these studies.

Sakoda and Suzuki (Sakoda and Suzuki 1984) solved the set of equation (19) to determine the variation of temperature in the adsorbent bed. The thermal capacitance of the container and heat exchanger were not considered in the heat transfer equation. Heat was transferred to adsorber by thermal radiation. Heat transfer between ambient and the adsorbent bed was included in their study. Almost uniform adsorbate concentration was considered in the bed since the packed bed was small. The thermal capacitance of the adsorbate in the bed was not included in heat transfer equation.

The set of equation (20) was solved by Sakoda and Suzuki (Sakoda and Suzuki 1986) to simulate transport of heat and adsorbate in closed type adsorption cooling system utilizing solar heat. Two energy equations one for container and other for the adsorbent particles were solved. The heat transfer to the adsorbent bed was contributed

by radiation. Additionally heat transfer between adsorbent and surrounding by convection was also taken into account.

Suzuki (Suzuki 1993) solved the energy equation in set of equation of (21) to simulate adsorption cooling system for automobiles. The adsorbent bed was heated or cooled by a working fluid. Mass transfer resistance in the adsorbent bed was neglected.

### 4.1.3.2. Non Uniform Temperature – Non Uniform Pressure Models

In these models, in addition to the terms including the derivative of the dependent variables with time, terms involve the gradients of the adsorptive temperature, pressure, density, and adsorbate concentration in space are also taken into account in heat and mass transfer equations. Thus, the number of terms in the governing equations is increased. The governing equation becomes more complex and special numerical methods should be employed to solve those coupled and non linear equations. The models involve heat and mass transfer resistances in the bed provide more reliable solutions compared to the models which neglect the heat and mass transfer resistances. In these models, the permeability of the adsorbent bed should be known in order to predict adsorptive transfer through the adsorbent bed. The permeability of the adsorbent bed may be determined experimentally or mathematical relation such as Blake-Kozeny. This relation can be used to determine permeability of an adsorbent bed theoretically. A non-uniform temperature – non uniform pressure problem can be one, two or three dimensional. The increase of dimension of the problem increases number of terms in the partial differential equations of heat and mass transfer. Hence, number of nodes or volumes increases and it causes the increase of computational time. Similar to the uniform temperature – uniform pressure model, two equations which are adsorption equilibria and mass balance equations for a particle should be clearly known for solving non uniform temperature – non uniform pressure heat and mass transfer equations. A review on the studies used non uniform temperature – non uniform pressure are summarized in this section.

Literature survey shows that Leong and Liu (Leong and Liu 2004a, 2004b, 2006, 2008, Liu and Leong 2005), and Yong and Sumathy (Yong and Sumathy 2004) considered heat and mass transfer resistances in the most of their studies. The set of equations of these studies are (1) and (23), respectively. The studied adsorbent bed is a

hallow cylinder and the studied problem was unsteady two dimensional. They found the variation of adsorbent temperature, and adsorptive pressure and velocity in radial and axial directions. The Darcy equation which provides relation between pressure of adsorptive and Darcy velocity were used to obtain adsorptive velocity distribution in the radial direction. Beside the inherent permeability of the adsorbent bed, the Knudsen and molecular diffusion mechanisms in the bed were also considered in their studies.

Sun et al. (Sun et al. 1995) also considered the variation of the dependent variables with respect to time and space. The set of equation (9) was used by them. The analyzed adsorbent bed is cylindrical however they do not considered the variation of dependent variable in radial direction and they solved problem only for axial direction. The porosity of the adsorbent particle was involved in their study. They used Ergun's equation and considered the inertia effect to obtain relation between adsorptive pressure and velocity. They made the governing equations non-dimensionalized and obtained results for dimensionless variables.

Ben Amar et al. (Ben Amar et al.1996) also performed study on the cylindrical adsorbent bed and considered variations of dependent variables in radial and axial directions (set of equation (10)). They employed thermodynamic relations to write continuity and energy equations in terms of temperature. They used Darcy law to obtain velocity in radial and axial directions based on adsorptive pressure difference.

Marletta et al. (Marletta et al.2002) employed a non-uniform temperature and pressure model of heat and mass transfer in compact adsorbent beds and the related set of equation are given as (12). The adsorbent bed is cylindrical and coated type. They considered the variation of temperature and adsorbate concentration in radial and axial directions and they included micropore and macropore porosity parameters in their analysis. They used both Fick's and Darcy laws to determine velocity in terms of pressure. Ergun's equation was also used to determine velocity in terms of adsorptive pressure. Hence, in addition to permeability of adsorbent bed, the inertia effect of adsorptive flow was also taken into account. For the mass balance equation, the variation of adsorptive pressure (or adsorptive density) in radial and axial directions were considered. Similar to the energy equation, macro and micropore porosities are taken into account in the mass balance equation. They made their equation dimensionless and found the solution for the non-dimensionalized equations.

The set of equation (13) was used by Restuccia et al. (Restuccia et al. 2002). They performed a simulation study for a coated zeolite adsorbent bed. The gradient of

temperature and adsorptive density only in radial direction was taken into account. The Darcy law was used to find adsorptive velocity in radial direction.

Maggio et al. (Maggio et al. 2006) solved the heat and mass transfer equations in a double bed for an adsorption machine as shown in the set of equation (15). The adsorbent bed is cylindrical and coated type. The variation of adsorbent temperature and adsorptive density was taken into account both in radial and axial directions. The relation between velocity and pressure was provided by Ergun's equation.

Demir et al. (Demir et al. 2009) simulated temperature and concentration in a granular adsorbent bed. The set of equation (22) was used by them. The variations of temperature and adsorptive density only in radial direction were considered. They used Darcy and Fick's laws to determine adsorptive velocity from pressure.

Zhang and Wang (Zhang and Wang 1999a, 1999b) considered variations of dependent variables in three directions of the cylindrical coordinates as used in the set of equation (24). The Darcy law was used to find the adsorptive velocity in the bed.

Also similar to Zhang and Wang's studies (Zhang and Wang 1999a, 1999b), Zhang (Zhang 2000) used the same set of equations (set of equation (24)) in a three dimensional non-equilibrium model.

### 4.1.3.3. Non Uniform Temperature – Uniform Pressure

In uniform pressure models, the interparticle mass transfer resistance in the adsorbent bed is neglected and the transfer of adsorptive in the adsorbent bed is assumed rapid. A change of adsorptive pressure in any point in the adsorbent bed is instantaneously propagated and adsorptive pressure attains to equilibrium condition immediately. Therefore, the pressure of adsorptive does not vary and it is constant at anywhere of adsorbent bed during the adsorption or desorption process. In another words, the adsorptive pressure at any location in the adsorbent bed is at evaporator pressure throughout the adsorption process and similarly the whole bed is at condenser pressure during desorption process. Although, no condition for the use of uniform pressure model was reported in literature, there is no doubt that the voids between particles should be sufficiently large to permits rapid motion of adsorptive from one point to another location.

Due to low thermal conductivity of adsorbents and voids between adsorbent particles which causes discontinuities in the media of bed, the use of uniform temperature may not be proper for simulation of adsorbent bed. Therefore the changes of temperature with space should be involved in the heat transfer equation. The solution of heat transfer equation and mass balance equation for the adsorbent particle assisted by adsorption equilibria yields temperature distribution in the bed for any instant of cycle. A review on studies employed uniform pressure – non uniform temperature are presented in this section.

Chua et al. (Chua et al. 2004) and Wang and Chua (Wang and Chua 2007b) solved the heat and mass transfer equations in the set of equations (6) and (8) for a two bed silica gel/water adsorption chiller, respectively. They solved the governing equations of a cylindrical adsorbent bed which was supported by metal fins. The gradient of adsorbent temperature only in radial direction was considered. The effect of the convective transport of heat in radial direction in the heat transfer equation was neglected. The amount of adsorbed or desorbed of adsorbate in the adsorbent bed was found based on a conservation of mass relation.

Saha et al. (Saha et al. 2009) performed a study on a cylindrical adsorbent bed which was banded and assisted by fins. As shown in the set of equation (17) the convective transport of heat was neglected in their study. The heat flow was considered both in r and z direction. A mass balance equation in terms of variation of dependent variables with time was written to determine the change of adsorptive rate in the bed.

Chahbani et al. (Chahbani et al. 2002, 2004) solved the heat and mass transfer equations of an adsorption heat pump as shown in the set of equation (18). The bed is cylindrical and variation of temperature in radial direction was included into the heat transfer equation. The convective transport of heat in their equation was neglected.

Alam et al. (Alam et al. 2000) solved the heat and mass transfer equations in the set of equations (25) for a two bed silica gel/water adsorption cooling unit. The temperature varies both in x and y directions in the bed. The mass and areas of the heat transfer fluid, adsorbent bed and the inert material were taken into account in the energy equation.

Ilis et al. (Ilis et al. 2010) solved the heat and mass transfer equations in the set of equations (26) of a silica gel/water adsorbent bed. The adsorptive assumed to be flow only in radial direction. They also non-dimensionalized the governing equations and found two dimensionless parameters. The effects of these parameters on adsorption

period were analyzed. In addition to this study, the effect of fins located inside of the adsorbent bed was also studied by Ilis et al. (Ilis et al. 2011). The heat transfer equation for the bed is two dimensional. The conduction heat transfer equation for the thin fin was also written and solved with the mass transfer equation of the particle and these equations are given in set of equation (27). They non-dimensionalized the these equations and effect of four different dimensionless numbers on the adsorption period was analyzed.

### 4.1.4. Classification of Mass Balance Equation for Adsorbent Particle

In addition to the heat and mass transfer equations for adsorbent bed, mass balance equation for adsorbent particle should be solved to determine adsorbate concentration in a particle. The adsorption or desorption process occurs in the bed until the adsorbent particles reach equilibrium which means that no change of adsorbate concentration within the particle occurs. Commercial adsorbents are generally used in the form of pellets which are prepared from microporous crystals and suitable binders. The binder affects adsorption by contributing secondary porosity in the form of macroporous and this results formation of an adsorbent particle having bidisperse pore structure.

The adsorption rate is controlled by diffusion mode of mass transport in an adsorbent particle since convective flow through the pores is negligible. Different diffusion mechanisms such as macropore, surface and/or micropore diffusion are used to describe adsorptive diffusion in an adsorbent particle. Macropore diffusion may occur by several distinct mechanisms as molecular, surface and Knudsen diffusions while micropore diffusion takes place only when the micropore size is close to the size of adsorbate molecules.

Although the theoretical determination of mass transfer diffusivity for different mechanism of diffusion has been reported in literature, practically effective mass transfer diffusivity involving different mechanism of mass transfer in an adsorbent particle is used. The effective mass transfer diffusivity can be determined by obtaining experimental transient uptake sorption curves. The isothermal diffusion can be found by exposing adsorbent samples in an ambient with changeable adsorptive concentration and comparing of the obtained uptake curves with theoretical ones. The rate of

adsorbate adsorbed or desorbed depends on the initial adsorbate concentration in the adsorbent particle, temperature of adsorbent and adsorptive and adsorptive pressure as well as the structure of adsorbent particle.

The rate of heat generated or dissipated in the bed depends on the change of adsorbate concentration in the adsorbent particles. Moreover, the change of adsorbate concentration in the adsorbent particle affects the density of adsorptive surrounds the adsorbent particle. Therefore, a mass balance equation for adsorbent particle should be considered in order to determine the average adsorbate concentration in the particles at any instant of the cycle. There are three models as solid diffusion model, linear driving force model and instantaneous equilibrium model which can be used to obtain the variation of adsorbate concentration in an adsorbent particle with time. The simulation studies of Table 4.2 are classified according to the mass balance equation for an adsorbent particle in this section.

### 4.1.4.1. Instantaneous Equilibrium Model

In this model, intraparticle mass transfer is assumed to be sufficiently rapid and so concentration is almost uniform in the particle. No internal and external mass transfer resistance in the particle exists. The adsorptive and the solid particles are thermodynamically in equilibrium at any instant of the cycle. Liu and Leong (Liu and Leong 2006), Sun et al. (Sun et al. 1995), Ben Amar et al. (Ben Amar et al.1996), Cacciola et al. (Cacciola et al.1993), Marletta et al. (Marletta et al. 2002), Restuccia et al. (Restuccia et al.2002, 2004), Maggio et al. (Maggio et al. 2006, 2009), Vasta et al. (Vasta et al. 2008), Freni et al. (Freni et al. 2008), Chahbani et al. (Chahbani et al. 2002, 2004) and Yong and Sumathy (Yong and Sumathy 2004), Ilis et al. (Ilis et al. 2010) were used equilibrium model in their studies to determine the change of average adsorbate concentration with time (Chahbani et al. 2004) as shown in the set of equations (2), (9), (10), (11), (12), (13), (14), (15), (16), (18), (23), and (26) in Table 4.2.

### 4.1.4.2. Linear Driving Force Model

Linear driving force (LDF) model was used by many investigators. In the linear driving force model, the change of the average adsorbate concentration with time is proportional to difference between adsorbate concentration and equilibrium concentrations under the same temperature and pressure. In LDF model the variation of average adsorbate concentration with time is also proportional to effective diffusivity however it has inverse relation with radius of particle. The model is very simple and provides accurate results. It is a fast model and saves computational time. Leong and Liu (Leong and Liu 2004a, 2004b, 2006, 2008, Liu and Leong 2005), Chua et al. (Chua et al. 1999, 2001, 2004), Saha et al. (Saha et al. 2003), Wang and Chua (Wang and Chua 2007a, 2007b), Saha et al. (Saha et al. 2009), Chahbani et al. (Chahbani et al. 2002, 2004), Sakoda and Suzuki (Sakoda and Suzuki 1984, 1986), Suzuki (Suzuki 1993), Demir et al. (Demir et al. 2009), Zhang and Wang (Zhang and Wang 1999a, 1999b), Zhang (Zhang 2000), Alam et al. (Alam et al. 2000), and Ilis et al. (Ilis et al. 2010, 2011) were used LDF model in their studies. The model was given in the set of equations (1), (3), (4), (6), (7), (8), (17), (18), (19), (20), (21), (22), (24), (25), (26), and (27) in Table 4.2.

### 4.1.4.3. Solid Diffusion Model

Solid diffusion model provides accurate variation of adsorbate concentration in the adsorbent particle for any instant of the cycle. The integration of adsorbate concentration over the entire of the adsorbent particle yields the average adsorbate concentration with time. Although this model provides accurate results, it requires long computational time. That's why this model was not used by investigators but only Chahbani et al. (Chahbani et al. 2002, 2004) and Ilis et al. (Ilis et al. 2010) used solid diffusion model to investigate the effect of the mass balance model of adsorbent particle on the heat and mass transfer through the adsorbent bed as given in the set of the equations (18) and (26) in Table 4.2.

### 4.1.5. Adsorbent Bed Permeability and Diffusivity Models

Permeability is a measure of the ability of the adsorbent to transmit the adsorptive. For the studies in which mass transfer resistance in the adsorbent bed is neglected, there is no need to determine the permeability of the adsorbent bed since adsorptive flows rapidly. However, if the mass transfer resistance in the bed is considered, a relation is required to define velocity distribution in the adsorbent bed for any instant in the cycle. Four models were used in the studies performed on the heat and mass transfer in the adsorbent bed of adsorption heat pump as Darcy law model, Darcy and Ficks laws model, Ergun's model and Ergun's and Fick's laws model.

#### 4.1.5.1. Darcy Law

In this model, inherent permeability is constant and the adsorptive velocity is found directly from pressure distribution. The Blake-Kozeny relation is generally used to calculate inherent permeability, whose value depends on the adsorbent particle diameter and porosity as given in the set of equations (10), (13), and (24). Ben Amar et al. (Ben Amar et al. 1996), Restuccia et al. (Restuccia et al. 2002), Zhang and Wang (Zhang and Wang 1999a, Zhang and Wang 1999b) and Zhang (Zhang 2000) used Blake-Kozeny relation to calculate inherent permeability.

#### 4.1.5.2. Darcy and Fick's Law Model

In this model, Darcy law ($\vec{V} = (-K_{app}/\mu)\overrightarrow{\nabla p}$) and Fick's law ($\vec{J} = -D_v\vec{\nabla}c$) are combined to simulate adsorptive velocity in the adsorbent bed. Hence, instead of use of inherent permeability K, an additional term related to the Fick's law is added and apparent permeability is defined.

Leong and Liu (Leong and Liu 2004a, 2004b, 2006, 2008, Liu and Leong 2005), Demir et al. (Demir et al. 2009), and Ilis et al. (Ilis et al. 2010, 2011) used Blake-Kozeny equation to determine inherent permeability and additionally Knudsen and molecular diffusion flows are included to contribute diffusion of adsorptive in the adsorbent bed as given in the set of equations (1), (23), (26), and (27). Then, the

apparent permeability was found based on the combination of equivalent diffusion and inherent permeability.

### 4.1.5.3. Ergun's Model

In this model, in addition to the inherent permeability of the adsorbent bed, the inertia effect of adsorptive is also considered. Therefore, another parameter (i.e. $k_E$, inertial effect term) is defined to describe inertia effect. Sun et al. (Sun et al. 1995) used this model to find the adsorptive velocity distribution from the pressure distribution of adsorptive (the set of equation (9)). Both inherent permeability and inertia effect parameters depend on the adsorbent particle parameter and porosity.

### 4.1.5.4. Ergun's with Fick's Law Model

In this model, both Ergun's and Fick's law models are considered which means that in addition to the Darcy and diffusion flows, the inertia effect is taken into account. Martella et al. (Martella et al. 2002) and Maggio et al. (Maggio et al. 2006) considered Knudsen and self diffusion flows in the adsorbent bed as given in the set of equations (12) and (15).

## 4.1.6. Equivalent Thermal Conductivity Equations

Different approaches were used to determine the equivalent conductivity in the adsorbent bed. There is no doubt that for the models whose neglect thermal resistance in the adsorbent bed, equivalent thermal conductivity is not required. Leong and Liu (Leong and Liu 2004a, 2004b, 2006, 2008, Liu and Leong 2005), Saha et al. (Saha et al. 2009), Li Yong and Sumathy (Li Yong and Sumathy 2004), Demir et al. (Demir et al. 2009), and Ilis et al. (Ilis et al. 2011) presented an equation for equivalent thermal conductivity which includes adsorptive thermal conductivity, porosity and ratio of adsorptive to adsorbent thermal conductivity to determine equivalent thermal conductivity of the adsorbent bed. No equation was found in the study of Chua et al. (Chua et al. 2004) but the value of the thermal conductivity in the bed was presented in

a table. Most probably some studies used an equation to determine equivalent thermal conductivity of adsorbent bed. However the source of the calculated value is not mentioned in their study and a constant value was given (Wang and Chua 2007b, Sun et al. 1995, Ben Amar et al. 1996, Marletta et al. 2002, Restuccia et al. 2002, Maggio et al. 2006, Chahbani et al. 2002). Martella et al. (Marletta et al. 2002) gave a constant value for equivalent thermal conductivity in the bed based on the experimental study. In the study of Chahbani et al. (Chahbani et al. 2004) the effect of the thermal conductivity on COP and SCP and time of cycle was investigated.

### 4.1.7. Adsorption Equilibria Relationships

In order to solve the heat and mass transfer equation for adsorbent bed, the rate of the adsorption or desorption of adsorbate should be known. As it was mentioned before, three models as instantaneous equilibrium, LDF, and solid diffusion models are used to find the rate of adsorption or desorption in the adsorbent particle. In these models, the equilibrium adsorbate concentration at any temperature and pressure of the adsorptive should be well known; otherwise the solution of the set of heat and mass transfer equations is impossible. For estimation of equilibrium condition between adsorbate and adsorbent, various theoretical and empirical approaches were proposed but none of them is completely satisfactory and valid for broad range of application. Although the most common models for establishing a relation between adsorbate concentration in the particle and adsorptive pressure and temperature at equilibrium state are isotherms but isosters are also widely used to demonstrate a cycle of an adsorption heat pump.

The simplest equilibria relationship of adsorption on surface is Langmuir isotherm. The local adsorption takes place on a uniform surface without any interaction between adsorbed molecules. Other isotherm is the Freundlich type equation. This equation is an empirical equation and can be defined by a curve which is relating the concentration of an adsorptive on the surface of an adsorbent, to the concentration of the adsorptive which it is in contact. Dubinin equation also can be derived from Freundlich equation. Another typical example of the expressions is the Toth's equation. It contains three parameters. Also Clapeyron approach can be used as an isotherm. The values of the equations against temperature are the polynomial functions in this equation.

Leong and Liu (Leong and Liu 2004a, 2004b, 2006, 2008, Liu and Leong 2005) and Sun et al. (Sun et al. 1995) used Langmuir equation to describe equilibrium condition of adsorbate as function of temperature and pressure for zeolite-water pair as given in their set of equations as (1) and (9), respectively. Liu and Leong (Liu and Leong 2006) used Langmuir equation for zeolite/water pair and Freundlich equation for silica gel/water pair in their studies for adsorption equilibria (set of equation (2)). Chua et al. (Chua et al. 1999), Saha et al. (Saha et al. 2003), and Alam et al. (Alam et al. 2000) used modified Freundlich equation based on manufacturer's proprietary data to determine the equilibrium condition for silica gel/water pair as given in set of equations (3), (5) and (25), respectively. Chua et al. (Chua et al. 2001) and Wang and Chua (Wang and Chua 2007a) stated that the generated data from the empirical isotherm equation are essentially in the low coverage regime and can be simply correlated by Henry's law correlation when the vapor phase assumed to be ideal (set of equations (4), (7)). Chua et al. (Chua et al. 2004), Wang and Chua (Wang and Chua 2007a), and Saha et al. (Saha et al. 2009) used Toth's equation to describe adsorption rate at equilibrium condition which is a function of pressure and temperature as illustrated in Table 4.2 in set of equations (6), (8), and (17). Ben Amar et al. (Ben Amar et al. 1996) used Dubinin equation for equilibria of carbon/ammonia and Langmuir equation of zeolite/water pair (set of equation (10)). Chahbani et al. (Chahbani et al. 2002, 2004) used Dubinin-Astakhov equation as given in set of equation (18) for the adsorption equilibria of ammonia/carbon. Sakoda and Suzuki (Sakoda and Suzuki 1984, 1986), Demir et al. (Demir et al. 2009), Ilis et al. (Ilis et al. 2010, 2011) used Freundlich equation for adsorption equilibria of silica gel/water (set of equations (19), (20), (22), (26), and (27)). Yong and Sumathy (Yong and Sumathy 2004) used Dubinin-Radushkevich equation for equilibria for activated carbon/ammonia pair as given as set of equation (23). Cacciola et al. (Cacciola et al. 1993), Marletta et al. (Marletta et al. 2002), Maggio et al. (Maggio et al. 2006), Zhang and Wang (Zhang and Wang 1999a, 1999b), and Zhang (Zhang 2000) used Clapeyron equation for representing isoster equation for zeolite/water pair as numbered set of equations as (11), (12), (15), and (24). Restuccia et al. (Restuccia et al. 2004) also used Clapeyron equation for SWS-1L (mesoporous silica gel impregnated with $CaCl_2$)/water pair (set of equation (14)). For active carbon/methanol pair the Clapeyron equation was used by Vasta et al. (Vasta et al. 2008), Freni et al. (Freni et al. 2008) and Maggio et al. (Maggio et al. 2009) as numbered set of equation as (16).

## 4.2. Literature Survey on Adsorption in an Adsorbent Particle

As given in previous section in details, the considerable theoretical and numerical studies on heat and mass transfer in an adsorbent bed for a cycle of adsorption heat pump were reviewed. To simulate the mass transfer in an adsorbent particle, instantaneous equilibrium model, LDF model, solid diffusion model were used. Literature survey shows that most of researchers used LDF model to determine the change of adsorbate concentration in an adsorbent particle. This means that the external mass transfer resistance for adsorbent particle was neglected in many theoretical studies. Moreover, in the most of the studies, the internal and external heat transfer resistances for the adsorbent particle were not taken into account. A uniform temperature distribution in the adsorbent particle was assumed.

Discussions on the mechanism of heat and mass transfer in an adsorbent particle can be found in some books and research papers. The heat and mass transfer equations for a single adsorbent particle with negligible and/or considerable internal and external heat and mass transfer resistances for isothermal and non-isothermal cases can be found in the references (Karger and Ruthven 1992, Ruthven 1984). In the text book of Suzuki (Suzuki 1990), the analytical solutions for an isothermal and non-isothermal case with negligible and considerable effect of external mass transfer resistance are presented. In the above textbooks, Henry isotherm in which the equilibrium adsorbate concentration linearly varies with adsorptive pressure is used to obtain analytical solution.

Haul and Stremming (Haul and Stremming 1984) studied the non-isothermal sorption kinetics in the porous adsorbents. They derived a general analytical solution by taking both the thermal conductivity within the adsorbent and the heat exchange with the ambient into account. The experimental analysis for benzene in single, spherical particle of mesoporous silica gel was done for comparison. In the theoretical study, the surface of the spherical adsorbent was at equilibrium with the fluid phase and the fluid was assumed to be at constant pressure.

Sun and Meunier (Sun and Meunier 1987a) proposed a model for analysis of non-isothermal sorption in a single microporous particle. The mass diffusion and heat conduction equations were simultaneously solved analytically. It is found that Lewis and thermal Biot number plays an important role on the use of isothermal model. In another study of Sun and Meunier (Sun and Meunier 1987b), a nonisothermal bidisperse

model was proposed by taking both macro and micropore diffusion and the diffusion within the micro particle into account. In this study, the rate of intrinsic adsorption at surface was assumed so high and accordingly, the adsorption is controlled within the pores.

Abdallah et al. (Abdallah et al. 1988) studied adsorption of water on NaX zeolite pellets, both experimentally and theoretically. The results showed that the heat dissipation plays a dominant role in the adsorption kinetics after a short initial stage that controlled by both the micropore and macropore diffusion.

Montastruc et al. (Montastruc et al. 2010) studied kinetic modeling of isothermal and non-isothermal adsorption in an adsorbent pellet. They showed that when heat transfer coefficient is very high or heat capacity is very large, the adsorption is isothermal. The diffusion mechanisms of $CO_2$ on commercial zeolite 4A and CaX pellets were theoretically and experimentally compared in the study of Ahn et al. (Ahn et al. 2004). They found that the modified dimensionless parameter called as $\gamma$ which is a criterion for the relative importance of the micropore diffusion and the effective macropore diffusion in the pellet. The dominant diffusion mechanism can be determined according to the value of this parameter.

Georgiou (Georgiou 2004) presented an asymptotically exact nonlinear driving force (NLDF) model of intra-particle mass-transfer rate for nonlinear isotherm systems with macropore diffusion control. They compared their solutions with the solutions of the Fickian diffusion and adsorption models. The solutions concluded that NLDF model was highly accurate on other known driving force models. Also NLDF model could be used with different sorption isotherms such as Langmuir and Freundlich. Kupiec and Georgiou (Kupiec and Georgiou 2005) worked on a new model that was applicable to systems with nonlinear adsorption isotherm. Both intraparticle and film mass-transfer resistances were accounted in the model when the intraparticle mass-transfer rate being controlled by pore diffusion. One result of their study was that the new model was applicable to the systems with a nonlinear isotherm and account for intraparticle (pore diffusion) and film mass transfer resistances as well as film heat transfer resistances.

In order to understand the mechanism of the heat and mass transfer in an adsorbent bed of adsorption heat pump, the mechanism of the heat and mass transfer in a single particle should be clearly recognized. The effects of internal and external heat and mass transfer resistances on adsorbate transport in an adsorbent particle should be well known. The external heat and mass transfer resistances play important role on

adsorbate transfer in an adsorbent particle. The above literature survey reveals that the external heat and mass transfer resistances and the internal heat transfer resistance were neglected in the most of studies without mentioning on validity of the assumptions. Moreover, literature survey showed that number of dimensionless studies on non-isothermal adsorption in an adsorbent particle considering both external heat and mass transfer resistances is limited due to complexity of heat and mass transport. In the most of performed studies on heat and mass in a single adsorbent particle, Henry isotherm was employed. The non-linear behavior of isotherms for many adsorbent-adsorbate pairs and complexity of boundary conditions particularly for mass transfer equation are reasons that cause difficulties for performing dimensionless analysis.

Table 4.1. A brief review on the performed studies

| | | |
|---|---|---|
| Leong and Liu 2004a | **Pair:**<br>zeolite NaX/water<br>**Aim & Result of the Study**:<br>This paper presents a two dimensional heat and mass transfer model of a combined heat and mass recovery adsorption cycle. This system consists of six major components including; two adsorber, external heat and cooling systems, a condenser and an evaporator. The mass recovery phase is very short (about 50s) compared to the whole cycle time for the specified operating conditions. By using only the mass recovery cycle, the COP and SCP can be improved by about 6% and 7%, respectively compared to the basic cycle. There is a significant increase in COP (by about 47%) compared to the basic cycle, there is an accompanied reduction in SCP by about 40%.<br>**Assumptions:**<br>(1) the adsorbed phase is considered as a liquid and the adsorbate gas is assumed to be an ideal gas, (2) the adsorbent bed is composed of uniform-size particles and has isotropic properties, (3) the properties of the fluid, the metal tube and adsorbate vapor are constant, (4) there are no heat losses in the adsorption cycle, (5) the thermal resistance between the metal tube and the adsorbent bed is neglected, (6) the flow of heat exchange fluid is assumed to be fully developed laminar flow, (7) the velocity distribution is parabolic in the radial direction and remains constant in axial direction. | 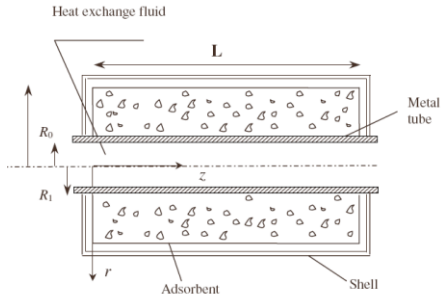 <br>Set of Equation (1) |

**(cont. on next page)**

Table 4.1 (cont.).

| | | |
|---|---|---|
| Leong and Liu 2004b | **Pair:**<br>zeolite 13X/water<br>**Aim & Result of the Study**:<br>A two-dimensional non-equilibrium numerical model describing the combined heat and mass transfer in adsorbent bed is presented. The effect of main configuration parameters such as the heat and mass transfer coefficients, thickness of the bed, diameter of the particle and porosity, on the thermal performance of the system are investigated. It is found that the performance can be strongly influenced by the adsorbent thickness and porosity of the adsorbent bed, while the variation of particle size has minimal effect on the performance.<br>**Assumptions:**<br>(1) the adsorbed phase is considered as a liquid, and the adsorbate gas is assumed to be an ideal gas, (2) the adsorbent bed is composed of uniform-size particles and has isotropic properties, (3) the properties of the fluid, the metal tube and adsorbate vapor are constant, (4) there are no heat losses in the adsorption cycle, (5) the thermal resistance between the metal tube and the adsorbent bed is neglected, (6) there are no heat losses in the adsorption cycle. | 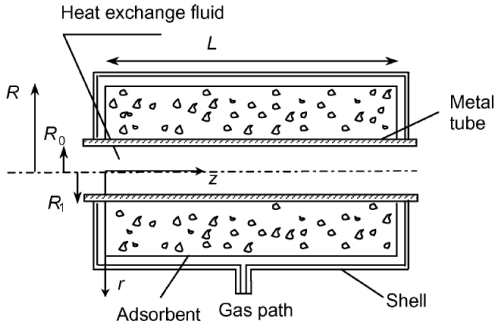 <br>Set of Equation (1) |

**(cont. on next page)**

Table 4.1 (cont.).

| | | |
|---|---|---|
| Leong and Liu 2005 | **Pair:**<br>zeolite 13X/water<br>**Aim & Result of the Study**:<br>In this study, the effect of operating conditions such as adsorption temperature ($T_a$), generation temperature ($T_g$), condensing temperature ($T_c$), evaporating temperature ($T_e$), the driven temperature of heat exchange fluid ($T_{h,in}$) and the velocity of heat exchange fluid, on system performance were investigated. The results show that $T_a$, $T_g$, $T_c$ and $T_e$ have significant effects on the system performance. The driven temperature, $T_{h,in}$ was found to have negligible effect on the coefficient of performance although the optimal cooling power increases with $T_{h,in}$.<br>**Assumptions:**<br>(1) the adsorbed phase is considered as a liquid, and the adsorbate gas is assumed to be an ideal gas, (2) the adsorbent bed is composed of uniform-size particles and has isotropic properties, (3) the properties of the fluid, the metal tube and adsorbate vapor are constant, (4) there are no heat losses in the adsorption cycle, (5) the thermal resistance between the metal tube and the adsorbent bed is neglected, (6) there are no heat losses in the adsorption cycle. | 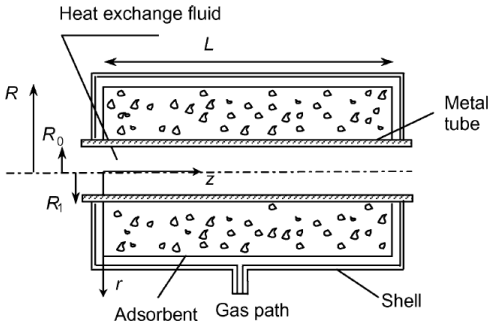 <br>Set of Equation (1) |

**(cont. on next page)**

Table 4.1 (cont.).

| | | |
|---|---|---|
| Leong and Liu 2006 | **Pair:**<br>zeolite/water<br>**Aim & Result of the Study**:<br>A numerical study on the effects of system design and operation parameters on the performance of a combined heat and mass recovery adsorption cycle is presented in this paper. The effects of bed dimensions, bed thermal conductivity, heat exchange fluid velocity, driven temperature and the degree of the heat recovery, defined in their study, on the system performance are investigated. The COP of the system increases while its SCP decreases with an increase in the degree of heat recovery. Both COP and SCP increase with an increase in the driven temperature of heat exchange fluid. Increasing the thermal conductivity has a positive effect on the system performance. For the analyzed adsorbent bed, the optimal velocity of the heat exchange fluid lies within the range of 0.1–0.5 m/s. The COP of the system increases while its SCP decreases with an increase in adsorbent bed thickness.<br>**Assumptions:**<br>(1) the adsorbed phase is considered as a liquid, and the adsorbate gas is assumed to be an ideal gas, (2) the adsorbent bed is composed of uniform-size particles, (3) the properties of the fluid, the metal tube and adsorbate vapor are constant, (4) there are no heat losses in the adsorption cycle, (5) the thermal resistance between the metal tube and the adsorbent bed is neglected, (6) the velocity distribution is assumed to be parabolic in the radial direction and remains constant in the axial direction. In addition, flow resistance arising from the water flowing in the pipeline is neglected, (7) the pressure in cond. or eva. is a constant value. | 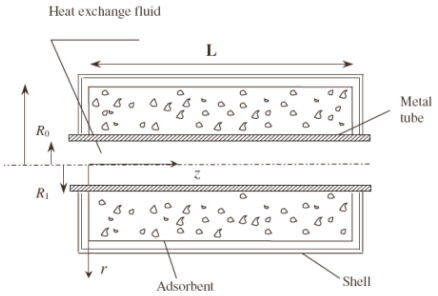 <br>Set of Equation (1) |

**(cont. on next page)**

Table 4.1 (cont.).

| | | |
|---|---|---|
| Liu and Leong 2006 | **Pair:**<br>zeolite/water ; silica gel/water<br>**Aim & Result of the Study**:<br>A novel cascading cycle based on two zeolite adsorbent beds and a silica gel adsorbent bed is presented in this paper. The following conclusions can be drawn: (1) the first and second heat recovery processes are very effective thus resulting in a higher COP, (2) there is a maximum value of COP within the range of $T_m$ investigated for a prescribed driven temperature, (3) both the COP and SCP increases with an increase in the driven temperature, (4) the COP value of 1.3 for this cascading cycle is more than two times that of an intermittent cycle (about 0.5).<br>**Assumptions:**<br>(1) the adsorption of the two working pairs is in equilibrium, (2) both the temperature and adsorbed uptake is uniform in the adsorber, (3) heat losses to the external environment are not taken into consideration, (4) the mass of water vapor is neglected, (5) the adsorber maintain its condensing or evaporating pressure, (6) water vapor mass transfer limitation is neglected. | 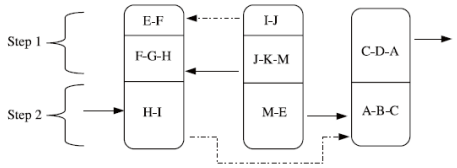 <br>(a) Schematic flow diagram<br> 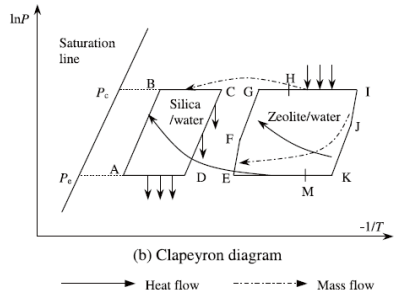 <br>(b) Clapeyron diagram<br>Set of Equation (2) |

**(cont. on next page)**

Table 4.1 (cont.).

| | | |
|---|---|---|
| Leong and Liu 2008 | **Pair:**<br>zeolite/water<br>**Aim & Result of the Study**:<br>Unlike the model used in the authors' previous studies, the condensing pressure (Pc) is not constant. The magnitude of the condensing pressure can be obtained by solving the energy balance equation of the condenser. The simulation results show that both COP and SCP increase with an increase in mass flow rate of cooling water in the condenser.<br>**Assumptions:**<br>(1) the adsorbed phase is considered as a liquid, and the adsorbate gas is assumed to be an ideal gas, (2) the adsorbent bed is composed of uniform-size particles and has isotropic properties, (3) except for the density of adsorbate vapor, the properties of the fluid, the metal tube and adsorbate vapor are constant, (4) there are no heat losses in the adsorption cycle, (5) the thermal resistance between the metal tube and the adsorbent bed is neglected, (6) there are no temperature and pressure variations in the condenser. | 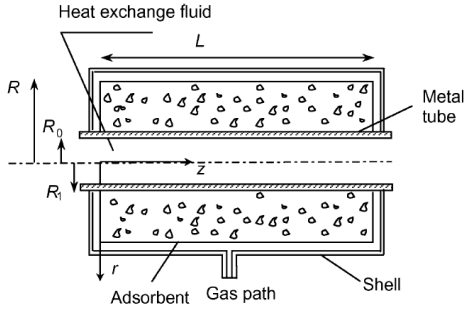 <br>Set of Equation (1) |

**(cont. on next page)**

Table 4.1 (cont.).

| | | |
|---|---|---|
| Chua et al. 1999 | **Pair:**<br>silica gel/water<br>**Aim & Result of the Study**:<br>In this study, the chiller exhibits very fast response time, and is able to hit cyclic-steady-state performance within four cycles. The resultant cyclic-steady-state condition is independent of the initial refrigerant mass distribution in the beds and evaporator. During cyclic-steady-state condition, provided the predicted refrigerant mass in the evaporator during switching phase matches with the experimental measurement, this model can be used to predict the cyclic-steady-state energetic performance.<br>**Assumptions:**<br>(1) interparticle mass transfer resistance is negligible, (2) the effect of the mass of refrigerant in the gas phase was ignored, (3) the temperature of adsorbent, adsorbate, and heat exchanging material assumed to be average temperature, (4) heat losses were ignored for the bed. | 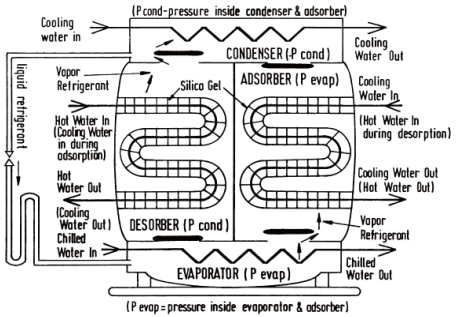 <br>Set of Equation (3) |

**(cont. on next page)**

Table 4.1 (cont.).

| | | |
|---|---|---|
| Chua et al. 2001 | **Pair:**<br>silica gel/water<br>**Aim & Result of the Study**:<br>A multi-bed regenerative adsorption chiller design was proposed. As a conclusion, The present study had demonstrated that it is possible to improve the recovery efficiency of low-grade waste heat via a multi-bed regenerative scheme. Compared with a two-bed scheme, a four-bed scheme improves the recovery efficiency by about 70%, and finally a multi-bed scheme makes it possible to start the beds one at a time.<br>**Assumptions:**<br>(1) interparticle mass transfer resistance is negligible, (2) heat losses were ignored for the bed, (3) the vapor phase is assumed to be ideal, (4) the volume of the adsorbent-adsorbed phase system changes negligibly with uptake, (5) operation assumed to be isosteric. | 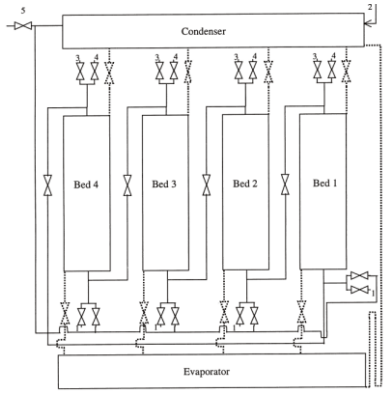 <br>Set of Equation (4) |

**(cont. on next page)**

Table 4.1 (cont.).

| | | |
|---|---|---|
| Saha et al. 2003 | **Pair:**<br>silica gel/water<br>**Aim & Result of the Study**:<br>The practical operational limits and performance characteristics with near-ambient temperature heat sources and small regenerating temperature lifts were investigated for the dual-mode, multi-stage, multi-bed regenerative adsorption chiller. In conclusion, the main advantage in the innovative dual mode cycle is its ability to utilize effectively low grade waste heat of temperature. Furthermore, with relatively higher driving source temperatures, the chiller in regenerative multi-bed mode yields higher performance.<br>**Assumptions:**<br>(1) the effect of the refrigerant mass in the gas phase was ignored, (2) the dependence of specific heat on temperature and of adsorption heat on concentration was neglected, (3) temperature was assumed to be uniform along the heat exchanger. | 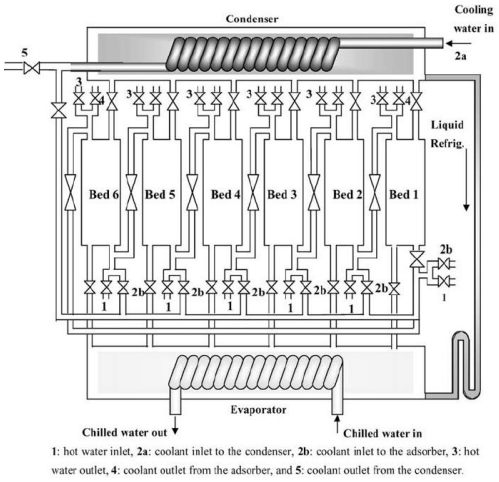 <br>Set of Equation (5) |

**(cont. on next page)**

Table 4.1 (cont.).

| | | |
|---|---|---|
| Chua et al. 2004 | **Pair:**<br>silica gel/water<br>**Aim & Result of the Study**:<br>This article presents a transient distributed-parameter model which simulates the performance of a two-bed adsorption chiller. The flow scheme was studied in this article is effectively a thermally regenerative scheme that recovers the energy of the hot adsorber and its associated piping. Found that, the shorter the distance of the silica gel from the heat transfer tube inlet, the faster is its adsorbed mass variation. Also, the switching phase plays an important role on the chiller's performance and may be indispensable. If the cycle time was taken 850 s as an example, the lumped-parameter model will under-predict the cooling capacity by 14%.<br>**Assumptions:**<br>(1) the adsorbed phase was a liquid, (2) the gaseous adsorbate was an ideal gas, (3) the condenser and the evaporator were ideal and possessed an infinite heat transfer coefficient, (4) the adsorption bed is composed of uniform size particles and the bed porosity is a constant. (5) the specific heat and the density of dry adsorbent are constant, (6) the physical properties of metal tube and fin are constant, (7) no heat losses from the adsorption/desorption bed are considered. | 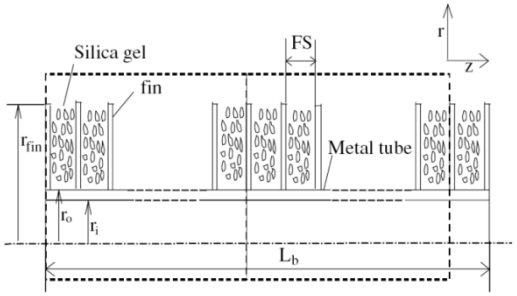 <br>Set of Equation (6) |

**(cont. on next page)**

Table 4.1 (cont.).

| | | |
|---|---|---|
| Wang and Chua 2007a | **Pair:**<br>silica gel/water<br>**Aim & Result of the Study**:<br>In this study, a water-circulation heat recovery scheme was investigated by the lump-parameter model. The prediction results from this model were compared with both the experimental data and the predictions from an experimentally verified distributed-parameter model. The difference in the performance predictions from the lump-parameter model and distributed-parameter model is about 10%.<br>**Assumptions:**<br>(1) interparticle mass transfer resistance is negligible, (2) heat losses were ignored for the bed. | 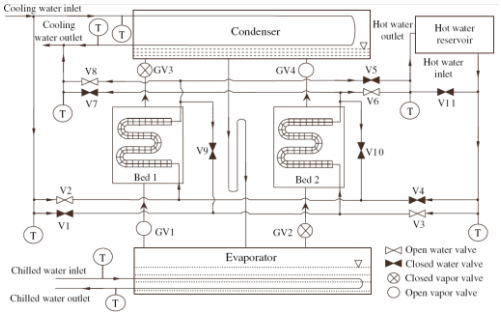 <br>Set of Equation (7) |

**(cont. on next page)**

Table 4.1 (cont.).

| | | |
|---|---|---|
| Wang and Chua 2007b | **Pair:**<br>silica gel/water<br>**Aim & Result of the Study**:<br>In this study, the efficiency of two distinct heat-recovery schemes as applied to the two-bed silica gel–water adsorption chiller was investigated. Passive heat-recovery scheme and water-circulation heat-recovery scheme, both improved the system COP without affecting cycle average cooling capacity. The passive heat-recovery scheme can be easily adopted in the commercial chiller with a simple modification of system control logic and may be able to replace the related company's' water-circulation heat recovery scheme at the design stage.<br>**Assumptions:**<br>The assumptions that are considered are not given clearly in this study: (1) only the density change inside the porous volume is omitted. | 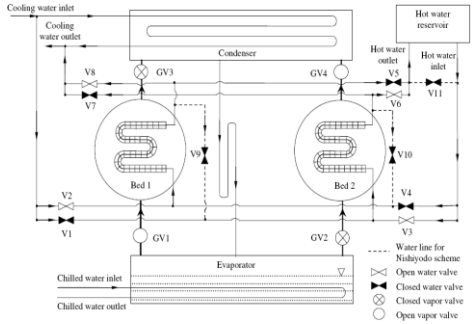 <br>Set of Equation (8) |

**(cont. on next page)**

Table 4.1 (cont.).

| | | |
|---|---|---|
| Sun et al. 1995 | **Pair:**<br>zeolite 13X/water ; zeolite 13X/ammonia<br>**Aim & Result of the Study**:<br>In this study, a theoretical analysis of coupled heat and mass transfers in an adsorbent bed heated by an external fluid was represented. Ammonia, whose operating pressures are much higher, resistances to mass transfer had found to be negligible even with very small values of the permeability. It was found that ammonia constitutes a good adsorbate for mass transfer considerations. The pressure assumption was considered as acceptable when ammonia was used as an adsorbate.<br>**Assumptions:**<br>(1) the system was considered to be one-dimensional. All radial effects were neglected, (2) the adsorbent bed is composed of uniform-size particles and the bed porosity is constant, (3) the solid phase is locally in equilibrium with the gaseous phase, (4) the gaseous phase is assumed to be an ideal gas, (5) the flow velocity in the adsorbent bed was determined by the Ergun equation, (6) the mass dispersion of the gaseous phase was neglected, (7) the properties of the fluid and the tube are constant, (8) the specific heats, adsorption heat and viscosity were considered as constant. | 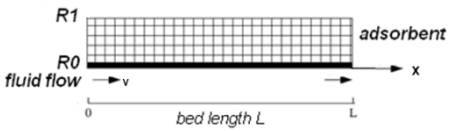 <br>Set of Equation (9) |

**(cont. on next page)**

Table 4.1 (cont.).

| | | |
|---|---|---|
| Ben Amar et al. 1996 | **Pair:**<br>zeolite NaX/water ; Activated carbon AX21-ammonia<br>**Aim & Result of the Study**:<br>In this study, the effects of operating parameters, such as cycle time, permeability and heating temperature on the cooling coefficient of performance and the power of cold production were discussed. The numerical results had shown that under ideal conditions, the performance of a temperature wave regenerative heat pump is considerably better than that of a basic uniform temperature heat pump.<br>**Assumptions:**<br>(1) the adsorbate gas is assumed to be an ideal gas, (2) the adsorbent bed is composed of uniform-size particles and the bed porosity is constant, (3) local equilibrium is maintained both for heat and mass transfer between the solid, adsorbed and gas phases, (4) the properties of the fluid and the tube are constant, (5) the specific heats, adsorption heat and viscosity were considered as constant, (5) the thermal energy induced by gas compression was neglected, (6) the thermal fluid and the tube were considered as unidimensional systems, (7) no heat losses in the circulating fluid loop were considered. | 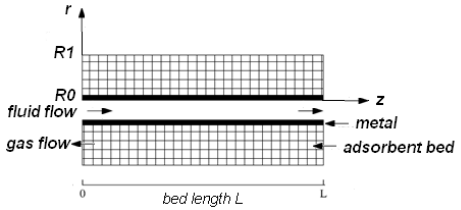 <br>Set of Equation (10) |

**(cont. on next page)**

Table 4.1 (cont.).

| | | |
|---|---|---|
| Cacciola et al. 1993 | **Pair:**<br>zeolite 4A/water<br>**Aim & Result of the Study**:<br>The non-dimensional form of the governing equations leads to a simple numerical method, which showed rapid convergence and yielded accurate results. The program represents an efficient tool for designing a two-reactor adsorption heat pump and for optimizing the component sizes in order to obtain the best system performance.<br>**Assumptions:**<br>(1) uniform temperature in each component, (2) adsorption equilibrium holds, (3) requires low heat-transfer rates or high adsorbent transfer properties, high thermal conductivity and mass diffusivity. | Set of Equation (11) |

**(cont. on next page)**

Table 4.1 (cont.).

| | | |
|---|---|---|
| Marletta et al. 2002 | **Pair:**<br>zeolite/water<br>**Aim & Result of the Study**:<br>This paper discusses a new dynamic two-dimensional model for the simulation of innovative consolidated-type adsorbent beds to use in adsorption energy systems. The aim of this paper is to propose a mathematical model, able to describe in a proper way the heat and mass transfer occurring in this new arrangement of the consolidated bed for the zeolite/water pair. As a result, It was possible to demonstrate that the proposed consolidated bed performs better than the competing arrangements. Indeed the proposed type allows a thermal cycle shorter in duration, and more efficient in terms of specific power than other bed configurations.<br>**Assumptions:**<br>(1) all the adsorbent particles have the same properties (including shape and size); they are uniformly distributed throughout the adsorbent, and in local thermal equilibrium with the adsorbate and the surrounding vapor phase ($T_s = T_v$), (2) the oil and the metal thermal gradients in radial direction are neglected; the corresponding equations become one-dimensional, (3) the gaseous phase behaves as an ideal gas, (4) the properties of the metal and the gaseous phase are assumed constant, (5) the properties of the thermal vector fluid, as well as those of the adsorbent, are considered temperature dependent, (6) all the thermal losses are negligible, (7) assumes non-uniform temperature and non-uniform pressure within the adsorbent bed, (8) The adsorption enthalpy is not constant. | 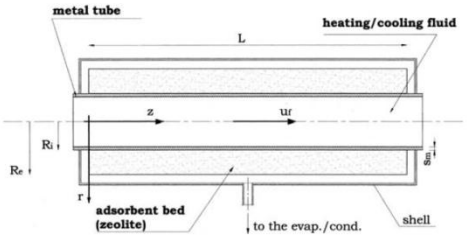 <br>Set of Equation (12) |

**(cont. on next page)**

Table 4.1 (cont.).

| | | |
|---|---|---|
| Restucci a et al. 2002 | **Pair:**<br>zeolite/water<br>**Aim & Result of the Study**:<br>The model calculates the pressure, temperature and water uptake distribution in the bed as a function of time. Results showed that the specific power was obtained with the new bed configuration is the best (600 W/kg), and about twenty times higher than that of the bed in grains. The results showed that the parameters that have the strongest influence on the specific power are the thickness of the bed and the permeability. On the contrary, for low values of the wall heat transfer coefficient the influence of the mass transfer resistance decreases. Furthermore, even if the thermal conductivity is low ($\lambda_{eq}$ = 0.2 W/mK), with the new bed proposed it is possible to obtain a very high specific cooling power, providing that the bed thickness is low and the permeability is higher than K = 5 x $10^{-12}$ $m^2$.<br>**Assumptions:**<br>(1) the cylindrical absorbers' pressure and temperature are non-uniform, (2) the axial gradients were neglected, (3) the temperature of the heating/cooling fluid was considered constant. | 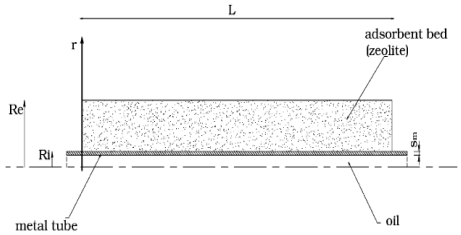 <br>Set of Equation (13) |

**(cont. on next page)**

Table 4.1 (cont.).

| | | |
|---|---|---|
| Restucci a et al. 2004 | **Pair:**<br>SWS-1L (mesoporous silicagel impregnated with $CaCl_2$/water<br>**Aim & Result of the Study**:<br>The aim of this work is to evaluate experimentally the performance of the SWS-1L for solid sorption air conditioning and to compare the experimental results with a dynamic simulation.<br>The use of SWS-1L material allows to reach the cooling COP up to 0.6 at the low desorption temperature of 90–95$^{o}$C. Despite the simplicity of the mathematical description of the cycle, good agreement between the model and the experimental measurements were found.<br>**Assumptions:**<br>(1) the mass transfer resistance has been neglected in the bed, (2) each component (adsorbent bed, condenser, and evaporator) was considered to be homogeneous, (3) the properties of the metal, the water vapor and the thermal vector fluids were assumed to be constant, (4) the thermal losses from the components were neglected. | 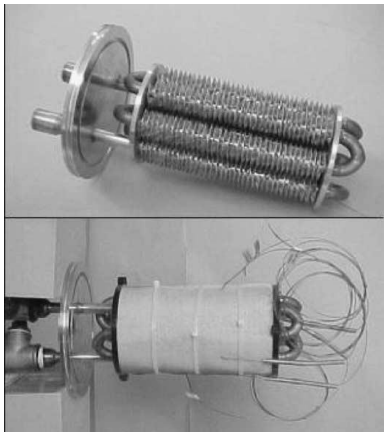 <br>Set of Equation (14) |

**(cont. on next page)**

Table 4.1 (cont.).

| | | |
|---|---|---|
| Maggio et al. 2006 | **Pair:**<br>zeolite 4A/water<br>**Aim & Result of the Study**:<br>A two-dimensional simulation model for adsorption machines, based on two thermally efficient consolidated beds with internal heat recovery, was presented in this paper. The results: The vapor permeability of the consolidated adsorbent beds must be higher than $5x10^{-12}$ $m^2$, in order to avoid a strong reduction of the performance of the system, the permeability and the wall heat transfer coefficient play an important role in defining the limiting process for the cycle evolution, the influence of the adsorbent bed thickness indicated the fundamental role of this parameter.<br>**Assumptions:**<br>(1) The two adsorbers have identical thermo-physical, structural and geometrical characteristics, (2) the losses during the heat recovery between the two reactors are neglected, (3) The cond.and eva. are ideal, they have a constant temperature during the isobaric phases, (4) all the adsorbent particles have the same properties; they are uniformly distributed throughout the adsorbent, and in local thermal equilibrium with the adsorbate and the surrounding gaseous, (5) thermal gradients in radial direction are neglected both for heat transfer fluid and metal, (6) The vapor velocity in the adsorbent is determined by Ergun's equation, (7) the gaseous phase is an ideal gas, (8) the properties of the metal and the gaseous phase are assumed to be constant, (9) the properties of the heat transfer fluid, adsorbent, are considered as temperature dependent, (10) thermal losses are neglected. | 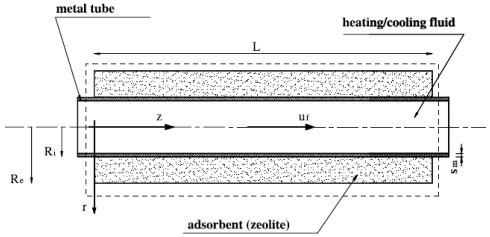 <br>Set of Equation (15) |

**(cont. on next page)**

Table 4.1 (cont.).

| | | |
|---|---|---|
| Vasta et al. 2008 | **Pair:**<br>active carbon/methanol<br>**Aim & Result of the Study**:<br>This paper discusses the dynamic model for simulation of an adsorptive ice-maker. In conclusion, the simulation results demonstrated that the design of the proposed ice-maker allows to provide a daily ice production of 5 kg, or slightly lower, for the most part of the year (from April to October).<br>**Assumptions:**<br>(1) All components are spatially isothermal and isobaric, (2) the resistances to the methanol diffusion through the adsorbent bed and through the components were neglected, (3) the adsorbent particles have uniform size, shape and distribution, (4) in the adsorbent bed, the solid phase is in local thermal equilibrium with the gaseous phase, (5) the gaseous phase behaves as an ideal gas, (6) all specific heats of the components and the heat transfer coefficients were assumed to be constant, (6) the thermal losses along the pipes were neglected. | 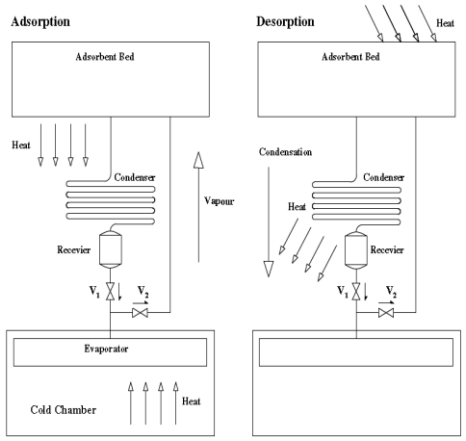 <br>Set of Equation (16) |

**(cont. on next page)**

Table 4.1 (cont.).

| | | |
|---|---|---|
| Freni et al. 2008 | **Pair:**<br>active carbon/methanol<br>**Aim & Result of the Study**:<br>The aim of this work is to utilize the dynamic model in order to: (a) carry out a parametric analysis for assessment of the key parameters of the system, (b) optimize the design of the solar-powered ice-maker. In results, FFD method was showed that the highest values of the average daily ice production and COPs, obtained for the 20-day period were considered (May 3–22, 2005), were respectively, 5.48 kg and 0.051. The FFD was made possible to assess that the two most influencing parameters on the system performance are the transmittance/absorptivity coefficient of the solar collector, and the heat transfer coefficient between the solar collector and the adsorbent material. Finally, by the Steepest Ascent Method (SAM) the optimal values of the key parameters had been identified.<br>**Assumptions:**<br>(1) All components are spatially isothermal and isobaric. Thus, the temperature of the adsorbent material and those of the system components are considered only time-variable, (2) the resistances to methanol diffusion, through the icemaker components, are neglected, (3) the adsorbent particles have uniform size, shape and distribution. (4) the solid phase is in local thermal equilibrium with the gaseous phase, (5) the gaseous phase behaves as an ideal gas, (6) the thermal losses along the pipes are neglected. | 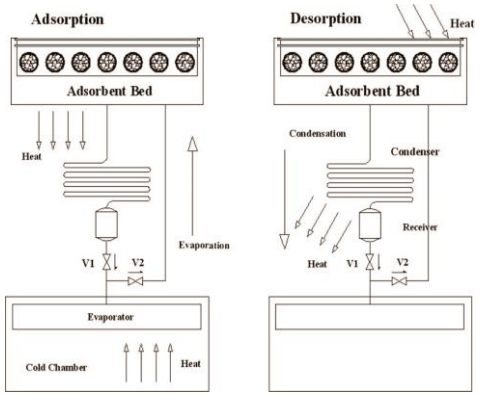 <br>Set of Equation (16) |

**(cont. on next page)**

Table 4.1 (cont.).

| | | |
|---|---|---|
| Maggio et al. 2009 | **Pair:**<br>silica gel with lithium chloride in pores/methanol<br>**Aim & Result of the Study**:<br>The aim of this work is to evaluate the performance of a solar-powered adsorptive ice-maker using the novel composite "lithium chloride in mesoporous silica gel. The results show that the utilization of innovative adsorbent materials with high sorption ability can improve the performance of adsorptive cooling systems. The novel composite sorbent ''lithium chloride in silica gel pores" makes it possible to design highly efficient solar-powered adsorptive ice-makers.<br>**Assumptions:**<br>All assumption in this study is referred. | 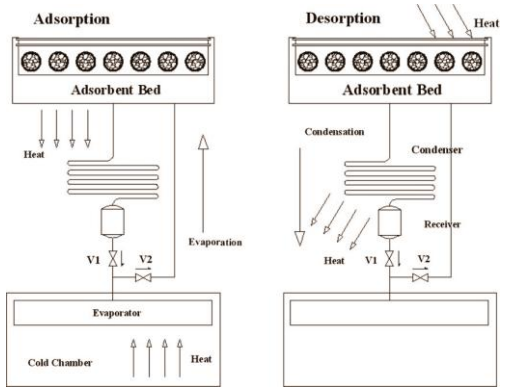 <br>Set of Equation (16) |

**(cont. on next page)**

Table 4.1 (cont.).

| | | |
|---|---|---|
| Saha et al. 2009 | **Pair:**<br>$CaCl_2$ confined to KSK silica gel/water<br>**Aim & Result of the Study**:<br>The aim of this study was to analyze the performances of SWS-1L in more optimized configuration similar to that used in commercial adsorption chillers. This article presents both the steady state and dynamic behaviors of SWS-1L in a two bed solid sorption cooling system using a transient distributed model. The results showed that the performances of adsorption chiller incorporating SWS-1L as adsorbents, in terms of cooling capacity, coefficient of performance and peak chilled water temperature, are better than those of the commercial available silica gel + water based adsorption chiller.<br>**Assumptions:**<br>(1) the heat transfer in the fin is assumed to be one-dimensional in the radial direction, (2) no mass transfers occur between the hot bed and the condenser or the cold bed and the evaporator, (3) heat flow in the adsorbent bed is considered both in r and z direction | 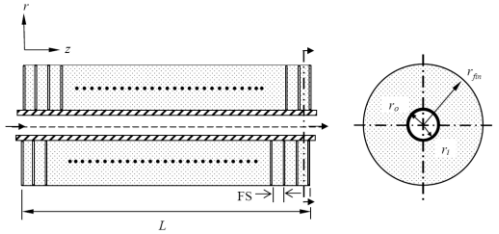 <br>Set of Equation (17) |

**(cont. on next page)**

Table 4.1 (cont.).

| | | |
|---|---|---|
| Chahbani et al. 2002 | **Pair:**<br>Carbon/$NH_3$<br>**Aim & Result of the Study**:<br>The paper addresses the effect of intraparticle mass transfer limitations. This paper investigates the effect of the choice of the intraparticle mass transfer kinetics model on the simulation of the performance of an adsorption cooling machine as characterized by the cooling coefficient of the performance (COP) and the specific cooling power (SCP). Mass transfer enhancement could lead to poorer heat transfer properties of the bed. Resorting to the equilibrium of the LDF models, instead of the solid diffusion model, can lead to erroneous simulation results. The equilibrium model overestimates the system performance whereas the LDF model tends to under evaluate it when used outside its domain of validity.<br>**Assumptions:**<br>(1) the pressure is uniform in the bed, (2) the solid and gaseous phases are in thermal equilibrium, (3) the gas behavior is ideal, (4) the thermal resistance of the tube is negligible, (5) the heat losses are negligible, (6) the bed is composed of particles of uniform size and the bed porosity is constant. | 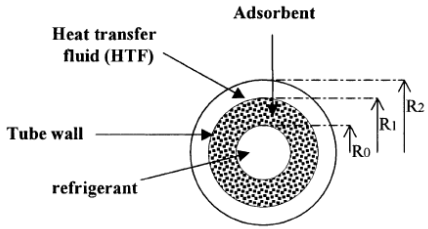 <br>Set of Equation (18) |

**(cont. on next page)**

Table 4.1 (cont.).

| | | |
|---|---|---|
| Chahbani et al. 2004 | **Pair:**<br>carbon/ammonia<br>**Aim & Result of the Study**:<br>This paper presents a study of the impacts of mass and heat transfers on the performance of thermal wave regenerative adsorption heat pumps. Emphasis was put on the effect of intraparticle mass transfer limitations. Simulation results clearly show that, in the case where the refrigerant is slow diffusing, the COP and the SCP are markedly reduced due to the fact that the quantity of refrigerant cycled is diminished. The shorter the cycle, the better the economic viability of the system.<br>**Assumptions:**<br>(1) the pressure is uniform in the bed, (2) the solid and gaseous phases are in thermal equilibrium, (3) the gas behavior is ideal, (4) the thermal resistance of the tube is negligible, (5) the heat losses are negligible, (6) the bed is composed of particles of uniform size and the bed porosity is constant. | 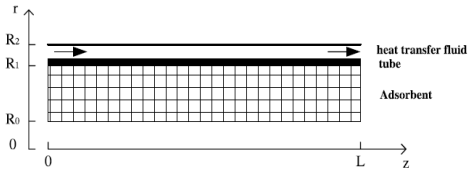 <br>Set of Equation (18) |

**(cont. on next page)**

Table 4.1 (cont.).

| | | |
|---|---|---|
| Sakoda and Suzuki 1986 | **Pair:**<br>silica gel/water<br>**Aim & Result of the Study**:<br>In this paper, experimental results were obtained with a model and interpreted by a theoretical model. The results shows that the solar COP of the model was controlled by the efficiency given as the ratio of heat used for the regeneration of adsorbents to the solar heat input and also that the efficiency was governed by the heat transfer area between the container of adsorbents and the inner adsorbent particles.<br>**Assumptions:**<br>(1) the mass in gas phase was neglected, (2) Both temperature in the beds and the amount adsorbed, $T_s$ and q, are uniform in the beds. | 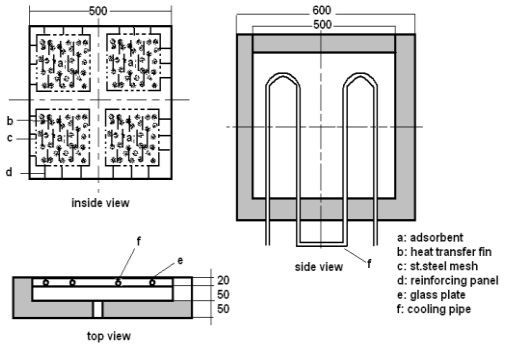 <br>Set of Equation (20) |
| Suzuki 1993 | **Pair:**<br>zeolite NaX/water<br>**Aim & Result of the Study**:<br>In this paper, the technological limits were associated with the application of adsorption system to passenger car air conditioning. Application of adsorption cooling system to automobiles could be possible if appropriate design of adsorbent beds makes improved heat transfer characteristics. For cooling system of 2,300 W, adsorbent amount of about 2 kg could be enough.<br>**Assumptions:**<br>(1) the mass in gas phase was neglected, (2) both temperature in the beds and the amount adsorbed are uniform in the beds, (3) the regeneration temperature is constant. | 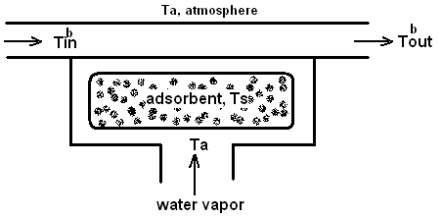 <br>Set of Equation (21) |

**(cont. on next page)**

Table 4.1 (cont.).

| | | |
|---|---|---|
| Demir et. al. 2009 | **Pair:**<br>silica gel/water<br>**Aim & Result of the Study**:<br>In this paper, the attentions are focused on the mechanism of heat and mass transfer in the adsorbent bed of adsorption heat pump. The influences of porosity on the variations of temperature, pressure, adsorbate concentration and adsorptive density profiles in a thick granular silica gel bed are studied. The increase of porosity reduces the thermal conductivity of the bed, heat transfer rate in the bed and the period of the adsorption process. Thermal resistance controls heat and mass transfer through the studied bed and the increase of thermal conductivity of the bed without decreasing mass diffusivity improves heat and mass transfer rates in the bed.<br>**Assumptions:**<br>(1) the adsorbent bed consists of uniform size adsorbent<br>granules, thus the bed porosity is assumed constant, (2) the adsorptive and adsorbent granules are in thermodynamic equilibrium, (3) the adsorptive behaves as an ideal gas, (4) thermal resistance within the adsorbent granule is neglected, (5) the temperature of an adsorbent granule equals to its surrounded adsorptive, (6) thermal properties of the adsorbent and adsorptive are constant, (7) heat transfer rate at $R=R_i$ is negligible. | 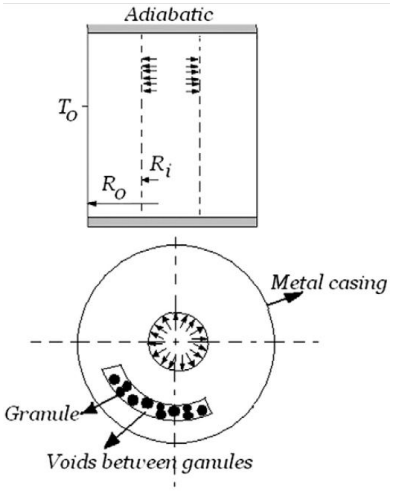 <br>Set of Equation (22) |

**(cont. on next page)**

Table 4.1 (cont.).

| | | |
|---|---|---|
| Li Yong and Sumathy 2004 | **Pair:**<br>monolith activated carbon/ammonia and activated carbon/methanol<br>**Aim & Result of the Study**:<br>the purpose of the present study is to analyze the influence of mass transfer on the temperature field as well as on sorption kinetics in adsorbent bed and to identify the factors that influence the mass transfer process through order of magnitude analysis, which could suggest a proper adsorber design. The results showed that there is a possibility to design a fast adsorption cycle with low mass transfer resistance, by either increasing the permeability of the adsorbent or reducing the thickness of the adsorbent bed.<br>**Assumptions:**<br>(1) the temperature of heat transfer fluid and all physical properties are assumed to be constant, (2) the adsorptive behaves as an ideal gas, (3) the initial temperature and pressure distribution is supposed to be uniform. | 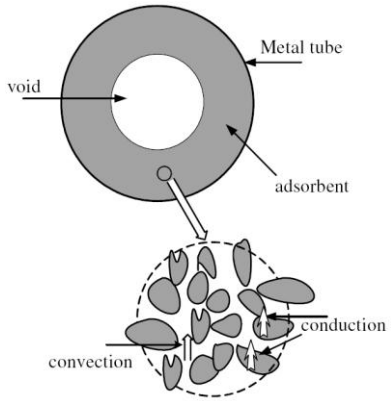 <br>Set of Equation (23) |

**(cont. on next page)**

Table 4.1 (cont.).

| | | |
|---|---|---|
| Zhang and Wang 1999a | **Pair:**<br>zeolite 13X/water vapor<br>**Aim & Result of the Study**:<br>the aim of the present study is to analyze the performance of a waste heat adsorption cooling system associated with the coupled heat and mass transfer mechanisms in the adsorbent numerically. The results showed that the system performance can be strongly influenced by the adsorber configurations such as the fin numbers, the adsorbent thickness, and the heat transfer coefficients.<br>**Assumptions:**<br>(1) the adsorbed phase is considered liquid, and the gaseous adsorbate is assumed as ideal gas, (2) the specific heat and the density of dry adsorbent is constant, (3) the adsorbent bed is composed of uniform-size particles and the bed porosity is constant, (4) the heat transfers in the heating/cooling fluids and in the metal tube are one-dimensional, and those in the fins are two-dimensional, (5) the temperature and the pressure in the space between the adsorbent and the outer tube are uniform, (6) the condenser and the evaporator are ideal. | 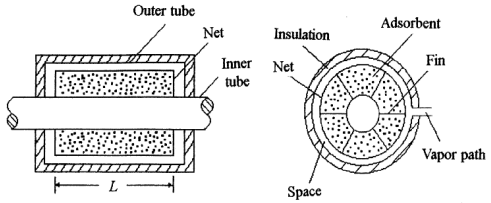 <br>Set of Equation (24) |

**(cont. on next page)**

Table 4.1 (cont.).

| | | |
|---|---|---|
| Zhang and Wang 1999b | **Pair:**<br>zeolite 13X/water vapor<br>**Aim & Result of the Study**:<br>the aim of the present study is to analyze numerically and experimentally of the coupled heat and mass transfer mechanisms in the adsorbent of a waste-heat adsorption cooling system. It has been found that for the isosteric phase, the heat pipe effect plays an important role in heat and mass transfer; on the other hand. The model can be used to optimize adsorption cooling cycles.<br>**Assumptions:**<br>(1) the adsorbed phase is considered liquid, and the gaseous adsorbate is assumed as ideal gas, (2) the specific heat and the density of dry adsorbent is constant, (3) the adsorbent bed is composed of uniform-size particles and the bed porosity is constant, (4) the heat transfers in the heating/cooling fluids and in the metal tube are one-dimensional, and those in the fins are two-dimensional, (5) the temperature and the pressure in the space between the adsorbent and the outer tube are uniform, (6) the condenser and the evaporator are ideal. | 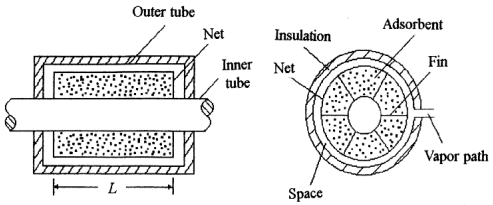 <br>Set of Equation (24) |

**(cont. on next page)**

Table 4.1 (cont.).

| | | |
|---|---|---|
| Zhang 2000 | **Pair:**<br>zeolite 13X/water vapor<br>**Aim & Result of the Study**:<br>the aim of the study is to simulate and compare with the experimental results of the performance of an intermittent adsorption cooling system driven by heat. The numeric results showed that the proposed model predicted by the dynamic response of the adsorption system well, compared with the experimental data.<br>**Assumptions:**<br>(1) the adsorbed phase is considered liquid, and the gaseous adsorbate is assumed as ideal gas, (2) the specific heat and the density of dry adsorbent is constant, (3) the adsorbent bed is composed of uniform-size particles and the bed porosity is constant, (4) the heat transfers in the heating/cooling fluids and in the metal tube are one-dimensional, and those in the fins are two-dimensional, (5) the temperature and the pressure in the space between the adsorbent and the outer tube are uniform, (6) the condenser and the evaporator are ideal. | 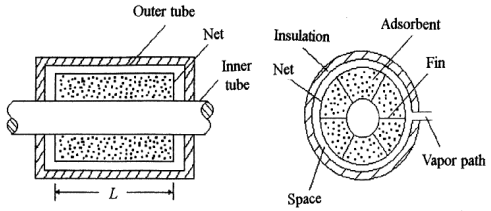 <br>Set of Equation (24) |

**(cont. on next page)**

Table 4.1 (cont.).

| | | |
|---|---|---|
| Alam et. al. 2000 | **Pair:**<br>silica gel/water<br>**Aim & Result of the Study**:<br>the aim of the study is to analyze the effect of heat exchanger design parameters on the system performance of a two-bed silica gel-water adsorption cooling unit. The results showed that the switching frequency *w*, bed NTU, Ar and bed Bi have strong effects on the system performance.<br>**Assumptions:**<br>(1) the bed has sufficiently unoccupied space and vapor pressure throughout the bed is uniform but varies with time, (2) the particles are small enough to be regarded as saturated, (3) constant thermophysical properties, (4) refrigerant vapor behaves as an ideal<br>gas, (5) adsorbed phase behaves as liquid. | 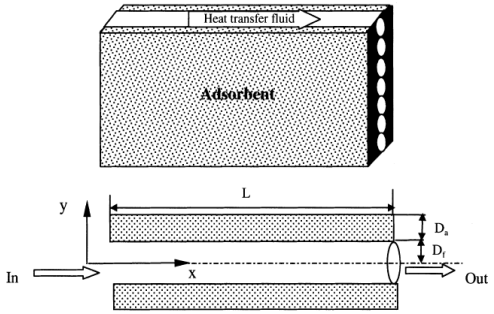 <br>Set of Equation (25) |

**(cont. on next page)**

Table 4.1 (cont.).

| | | |
|---|---|---|
| Ilis et. al. 2010 | **Pair:**<br>silica gel/water<br>**Aim & Result of the Study**:<br>the aim of present study is to investigate the heat and mass transfer in a granular adsorbent bed for an isobaric adsorption process numerically. Under the performed assumptions, nine independent variables which effect heat and mass transfer in the bed are combined only in two independent variables as G and Γ. The effects of G and Γ parameters on local and average temperature and adsorbate concentration in the adsorbent bed for the adsorption process are studied. Moreover, a study on comparison of three models used to simulate mass transfer through an adsorbent granule as instantaneous equilibrium, linear driving force (LDF), and solid diffusion models is performed and the obtained results based on G and Γ parameters are discussed.<br>**Assumptions:**<br>(1) pressure distribution in the bed is uniform and adsorptive can be transferred rapidly between particles, (2) the adsorbent bed consists of uniform size adsorbent particles and the bed porosity is constant, (3) the adsorptive and adsorbent granules are in thermodynamic equilibrium, (4) thermal resistance within the adsorbent granule is neglected, (5) thermal properties of the adsorbent, adsorptive and adsorbate are constant, (6) heat transfer rate at $R = R_i$ is negligible, and (7) wall thermal resistance between bed surface and granule is not considered the adsorbent bed consists of uniform size adsorbent particle. | 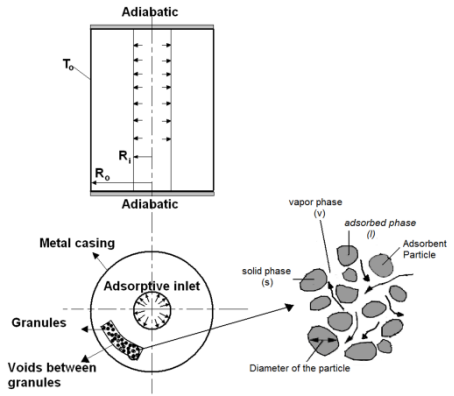 <br>Set of Equation (26) |

**(cont. on next page)**

Table 4.1 (cont.).

| | | |
|---|---|---|
| Ilis et. al. 2011 | **Pair:**<br>silica gel/water<br>**Aim & Result of the Study**:<br>the aim of present study is to perform a dimensionless analysis on heat and mass transfer through an annular adsorbent bed assisted with radial fins during an isobaric adsorption process. The non-dimensionalization of the governing equations yields two dimensionless parameters as Ku and Γ. The effect of these dimensionless parameters on heat and mass transfer in an adsorbent bed is analyzed.<br>**Assumptions:**<br>(1) the adsorbent bed consists of uniform size adsorbent particle, (2) adsorptive and adsorbent particles are in thermodynamic equilibrium, (3) the internal and external thermal resistances are neglected for the adsorbent particle, (4) thermal properties of the adsorbent, adsorptive and adsorbate are constant, and (5) the wall thermal resistance between the bed surface and adsorbent particle is not considered. | 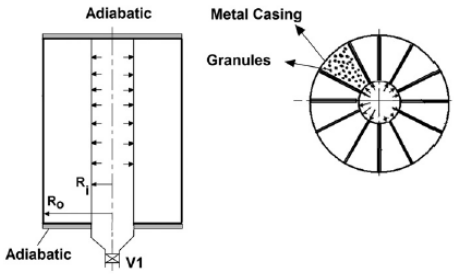 <br>Set of Equation (27) |

Table 4.2. The set of equations, the considered equations which was used in the studies

| | |
|---|---|
| (1) | **Adsorption Equilibria:**<br>$$q_{eq} = \frac{q_{s,1} b_1 P}{1 + b_1 P} + \frac{q_{s,2} b_2 P}{1 + b_2 P} + \frac{q_{s,3} b_3 P}{1 + b_3 P}$$<br>$$q_{s,k} = a_{0,k} + \frac{a_{1,k}}{T_s} + \frac{a_{1,k}}{T_s^2} + \frac{a_{1,k}}{T_s^3};\ q_{s,3} = 0.267 - q_{s,1} - q_{s,2}\ ;\ b_k = b_{0,k} \exp\left(-\frac{E_k}{T_s}\right)$$<br>**Mass Transfer Equation for Particle:**<br>$$\frac{\partial \bar{q}}{\partial t} = \frac{15 D_e}{r_p^2}(q_{eq} - \bar{q})$$<br>**Mass Transfer Equation for Bed and Velocity:**<br>$$\frac{\partial \varepsilon \rho_g}{\partial t} + \nabla.\left(\rho_g \boldsymbol{u}\right) + \rho_s \frac{\partial \bar{q}}{\partial t} = 0 \qquad \boldsymbol{u} = -\frac{K_{ap}}{\mu}\nabla P$$<br>**Heat Transfer Equation for Adsorbent Bed:**<br>$$\left(\rho_s C_{ps} + \rho_s q C_{pa} + \varepsilon \rho_g C_{pg}\right)\frac{\partial T_s}{\partial t} + \frac{\partial\left(\rho_g C_{pg} u T_s\right)}{\partial z} + \frac{1}{r}\frac{\partial}{\partial r}\left(r \rho_g C_{pg} v T_s\right) = \frac{\partial}{\partial z}\left(\lambda_{eq}\frac{\partial T_s}{\partial z}\right) + \frac{1}{r}\frac{\partial}{\partial r}\left(r \lambda_{eq}\frac{\partial T_s}{\partial r}\right) + \rho_s \Delta H \frac{\partial \bar{q}}{\partial t}$$<br>**Equivalent Conductivity Equation:**<br>$$\lambda_{eq}/\lambda_f = \frac{0.01(1-\varepsilon)^{1/2}}{\Lambda} + \frac{0.99(1-\varepsilon)^{1/2}}{1 + (\Lambda - 1)0.01(1-\varepsilon)^{1/2}} + \frac{1 - (1-\varepsilon)^{1/2}}{1 + 0.01(\Lambda - 1)(1-\varepsilon)^{1/2}}$$<br>**Diffusivity Equations:**<br>$$D_e = D_0 \exp\left(-\frac{E_D}{RT_s}\right) \qquad D_g = \frac{1}{\frac{1}{D_m} + \frac{1}{D_k}} \qquad D_m = 0.02628 \frac{\sqrt{T^3/M}}{P\sigma^2\Omega} \qquad D_k = \frac{200 r_p}{3}\left(\frac{8RT}{\pi M}\right)^{1/2} = 9 r_p \left(\frac{T}{M}\right)^{1/2}$$<br>**Permeability Equations:**<br>$$K = \frac{\varepsilon_a^3 a^2}{150\ (1-\varepsilon_a)^2} \qquad K_{ap} = K + \frac{\varepsilon_a \mu}{\tau P} D_g$$<br>***Important parameters:*** $q_{eq}$: equilibrium amount adsorbed (kg kg$^{-1}$), u: adsorptive velocity (ms$^{-1}$), $T_s$: adsorbent temperature (K), P: pressure (Pa). |

**(cont. on next page)**

Table 4.2 (cont.).

| | |
|---|---|
| (2) | **Adsorption Equilibria:**<br>$$q_{eq} = \frac{q_{s,1} b_1 P}{1 + b_1 P} + \frac{q_{s,2} b_2 P}{1 + b_2 P} + \frac{q_{s,3} b_3 P}{1 + b_3 P}$$<br>$$q_{s,k} = a_{0,k} + \frac{a_{1,k}}{T_s} + \frac{a_{1,k}}{T_s^2} + \frac{a_{1,k}}{T_s^3};\ q_{s,3} = 0.267 - q_{s,1} - q_{s,2};\ b_k = b_{0,k} \exp\left(-\frac{E_k}{T_s}\right);\ q = k\left(P/P_s\right)^{1/n}$$<br>$$lnP_s = 25.1948 - 5098.26/T$$<br>**Mass Transfer Equation for Particle:**<br>Adsorptive and adsorbent are thermodynamically in equilibrium<br>**Mass Transfer Equation for Bed:**<br>No mass transfer resistance<br>**Heat Transfer Equation for Adsorbent Bed:**<br>$$\sum m_i C_{pi} \frac{\partial T_{s1}}{\partial t} = m_s \Delta H \frac{\partial q}{\partial t}$$<br>$$\sum m_i C_{pi} \frac{\partial T_{s2}}{\partial t} = m_s \Delta H \frac{\partial q}{\partial t} + m_s \frac{\partial q}{\partial t} C_{pg} (T_{s1} - T_{s2})$$<br>**Equivalent Conductivity Equation:**<br>Not required<br>**Diffusivity Equations:**<br>Not required<br>**Permeability Equations:**<br>Not required<br>***Important parameters:***<br>q: adsorbed concentration (kg kg$^{-1}$), $T_s$: adsorbent temperature (K), P: pressure (Pa). |

**(cont. on next page)**

Table 4.2 (cont.).

| | |
|---|---|
| (3) | **Adsorption Equilibria:**<br>$$q^* = A(T_{sg})\left[\frac{P_{sat}(T_{ref})}{P_{sat}(T_{sg})}\right]^{B(T_{sg})}$$<br>$$A(T_{sg}) = A_0 + A_1T_{sg} + A_2T_{sg}^2 + A_3T_{sg}^3; B(T_{sg}) = B_0 + B_1T_{sg} + B_2T_{sg}^2 + B_3T_{sg}^3$$<br>**Mass Transfer Equation for Particle:**<br>$$\frac{\partial q}{\partial t} = \frac{15D_{so}\exp(-E_a/RT)}{R_p^2}(q^* - q)$$<br>**Mass Transfer Equation for Bed:**<br>No mass transfer resistance<br>**Heat Transfer Equation for Adsorbent Bed:**<br>$$\left(M_{sg}c_{p,sg} + M_{Hex}c_{p,Hex}\right)\frac{\partial T_{bed,i}}{\partial t} + M_{sg}q_{bed,i}\frac{\partial h_{ads}}{\partial t}$$<br>$$= M_{sg}\frac{\partial q_{bed,i}}{\partial t}\left[\delta\{h_g(T_{evap}) - h_g(P_{evap} - T_{bed,i}) + \Delta H_{ads}\} + (1-\delta)\Delta H_{ads}\right] - U_{cooling}\frac{A_{bed}}{N}\sum_{k=1}^{N}(T_{bed,i} - T_k)$$<br>**Equivalent Conductivity Equation:** Not required<br>**Diffusivity Equations:**<br>Not required for adsorbent bed<br>**Permeability Equations:**<br>Not required<br>***Important parameters:*** q: mean adsorbed concentration (kg kg$^{-1}$), q$^*$: equilibrium amount adsorbed (kg kg$^{-1}$),T: temperature ($^o$C), P: pressure (Pa), $h_{ads}$: partial enthalpy of adsorbate in adsorbent-adsorbate system (J kg$^{-1}$). |

**(cont. on next page)**

Table 4.2 (cont.).

| | |
|---|---|
| (4) | **Adsorption Equilibria:**<br>$$q^* = K_o \exp\left(\frac{18\Delta H_{ads}}{RT}\right) P^*$$<br>**Mass Transfer Equation for Particle:**<br>$$\partial q/\partial \tau = \frac{15 t_{cycle} D_{so} \exp(-E_a/RT)}{R_p^2}\left[q^*(P,T) - q\right]$$<br>**Mass Transfer Equation for Bed:**<br>No mass transfer resistance<br>**Heat Transfer Equation for Adsorbent Bed:**<br>$$\left(1 + \alpha_{Hex} + q_{bed,i} c_{ads}\right)\frac{d\Theta_{bed,i}}{d\tau} =$$<br>$$\frac{dq_{bed,i}}{d\tau}\left[\delta_{bed,i}\left[\bar{h}_g\left(T_{evap}\right) - \bar{h}_{ads}\left(P^*, T_{bed,i}, q_{bed,i}\right)\right] - (1-\delta_{bed,i})\left[\bar{h}_g\left(P_{evap}, T_{bed,i}\right) - \bar{h}_{ads}\left(P^*, T_{bed,i}, q_{bed,i}\right)\right]\right] - NTU_{cooling}\omega c_{cooling}^{in}\sum_{k=1}^{N}\left(\Theta_{bed,i} - \Theta_k\right)$$<br>$$\left(1 + \alpha_{Hex} + q_{bed,j} c_{ads}\right)\frac{d\Theta_{bed,j}}{d\tau} =$$<br>$$\frac{dq_{bed,j}}{d\tau}\left[\theta_{bed,j}\left[\bar{h}_g\left(P_{cond}, T_{bed,j}\right) - \bar{h}_{ads}\left(P^*, T_{bed,j}, q_{bed,j}\right)\right] - (1 -$$<br>$$\theta bed,i)hgTcond - hadsP*,Tbed,j,qbed,j - NTUheatingdM heatingdt\omega cheatingink=1N\Theta bed,j - \Theta k$$<br>**Equivalent Conductivity Equation:** Not required<br>**Diffusivity Equations:**<br>Not required for adsorbent bed<br>**Permeability Equations:** Not required<br>***Important parameters:*** q: mean adsorbed concentration (kg kg$^{-1}$), q$^*$: equilibrium amount adsorbed (kg kg$^{-1}$), P: pressure (Pa), h: specific enthalpy (kJ kg$^{-1}$), M: mass (kg). |

**(cont. on next page)**

Table 4.2 (cont.).

| | |
|---|---|
| (5) | **Adsorption Equilibria:**<br>$$q^* = A(T_s)\left[\frac{P_s(T_w)}{P_s(T_s)}\right]^{B(T_s)}$$<br>$$A(T_s) = A_0 + A_1T_s + A_2T_s^2 + A_3T_s^3$$<br>$$B(T_s) = B_0 + B_1T_s + B_2T_s^2 + B_3T_s^3$$<br>**Mass Transfer Equation for Particle:**<br>$$\frac{\partial q}{\partial t} = \frac{15D_s}{R_p^2}(q^* - q)$$<br>**Mass Transfer Equation for Bed:**<br>No mass transfer resistance<br>**Heat Transfer Equation for Adsorbent Bed:**<br>$$\frac{d}{dt}\{W_s(C_{ps} + C_{pw}q) + (C_{pCu}W_{kHex} + C_{pAl}W_{fHex})\}T_{ad} = Q_{st}W_s\frac{dq}{dt} + m_{water}C_{pwater}(T_{water1N} - T_{waterout}) - \delta W_sC_{pv}(T_{ad} - T_{eva})\frac{dq}{dt}$$<br>**Equivalent Conductivity Equation:**<br>Not required<br>**Diffusivity Equations:**<br>$$D_s = D_{so}exp\left(\frac{E_a}{RT}\right)$$<br>**Permeability Equations:**<br>Not required<br>***Important parameters:***<br>q: mean adsorbed concent. (kg kg$^{-1}$), q$^*$: equilibrium amount adsorbed (kg kg$^{-1}$),T: temperature ($^o$C), W: mass (kg), $Q_{st}$: adsorption heat (J kg$^{-1}$). |

**(cont. on next page)**

Table 4.2 (cont.).

| | |
|---|---|
| (6) | **Adsorption Equilibria:**<br>$$q^* = \frac{K_o \exp\left\{\frac{\Delta H_{ads}}{RT}\right\} P}{[1 + \{K_o/q_\infty exp\Delta H_{ads}/(RT)P\}^t]^{\frac{1}{t}}}$$<br>**Mass Transfer Equation for Particle:**<br>$$\frac{\partial q}{\partial t} = \frac{15 D_o \exp\left(-E_a/RT_s\right)}{R_p^2}(q^* - q)$$<br>**Mass Transfer Equation for Bed:**<br>$$\int_V \left[\varepsilon_t \frac{\partial \rho_v}{\partial t} + (1-\varepsilon_t)\rho_s \frac{\partial q}{\partial t}\right] = \dot{m}_{\bar{c},v}^{e}$$<br>$$\varepsilon_t = \varepsilon_b + (1-\varepsilon_b)\varepsilon_p$$<br>**Heat Transfer Equation for Adsorbent Bed:**<br>$$(1-\varepsilon_t)\left[\rho_s C_{ps}\frac{\partial T_s}{\partial t} + \rho_s\left(h_g - \Delta H_{ads}\right)\frac{\partial q}{\partial t} + \rho_s q C_{pg}\frac{\partial T_s}{\partial t}\right] + \varepsilon_t \frac{\partial(\rho_v u_v)}{\partial t} = \frac{\partial\left(k_s \frac{\partial T_s}{\partial r} r\right)}{\partial r} + \frac{h_{fin,s}}{FS}\left(T_{fin,1} - T_s\right) - \frac{h_{fin,s}}{FS}\left(T_s - T_{fin,r}\right)$$<br>**Equivalent Conductivity Equation:** A constant value is given<br>**Diffusivity Equations:**<br>Not required for adsorbent bed<br>**Permeability Equations:**<br>Not required<br>***Important parameters:***<br>q: mean adsorbed concentration (kg kg$^{-1}$), q$^*$: equilibrium amount adsorbed (kg kg$^{-1}$),h: heat transfer coefficient (W m$^{-2}$K$^{-1}$), FS: fin space (m). |

**(cont. on next page)**

Table 4.2 (cont.).

| | |
|---|---|
| (7) | **Adsorption Equilibria:**<br>$$q^* = K_o \exp\left(\frac{18\Delta H_{ads}}{RT}\right) P^*$$<br>**Mass Transfer Equation for Particle:**<br>$$\frac{\partial q}{\partial t} = \frac{15 D_{so} \exp\left(-E_a/RT_s\right)}{R_p^2}(q^* - q)$$<br>**Mass Transfer Equation for Bed:**<br>No mass transfer resistance<br>**Heat Transfer Equation for Adsorbent Bed:**<br>$$\left(M_{sg}c_{v,sg} + M_{Hex}c_{v,Hex} + M_{sg}q_{bed,i}c_{vg}\right)\frac{\partial T_{bed,i}}{\partial t}$$<br>$$= M_{sg}\frac{\partial q_{bed,i}}{\partial t}\left[\delta\left\{h_g\left(T_{evap}\right) - h_g\left(P_{evap} - T_{bed,i}\right) + \Delta H_{ads}\right\} + (1-\delta)\Delta H_{ads}\right] - U_{cooling}\frac{A_{bed}}{N}\sum_{k=1}^{N}\left(T_{bed,i} - T_k\right)$$<br>**Equivalent Conductivity Equation:** Not required<br>**Diffusivity Equations:**<br>Not required for adsorbent bed<br>**Permeability Equations:**<br>Not required<br>***Important parameters:***<br>q: mean adsorbed concentration (kg kg$^{-1}$), q$^*$: equilibrium amount adsorbed (kg kg$^{-1}$),T: temperature ($^o$C), P: pressure (Pa), M: mass (kg), U: heat transfer coefficient (W m$^{-2}$K$^{-1}$). |

**(cont. on next page)**

Table 4.2 (cont.).

| | |
|---|---|
| (8) | **Adsorption Equilibria:**<br>$$q^* = \frac{K_o \exp\left\{\frac{\Delta H_{ads}}{RT}\right\} P}{[1 + \{K_o/q_\infty exp\Delta H_{ads}/(RT)P\}^t]^{\frac{1}{t}}}$$<br>**Mass Transfer Equation for Particle:**<br>$$\frac{\partial q}{\partial t} = \frac{15 D_o \exp\left(-E_a/RT_s\right)}{R_p^2}(q^* - q)$$<br>**Mass Transfer Equation for Bed:**<br>$$\int_V \left[\varepsilon_t \frac{\partial \rho_v}{\partial t} + (1-\varepsilon_t)\rho_s \frac{\partial q}{\partial t}\right] = \dot{m}_{\bar{e},v}$$<br>$$\varepsilon_t = \varepsilon_b + (1-\varepsilon_b)\varepsilon_p$$<br>**Heat Transfer Equation for Adsorbent Bed:**<br>$$\frac{(1-\varepsilon_t)\partial\left[\rho_s C_{ps} T_s + \rho_s(h_v - \Delta H_{ads})q + \rho_s q C_{pg} T_s\right] + \varepsilon_t(\rho_v u_v)}{\partial t} = \frac{\partial\left(k_s \frac{\partial T_s}{\partial r} r\right)}{r\partial r} + \frac{\bar{h}_{fin,s}}{FS}\left(T_{fin,1} - T_s\right) - \frac{\bar{h}_{fin,s}}{FS}\left(T_s - T_{fin,r}\right)$$<br>**Equivalent Conductivity Equation:** A constant value is given (referred)<br>**Diffusivity Equations:**<br>Not required for adsorbent bed<br>**Permeability Equations:**<br>Not required<br>***Important parameters:***<br>q: mean adsorbed concentration (kg kg$^{-1}$), q$^*$: equilibrium amount adsorbed (kg kg$^{-1}$),T: temperature ($^o$C), P: pressure (Pa), $\bar{h}$: heat transfer coefficient (W m$^{-2}$K$^{-1}$), h: enthalpy (J kg$^{-1}$), FS: fin spacing (m), k: thermal conductivity (W m$^{-1}$K$^{-1}$). |

**(cont. on next page)**

Table 4.2 (cont.).

| | |
|---|---|
| (9) | **Adsorption Equilibria:**<br>$$q_{eq} = \frac{q_{s,1} b_1 P}{1 + b_1 P} + \frac{q_{s,2} b_2 P}{1 + b_2 P} + \frac{q_{s,3} b_3 P}{1 + b_3 P}$$<br>$$q_{s,k} = a_{0,k} + \frac{a_{1,k}}{T_s} + \frac{a_{1,k}}{T_s^2} + \frac{a_{1,k}}{T_s^3};\ q_{s,3} = 0.267 - q_{s,1} - q_{s,2};\ b_k = b_{0,k} \exp\left(-\frac{E_i}{T_s}\right)$$<br>**Mass Transfer Equation for Particle:**<br>Adsorptive and adsorbent are in thermodynamically in equilibrium<br>**Mass Transfer Equation for Bed and Velocity:**<br>$$[\varepsilon_b + (1 - \varepsilon_b)\varepsilon_b]\frac{\partial \rho}{\partial t} + \frac{\partial (u\rho)}{\partial x} = -(1 - \varepsilon_b)(1 - \varepsilon_b)\frac{\partial q}{\partial t} \qquad u = -\frac{2k_D \mu^{-1} {\partial \mathrm{P}}/{\partial \mathrm{x}}}{1 + \sqrt{1 + 4\rho k_D k_E \mu^{-2} \left|{\partial \mathrm{P}}/{\partial \mathrm{x}}\right|}}$$<br>**Heat Transfer Equation for Adsorbent Bed:**<br>$$\frac{\partial (C_\Sigma T)}{\partial t} + \frac{\partial \left(u\rho C_{\mathrm{g}} T\right)}{\partial x} - \frac{\partial}{\partial x}\left(\lambda \frac{\partial T}{\partial x}\right) = (1 - \epsilon_{\mathrm{b}})(1 - \epsilon_{\mathrm{b}})|\Delta \mathrm{H}| \frac{\partial \mathrm{q}}{\partial \mathrm{t}} + \frac{\mathrm{h_{ms}} \mathrm{A_{ms}}}{\mathrm{V_s}} (\mathrm{T_m} - T)$$<br>$$C_\Sigma = [\epsilon_b + (1 - \epsilon_b)\epsilon_b]\rho C_g + (1 - \epsilon_b)(1 - \epsilon_b)(\rho_s C_s + q C_a)$$<br>**Equivalent Conductivity Equation:** A constant value is given<br>**Diffusivity Equations:**<br>Not required<br>**Permeability Equations:**<br>$$k_D = \frac{\varepsilon_b^3 {d_p}^2}{150\,(1 - \varepsilon_b)^2} \qquad k_E = \frac{1.75 d_p}{150(1 - \varepsilon_b)}$$<br>***Important parameters:***<br>q: mean adsorbed concent. (kg kg$^{-1}$), T: temp. (K), P: press. (Pa), u: adsorptive vel. (ms$^{-1}$), h: heat trnf coef. (W m$^{-2}$K$^{-1}$), λ: cond. (W m$^{-1}$K$^{-1}$). |

**(cont. on next page)**

Table 4.2 (cont.).

| | |
|---|---|
| (10) | **Adsorption Equilibria:**<br>$$q_{eq} = \frac{q_{s,1} b_1 P}{1 + b_1 P} + \frac{q_{s,2} b_2 P}{1 + b_2 P} + \frac{q_{s,3} b_3 P}{1 + b_3 P}$$<br>$$q_{s,k} = a_{0,k} + \frac{a_{1,k}}{T_s} + \frac{a_{1,k}}{T_s^2} + \frac{a_{1,k}}{T_s^3}; q_{s,3} = 0.267 - q_{s,1} - q_{s,2}; b_k = b_{0,k} \exp\left(-\frac{E_i}{T_s}\right)$$<br>$$q = 0.549\ exp\left[-1.617 * 10^{-6}\left(T\ ln\frac{P_s}{P}\right)^2\right]$$<br>**Mass Transfer Equation for Particle:**<br>Adsorptive and adsorbent are in thermodynamically in equilibrium<br>**Mass Transfer Equation for Bed and Velocity:**<br>$$\varepsilon_t \frac{\partial \rho_g}{\partial t} + \nabla.\left(\rho_g u\right) + \rho_b \frac{\partial \bar{q}}{\partial t} = 0 \qquad u = -\frac{K}{\mu}\nabla P$$<br>**Heat Transfer Equation for Adsorbent Bed:**<br>$$\rho C_p \frac{\partial T_s}{\partial t} + \rho_g C_{pg} u \nabla T_s = \nabla(\lambda_s \nabla T_s) + \rho_b \Delta H \frac{\partial q}{\partial t}$$<br>**Equivalent Conductivity Equation:** A constant value is given<br>**Diffusivity Equations:**<br>Not required<br>**Permeability Equations:**<br>$$K = \frac{\varepsilon_a^3 d^2}{150\ (1-\varepsilon_a)^2}$$<br>***Important parameters:***<br>$\bar{q}$: mean adsorbed concentration (kg kg$^{-1}$), T: temperature (K), P: pressure (Pa), u: adsorptive velocity (ms$^{-1}$), λ: thermal conductivity (W m$^{-1}$K$^{-1}$). |

**(cont. on next page)**

Table 4.2 (cont.).

| | |
|---|---|
| (11) | **Adsorption Equilibria:**<br>$$\ln(p_{sk}) = a(w_k) + \frac{b(w_k)}{T_{zk}}$$<br>$$A(w) = a_0 + a_1 w + a_2 w^2 + a_3 w^3$$<br>$$B(w) = b_0 + b_1 w + b_2 w^2 + b_3 w^3$$<br>**Mass Transfer Equation for Particle:**<br>Adsorptive and adsorbent are thermodynamically in equilibrium<br>**Mass Transfer Equation for Bed:**<br>No mass transfer resistance<br>**Heat Transfer Equation for Adsorbent Bed:**<br>$$M_{zi}\left[B_i\left(\frac{\partial T_{h,b}}{\partial t} + \Delta H_i\left(\frac{\partial W_i}{\partial t}\right)\right)\right] = E_i m_{hb} C_{ph}\left(T_{h,b} - T_{zi}\right)$$<br>**Equivalent Conductivity Equation:**<br>Not required<br>**Diffusivity Equations:**<br>Not required<br>**Permeability Equations:**<br>Not required<br>***Important parameters:***<br>W: uptake, T: temperature, M: mass. |

**(cont. on next page)**

Table 4.2 (cont.).

| | |
|---|---|
| (12) | **Adsorption Equilibria:**<br>$$\ln(p) = a(w) + \frac{b(w)}{T}$$<br>**Mass Transfer Equation for Particle:**<br>Adsorptive and adsorbent are thermodynamically in equilibrium<br>**Mass Transfer Equation for Bed and Velocity:**<br>$$\left\{[\varepsilon_{ma} + (1-\varepsilon_{ma})\varepsilon_{mi}]\frac{1}{RT_s} + (1-\varepsilon_{ma})(1-\varepsilon_{mi})\left.\frac{\partial q_a}{\partial p}\right|_{T_s}\right\}\frac{\partial p}{\partial t} - \left\{[\varepsilon_{ma} + (1-\varepsilon_{ma})\varepsilon_{mi}]\frac{p}{RT_s{}^2} - (1-\varepsilon_{ma})(1-\varepsilon_{mi})\left.\frac{\partial q_a}{\partial T_s}\right|_{p}\right\} \times \frac{\partial T_s}{\partial t} + \frac{1}{r}\frac{\partial}{\partial r}\left(r\frac{v_{or}p}{RT_s}\right) + \frac{\partial}{\partial z}\left(\frac{v_{oz}p}{RT_s}\right) =$$<br>$$0; \qquad v_o + \frac{\rho_v}{\mu_v}k_E v_o|v_o| = -\frac{k_{D_{eq}}}{\mu_v}\nabla \mathrm{p}$$<br>**Heat Transfer Equation for Adsorbent Bed:**<br>$$\left\{[\varepsilon_{ma} + (1-\varepsilon_{ma})\varepsilon_{mi}]\frac{C_{pv}}{R} - (1-\varepsilon_{ma})(1-\varepsilon_{mi}) \times \left[|\Delta H| - \left(c_{peq} + (\rho_s + q_a)\left.\frac{\partial c_{peq}}{\partial q_a}\right|_{T_s}\right)T_s\right]\left.\frac{\partial q_a}{\partial p}\right|_{T_s}\right\}\frac{\partial p}{\partial t} + (1-\varepsilon_{ma})(1-\varepsilon_{mi})\left\{(\rho_s + q_a)\left(c_{peq} +\right.\right.$$<br>$$Ts\partial cpeq\partial Tsqa - \Delta H - cpeq + \rho s + qa\partial cpeq\partial qaTsTs\partial qa\partial Tsp\partial Ts\partial t + 1r\partial\partial rrcpvR + 1pvor + \partial\partial zcpvR + 1pvoz = \lambda eq1r\partial\partial rr\partial Ts\partial r + \partial 2Ts\partial z2$$<br>**Equivalent Conductivity Equation:** A constant value is given<br>**Diffusivity Equations:**<br>$$D_v = \left(\frac{1}{D^*} + \frac{1}{D_K}\right)^{-1}\frac{\varepsilon_{ma}}{\eta_T};\ D^* = 0.02628\frac{\sqrt{T^3/MM_v}}{p\sigma^2\Omega_D};\ D_K = 48.5 d_{pore}\sqrt{\frac{T}{MM_v}}$$<br>**Permeability Equations:** $k_D = \frac{\varepsilon_{ma}^3 D_p^2}{150-(1-\varepsilon_{ma})^2};\ k_E = \frac{1.75 D_p}{150-(1-\varepsilon_{ma})}$ $\quad k_{D_{eq}} = k_D + \frac{D_v \mu_v}{p}$ |

**(cont. on next page)**

Table 4.2 (cont.).

| | |
|---|---|
| (13) | **Adsorption Equilibria:**<br>Not referred<br>**Mass Transfer Equation for Particle:**<br>Adsorptive and adsorbent are thermodynamically in equilibrium<br>**Mass Transfer Equation for Bed and Velocity:**<br>$\varepsilon_t \frac{\partial \rho_v}{\partial t} + \frac{1}{r}\frac{\partial (\mathrm{r}\rho_\mathrm{v}\mathrm{v_o})}{\partial \mathrm{r}} + (1-\varepsilon_t)\rho\frac{\partial w}{\partial t} = 0 \qquad v_o = -\frac{K}{\mu_v}\frac{\partial \mathrm{P}}{\partial \mathrm{r}}$<br>**Heat Transfer Equation for Adsorbent Bed:**<br>$(1-\varepsilon_t)\frac{\partial}{\partial t}\left[\rho(1+w)C_{peq}T_s\right] + \frac{1}{r}\frac{\partial}{\partial r}\left(r\rho_v C_{pv} T_s v_o\right) + \varepsilon_t \frac{\partial\left(\rho_v C_{pv} u T_s\right)}{\partial t} = \lambda_{eq}\frac{\partial}{\partial r}\left(r\frac{\partial T_s}{\partial r}\right) + (1-\varepsilon_t)\rho|\Delta H|\frac{\partial w}{\partial t}$<br>**Equivalent Conductivity Equation:**<br>Constant values are given<br>**Diffusivity Equations:**<br>Not required<br>**Permeability Equations:**<br>$K = \frac{\varepsilon_a^3 d^2}{150\,(1-\varepsilon_a)^2}$ (referred)<br>***Important parameters:***<br>w: mean adsorbed concentration (kg kg$^{-1}$), T: temperature (K), p: pressure (Pa), $v_o$: adsorptive velocity (ms$^{-1}$), λ: thermal conductivity (W m$^{-1}$K$^{-1}$). |

**(cont. on next page)**

Table 4.2 (cont.).

| | |
|---|---|
| (14) | **Adsorption Equilibria:**<br>$$\ln(p) = A(w) + \frac{B(w)}{T}$$<br>**Mass Transfer Equation for Particle:**<br>Adsorptive and adsorbent are thermodynamically in equilibrium<br>**Mass Transfer Equation for Bed:**<br>No mass transfer resistance<br>**Heat Transfer Equation for Adsorbent Bed:**<br>$$\left[m_s(1+w)C_{peq} + m_{ex}C_{pex}\right]\frac{dT_s}{dt} = \left[\dot{m}_f C_{pf}\varepsilon(T_{f-bed} - T_s)\right]_{bed}$$<br>$$\left[\dot{m}_f C_{pf}\varepsilon(T_{f-bed} - T_s)\right]_{bed} = \left[\dot{m}_f C_{pf}(T_{in} - T_{out})\right]_{bed}$$<br>$$\left[m_s(1+w)C_{peq} + m_{ex}C_{pex}\right]\frac{dT_s}{dt} - m_s\frac{dw}{dt}\Delta H = \left[\dot{m}_f C_{pf}\varepsilon(T_{f-bed} - T_s)\right]_{bed}$$<br>$$\left[\dot{m}_f C_{pf}\varepsilon(T_{f-bed} - T_s)\right]_{bed} = \left[\dot{m}_f C_{pf}(T_{in} - T_{out})\right]_{bed}$$<br>**Equivalent Conductivity Equation:** Not required<br>**Diffusivity Equations:**<br>Not required<br>**Permeability Equations:**<br>Not required<br>***Important parameters:***<br>w: mean adsorbed concentration (kg kg$^{-1}$), T: temperature ($^{o}$C), P: pressure (Pa), $\dot{m}$: mass flow rate (kg s$^{-1}$), m: mass (kg). |

**(cont. on next page)**

Table 4.2 (cont.).

| | |
|---|---|
| (15) | **Adsorption Equilibria:**<br>$$\ln(p) = A(w) + \frac{B(w)}{T}$$<br>**Mass Transfer Equation for Particle:**<br>Adsorptive and adsorbent are thermodynamically in equilibrium<br>**Mass Transfer Equation for Bed and Velocity:**<br>$$\varepsilon_t \frac{\partial \rho_g}{\partial t} + \frac{1}{r}\frac{\partial (r v_{or} \rho_g)}{\partial r} + \frac{\partial (v_{oz} \rho_g)}{\partial r} + (1-\varepsilon_t)\rho_s \frac{\partial w}{\partial t} = 0$$<br>$$v_o + \frac{\rho_g}{\mu_g} k_E v_o |v_o| = -\frac{k_a}{\mu_g} \text{grad(p)}$$<br>**Heat Transfer Equation for Adsorbent Bed:**<br>$$\varepsilon_t \frac{\partial (\rho_g c_{pg} T_s)}{\partial t} + (1-\varepsilon_t)\frac{\partial}{\partial t}\left[(1-w)c_{peq} T_s\right] + \frac{1}{r}\frac{\partial}{\partial r}\left[r\left(\rho_g c_{pg} T_s + p\right) v_{or}\right] + \frac{\partial}{\partial z}\left[\left(\rho_g c_{pg} T_s + p\right) v_{oz}\right] = \lambda_{eq}\left[\frac{1}{r}\frac{\partial}{\partial r}\left(r\frac{\partial T_s}{\partial r}\right) + \frac{\partial^2 T_s}{\partial z^2}\right] + (1-\varepsilon_t)\rho_s |\Delta H| \frac{\partial w}{\partial t}$$<br>**Equivalent Conductivity Equation:** A constant value is given<br>**Diffusivity Equations:**<br>$$D_g = \left(\frac{1}{D^*} + \frac{1}{D_K}\right)^{-1} \frac{\varepsilon}{\eta_T} \qquad D^* = 0.02628 \frac{\sqrt{T^3/MM_g}}{p\sigma^2 \Omega_D} \qquad D_K = 48.5 d_{pore} \sqrt{\frac{T}{MM_g}}$$<br>**Permeability Equations:**<br>$$k_E = \frac{1.75 D_p}{150(1-\varepsilon)} \qquad k_a = k_d + \frac{D_g \mu_g}{p} \qquad k_d = \frac{\varepsilon^3 {D_p}^2}{150(1-\varepsilon)^2}$$<br>***Important parameters:***<br>w: mean adsorbed concentration (kg kg$^{-1}$), T: temperature (K), p: pressure (Pa), λ: thermal conductivity (W m$^{-1}$K$^{-1}$). |

**(cont. on next page)**

Table 4.2 (cont.).

| | |
|---|---|
| (16) | **Adsorption Equilibria:**<br>$$\ln(p) = A(w) + \frac{B(w)}{T}$$<br>$$A(w) = a_0 + a_1 w + a_2 w^2 + a_3 w^3$$<br>$$B(w) = b_0 + b_1 w + b_2 w^2 + b_3 w^3$$<br>**Mass Transfer Equation for Particle:**<br>Adsorptive and adsorbent are thermodynamically in equilibrium<br>**Mass Transfer Equation for Bed:**<br>No mass transfer resistance<br>**Heat Transfer Equation for Adsorbent Bed:**<br>$$U_2 A_2 (T_m - T_s) = (m_s c_s + w_s c_a) \frac{dT_s}{dt} - K_1 m_s \Delta H(w) \frac{dw}{dt}$$<br>**Equivalent Conductivity Equation:**<br>Not required<br>**Diffusivity Equations:**<br>Not required<br>**Permeability Equations:**<br>Not required<br>***Important parameters:***<br>w: mean adsorbed concentration (kg kg$^{-1}$), T: temperature (K), U: heat transfer coefficient (W m$^{-2}$K$^{-1}$), m: mass(kg). |

**(cont. on next page)**

Table 4.2 (cont.).

| | |
|---|---|
| (17) | **Adsorption Equilibria:**<br>$$x^* = \frac{x_m K_o \exp(\Delta H_{ads}/RT)P}{[1 + \{K_o \exp(\Delta H_{ads}/RT)P\}^{t_1}]^{1/t_1}}$$<br>**Mass Transfer Equation for Particle:**<br>$$\frac{\partial x}{\partial t} = \frac{15 D_{so} e^{-\frac{E_a}{RT}}}{R_p^2}(x^* - x)$$<br>**Mass Transfer Equation for Bed:**<br>$$\frac{\partial M_{ref}}{\partial t} = -M^{sg}\left\{\frac{\partial x_{des}^{bed}}{\partial t} + \frac{\partial x_{ads}^{bed}}{\partial t}\right\}$$<br>**Heat Transfer Equation for Adsorbent Bed:**<br>$$\left(\rho^{sg} {C_p}^{sg} + \rho^g x {C_p}^a\right)\frac{\partial T^{sg}}{\partial t} = \nabla(\lambda^{eff}\,\nabla T^{sg}) + \rho^{sg}\Delta H_{ads}\frac{\partial x}{\partial t} - \frac{h_{fin-s}A^{fin}}{V^{fin}}(T^{fin} - T^{sg}) - \frac{h_{m-s}^{tube}}{A}V^{tube}(T^{tube} - T^{sg})$$<br>**Equivalent Conductivity Equation:**<br>$$\lambda^{eff} = \lambda^g/(\emptyset + 2/3\ \lambda^g/\lambda^{sg})$$<br>**Diffusivity Equations:**<br>Not given (close to Knudsen diffusivity)<br>**Permeability Equations:**<br>Not required<br>***Important parameters:***<br>x: mean adsorbed concentration (kg kg$^{-1}$), $x^*$: equilibrium amount adsorbed (kg kg$^{-1}$),T: temperature ($^o$C), P: pressure (Pa), λ: thermal conductivity (W m$^{-1}$K$^{-1}$), M: mass (kg), h heat transfer coefficient (W m$^{-2}$K$^{-1}$), V: volume (m$^3$). |

**(cont. on next page)**

Table 4.2 (cont.).

| | |
|---|---|
| (18) | **Adsorption Equilibria:**<br>$$q^* = q^o \exp\left(-k\left(\frac{T}{T_{sat}} - 1\right)^n\right)$$<br>**Mass Transfer Equation for Particle:**<br>$$\frac{\partial \bar{q}}{\partial t} = \frac{\partial q^*}{\partial t} \qquad \frac{\partial q}{\partial t} = \frac{1}{r_p^2}\frac{\partial}{\partial r}\left(r_p^2 D_s \frac{\partial q}{\partial r}\right) \qquad \frac{\partial \bar{q}}{\partial t} = \frac{15 D_s}{r_p^2}(q^* - \bar{q})$$<br>**Mass Transfer Equation for Bed:**<br>No mass transfer resistance<br>**Heat Transfer Equation for Adsorbent Bed:**<br>$$\left(\rho_s C_{ps} + \bar{q} C_{pa}\right)\frac{\partial T_s}{\partial t} - \Delta H \frac{\partial \bar{q}}{\partial t} = \frac{\lambda_s}{r}\frac{\partial}{\partial r}\left(r\frac{\partial T_s}{\partial r}\right)$$<br>**Equivalent Conductivity Equation:**<br>is a variable parameter (Maggio et al. 2009), a constant value is given (Freni et al. 2008)<br>**Diffusivity Equations:**<br>Not required for adsorbent bed<br>**Permeability Equations:**<br>Not required<br>***Important parameters:***<br>$\bar{q}$: mean adsorbed concentration (kg kg$^{-1}$), q$^*$: equilibrium amount adsorbed (kg kg$^{-1}$),T: temperature (K), P: pressure (Pa), λ: thermal conductivity (W m$^{-1}$K$^{-1}$). |

**(cont. on next page)**

Table 4.2 (cont.).

| | |
|---|---|
| (19) | **Adsorption Equilibria:**<br>$$q = k\left(P/P_s\right)^{\frac{1}{n}}$$<br>**Mass Transfer Equation for Particle:**<br>$$\frac{\partial \bar{q}}{\partial t} = \frac{15 D_s}{R_p^2}(q^* - q)$$<br>**Mass Transfer Equation for Bed:**<br>No mass transfer resistance<br>**Heat Transfer Equation for Adsorbent Bed:**<br>$$W_s C_{ps}\frac{\partial T_s}{\partial t} = W_s Q_{st}\frac{\partial q}{\partial t} - A_s h_s(T_s - T_a) + A_s Q$$<br>**Equivalent Conductivity Equation:**<br>Not required<br>**Diffusivity Equations:**<br>$$D_s = D_{so}\exp\left(-\frac{E_a}{RT}\right)$$<br>**Permeability Equations:**<br>Not required<br>***Important parameters:***<br>$\bar{q}$: mean adsorbed concentration (kg kg$^{-1}$), q$^*$: equilibrium amount adsorbed (kg kg$^{-1}$), T: temperature (K), Q: effective heat influx into adsorbent bed by radiation (W m$^{-2}$), A: heat transfer area (m$^2$). |

**(cont. on next page)**

Table 4.2 (cont.).

| | |
|---|---|
| (20) | **Adsorption Equilibria:**<br>$$q^* = q\infty \left({}^{P}/_{P_s}\right)^{\frac{1}{n}}$$<br>**Mass Transfer Equation for Particle:**<br>$$\frac{\partial \bar{q}}{\partial t} = \frac{15 D_s}{R_p^2}(q^* - q)$$<br>**Mass Transfer Equation for Bed:**<br>No mass transfer resistance<br>**Heat Transfer Equation for Adsorbent Bed:**<br>$$\frac{\partial}{\partial t}(C_b W_b T_b) = -h_{1,b} A_{1,b}(T_b - T_a) - h_{2,b} A_{2,b}(T_b - T_s) + F_b C_w \left(T_{in,b} - T_{out,b}\right)$$<br>$$\frac{\partial}{\partial t}(C_b W_b T_b) = -h_{1,b} A_{1,b}(T_b - T_a) - h_{2,b} A_{2,b}(T_b - T_s) + Q_{solar} A_{1,b}$$<br>**Equivalent Conductivity Equation:** Not required<br>**Diffusivity Equations:**<br>$$D_s = D_{so} \exp\left(-\frac{E_a}{RT}\right)$$<br>**Permeability Equations:**<br>Not required<br>***Important parameters:***<br>$\bar{q}$: mean adsorbed concentration (kg kg$^{-1}$), q$^*$: equilibrium amount adsorbed (kg kg$^{-1}$), T: temperature (K), A: heat transfer area (m$^2$), h: heat transfer coefficient (W m$^{-2}$K$^{-1}$), W: weight (kg), F: flow rate of water (kg s$^{-1}$). |

**(cont. on next page)**

Table 4.2 (cont.).

| | |
|---|---|
| (21) | **Adsorption Equilibria:**<br>Not referred<br>**Mass Transfer Equation for Particle:**<br>$$\frac{\partial \bar{q}}{\partial t} = \frac{15 D_s}{R_p^2}(q^* - q)$$<br>**Mass Transfer Equation for Bed:**<br>No mass transfer resistance<br>**Heat Transfer Equation for Adsorbent Bed:**<br>$$\frac{\partial}{\partial t}(C_s W_s T_s) = Q_{st} W_s \frac{\partial q}{\partial t} - (h_o A)^b (T_s - T_b)$$<br>**Equivalent Conductivity Equation:**<br>Not required<br>**Diffusivity Equations:**<br>Referred<br>**Permeability Equations:**<br>Not required<br>***Important parameters:***<br>$\bar{q}$: mean adsorbed concentration (kg kg$^{-1}$), q$^*$: equilibrium amount adsorbed (kg kg$^{-1}$), T: temperature (K), A: heat transfer area (m$^2$), h: heat transfer coefficient (W m$^{-2}$K$^{-1}$), W: weight (kg), $Q_{st}$: heat of adsorption (J kg$^{-1}$).. |

**(cont. on next page)**

Table 4.2 (cont.).

| | |
|---|---|
| (22) | **Adsorption Equilibria:**<br>$$W_\infty = W_o \left({}^{P_{sat}}/_{P}\right)^{\frac{1}{n}}$$<br>**Mass Transfer Equation for Particle:**<br>$$\frac{\partial W}{\partial t} = \frac{15 D_{eff}}{r_p^2}(W_\infty - W)$$<br>**Mass Transfer Equation for Bed and Velocity:**<br>$$\frac{\partial \rho_w}{\partial t} + \frac{1}{\varepsilon}\rho_s \frac{\partial W}{\partial t} + \frac{1}{\varepsilon R}\frac{\partial}{\partial R}(R\rho_w u) = 0 \qquad u = -K_{app}\frac{R}{M\mu}\frac{\partial(\rho_w T_w)}{\partial r}$$<br>**Heat Transfer Equation for Adsorbent Bed:**<br>$$\left[\left(\rho C_p\right)_{eff} + \rho_s C_{pw} W\right]\frac{\partial T}{\partial t} = \lambda_{eq}\frac{1}{R}\frac{\partial}{\partial R}\left(R\frac{\partial T}{\partial R}\right) - \frac{1}{R}\frac{\partial}{\partial R}\left(\rho_w C_{pw} R u T\right) + \rho_s \Delta H_{st}\frac{\partial W}{\partial t}$$<br>**Equivalent Conductivity Equation:**<br>$$\lambda_{eff} = \lambda_s^{1-\varepsilon}\,\lambda_w^{\varepsilon}$$<br>**Diffusivity Equations:**<br>$$\frac{1}{D_{bed}} = \frac{1}{D_m} + \frac{1}{D_k} \qquad D_m = 0.02628\frac{\sqrt{{}^{T^3}/_{M}}}{P\sigma^2\Omega} \qquad D_k = 97 r_p\sqrt{{}^{T}/_{M}}$$<br>**Permeability Equations:**<br>$$K = \frac{\varepsilon^3 r_p^2}{150\,(1-\varepsilon)^2} \qquad K_{app} = K + \frac{\varepsilon\mu}{\tau P}D_{bed}$$<br>***Important parameters:*** W: mean adsorbed concentration (kg kg$^{-1}$), $W_\infty$: equilibrium amount adsorbed (kg kg$^{-1}$), T: temperature (K), u: adsorptive velocity (ms$^{-1}$), $\lambda$: heat transfer coefficient (W m$^{-1}$K$^{-1}$). |

**(cont. on next page)**

Table 4.2 (cont.).

| | |
|---|---|
| (23) | **Adsorption Equilibria:**<br>$$w = w_o \exp\left(-k\left(\frac{T}{T_{sat}} - 1\right)^n\right)$$<br>**Mass Transfer Equation for Particle:**<br>Adsorptive and adsorbent are thermodynamically in equilibrium<br>**Mass Transfer Equation for Bed and Velocity:**<br>$$\frac{\partial \rho_v}{\partial t} + \frac{1}{\mathrm{r}}\frac{\partial}{\partial r}(r\rho_v u_r) = -\rho_z \frac{\partial w}{\partial t} \qquad u_r = -\frac{k_D}{\mu}\frac{\partial \mathrm{P}}{\partial \mathrm{r}}$$<br>**Heat Transfer Equation for Adsorbent Bed:**<br>$$\frac{\partial\left(\rho C_p T_z\right)}{\partial t} + \frac{1}{\mathrm{r}}\frac{\partial}{\partial r}(r\rho_v C_{pv} u_r T_z) = \frac{1}{r}\frac{\partial}{\partial r}\left(k_{eff} r \frac{\partial T_z}{\partial r}\right) + \rho_z \Delta H \frac{\partial w}{\partial t}$$<br>**Equivalent Conductivity Equation:**<br>$$k_{eff} = k_z^{1-\varepsilon_t}\, k_v^{\varepsilon_t}$$<br>**Diffusivity Equations:**<br>Not required<br>**Permeability Equations:**<br>Variable parameter<br>***Important parameters:***<br>W: mean adsorbed concentration (kg kg$^{-1}$), T: temperature (K), u: velocity (m s$^{-1}$), u: adsorptive velocity (ms$^{-1}$), $k_{eff}$: thermal conductivity (W m$^{-1}$K$^{-1}$). |

**(cont. on next page)**

Table 4.2 (cont.).

| | |
|---|---|
| (24) | **Adsorption Equilibria:**<br>$$\ln(P_z) = a(w_{eq}) + \frac{b(w_{eq})}{T_z}$$<br>$$a(w_{eq}) = a_0 + a_1 w_{eq} + a_2 {w_{eq}}^2 + a_3 {w_{eq}}^3; \quad b(w_{eq}) = b_0 + b_1 w_{eq} + b_2 {w_{eq}}^2 + b_3 {w_{eq}}^3$$<br>**Mass Transfer Equation for Particle:**<br>$$\frac{\partial w}{\partial t} = \frac{60 D_s}{d_p^2}(w_{eq} - w)$$<br>**Mass Transfer Equation for Bed and Velocity:**<br>$$\varepsilon_t \frac{\partial \rho_v}{\partial t} + \nabla(u\rho_v) + \rho_z \frac{\partial w}{\partial t} = 0 \qquad u = \frac{-k_D}{\mu}\nabla P_z$$<br>**Heat Transfer Equation for Adsorbent Bed:**<br>$$\frac{\partial(\rho C_p T_z)}{\partial t} + \nabla(\rho_v C_{pv} u T_z) - \nabla(\lambda_z \nabla T_z) - \rho_z q_{st}\frac{\partial w}{\partial t} = 0$$<br>**Equivalent Conductivity Equation:** is a constant parameter<br>**Diffusivity Equations:**<br>$$D_s = D_{s0}\exp\left(-\frac{E_a}{RT_z}\right)$$<br>**Permeability Equations:**<br>$$k_D = \frac{{\varepsilon_b}^3 d_p^2}{150\,(1-\varepsilon_b)^2}$$<br>***Important parameters:*** w: mean adsorbed concentration (kg kg$^{-1}$), $w_{eq}$: equilibrium amount adsorbed (kg kg$^{-1}$), T: temperature (K), u: adsorptive velocity (ms$^{-1}$), $\lambda$: heat transfer coefficient (W m$^{-1}$K$^{-1}$). |

**(cont. on next page)**

Table 4.2 (cont.).

| | |
|---|---|
| (25) | **Adsorption Equilibria:**<br>$$q_e = K\left[\frac{P_s(T_v)}{P_s(T_b)}\right]^{1/n}$$<br>**Mass Transfer Equation for Particle:**<br>$$\frac{\partial q}{\partial t} = \mu(q_e - q)$$<br>**Mass Transfer Equation for Bed and Velocity:**<br>No mass transfer resistance<br>**Heat Transfer Equation for Adsorbent Bed:**<br>$$M_a c_a\left(1 + \frac{c_r}{c_a}q + \frac{M_m c_m}{M_a c_a}\right)\frac{\partial T_b}{\partial t} - \rho_a \mathrm{A_a L Q_{st}}\frac{\partial q}{\partial t} = k_{eff}\mathrm{A_a L}\left(\frac{\partial^2 T_b}{\partial x^2} + \frac{\partial^2 T_b}{\partial y^2}\right)$$<br>**Equivalent Conductivity Equation:**<br>is a constant parameter<br>**Diffusivity Equations:**<br>Not required for adsorbent bed<br>**Permeability Equations:**<br>Not required<br>***Important parameters:***<br>$q$: adsorbed concentration (kg kg$^{-1}$), $q_e$: equilibrium amount adsorbed (kg kg$^{-1}$), T: temperature (K), M: mass (kg). |

**(cont. on next page)**

Table 4.2 (cont.).

| | |
|---|---|
| (26) | **Adsorption Equilibria:**<br>$$W_\infty = k\left({}^{P}/_{P_{sat}}\right)^{\frac{1}{n}}$$<br>**Mass Transfer Equation for Particle:**<br>$$\frac{\partial \overline{W}}{\partial t} = \frac{\partial \overline{W}_\infty}{\partial t} \qquad \frac{\partial \overline{W}}{\partial t} = \frac{15 D_{eff}}{r_p^2}\left(\overline{W}_\infty - \overline{W}\right) \qquad \frac{\partial W}{\partial t} = \frac{1}{r^2}\frac{\partial}{\partial r}\left(r^2 D_{eff}\ \frac{\partial W}{\partial r}\right)$$<br>**Mass Transfer Equation for Bed and Velocity:**<br>No mass transfer resistance<br>**Heat Transfer Equation for Adsorbent Bed:**<br>$$(\rho C_p)_{eff}\ \frac{\partial T}{\partial t} = \lambda_{eff}\ \frac{1}{R}\frac{\partial}{\partial R}\left(R\frac{\partial T}{\partial R}\right) + (1-\varphi)\rho_S \Delta H_{ads}\ \frac{\partial \overline{W}}{\partial t}$$<br>**Equivalent Conductivity Equation:**<br>$$\lambda_{eff}\ = (1-\varphi)\lambda_S + \varphi\lambda_V$$<br>**Diffusivity Equations:**<br>Not required for adsorbent bed<br>**Permeability Equations:**<br>Not required<br>***Important parameters:***<br>W: mean adsorbed concentration (kg kg$^{-1}$), $W_\infty$: equilibrium amount adsorbed (kg kg$^{-1}$), T: temperature (K), $\lambda$: heat transfer coefficient (W m$^{-1}$K$^{-1}$). |

**(cont. on next page)**

Table 4.2 (cont.).

| | |
|---|---|
| (27) | **Adsorption Equilibria:**<br>$$W_{\infty} = k\left(P/P_{sat}\right)^{\frac{1}{n}}$$<br>**Mass Transfer Equation for Particle:**<br>$$\frac{\partial \overline{W}}{\partial t} = \frac{15 D_{eff}}{r_P^2}\left(\overline{W}_{\infty} - \overline{W}\right)$$<br>**Mass Transfer Equation for Bed and Velocity:**<br>No mass transfer resistance<br>**Heat Transfer Equation for Adsorbent Bed and Fins:**<br>$$\frac{\partial T}{\partial t} = \alpha_{eff}\frac{1}{R}\frac{\partial}{\partial R}\left(R\frac{\partial T}{\partial R}\right) + \alpha_{eff}\frac{1}{R^2}\frac{\partial^2 T}{\partial \phi^2} + \frac{(1-\varphi)\rho_S}{(\rho C_p)_{eff}}\Delta H_{ads}\frac{\partial W}{\partial t}\ ;\ \left(\rho C_p\right)_{fin}\delta\frac{\partial T_{fin}}{\partial t} = k_S\frac{1}{R}\frac{\partial T_{fin}}{\partial \phi}\bigg|_{fs} + k_{fin}\frac{\partial^2 T_{fin}}{\partial R^2}\delta$$<br>**Equivalent Conductivity Equation:**<br>$$\lambda_{eff} = (1-\varphi)\lambda_S + \varphi\lambda_V$$<br>**Diffusivity Equations:**<br>Not required for adsorbent bed<br>**Permeability Equations:**<br>Not required<br>***Important parameters:***<br>W: mean adsorbed concentration (kg kg$^{-1}$), $W_{\infty}$: equilibrium amount adsorbed (kg kg$^{-1}$), T: temperature (K), $\lambda$: heat transfer coefficient (W m$^{-1}$K$^{-1}$), $\delta$ : thickness of the fin. |

# CHAPTER 5

# HEAT AND MASS TRANSFER EQUATIONS FOR ADSORPTION IN A SINGLE PARTICLE

The heat and mass transfer equations in a single particle during an adsorption process is explained in this chapter. The single adsorbent particle is located in an infinite adsorptive media which is at specified pressure and temperature. Four cases are considered for analyzing heat and mass transfer in a single particle. The studied cases are a) isothermal mass transfer in a single particle with negligible effect of external mass transfer resistance, b) isothermal mass transfer in a single particle with considerable effect of external mass transfer resistance, c) heat and mass transfer in a single adsorbent particle with negligible effects of external heat and mass transfer resistances, d) heat and mass transfer in a single adsorbent particle with considerable effects of external heat and mass transfer resistances.

## 5.1. The Considered Adsorbent Particle and Ambient

Figure 5.1 shows the schematic view of the analyzed adsorbent particle for four cases. As is seen, the adsorbent particle located in an infinite adsorptive media. The pressure, density, and temperature of adsorptive are $P_\infty$, $\rho_\infty$, and $T_\infty$ which are constant. Figure 5.1(a) represents Case I in which the adsorption is assumed to be isothermal and no external mass transfer resistances exist. Hence, the equilibrium adsorbate concentration at the surface of the particle can be calculated from the temperature and density of ambient adsorptive. Figure 5.1(b) shows the considered adsorbent particle for an isothermal adsorption with considerable external mass transfer resistance. The external mass transfer resistance at the outer region of adsorbent particle causes a significant density gradient around the particle and the adsorptive density at the surface of particle will be different than the density of ambient adsorptive. Figure 5.1(c) shows the adsorbent particle for a non-isothermal case with negligible heat and mass transfer resistance. The temperature of adsorbent is different than the ambient

temperature. The negligible external heat and mass transfer resistance causes the density and temperature at the surface of adsorbent particle become close to the ambient temperature and density. Figure 5.1(d) shows the considered adsorbent particle for non-isothermal adsorption case with considerable external heat and mass transfer resistances. As is seen, the values of both temperature and density at the interface are different than the ambient values due to the considerable external heat and mass transfer resistances.

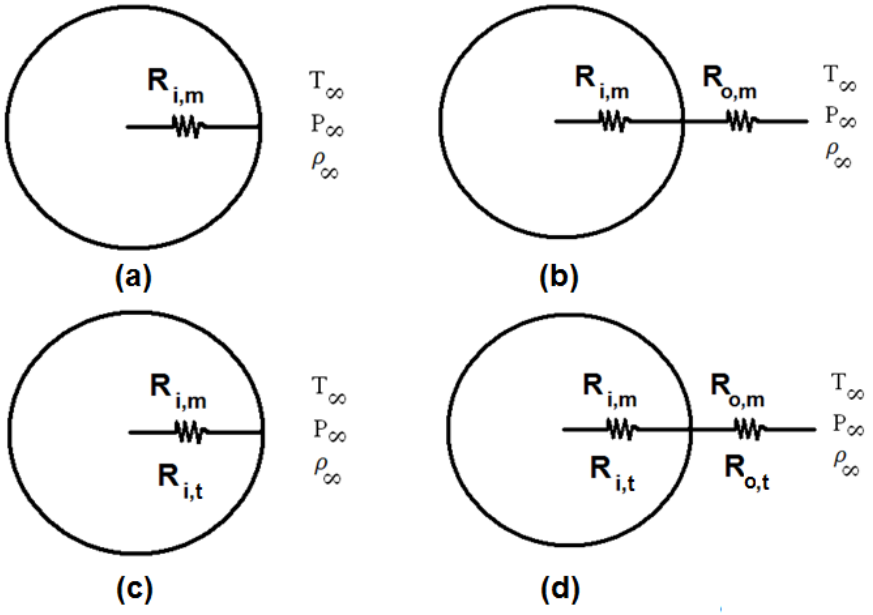


Figure 5.1. The schematic view of the studied adsorbent particles, a) isothermal particle with negligible external mass transfer resistance, b) isothermal particle with considerable external mass transfer, c) negligible external mass transfer but considerable internal heat transfer resistance, d) non-isothermal particle with considerable external heat and mass transfer resistances

The adsorbent particle is considered as spherical with a radius of $r_p$. The study is performed for Freundlich isotherm of adsorption equilibria for silica gel-water pair. The thermophysical properties of silica gel particle and water is given in Appendix A in Table A1 (Ilis et al. 2010). Generally, the Freundlich isotherm equation is written based on pressure ratio as:

$$W_{\infty} = k(P / P_{sat})^{1/n} \tag{5.1}$$

where k and n are constants and their values for silica gel-water (Davison A) pair are 0.552 and 1.6, respectively (Liu and Leong 2006, Sakoda and Suzuki 1984, 1986, Demir et al. 2009, Chua et al. 2001, Wang and Chua 2007a). The ideal gas relation can be used to define the isotherm equations based on adsorptive density, since temperature is not changed for an isotherm. Then, the Freundlich adsorption equilibria based on density ratio can be written as;

$$W_{\infty} = k(\rho / \rho_{sat})^{1/n} \tag{5.2}$$

The effective thermal capacity, thermal conductivity, and effective diffusivity are calculated by using the following relations:

$$(\rho C_p)_{eff} = (\rho C_p)_s + \rho_s C_{pl} \overline{W} \tag{5.3}$$

$$\lambda_{eff} = \overline{W} \lambda_l + (1 - \overline{W}) \lambda_s \tag{5.4}$$

$$D_{eff} = D_o e^{-E/RT} \tag{5.5}$$

where $D_o$ is the reference diffusivity and E is the diffusion activation energy and their values are $2.54 \times 10^{-4}$ $m^2/s$ and $4.2\ 10^4$ J/mol for the studied silica gel-water, respectively (Demir et al. 2009).

As it was mentioned before heat and mass transfer in adsorbent particle is too complex and requires assumptions. Following assumptions are made in the present study; a) surface diffusion is dominant mode of mass transfer diffusion, b) radiation heat transfer between particle and ambient is neglected, c) thermophysical properties of adsorbent and adsorbate are constant, d) the study is performed for adsorptive pressure as P = 2 kPa, e) the ideal gas relation is used as the state equation for adsorptive, f) the heat of adsorption is assumed constant.

## 5.2. Dimensionless Equilibrium Isotherm

The dimensional isotherms for the considered silica gel/water pair represented by Eq. (5.2) are shown in Figure 5.2 for different temperatures as 303, 323, 343, and 363 K. As is seen from this figure, the variation of equilibrium concentration with density for Freundlich isotherm has a non-linear behavior. As seen, by changing of temperature isotherm function is changed.

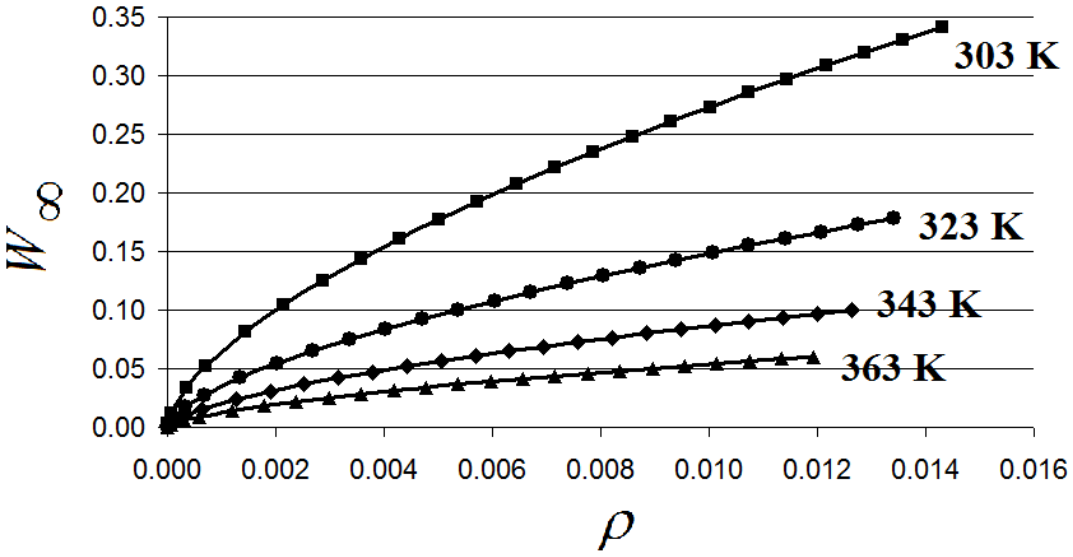


Figure 5.2. The dimensional isotherms, the variation of equilibrium adsorbate concentration with density for the Freundlich isotherm for the considered silica gel/water pair

The isotherm function can be non-dimensionalized by using the following parameters:

$$W^* = \frac{W - W_i}{W_\infty - W_i};\ \ \rho^* = \frac{\rho}{\rho_\infty} \tag{5.6}$$

The non-dimensionalization of these parameters ( $\rho$ and $W$ ) can be useful to find a function which is valid for different temperatures. For Freundlich isotherm type, the dimensionless isotherms overlap each others. Thus, it is possible to use a unique dimensionless isotherm equation to determine dimensionless adsorbate concentration in terms of dimensionless density. The dimensionless form of the Freundlich isotherm does not depend on the temperature. The dimensionless isotherm equation changes from

pair to pair. For different kind of silica gel-water pairs, these functions are plotted in Figure 5.3 (Afonso et al. 2005, Xia et al. 2008).

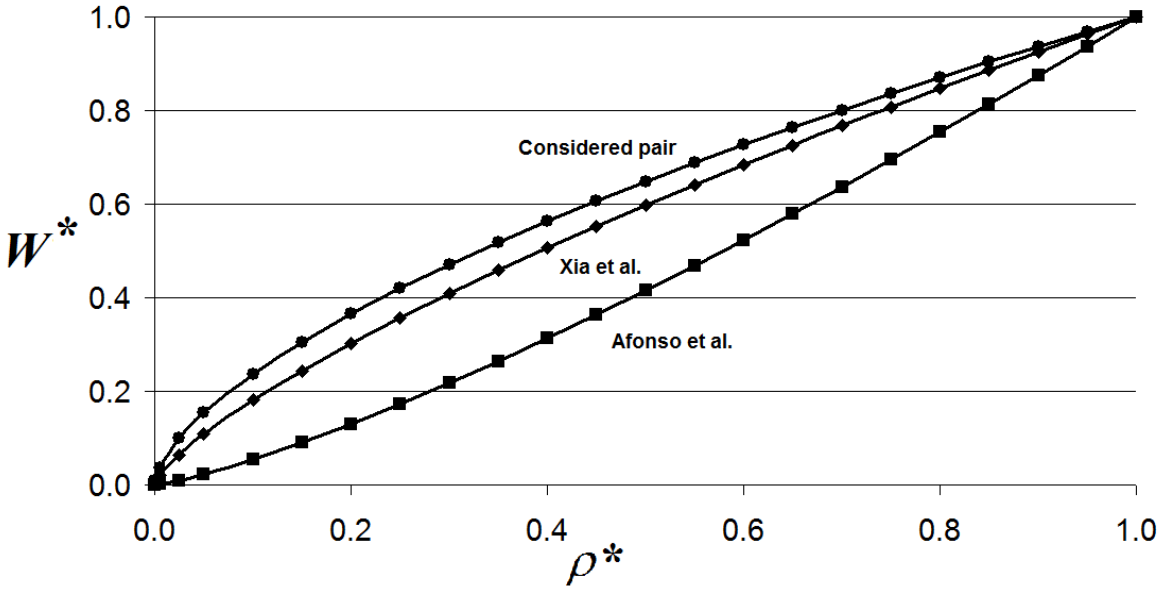


Figure 5.3. The dimensionless Freundlich isotherms for different silica gel/water pairs (Source: Afonso et al. 2005, Xia et al. 2008)

For an adsorbent-adsorbate pair with Freundlich isotherm type, the unique dimensionless isotherm can be written as:

$$W^* = \Gamma(\rho^*) \tag{5.7}$$

For the considered silica gel-water pair, the function of Γ is:

$$W^* = -1.6874(\rho^*)^4 + 4.1626(\rho^*)^3 - 3.8241(\rho^*)^2 + 2.3127(\rho^*) + 0.0301 \tag{5.8}$$

## 5.3. Governing Equations

The governing equations, the initial and boundary conditions are written for each case. The dimensionless forms of these governing equations and initial and boundary conditions are given for all cases.

### 5.3.1. Case I

The problem is isothermal and the external heat and mass transfer resistances are neglected for this case. For water diffusion in a silica gel particle, the Knudsen and molecular diffusions can be neglected and the surface diffusion can be considered as the dominant mechanism affecting mass diffusion rate in a silica gel (Leong and Liu 2004b, 2006, Liu and Leong 2005, Wang and Chua 2007a, Sakoda and Suzuki 1986). The solid diffusion model based on Fick's law is used to derive the following partial differential equation and to obtain the variation of local adsorbate concentration in the adsorbent particle during adsorption stage;

$$\frac{\partial W}{\partial t} = \frac{1}{r^2}\frac{\partial}{\partial r}\left( r^2 D_{eff}\ \frac{\partial W}{\partial r} \right) \tag{5.9}$$

where $D_{eff}$ is the effective diffusivity and it includes all possible diffusion mechanisms such as surface, pore diffusion etc. The initial and boundary conditions for Eq. (5.9) can be written as;

$$t = 0 \qquad W = 0 \tag{5.10}$$

$$\text{r} = 0 \qquad \frac{\partial W}{\partial r} = 0 \tag{5.11}$$

$$\text{r} = \text{r}_\text{p} \qquad W = W_\infty \tag{5.12}$$

where $W_\infty$ can be found from isotherm relation (Eq.(5.2)). The following dimensionless parameters can be used to obtain the dimensionless form of the mass transfer equation (Eq. (5.2)) and related initial and boundary conditions;

$$W^* = \frac{W - W_i}{W_\infty - W_i};\ r^* = \frac{r}{r_p};\ \tau = \frac{D_{eff}\, t}{r_p^2};\ \rho^* = \frac{\rho}{\rho_\infty} \tag{5.13}$$

where $\rho_\infty$ is the density of ambient adsorptive and $W_\infty$ represents the adsorbate concentration for the ambient adsorptive at $\rho_\infty$ and $T_\infty$. For the present study, it is

assumed that $W_i = 0$. By using the above dimensionless parameters, the dimensionless form of mass transfer equation for an adsorbent particle of Case I become as:

$$\frac{\partial W^*}{\partial \tau} = \frac{1}{r^{*2}} \frac{\partial}{\partial r^*} \left( r^{*2} \frac{\partial W^*}{\partial r^*} \right) \tag{5.14}$$

The dimensionless initial condition for the problem can be written as:

$$\tau = 0; \qquad W^* = 0 \tag{5.15}$$

While the boundary conditions for the problem are;

$$r^* = 0; \qquad \frac{\partial W^*}{\partial r^*} = 0 \tag{5.16}$$

$$r^* = 1; \qquad W^* = 1 \tag{5.17}$$

The dimensionless mass transfer equation (Eq. (5.14)) and the initial and boundary conditions (Eqs. (5.15)-(5.17)) show that the change of dimensionless adsorbate concentration in the particle with dimensionless time is unique and does not depend on isotherm relation.

### 5.3.2. Case II

The mass transfer problem is isothermal but the external mass transfer resistance is taken into consideration. The dimensional mass transfer equation for Case II is the same with Case I (Eq. (5.9)). The initial and boundary condition at the center of the particle are not changed and Eqs. (5.10) and (5.11) are valid. However; the boundary condition at the surface of the particle should be revised due to the considerable external mass transfer resistance as;

r = $r_p$ $$-D_{eff}\,\rho_s\,\frac{\partial W}{\partial r} = h_m(\rho|_{r=r_p} - \rho_\infty) \tag{5.18}$$

The dimensionless parameter groups defined for the Case I (Eq. (5.13)) can be used for the present case. The dimensionless form of the boundary condition at the outer surface of the particle takes the following form:

$$r^* = 1; \qquad \frac{\partial W^*}{\partial r^*} = Bi_m^{'}\left(1-\rho^*\Big|_{r^*=1}\right) \tag{5.19}$$

$Bi_m^{'}$ is called as modified mass transfer Biot number and it can be calculated from the following equation;

$$Bi_m^{'} = Bi_m G \tag{5.20}$$

where $Bi_m$ is the classical mass transfer number. $Bi_m$ and G are obtained as;

$$Bi_m = \frac{h_m r_p}{D_{eff}} \tag{5.21}$$

$$G = \frac{\rho_\infty}{\rho_s(W_\infty - W_i)} \tag{5.22}$$

The modified Biot mass number ($Bi_m^{'}$) is defined to combine $Bi_m$ and G dimensionless parameter groups. The right side of Eq. (5.19) depends $W^*$ while the left side contains $\rho^*$. The dimensionless isotherm equation provides relation between $W^*$ and $\rho^*$. The dimensionless mass transfer equation (Eq.(5.14)), the initial and boundary conditions (Eqs. (5.15), ( 5.16) and (5.17)) and the dimensionless relation between $\rho^*$ and $W^*$ show that the change of dimensionless adsorbate concentration in the adsorbent

particle of Case II with time depends on modified mass transfer Biot number and $\Gamma_i$ function.

### 5.3.3. Case III

The problem of Case III is a non isothermal heat and mass transfer with negligible external heat and mass transfer resistances. Since the problem is non-isothermal, heat transfer equation should be written for the adsorbent particle to obtain temperature distribution in the particle.

$$(\rho C_p)_{eff} \frac{\partial T}{\partial t} = \lambda_{eff} \frac{1}{r^2} \frac{\partial}{\partial r}\left( r^2 \frac{\partial T}{\partial r} \right) + \rho_s \Delta H_{ads} \frac{\partial W}{\partial t} \tag{5.23}$$

where $(\rho C_p)_{eff}$ and $\lambda_{eff}$ are the effective thermal capacitance and thermal conductivity of the adsorbent particle. The effect of adsorption in the adsorbent particle is contributed by $\partial W / \partial t$. The initial and boundary conditions for heat transfer equation (Eq. (5.23)) can be written as:

$$\text{t} = 0; \qquad T = T_i \tag{5.24}$$

$$\text{r}_\text{p} = 0; \qquad \frac{\partial T}{\partial r} = 0 \tag{5.25}$$

$$\text{r} = \text{r}_\text{p}; \qquad T = T_\infty \tag{5.26}$$

The set of dimensionless parameter is defined by Eq. (5.13) can be used to obtained the dimensionless form of heat transfer equation and initial and boundary conditions of Case III. However; an additional relation for dimensionless temperature should be defined:

$$\theta = \frac{T - T_\infty}{T_i - T_\infty}, \tag{5.27}$$

where $T_i$ represents initial temperature. By using Eqs. (5.13) and (5.27), the dimensionless form of heat transfer equation (Eq. (5.23)) for Case I can be obtained as;

$$\frac{\partial \theta}{\partial \tau} = Le \frac{1}{r^{*2}} \frac{\partial}{\partial r^*} \left( r^{*2} \frac{\partial \theta}{\partial r^*} \right) + Ku \frac{\partial W^*}{\partial \tau} \tag{5.28}$$

The dimensionless initial and boundary conditions for heat transfer equation (Eq. (5.24-26)) can be written as:

$$\tau = 0; \qquad \theta = 1 \tag{5.29}$$

$$r^* = 0; \qquad \frac{\partial \theta}{\partial r^*} = 0 \tag{5.30}$$

$$r^* = 1; \qquad \theta = 0 \tag{5.31}$$

where *Ku* and *Le* are dimensionless independent parameter groups as Kutateladze and Lewis numbers, respectively and they are defined as:

$$Ku = \frac{\rho_S \Delta H_{ads} (W_\infty - W_i)}{(\rho C_p)_{eff} (T_i - T_\infty)} \tag{5.32}$$

$$Le = \frac{\alpha_{eff}}{D_{eff}} \tag{5.33}$$

The dimensionless parameter Ku represents the ratio of heat of adsorption to the sensible thermal energy storage (5.32). The Le parameter refers to the ratio of heat transfer diffusion to the mass transfer diffusion in the radial direction of the adsorbent particle.

The dimensionless mass transfer equation, initial and boundary conditions for Case III is identical with that of Case I (i.e. Eq. (5.14)) since negligible external mass transfer resistance exists. It should be mentioned that since external heat transfer resistance is negligible, the surface temperature is assumed at temperature of ambient and hence $\theta = 0$ for particle surface. The dimensionless heat and mass transfer equations (Eqs. (5.14) and (5.28)), the dimensionless initial conditions (Eqs. (5.15) and (5.29)) and dimensionless boundary conditions (Eqs.(5.16), (5.17), (5.30) and (5.31)) show that the dimensionless adsorbate distribution in the particle of Case III depends on *Ku* and *Le* numbers.

### 5.3.4. Case IV

The problem of Case IV is defined as non-isothermal with considerable external heat and mass transfer resistances. The dimensionless heat transfer equation, initial and boundary condition at the center of particle are the same with Case III (Eqs. (5.28)-( 5.30)). However, the thermal boundary condition at the particle surface should be defined as follow due to existence of considerable heat transfer resistance.

$$r = r_p \qquad -\lambda_s \frac{\partial T}{\partial r} = h_f (T - T_\infty) \tag{5.34}$$

The use of dimensionless parameters (Eqs.(5.13) and (5.27)) yields the dimensionless boundary condition for the outer surface of the particle.

$$r^* = 1; \qquad \frac{\partial \theta}{\partial r^*} = -Bi_h \theta \tag{5.35}$$

where $Bi_h$ is heat transfer Biot number it is defined as:

$$Bi_h = \frac{h_f r_p}{\lambda_{eff}} \tag{5.36}$$

The dimensionless mass transfer equation, initial and boundary conditions for Case IV are identical with those equations of Case II (Eqs. (5.14), (5.15), (5.16)). The dimensionless heat and mass transfer equations (Eqs. (5.14) and (5.28)), the dimensionless initial conditions (Eqs. (5.15) and (5.29)) and dimensionless boundary conditions (Eqs.(5.16), (5.19), (5.30) and (5.35)) show that at the dimensionless adsorbate distribution and temperature in the particle of Case IV depends on *Ku*, *Le*, $Bi_h$, and $Bi'_m$ function.

# CHAPTER 6

# HEAT AND MASS TRANSFER EQUATIONS FOR ADSORPTION PROCESS IN AN ADSORBENT BED

The heat and mass transfer equations for an adsorption process in an adsorbent bed are explained in this chapter. Basically, two main approaches are used to analyze heat and mass transfer in an adsorbent bed as uniform and non-uniform pressure approaches. These approaches are studied in this section. Besides, the heat and mass transfer equations for an adsorbent bed assisted by fins are presented in this chapter.

## 6.1. Definition on Uniform and Non-Uniform Pressure Approach

In an adsorption process, the solid and the fluid adsorbed on the solid surface are called as adsorbent (e.g. silica gel) and adsorbate (e.g. adsorbed water), while the adsorbable substance which is in the gas phase is called as adsorptive (e.g. water vapor). Adsorptive tends to be diffused into the pores of the adsorbent. Adsorbent bed, in which adsorption and desorption processes occur, is the crucial part of an adsorption heat pump. The adsorbent bed used in adsorption heat pump is a closed type operating under low or high pressures. It enables combination of heat storage and heat pumping functions in the same system.

Mass transfer within the adsorbent particle (intraparticle mass transfer) and mass transfer in voids between adsorbent particles (interparticle mass transfer) occur in a closed type granular adsorbent bed. The intraparticle mass transfer is generally formed by diffusion mode of transport in the adsorbent particle. The solid diffusion or LDF model is used to determine the adsorbate concentration change with time in the adsorbent particle. The interparticle mass transfer mostly occurs due to the gradient of adsorptive concentration (pressure) in the adsorbent bed and it can be represented by Darcy law. Two approaches which are uniform and non-uniform pressure approaches can be used for the simulation of heat and mass transfer in a closed adsorbent bed:

*Uniform pressure approach:* In this approach, the interparticle mass transfer resistance is assumed negligible; hence the adsorptive pressure in the entire adsorbent bed is uniform as shown in Figure 6.1(a). The temperature gradient and intraparticle mass transfer resistance are two parameters that influence adsorbate concentration gradient inside the bed. The temperature in the bed changes both in time and space. A heat transfer equation without convective term is solved to determine local temperature throughout the adsorption process.

*Non-uniform pressure approach*: The interparticle mass transfer resistance is taken into account as shown in Figure 6.1(b), and the space gradient of adsorptive pressure is determined. The convective transport term appears in the heat transfer equation. Two simultaneous additional equations (i.e. continuity and Darcy equations) should be solved to obtain the adsorptive concentration profile and adsorptive velocity in the bed.

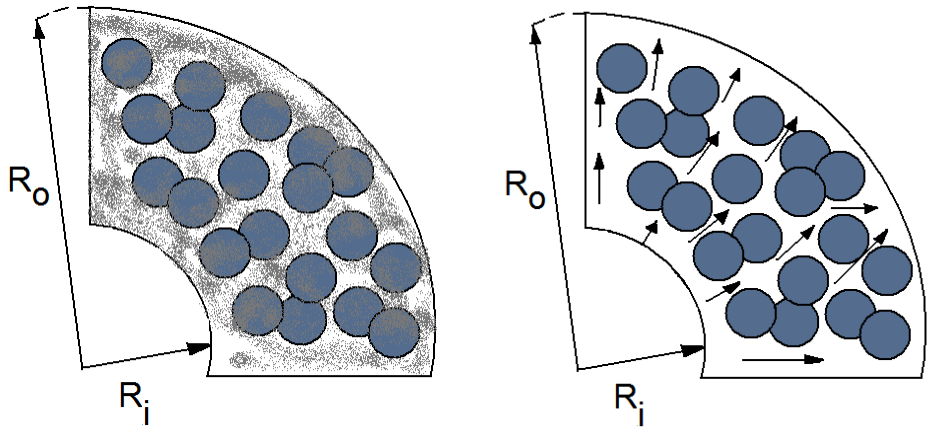


(a) (b)

Figure 6.1. A section of adsorbent bed, a) uniform pressure approach, b) non-uniform pressure approach

The heat and mass transfer in a granular adsorbent bed are coupled and complicated; hence some assumptions have to be made to pose the governing equations. The made assumptions are; 1) the adsorbent bed consists of uniform size spherical adsorbent particles, 2) the particles arrangement is assumed cubical and thus the bed porosity is constant for different particle sizes, 3) the adsorptive and adsorbent particle are in thermal equilibrium, 4) the thermal resistance within the adsorbent particle is neglected, 5) thermal properties of the adsorbent, adsorptive and adsorbate are constant,

6) heat transfer rate at inner radius of bed (i.e., $R = R_i$) is negligible, 7) wall thermal resistance between the bed surface and particle is not considered, 8) the heat of adsorption is assumed constant.

Figure 6.2 shows the schematic view of the analyzed annulus adsorbent bed filled with the adsorbent particles. The adsorbent bed has a cylindrical shape. The upper and bottom surfaces of the adsorbent bed are insulated and the transfer of heat and mass occurs only in radial direction. The space at the center of the bed is sufficiently large and the bed height is very small when compared with the bed thickness. Hence, the gradient of the adsorptive velocity through the length of the bed is neglected. The thermal resistance of the metal casing is neglected. The adsorptive can easily flow from inner surface, $R = R_i$, toward the outer surface, $R = R_o$.

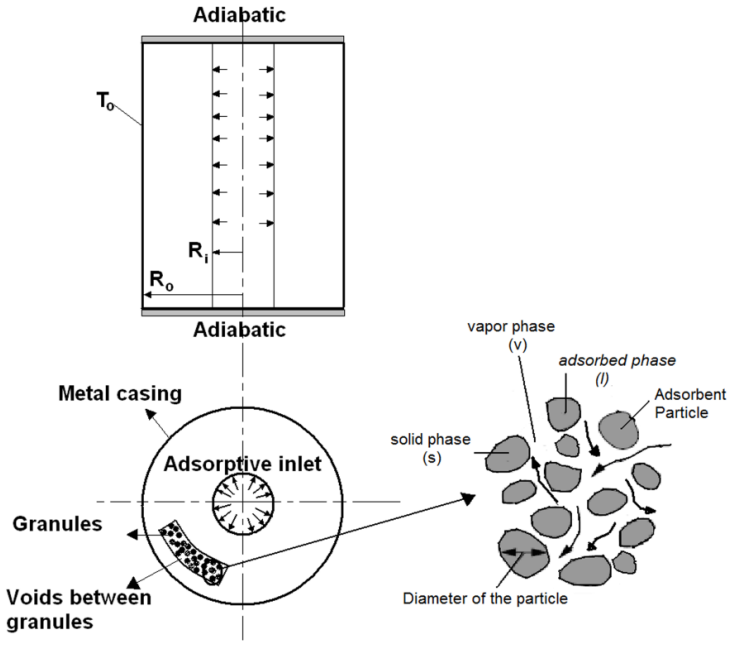


Figure 6.2. The schematic view of analyzed annular adsorbent bed filled with the adsorbent granules

The governing equations of uniform and non-uniform approaches used in the analysis of the heat and mass transfer in the adsorbent bed are separately presented in the following subsections. The derivations of the governing equations are given in details in the Appendix B. Heat of adsorption and effective diffusivity values are assumed constant to find the dimensionless numbers. This assumption might be valid for narrow range of adsorption or at the average temperature, pressure range of adsorption.

## 6.2. Governing Equations of Uniform Pressure Approach

The governing equations are given for both the dimensional and dimensionless forms for uniform pressure approach in this section. The initial and boundary conditions are given in tables for each dimensional and dimensionless form of the uniform pressure approach used in the theoretical studies.

### 6.2.1. Dimensional Form

The interparticle mass transfer resistance is assumed negligible in this approach. The voids between particles are large and adsorptive motion is sufficiently fast to assume a uniform pressure in the entire adsorbent bed. The heat transfer equation for the adsorbent bed (the derivation of the equation is given in Appendix B) can be written as:

$$(\rho C_p)_{eff} \frac{\partial T}{\partial t} = \lambda_{eff} \frac{1}{R} \frac{\partial}{\partial R}\left( R \frac{\partial T}{\partial R} \right) + (1-\varphi)\rho_S \Delta H_{ads} \frac{\partial \overline{W}}{\partial t} \tag{6.1}$$

where $(\rho C_p)_{eff}$ and $\lambda_{eff}$ are the effective thermal capacitance and conductivity of the adsorbent bed. The effect of adsorbate adsorption in the adsorbent particle is contributed by $\partial \overline{W} / \partial t$ in Eq. (6.1). Since the pressure inside of the bed is uniform, there is no need to write a mass transfer equation for water vapor flow through the bed. However, an equation is required for determination of adsorption rate in the adsorbent particle. Three different models can be written as;

a) the instantaneous equilibrium model;

$$\frac{\partial \overline{W}}{\partial t} = \frac{\partial \overline{W}_\infty}{\partial t} \tag{6.2}$$

where $\overline{W}$ and $\overline{W}_\infty$ are the average adsorbate concentration in the adsorbent particle and equilibrium adsorbate concentration.

b) LDF model;

According to this model, which is based on Fick's law, the change of mean adsorbate concentration with time is proportional to the difference between the adsorbed and equilibrium concentrations;

$$\frac{\partial \overline{W}}{\partial t} = \frac{15 D_{eff}}{r_p^2} \left( \overline{W}_\infty - \overline{W} \right) \tag{6.3}$$

c) The solid diffusion model;

The model is based on Fick's law and the following partial differential equation should be solved to obtain the variation of local adsorbate concentration with time in the particle;

$$\frac{\partial W}{\partial t} = \frac{1}{r^2} \frac{\partial}{\partial r} \left( r^2 D_{eff} \frac{\partial W}{\partial r} \right) \tag{6.4}$$

where $D_{eff}$ and $r_p$ represent effective diffusivity and radius of the adsorbent particle. $D_{eff}$ can be found from Arrhenius equation (Ben Amar et al. 1996):

$$D_{eff} = D_o e^{-E/RT} \tag{6.5}$$

where $D_o$ is the reference diffusivity and E is the diffusion activation energy (Appendix A Table A2). In order to solve mass transfer equation for the particle (Eq. (6.3)), a relation for equilibrium state (i.e. $\overline{W}_\infty$) must be known. The following isotherm equation can be used to determine adsorbate equilibrium concentration in the silica gel particle for a given pressure and temperature (Leong and Liu 2004, Sakoda and Suzuki 1984, Sakoda and Suzuki 1986):

$$\overline{W}_\infty = k \left( P / P_{sat} \right)^{1/n} \tag{6.6}$$

where k and n are the constants for the specific adsorbent-adsorbate pair. The symbol $P_{sat}$ represents water vapor saturation pressure at the considered temperature. As given in Chapter 2, the effective thermal capacity and thermal conductivity are calculated by using the following relations:

$$(\rho C_p)_{eff} = (1-\varphi)\left\{(\rho C_p)_s + \rho_s C_{p_l} \overline{W}\right\} + \varphi(\rho C_p)_v \tag{6.7}$$

$$\lambda_{eff} = (1-\varphi)\lambda_s + \varphi\lambda_v \tag{6.8}$$

The initial and boundary conditions of the problem for uniform pressure approach are given in Table 6.1.

## 6.2.2. Dimensionless Form

The following dimensionless parameters are defined to obtain the dimensionless form of the governing equations (Eqs. (6.1-6.4)):

$$R^* = \frac{R}{R_i},\ \theta = \frac{T - T_{ref}}{\Delta T}, \tau = \frac{\alpha_{eff}\, t}{R_i^2};\ W^* = \frac{W - W_{ref}}{\Delta W}; r^* = \frac{r}{r_p} \tag{6.9}$$

Table 6.1. The initial and boundary conditions of the problem for the uniform pressure approach

| Uniform Pressure Approach | | | |
|---|---|---|---|
| **Dependent variable** | **B.C at R=$R_i$** | **B.C atR=$R_o$** | **Initial conditions** |
| Temperature (K) | $\partial T / \partial R = 0$ | $T = T_a$ | $T = T_d$ |
| Adsorptive pressure (kPa) | $P = P_{const}$ | $P = P_{const}$ | $P = P_{const}$ |
| Amount of adsorbate ($kg_v\ kg_s^{-1}$) | $W = f(P,T)$ | $W = f(P,T)$ | $W$ = initial value @$T_d$ |

The definitions of $W_{ref}$ and $\Delta W$ depend on the process. Figure 6.3 shows an isobaric adsorption process on Clapeyron diagram. The adsorption process is started when

adsorbate concentration in the adsorbent bed is $W_d$ and bed temperature is at $T_d$. The process is finished when the adsorbate concentration is attained to $W_a$ while the bed temperature is decreased to $T_a$. For adsorption process, $W_{ref}$ and $\Delta W$ can be defined as $W_d$ and $(W_a - W_d)$, respectively. Similarly, $T_{ref}$ and $\Delta T$ in Eq.(6.7) are $T_a$ and ( $T_d - T_a$).

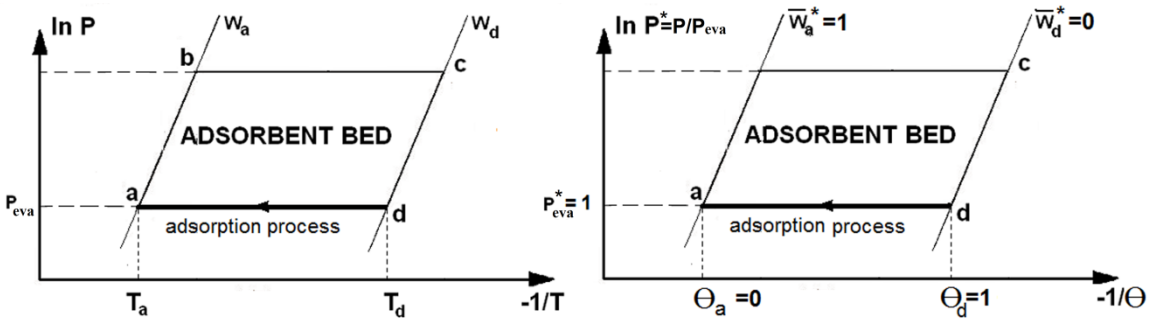


(a) (b)

Figure 6.3. A schematic view of adsorption process on Clapeyron diagram, (a) dimensional isoster, (b) dimensionless isoster.

By using the above dimensionless parameters, the dimensionless form of heat transfer equation for the bed become as:

$$\frac{\partial \theta}{\partial \tau} = \frac{1}{R^*}\frac{\partial}{\partial R^*}\left(R^* \frac{\partial \theta}{\partial R^*}\right) + Ku\frac{\partial \overline{W}^*}{\partial \tau} \tag{6.10}$$

while the dimensionless forms of mass transfer models for adsorbent particle are;

$$\frac{\partial \overline{W}^*}{\partial \tau} = \frac{\partial \overline{W}_\infty^*}{\partial \tau} \tag{6.11}$$

$$\frac{\partial \overline{W}^*}{\partial \tau} = 15\Gamma\left(\overline{W}_\infty^* - \overline{W}^*\right) \tag{6.12}$$

$$\frac{\partial \overline{W}^*}{\partial \tau} = \frac{\Gamma}{r^{*2}}\frac{\partial}{\partial r^*}\left(r^{*2}\frac{\partial \overline{W}^*}{\partial R^*}\right) \tag{6.13}$$

where Ku and Γ in the above equations are dimensionless independent parameters and they are defined as:

$$Ku = \frac{\rho_s \, \Delta H_{ads} \Delta \overline{W} (1-\varphi)}{(\rho C_p)_{eff} \, \Delta T} \tag{6.14}$$

$$\Gamma = \frac{D_{eff} \ / r_p^2}{\alpha_{eff} \ / R_i^2} \tag{6.15}$$

The dimensionless parameter Ku represents the ratio of heat of adsorption to the sensible thermal energy storage (Federov and Viskanta 1999). The Γ parameter refers to the ratio of mass transfer diffusion in the radial direction of adsorbent particle to the heat transfer diffusion in the radial direction of the adsorbent bed.

The dimensionless initial and boundary conditions of the problem for uniform pressure approach are given in Table 6.2.

Table 6.2. The dimensionless initial and boundary conditions of the problem with for the uniform pressure approach

| **Uniform Pressure Approach** | | | |
|---|---|---|---|
| **Dependent variable** | **B.C at $R^*$=1** | **B.C at $R^*$=$R_o$/ $R_i$** | **Initial conditions** |
| Dimensionless Temperature | $\partial\theta / \partial R^* = 0$ | $\theta = 0$ | $\theta = 1$ |
| Dimensionless adsorptive pressure | $P^* = 0$ | $P^* = 0$ | $P^* = 0$ |
| Dimensionless amount of adsorbate | $W^* = f(P^*, \theta)$ | $W^* = f(P^*, \theta)$ | $W^* = 0$ |

## 6.3. Non-Uniform Pressure Approach

For both the dimensional and dimensionless forms of the non-uniform pressure approach, the governing equations are given in this section. The initial and boundary conditions are also mentioned in tables for each dimensional and dimensionless form of the non-uniform pressure approach used in the theoretical studies.

### 6.3.1. Dimensional Form

In this approach, the effect of interparticle mass transfer resistance is taken into account. The change of water vapor pressure in the voids between silica gel particles during the adsorption process is considered (Figure 6.2(b)). The continuity equation based on conservation of mass for water vapor flow through the adsorbent bed (the derivation of the equation is given in Appendix B) can be written as:

$$\varphi \frac{\partial \rho_v}{\partial t} + \frac{1}{R}\frac{\partial}{\partial R}\left(R\rho_v V_r\right) + (\varphi - 1)\rho_s \frac{\partial \overline{W}}{\partial t} = 0 \tag{6.16}$$

The heat transfer equation for the adsorbent bed involving silica gel particle(the derivation of the equation is given in Appendix B), water vapor and adsorbed water can be written as:

$$\left(\rho C_p\right)_{eff} \frac{\partial T}{\partial t} + \frac{1}{R}\frac{\partial}{\partial R}\left(R\rho_v V_r C_{p_v} T\right) = \lambda_{eff} \frac{1}{R}\frac{\partial}{\partial R}\left(R\frac{\partial T}{\partial R}\right) + (1-\varphi)\rho_s \Delta H_{ads} \frac{\partial \overline{W}}{\partial t} \tag{6.17}$$

In the above equation, $V_r$ is facial water vapor velocity and can be calculated by Darcy law. As it was mentioned before Darcy's law is a simple proportional relationship among the fluid flow rate through a porous medium, the fluid viscosity and the pressure drop for a given distance. For the present problem, it can be written as:

$$V_r = \frac{K_{app}}{\mu}\left(-\frac{\partial P}{\partial x}\right) \tag{6.18}$$

where $K_{app}$ and $\mu$ are apparent permeability of the silica gel bed and the water vapor viscosity. The ideal gas relation is used to calculate the pressure change of the water vapor in the silica gel bed. The apparent permeability of the silica gel bed, $K_{app}$, can be calculated by the following relation (Leong and Liu 2004):

$$K_{app} = K_{inh} + \frac{\varphi\mu}{\tau P} D_{bed} \tag{6.19}$$

where $K_{inh}$ is the inherent permeability and $D_{bed}$ is the mass diffusivity of the bed. The inherent permeability can be obtained by using Blake–Kozeny relation which is valid for void fractions less than φ=0.5 (Bird et al. 2002):

$$K_{inh} = \frac{r_p^2 \varphi^3}{37.5(1-\varphi)^2} \tag{6.20}$$

The adsorbate can also be diffused in the voids between adsorbent particles. Two diffusion mechanisms which are Knudsen and molecular diffusions should be taken into account. As known, when the collisions between a molecule and the pore walls occur more frequently than collisions between diffusing molecules, the diffusion is called as Knudsen diffusion, and it can be calculated from the following equation:

$$D_k = 97 r_{pore} \sqrt{T/M} \tag{6.21}$$

When the pore diameter is larger than the average distance between molecular collisions and the collisions between diffusing molecules occur more frequently than collisions between molecules and the pores wall, the diffusion mechanism is called as molecular diffusion. The molecular diffusivity can be obtained from Eq. (6.22).

$$D_m = 0.02628 \frac{\sqrt{T^3/M}}{P\sigma^2\Omega} \tag{6.22}$$

As explained in Chapter 2, for remindy, the effect of overall diffusion in the voids between the particles in the adsorbent bed can be obtained by considering both effects of Knudsen and molecular diffusion (Karger and Ruthven 1992):

$$\frac{1}{D_{bed}} = \frac{1}{D_m} + \frac{1}{D_k} \tag{6.23}$$

For the non-uniform approach, the LDF relation (Eq. (6.3)) is also used to determine the change of mean adsorbate concentration in the adsorbent particle at the given temperature and pressure.

The initial and boundary conditions of the problem for non-uniform pressure approach are given in Table 6.3.

Table 6.3. The initial and boundary conditions of the problem for non-uniform pressure approach

| **Non-uniform Pressure Approach** | | | |
|---|---|---|---|
| **Dependent variable** | **B.C at R=$R_i$** | **B.C atR=$R_o$** | **Initial conditions** |
| Temperature (K) | $\partial T / \partial R = 0$ | $T = T_a$ | $T = T_d$ |
| Adsorptive pressure (kPa) | $P = P_{const}$ | $\partial P / \partial R = 0$ | $P = f(\rho, T)$ |
| Adsorptive density (kg $m^3$) | $\rho_v = f(P,T)$ | $\rho_v = f(P,T)$ | $\rho_v$ = initial value @ $T_d$ |
| Amount of adsorbate ($kg_v$ $kg_s^{-1}$) | $W = f(P,T)$ | $W = f(P,T)$ | $W$ = initial value @ $T_d$ |
| Adsorptive velocity (m $s^{-1}$) | $V_r = f(\rho_v)$ | $V_r = 0$ | $V_r = 0$ |

## 6.3.2. Dimensionless Form

The following dimensionless parameters are defined to obtain the dimensionless form of the governing equations (Eqs. (6.16-6.18)):

$$R^* = \frac{R}{R_i},\ \theta = \frac{T - T_a}{T_d - T_a},\ \tau = \frac{\alpha_{eff}\, t}{R_i^2};\ W^* = \frac{W - W_d}{W_a - W_d};$$

$$\rho^* = \frac{\rho - \rho_d}{\rho_a - \rho_d};\ P^* = \frac{P - P_d}{P_a - P_d};\ V_r^* = \frac{V R_i}{\alpha_{eff}} \qquad (6.24)$$

By using the above dimensionless parameters, the dimensionless form of the continuity equation for the bed become as:

$$\frac{\partial \rho^*}{\partial \tau} + \frac{1}{\varphi}\frac{1}{R^*}\frac{\partial}{\partial R^*}\left(R^* \rho^* V_r{}^*\right) + \frac{(\varphi - 1)}{\varphi} G \frac{\partial \overline{W}^*}{\partial \tau} = 0 \tag{6.25}$$

Dimensionless heat transfer equation for the adsorbent bed can be written as:

$$\frac{\partial \theta}{\partial \tau} + \Pi \frac{1}{R^*}\frac{\partial}{\partial R^*}\left(R^* \rho^* V_r{}^* \theta\right) = \frac{1}{R^*}\frac{\partial}{\partial R^*}\left(R^* \frac{\partial \theta}{\partial R^*}\right) + Ku \frac{\partial \overline{W}^*}{\partial \tau} \tag{6.26}$$

while the dimensionless forms of mass transfer model for adsorbent particle is same as Eq. (6.12)

$$\frac{\partial \overline{W}^*}{\partial \tau} = 15\Gamma\left(\overline{W}_\infty^* - \overline{W}^*\right) \tag{6.12}$$

The Darcy flow also can be written as;

$$V_r{}^* + \mathrm{K}\frac{\partial P^*}{\partial R^*} = 0 \tag{6.27}$$

where $Ku, \Pi, G, \Gamma$, and $\mathrm{K}$ in the above equations are dimensionless independent parameters and they are defined as:

$$Ku = \frac{\rho_S \, \Delta H_{ads} (1-\varphi)(W_a - W_d)}{(\rho C_p)_{eff} (T_d - T_a)} \tag{6.14}$$

$$\Pi = \frac{C_{p_v} (\rho_a - \rho_d)}{(\rho C_p)_{eff}} \tag{6.28}$$

$$G = \frac{\rho_S (W_a - W_d)}{(\rho_a - \rho_d)} \tag{6.29}$$

$$\Gamma = \frac{D_{eff} / r_p^2}{\alpha_{eff} / R_i^2} \tag{6.15}$$

$$\mathrm{K} = \frac{K_{app}\ \Delta P_{\max}}{\mu \alpha_{eff}} \tag{6.30}$$

where $\Delta P_{\max}$ = max pressure drop in radial direction

The dimensionless parameter Ku represents the ratio of heat of adsorption to the sensible thermal energy storage. The Γ parameter refers to the ratio of mass transfer diffusion in the radial direction of adsorbent particle to the heat transfer diffusion in the radial direction of the adsorbent bed. K represents the dimensionless potential velocity and the ratio of the interparticle mass transfer to the heat diffusion in the bed. Π is the ratio of adsorptive thermal capacitance to the effective thermal capacitance of the adsorbent bed where G gives the slope of the isotherm.

The dimensionless initial and boundary conditions of the problem for non-uniform pressure approach are given in Table 6.4.

Table 6.4. The dimensionless initial and boundary conditions of the problem for the non-uniform pressure approach

| **Non-uniform Pressure Approach** | | | |
|---|---|---|---|
| **Dependent variable** | **B.C at R=1** | **B.C at $R^*=R_o/R_i$** | **Initial conditions** |
| Dimensionless Temperature | $\partial\theta / \partial R^* = 0$ | $\theta = 0$ | $\theta = 1$ |
| Dimensionless adsorptive pressure | $P^* = 0$ | $\partial P^* / \partial R^* = 0$ | $P^* = f(\rho^*, \theta)$ |
| Dimensionless adsorptive density | $\rho_v^* = f(P^*, \theta)$ | $\rho_v^* = f(P^*, \theta)$ | $\rho_v^* = 0$ |
| Dimensionless amount of adsorbate | $W^* = f(P^*, \theta)$ | $W^* = f(P^*, \theta)$ | $W^* = 0$ |
| Dimensionless adsorptive velocity | $V_r^* = f(\rho_v^*)$ | $V_r^* = 0$ | $V_r^* = 0$ |

## 6.4. Uniform Pressure Approach Assisted with Fins

The governing equations, initial and boundary conditions where the uniform pressure approach is used for the adsorbent bed assisted with fins are given in this section. The governing equations, initial and boundary conditions are written both for the dimensional and dimensionless forms.

### 6.4.1. Dimensional Form

The analyzed adsorbent bed is an annular bed with inner fins in radial direction as shown in Figure 6.4. It is assumed that the upper and lower surfaces of bed are well insulated and the adsorbent bed is enough long, so the end effects can be neglected. The heat and mass are transferred only in radial and angular directions of the bed. Initially, the adsorbent bed is at $T_d$ temperature and adsorbate concentration in the bed is $W_d$ as shown in Figure 6.2(a). Suddenly, the temperature of the bed outer surface falls to $T_a$ and the valve between the adsorbent bed and the evaporator (V1 valve) is opened to allow the transfer of adsorptive (i.e., water vapor) to the bed. The adsorptive can flow easily between the adsorbent particles. The interparticle mass transfer resistance is neglected. The process is isobaric and the bed pressure is not changed during the adsorption process. The bed final temperature is $T_a$ and the corresponding adsorbate concentration is $W_a$. A schematic view of dimensionless adsorption equilibria is shown in Figure 6.2(b).

The isotherm equation Eq. (6.4) can be used to determine adsorbate equilibrium concentration in the particle for a given pressure and temperature.

The heat transfer equation for the adsorbent bed assisted with fins (the derivation of the equation is given in Appendix B) can be written as:

$$\frac{\partial T}{\partial t} = \alpha_{eff}\ \frac{1}{R}\frac{\partial}{\partial R}\left(R\frac{\partial T}{\partial R}\right) + \alpha_{eff}\ \frac{1}{R^2}\frac{\partial^2 T}{\partial \phi^2} + \frac{(1-\varphi)\rho_S}{(\rho C_p)_{eff}}\Delta H_{ads}\frac{\partial W}{\partial t} \quad (6.31)$$

where $\alpha_{eff}$ is the effective thermal diffusivity. An equation for determination of adsorption rate in the adsorbent particle is required. In this study, the LDF method is used to determine the adsorption rate in the adsorbent particle as given in Eq. (6.3).

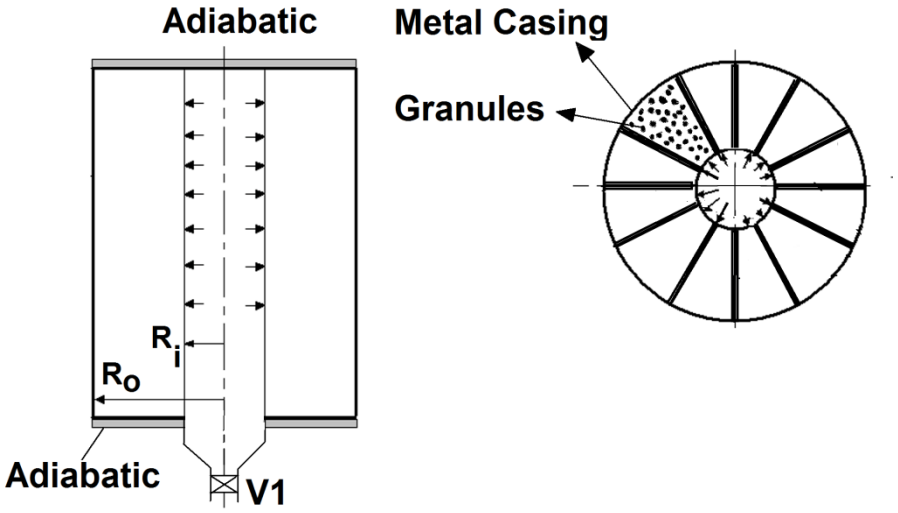


Figure 6.4. The front and top views of the analyzed adsorbent bed with 12 fins inside

Uniform temperature distribution can be assumed in the cross section of the thin fin, (i.e., $T_{fin} = f(R,t)$). The conduction heat transfer equation for the thin fin (the derivation of the equation is given in Appendix B) can be written as:

$$\left(\rho C_p\right)_{fin} \delta \frac{\partial T_{fin}}{\partial t} = \lambda_s \frac{1}{R} \frac{\partial T_{fin}}{\partial \phi}\bigg|_{fs} + \lambda_{fin} \frac{\partial^2 T_{fin}}{\partial R^2} \delta \qquad (6.32)$$

The second term of Eq. (6.28) represents the rate of heat enters or leaves the bed lateral surfaces (Figure 6.5).

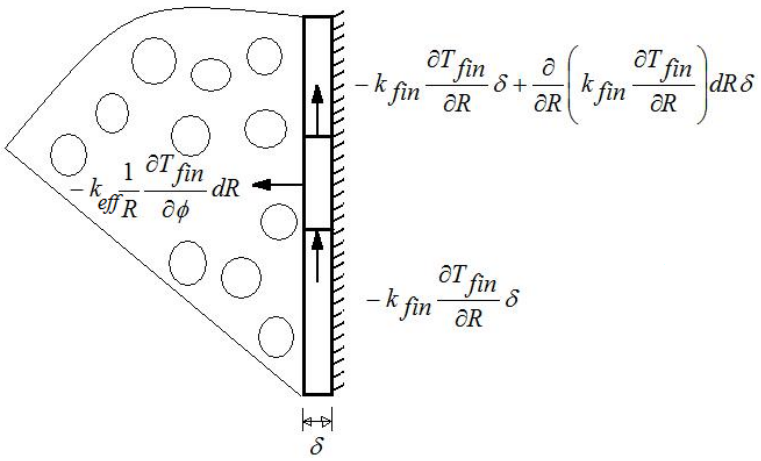


Figure 6.5. The schematic view of the derivation of fin equation

The initial and boundary conditions of the problem for uniform pressure approach assisted with fins are given in Table 6.5.

Table 6.5. The initial and boundary conditions of the problem for the uniform pressure approach assisted with fins

| **Uniform Pressure Approach Assisted with Fins** | | | |
|---|---|---|---|
| **Dependent variable** | **B.C at R=$R_i$** | **B.C atR=$R_o$** | **Initial conditions** |
| Temperature (K) | $\partial T/\partial R = 0$ | $T = T_a$ | $T = T_d$ |
| Adsorptive pressure (kPa) | $P = P_{const}$ | $P = P_{const}$ | $P = P_{const}$ |
| Amount of adsorbate ($kg_v\ kg_s^{-1}$) | $W = f(P,T)$ | $W = f(P,T)$ | $W$ = initial value @ $T_d$ |
| | **B.C at $\phi$ =0** | **B.C at $\phi = \phi_o$** | |
| Fin Temperature (K) | $\partial T/\partial R = 0$ | $T = T_{fin}$ | |

## 6.4.2. Dimensionless Form

Eqs. (6.31), (6.3), and (6.32) can be non-dimensionalized by using the dimensionless parameters as given in Eq. (6.9). By using these dimensionless parameters, the dimensionless forms of the bed heat transfer equation, particle mass balance equation and fin heat conduction equation become as:

$$\frac{\partial \theta}{\partial t} = \frac{1}{R^*}\frac{\partial}{\partial R^*}\left(R^*\frac{\partial \theta}{\partial R^*}\right) + \frac{1}{R^{*2}}\frac{\partial^2 \theta}{\partial \phi^2} + Ku\frac{\partial \overline{W}^*}{\partial t} \tag{6.33}$$

$$\frac{\partial W^*}{\partial t} = 15\Gamma\left(W_\infty{}^* - W^*\right) \tag{6.12}$$

$$\alpha^*\frac{\partial \theta_{fin}}{\partial \tau} = \Lambda\frac{1}{R^*}\frac{\partial \theta}{\partial \phi}\bigg|_{fs} + \frac{\partial^2 \theta_{fin}}{\partial R^{*2}} \tag{6.34}$$

where dimensionless parameters of Ku, $\Gamma$, $\Lambda$, and $\alpha^*$ are:

$$Ku = \frac{\rho_s \Delta H_{ads}(1-\varphi)\Delta W}{(\rho C_p)_{eff}\,\Delta T};\ \Gamma = \frac{D_{eff}/r_p^2}{\alpha_{eff}/R_i^2};\ \Lambda = \frac{\lambda_{eff}}{\lambda_{fin}}\frac{R_i}{\delta};\ \alpha^* = \frac{\alpha_{eff}}{\alpha_{fin}} \tag{6.35}$$

As mentioned before Ku represents Kutateladze number which is a dimensionless parameter shows the ratio of the generated heat due to adsorption and the sensible thermal energy storage in adsorbent bed (Federov and Viskanta 1999). The dimensionless $\Gamma$ parameter compares the adsorbate diffusion in the adsorbent particle to the transport of heat transfer throughout the adsorbent bed. The dimensionless parameter of $\Lambda$ is the dimensionless fin coefficient and refers to the ratio of heat transfer from the fin lateral surface to the diffusion of heat in radial direction of the fin. Finally, $\alpha^*$ parameter is the ratio of effective thermal diffusivities of adsorbent medium and fin.

The dimensionless initial and boundary conditions of the problem for uniform pressure approach assisted with fins are given in Table 6.6.

## 6.5. Two Dimensional Uniform Pressure Approach (r and z)

As mention in the first section, the interparticle mass transfer resistance is assumed negligible in uniform pressure approach. The equations given in this section is used in the numeric program which was used to validate the experimental results of this study. The equations consist of two directions for the bed as r and z directions. The z

direction is taken due to the temperature difference in the z direction. The heat transfer equation for the adsorbent bed can be written as:

$$(\rho C_p)_{eff}\ \frac{\partial T}{\partial t} = \lambda_{eff}\ \frac{1}{R}\frac{\partial}{\partial R}\left(R\frac{\partial T}{\partial R}\right) + \lambda_{eff}\ \frac{\partial}{\partial z}\left(\frac{\partial T}{\partial z}\right) + (1-\varphi)\rho_S \Delta H_{ads}\ \frac{\partial \overline{W}}{\partial t} \qquad (6.36)$$

where $(\rho C_p)_{eff}$ and $\lambda_{eff}$ are the effective thermal capacitance and conductivity of the adsorbent bed. The effect of adsorbate adsorption in the adsorbent particle is contributed by $\partial \overline{W} / \partial t$. In this approach, there is no need to write a mass transfer equation for water vapor flow through the bed.

The Linear Drive Force (LDF) model is used to determine the change of mean adsorbate concentration with time;

$$\frac{\partial \overline{W}}{\partial t} = \frac{15 D_{eff}}{r_p^2}\left(\overline{W}_\infty - \overline{W}\right) \qquad (6.3)$$

where $D_{eff}$ and $r_p$ represent effective diffusivity and radius of the adsorbent particle.

The effective thermal capacity and thermal conductivity are calculated by using the following relations:

$$(\rho C_p)_{eff} = (1-\varphi)\left\{(\rho C_p)_S + \rho_S C_{p_l} \overline{W}\right\} + \varphi(\rho C_p)_V \qquad (6.7)$$

$$\lambda_{eff} = (1-\varphi)\lambda_S + \varphi\lambda_V \qquad (6.8)$$

Table 6.6. The dimensionless initial and boundary conditions of the problem for the uniform pressure approach assisted with fins

| **Uniform Pressure Approach Assisted with Fins** | | | |
|---|---|---|---|
| **Dependent variable** | **B.C at $R^*=1$** | **B.C at $R^*=R_o/R_i$** | **Initial conditions** |
| Dimensionless Temperature | $\partial\theta / \partial R^* = 0$ | $\theta = 0$ | $\theta = 1$ |
| Dimensionless adsorptive pressure | $P^* = 0$ | $P^* = 0$ | $P^* = 0$ |
| Dimensionless amount of adsorbate | $W^* = f(P^*, \theta)$ | $W^* = f(P^*, \theta)$ | $W^* = 0$ |
| Dimensionless Fin Temperature | $\partial\theta_{fin} / \partial R^* = 0$ | $\theta_{fin} = 0$ | |
| | **B.C at $\phi$ =0** | **B.C at $\phi = \phi_o$** | |
| Fin Temperature (K) | $\theta = \theta_{fin}$ | $\partial\theta / \partial R^* = 0$ | $\theta_{fin} = 1$ |

The initial and boundary conditions of the problem for uniform pressure approach in r and z directions are given in Table 6.7.

Table 6.7. The initial and boundary conditions of the problem for the uniform pressure approach in r and z directions

| **Uniform Pressure Approach** | | | | |
|---|---|---|---|---|
| **Dependent variable** | **B.C at R=$R_i$** | **B.C at R=$R_o$** | **B.C at z=$z_{upper}$**<br>**B.C at z=$z_{lower}$** | **Initial conditions** |
| Temperature (K) | $\partial T / \partial R = 0$ | $T = T_{bs}$ | $T = T_{up}$<br>$T = T_{lo}$ | $T = T_{bs}$ |
| Adsorptive pressure (kPa) | $P = P_{const}$ | $P = P_{const}$ | $P = P_{const}$ | $P = P_{const}$ |
| Amount of adsorbate ($kg_v\ kg_s^{-1}$) | $W = f(P,T)$ | $W = f(P,T)$ | $W = f(P,T)$ | $W = 0$ |

# CHAPTER 7

# EXPERIMENTAL SETUP AND PROCEDURE

In this chapter, an experimental setup which had been designed and constructed is explained. The setup was designed to investigate heat and mass transfer in an adsorbent bed of an adsorption heat pump and to validate the obtained numerical results. The silica gel/water pair was used. The adsorbent bed is an annular bed. The main objective of this setup is to find out temperature profiles in a granular adsorbent bed during adsorption process. The numerically obtained results were compared with the temperature profiles of the experiments. The comparisons of numerical and experimental results are given in Chapter 9.

## 7.1. The Designed Setup

The designed adsorbent bed is cylindrical in shape. The setup was constructed from a stainless steel pipe (type 304). The setup has two main components as adsorbent bed and an evaporator. The evaporator was filled with water while the adsorbent bed was filled with silica gel particles. The porosity of the silica gel inside of the bed was assumed as 0.45 (Collins 1961, Heinemann 2005). As seen from the Figure 7.1, the constructed setup has only one adsorbate container functions as both condenser and evaporator. The adsorbent bed and evaporator were fixed on a steel frame. A vacuum tight valve was located between the adsorbent bed and adsorbate container. The level of adsorbate can be measured from the sight glasses mounted on the casing of adsorbate container. An outlet was provided for filling of adsorbate to the container on top of the adsorbate container. There is a drain pipe for draining of adsorbate on the bottom of container. A heat exchanger was located in the container to provide heat transfer between adsorbate and a working fluid.

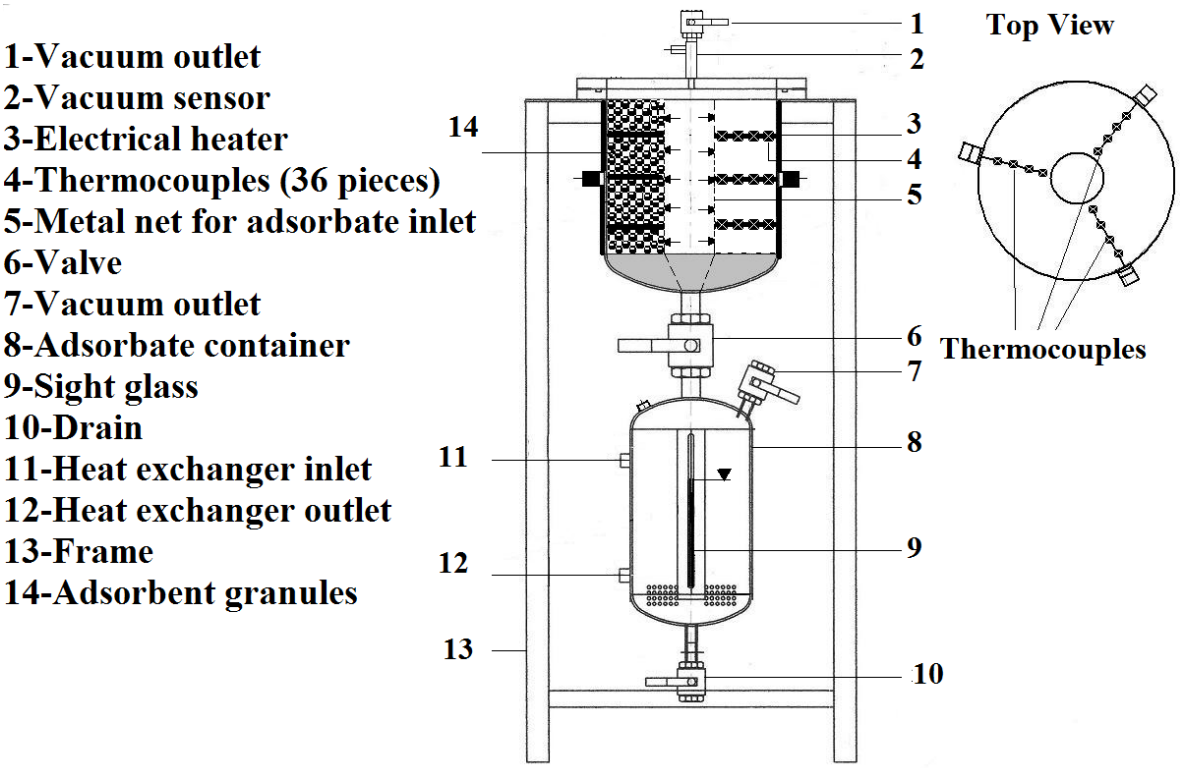


Figure 7.1. A schematic view of the first designed setup

A vacuum outlet and a vacuum sensor were connected to the adsorbent bed. During the adsorption and desorption processes, the adsorbent bed was cooled and heated from the outer surface of annulus bed. The adsorbent bed was heated by electrical resistance which is surrounded around its outer surface. The constructed setup and its components can be seen in Figure 7.2.

.

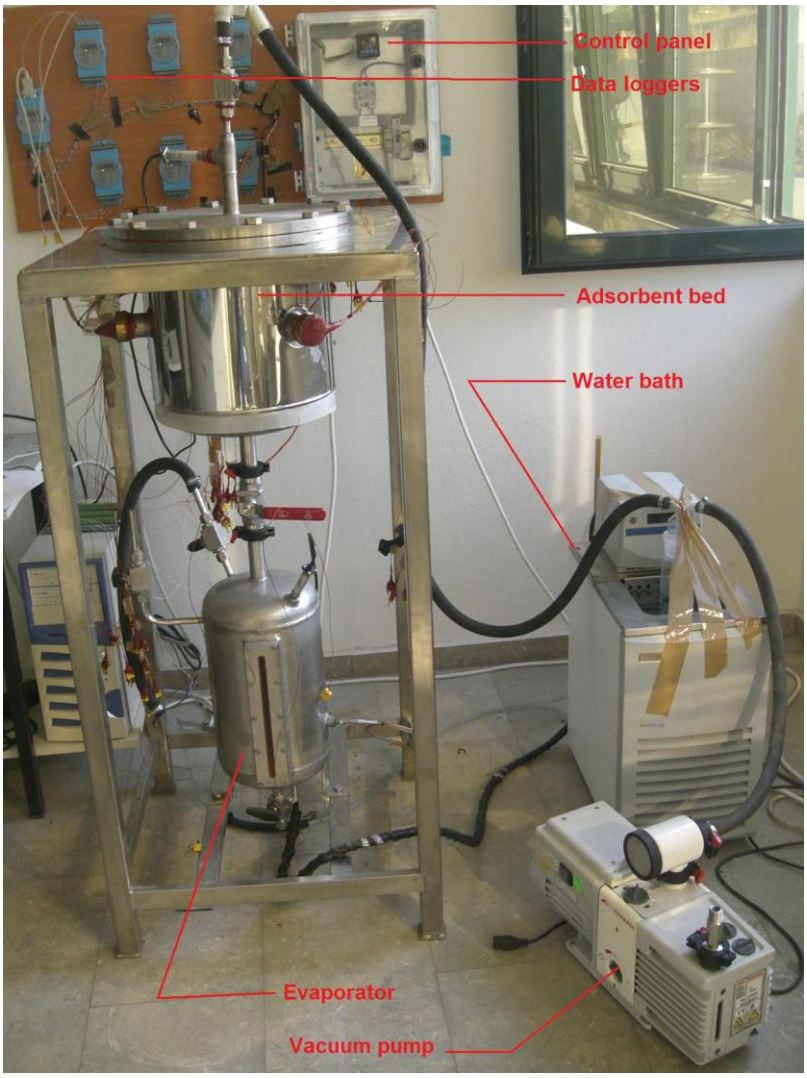


Figure 7.2. A view of the experimental setup

The temperature and pressure were measured by sensors and acquired by using a data logger card and software. The data were transferred to a computer and automatically saved. The picture of data loggers and the control panel of the resistance is illustrated in Figure 7.3.

Figure 7.3. Data logger set and the electrical resistance control panel

## 7.2. Components of the Experimental Setup

As mentioned, the experimental setup consists of equipments. Detailed information about the equipments used in the experimental setup is given in this chapter.

### 7.2.1. The Evaporator/Condenser

The setup has one evaporator/condenser tank which has a volume of 10 lt. The evaporator basically consists of a stainless steel container, a pressure transducer, a thermocouple, and four vacuum valves (a valve for water supply inlet, a valve for vacuum connector, a valve to drain water and a valve between the evaporator and the adsorbent bed) as shown in Figure 7.4. A heat exchanger was located inside the evaporator; this heat exchanger was used to transfer heat from water flowing from the water bath to the water inside the container and provide boiling of water. The inlet and outlet of the heat exchanger were connected to water bath. The length of the heat exchanger is 12 m and the diameter is 6 mm. The water level in the container can be observed from the sight glass located in front of the evaporator. The amount of the adsorbed water can be determined by this way. A thermocouple located inside the evaporator measures the temperature of the water in the container. The evaporator was insulated by flexible insulation plates.

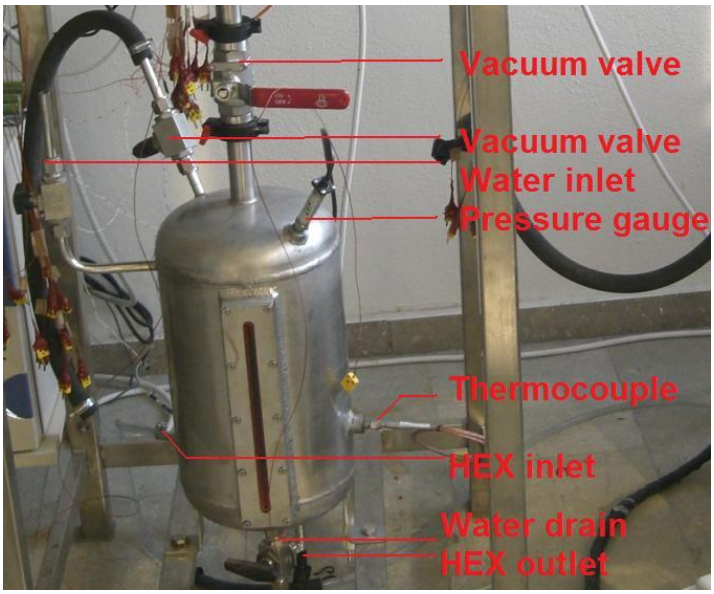


Figure 7.4. The evaporator and its components

### 7.2.2. The Adsorbent Bed

As illustrated in Figure 7.2, the adsorbent bed is an annular steel container (type 304) and with 4 mm thickness and 309 mm inner diameter. The height of the bed is 290 mm. In the middle of the adsorbent bed, a free space with 50 mm diameter in the vertical direction provided for free transfer of adsorptive. On the adsorbent bed, there is a valve used to connect the adsorbent bed to vacuum pump and there is a pressure transducer. There are three outlets for the thermocouples on the adsorbent bed located at the circumferences of the container with $120^{o}$ angle between them. Inner design of the adsorbent bed was obligated to be modified during the experiments due to the desorption constraints. The detailed information of the inner design of the bed is given below. Two different adsorbent bed were designed and constructed in this study. There were difficulties with the first experimental setup and the change of the adsorbent bed was required. Both the first and the second adsorbent beds are explained in the following sections.

#### 7.2.2.1. The First Constructed Adsorbent Bed

To obtain the temperature variation inside of the adsorbent bed, totally 36 thermocouples were located inside of the bed. The locations of thermocouples are also

shown in Figure 7.5. The thermocouples were located at 0, 120, and 240 degrees in θ direction and the distance between thermocouples in radial and z direction are 25 mm and 90 mm, respectively (total 36 measurement points).

Figure 7.5. An inside view of the designed adsorbent bed and locations of the thermocouples

A metal mesh made of steel was located in the middle of the adsorbent bed for free transferring of the adsorptive into the adsorbent bed in radial direction. Then, the adsorbent bed was filled with 17.4 kg silica gel particles. To close the cover of the adsorbent bed, red silicone (Loctite Co.) which has a resistance up to 300$^{o}$C were filled to seal ring red groove. The groove has a resistance temperature up to 300$^{o}$C. Then, the cover of the bed was closed with 12 cap screws.

The outer surface of the adsorbent bed was covered with an electrical heater and the heater was controlled by a PID temperature controller during vacuum period and had 1kW heating capacity.

### 7.2.2.2. The Modified Adsorbent Bed

The experiments performed by the first setup failed due to the desorption difficulties. So, the amount of silica gel was reduced in the second design. By this method, the desorption process time was shortened due to the less mass of the silica gel in the adsorbent bed. In the second experimental setup, the bed was divided into three parts. The silica gel was located in the mid part of the bed. The amount of the silica gel was reduced. The design steps are shown in Figure 7.6. As seen from Figure 7.6 (a) and

(b), the upper and lower thermocouples were removed and the thermocouples in the mid part of the bed were not changed. Three rectangular metal supporters made of stainless steel (Figure 7.6 (c)) were placed at the bottom of the bed (Figure 7.6 (d)). Teflon sheet was placed over these metal supporters to close (or cancel) the bottom part of the bed. The metal supporters were fixed by an adhesive band which is durable to high temperature. The bottom part of the bed was filled with Teflon chips as a thermal insulator as seen from Figure 7.6 (e). The Teflon was chosen because of resistance to high temperature and no water adsorptivity. The Loctite 5368 material was applied to the bed inner surface acts as a gasket (Figure 7.6 (f)) for the Teflon sheet that was placed over this sealant. The bottom part of the bed was covered by 2 mm thick Teflon sheet and the applied sealant completely separated the bottom and the mid part of the bed (Figure 7.6 (g)). A metal net which has 0.08 m radius was replaced on the Teflon sheet. This metal net was placed (Figure 7.6 (h)) for free transferring of the adsorptive into the adsorbent bed in radial direction. Then the thermocouples (totally 6 thermocouples) near the inner part of the adsorbent bed were removed. Three of these thermocouples were placed on the surface of the Teflon sheet on three different points (0, 120, 240 degrees) for measuring the temperature of upper part of the sheet. Then the silica gel granules which are totally 3.16 kg were placed between the metal net and the outer surface as illustrated in Figure 7.6 (i). After these steps, 2 mm Teflon sheet was placed over them and sealed with the same sealant and by the same isolation procedure (Figure 7.6 (j)) followed for the first Teflon sheet at the bottom of the silica gel granules. The other three thermocouples were fixed under the upper Teflon sheet to measure the lower side temperature of the sheet.

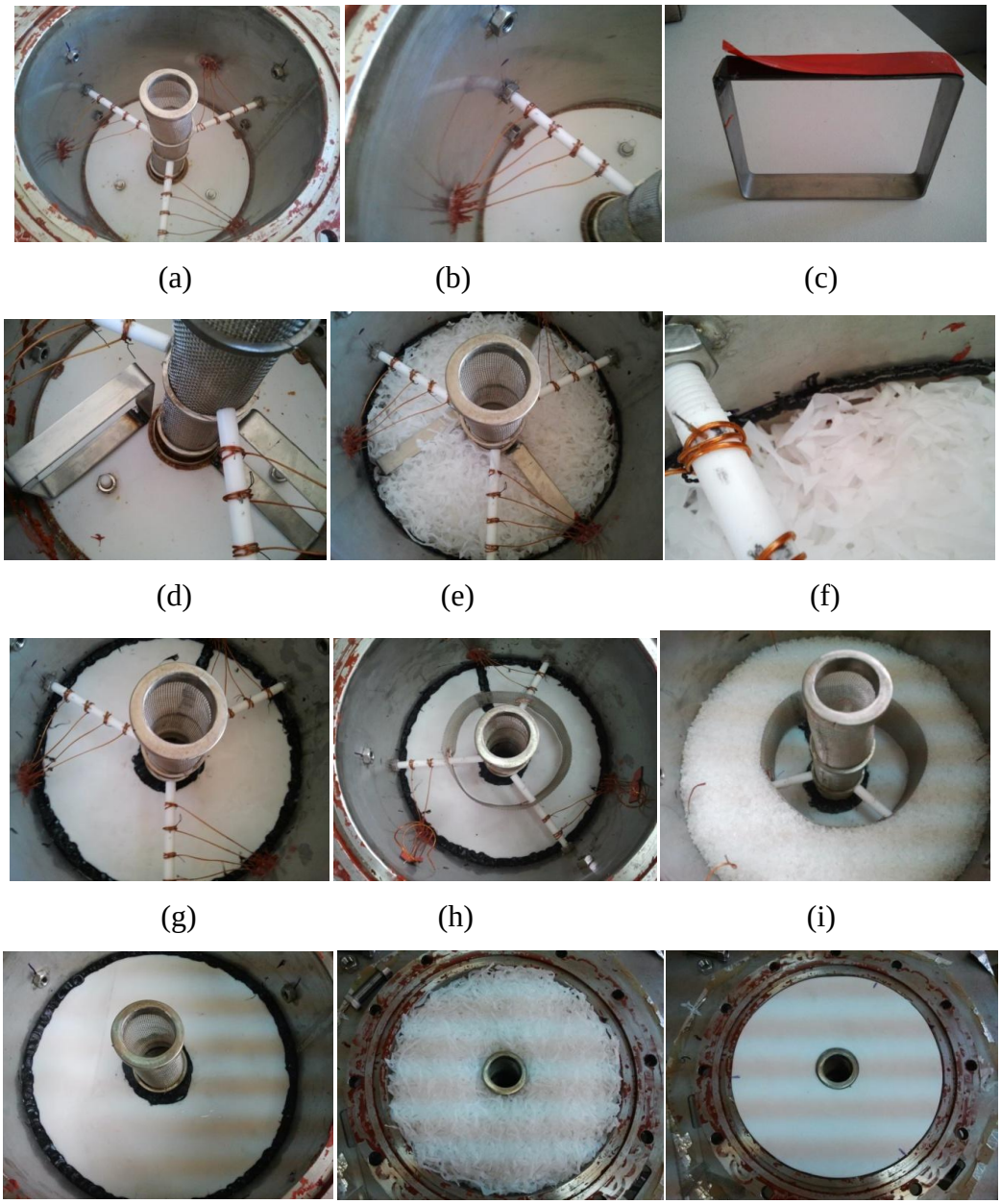

(a) (b) (c)

(d) (e) (f)

(g) (h) (i)

(j) (k) (l)

Figure 7.6. The construction details of the modified adsorbent bed

By using these six thermocouples (three on the surface of the first sheet, three over the surface of the second sheet), the upper and the lower surface temperatures of the silica gel volume were measured. Teflon chips were placed to the upper part of the bed over the second Teflon sheet (Figure 7.6 (k)). Before the Teflon chips placed in the bed, the weight of them was measured and the porosity of the Teflon chips was calculated. Finally, the third Teflon sheet was placed on the top of the bed (Figure 7.6 (l)) and the cover of the bed was closed. The cover was mounted to the bed by screws. The schematic view of the modified adsorbent bed is illustrated in Figure 7.7.

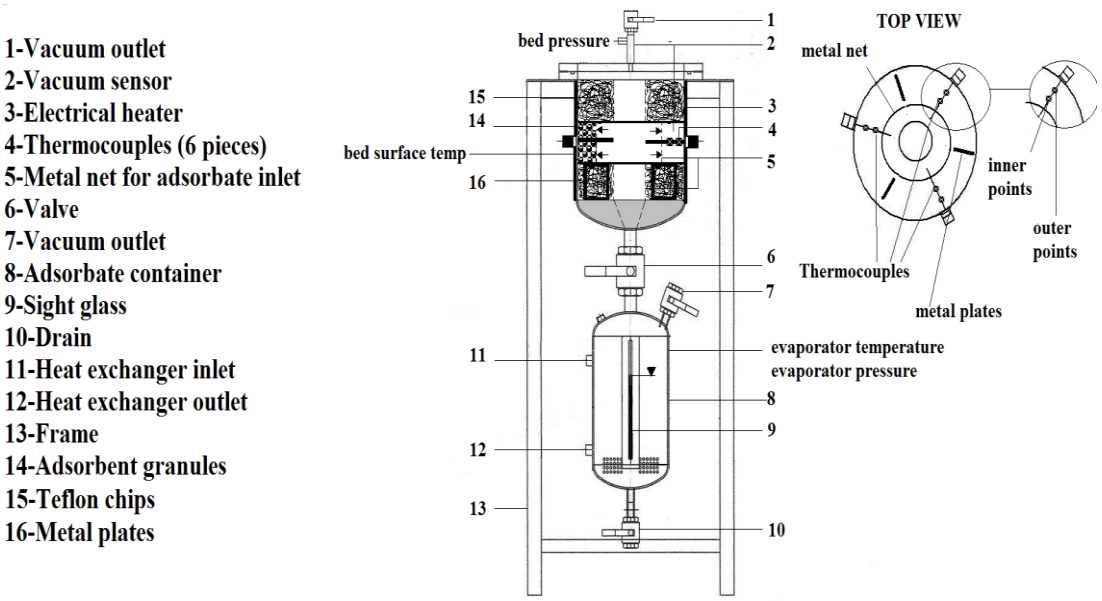


Figure 7.7. A schematic view of the modified setup

## 7.2.3. Silica Gel

The silica gel used in the adsorbent bed was supplied from Merck Co.. The shape of silica gel is assumed spherical and the equivalent diameter of adsorbent granules varies between 3 - 5 mm. It has 25% water adsorption capacity by weight. BET (Braunauer Emmet and Teller - the physical adsorption of gas molecules on a solid surface) surface area and average pore diameter of silica gel were given as 626 $m^2g^{-1}$ and 2.0-2.5 nm respectively. The specific heat and the density of the silica gel were given as 1 kJ/kg$^o$C and 750 kg/$m^3$, respectively. The heat of adsorption per kg adsorbed water is taken as 2644 kJ from the Ref (Demir et al. 2011).

## 7.2.4. The Water Bath

The temperature stability of the inlet water for the heat exchanger (serpentine) was maintained by a constant temperature water bath which has 7 lt water capacity and its operating temperature range changes from -40 to 200$^o$C with ±0.01$^o$C stability. The temperature setting is digital. The bath has been made out of stainless steel.

### 7.2.5. The Vacuum Pump

A small wet/dry RV rotary vane vacuum pump from Edwards Co. was used for vacuuming. The vacuum pump is oiled type with 1 lt oil capacity. At high vacuum mode, the ultimate min. pressure of the pump is $2x10^{-3}$ mbar. The motor powers at 50 Hz is 450 W and at 60 Hz is 550 W.

### 7.2.6. The Data Loggers

The thermocouples located in the adsorbent bed, in the evaporator, and on the other parts of the setup are K type thermocouples. Six data loggers and a module are used to collect the data from the thermocouples and pressure gauges. The data loggers each have 16-bit 8-channel analog input module that provides programmable input ranges on all channels. Each input provides 3000 V DC of isolation between the analog input and the module. The data loggers use a 16-bit microprocessor-controlled sigma-delta A/D converter to convert sensor voltage or current into digital data. The module sends the data to the host computer through a standard RS-485 interface. Sampling rate is 2 secs. for 18 hours.

### 7.2.7. The Control Panel

The control panel was used to control the electrical heater on the adsorbent bed. A thermocouple was located between the heater and the adsorbent bed and by this thermocouple, the temperature was measured and the electrical heater was controlled. This thermocouple was connected to the control panel which is controlled by step control module. For desorption and adsorption processes, this control panel controls the current or voltage to the electrical resistance. It has 2 unit relay output and 1 unit transmitter output.

### 7.2.8. The Pressure Gauge

Two identical pressure gauges were used on the setup the pressures of the evaporator and the adsorbent bed. These pressure gauges have ±0.4% accuracy and have a range 1 to 5 V output. The stainless steel pressure gauges have a measurement range 101.6 kPa to 0 kPa. They can endure temperatures range -29 to 71$^{o}$C.

### 7.2.9. The Thermocouples in the Adsorbent Bed

The K type thermocouples were located inside of the adsorbent bed which all of them are thermally insulated probes with a flexible wire. They measure the local temperature at the located position. The response time of the K type thermocouples is 0.5 sec. Their operation temperature is from -250 to 404$^{o}$C.

### 7.2.10. The Software

The software used for monitoring and data logging includes task, script, and display configuration and provided by the Advantech Co. named as Advantech Genidaq. The software provides an object based graphical interface that simplifies control and display setup. The software provides to configure the parameters and connect the toolbox. The data are saved automatically and can be transferred to Excel data file.

## 7.3. Leakage Problems of the Adsorbent Bed and Employed Solution

Even though the experimental setup was designed and constructed to work under vacuum, many leakage problems were observed. To overcome the air leakage, many methods were applied:

Firstly, the thermocouple cables which are connected to the inside of three cable ports were placed in a thick plastic hose to prevent leakage from the cable coating of the thermocouples as illustrated in Figure 7.8 (a). The thermocouple cable ports which are coming out of the adsorbent bed were covered with a red silicone sealant (Loctite Co.)

which has thermally resists up to 300$^{o}$C (Figure 7.8 (b)). Based on our observation, the most important leakage problem occurs from thermocouple jacks. To overcome the leakage from the tip points of the thermocouples, the thermocouples were removed from their jacks and cables were connected to an electric terminal. Data were transfered to dataloggers by these terminals. Electric terminals were located into 3 boxes (Figure 7.8 (c)). An insulation material (Loctite 3090) was applied into the boxes (Figure 7.8 (d)). The electric terminal boxes were filled with Epoxy based SC 700 material to block the air contact of the thermocouple cables (Figure 7.8 (e)). Finally, after the final insulations were applied to the thermocouple cables, the leakage rate was found only 1 kPa/24 hours from all of the setup.

The final view of the experimental setup is illustrated in Figure 7.9.

## 7.4. The Experiment Procedure

Three steps were followed to perform an experiment by the setup. These steps are given below:

**Step 1: Evacuation and Desorption**:

Before the adsorption process, the whole system has to be vacuumed.

1. The evaporator which was filled with 9 lt deionized water was connected to the vacuum pump by a flexible hose. By opening the valve on the evaporator, the evaporator was vacuumed to the set pressure of the adsorption process. To vacuum the evaporator completely, the valve was opened and closed more than five times. The vacuum procedure takes approximately 1 hour.
2. After the evacuation of the evaporator, the adsorbent bed was evacuated while being heated to remove water content in the silica gel. During this drying process, valves on top and the bottom of the adsorbent bed were closed and the bed was heated by the electrical resistance on the outer surface of the adsorbent bed up to 100$^{o}$C. The bed was connected to the vacuum pump by a flexible hose. The valve on top of the adsorbent bed was opened and the drying process of silica gel continued for four days while the bed is still at 100$^{o}$C.

(a) (b) (c)

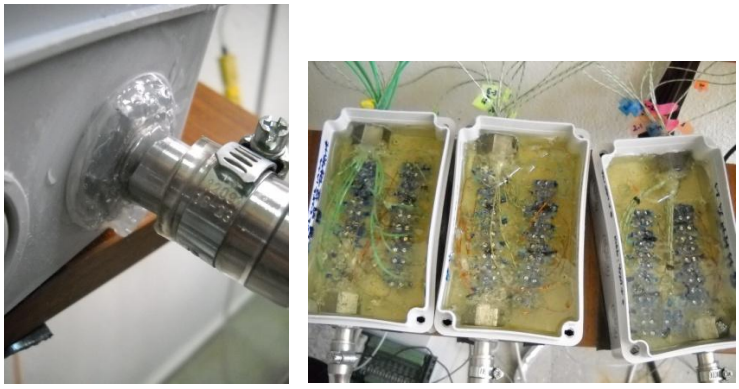

(d) (e)

Figure 7.8. The leakage blockage procedure from thermocouple cable and thermocouple tips

**Step 2: Temperature Stabilization**:

After the evacuation process, the temperatures of bed and evaporator should be stabilized to the set temperature.

1. The water bath was fixed to a temperature to heat or cool the water inside of the evaporator.
2. Meanwhile, the electrical heater was set to a temperature where the adsorption process will be started.
3. Then, to start the experiment, the water inside of the temperatures of evaporator and the bed should become steady to the set temperatures.
4. During this period, vacuum process continued from the bed.

**Step 3: Adsorption**:

Finally, the adsorption process was performed by the following steps:

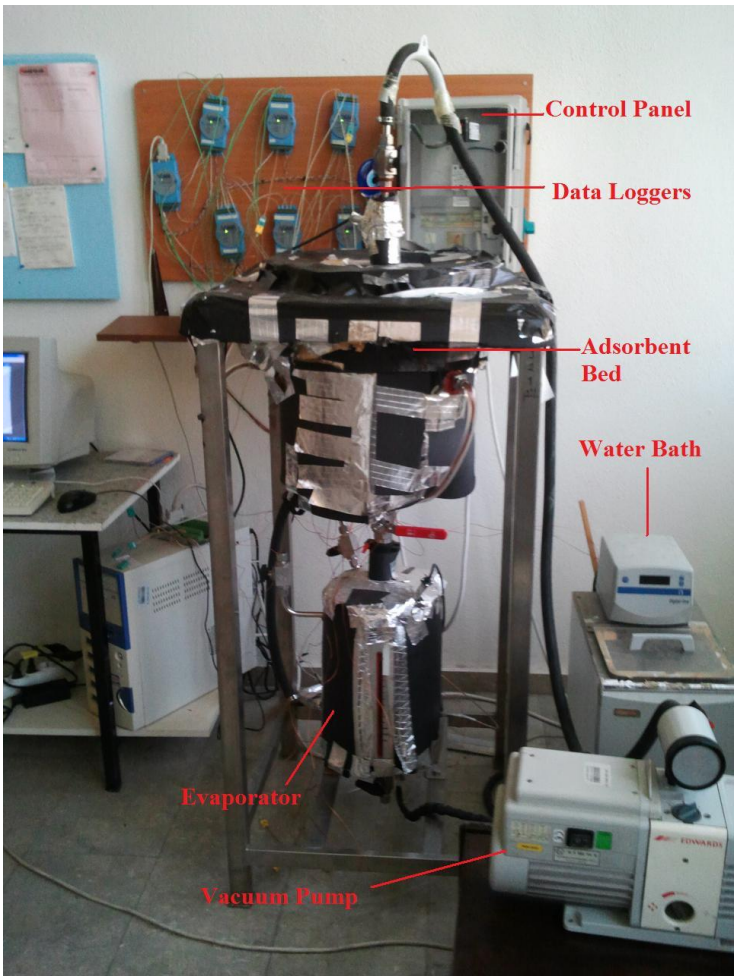


Figure 7.9. A view of the modified setup and its equipments

1. The valve at the top of the bed where the bed was connected to the pump was closed. The vacuum pump was switched off.
2. When the adsorbent bed and evaporator temperatures were fixed to the beginning of the adsorption process temperature, the valve between evaporator and adsorbent bed was fully opened and adsorption process was started.
3. Before opening the valve between the evaporator and the bed, the water level inside of the evaporator was marked.
4. During the adsorption process, the evaporated water from the evaporator was adsorbed by silica gel. Throughout the adsorption process, the outer surface temperature of adsorbent bed was held at desired temperature by the electrical heater.
5. The water level inside of the evaporator was marked in certain time intervals, during adsorption process. The level of the water measurements were marked at regular intervals during the experiments.

6. After a complete adsorption process, the valve between the adsorbent bed and the evaporator was closed.
7. The isobaric adsorption process was continued until the level of water inside the evaporator becomes fixed which indicates that the silica gel particles reach their equilibrium condition.
8. During the adsorption process, the inner and outer region temperatures in the bed were measured.

# CHAPTER 8

# NUMERICAL METHOD FOR SOLUTION OF GOVERNING EQUATIONS

In this chapter, the brief description on finite difference method is given. The computational domains of the considered problems solved in this thesis are explained. The nodal equations of the governing equations of different analyzed cases are derived and the numerical procedures used in the written codes for finding temperature and concentration are explained. Implicit method is used to find values of dependent variable for each time step. FORTRAN programming language is used to write the computer codes. Details on solution procedures such as number of grids, convergence criterion, and determination of averages of the unknowns are explained.

## 8.1. Finite Difference Method

In many engineering applications, the governing differential equations are not linear or they cannot be linearized. The considered region is irregular or boundary conditions highly depend on time. Hence, the analytical solution of the differential equations is very difficult or sometimes impossible. Numerical approaches provide an alternative solution of the aforementioned equations. However, the disadvantage of numerical methods is that they yield tabulated data rather than a function. Numerical analysis is the study of algorithms that use numerical approximations for the problems. To find the solution of a function with numerical analysis, several approaches can be used such as finite element, finite difference, finite volume, boundary element method etc. The finite difference method is one of the numerical approaches to predict the solutions of the differential equations. Particularly, it can be an appropriate method for solving boundary value problems. The governing equations and differential equations described in Chapter 5 and 6 are solved numerically by method of finite difference.

The finite difference method converts the differential equation into an algebraic equation for a point. Then, it can be applied to the all nodes, obtained by discritization

of domain, and set of algebraic equations will be generated. The solution of these linear algebraic equation yields results for each node. Two types of discritization are faced in engineering problems. A differential equation can be discritized in a space as shown in Figure 8.1 (a) or it can be discritized in time indicated in Figure 8.1(b).

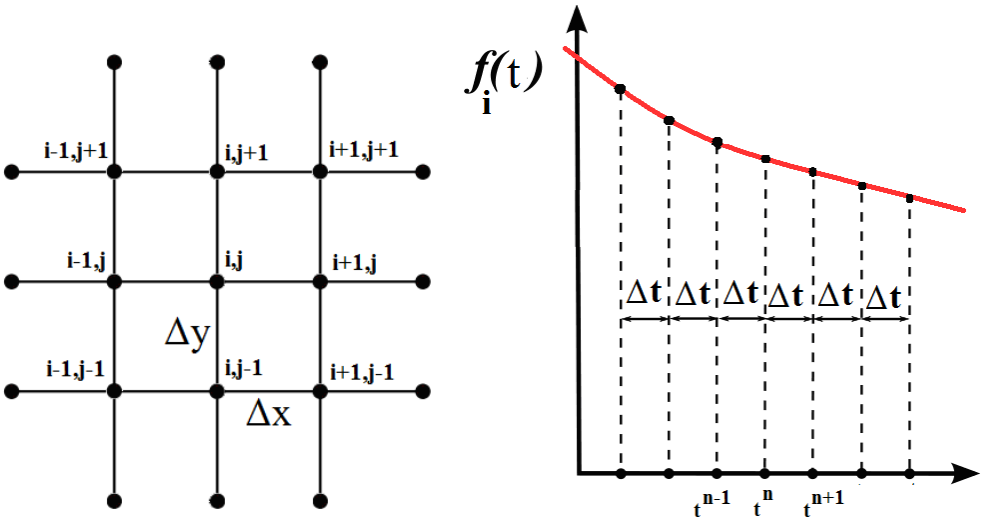


(a) (b)

Figure 8.1. A differential equation can be discritized (a) in a space, (b) in a time

In finite difference method, the domain should be divided into grids, the nodal equation of the given differential equation and boundary conditions should be obtained, the nodal equation should be applied to all nodes, and the obtained algebraic equations should be solved to achieve results. Forward, backward and central difference formulas are applied to obtain the nodal equation for the first and second derivatives. These formulas are defined as follows:

- Forward Difference:

$$f'(x_i) = \frac{y_{i+1} - y_i}{x_{i+1} - x_i} \qquad f''(x_i) = \frac{y_{i+2} - 2y_{i+1} + y_i}{(\Delta x)^2} \tag{8.1}$$

- Backward Difference:

$$f'(x_i) = \frac{y_i - y_{i-1}}{x_i - x_{i-1}} \qquad f''(x_i) = \frac{y_{i-2} - 2y_{i-1} + y_i}{(\Delta x)^2} \tag{8.2}$$

- Central Difference:

$$f'(x_i) = \frac{y_{i+1} - y_{i-1}}{x_{i+1} - x_{i-1}} \qquad f''(x_i) = \frac{y_{i+1} - 2y_i + y_{i-1}}{(\Delta x)^2} \tag{8.3}$$

### 8.1.1. Implicit Method

Many numerical approaches are used to solve differential equations depends on time. For time dependent engineering problems, the governing equation should also be discritized according to time. The implicit method is one of the common used approaches and finds accurate solution for the time dependent differential equation. The value of a dependent variable for a time step is obtained by using the dependent variables of neighboring nodes at the same time step. In this thesis, the implicit method is used to solve the problems. Generally, backward difference is used to write the first order derivative of dependent variable respect to time:

$$\left|\frac{\partial T}{\partial t}\right|^{n+1} = \frac{T^{n+1} - T^n}{\Delta t} \tag{8.4}$$

## 8.2. Discritization of Considered Adsorbent Bed

As illustrated in Figure 6.2, the analyzed annulus adsorbent bed is filled with the adsorbent granules. The adsorbent bed has a cylindrical shape. The adsorptive can easily flow from inner surface, $R=R_i$, toward the outer surface, $R=R_o$. For a three dimensional annular bed, the domain should be discritized in radial, angular and axial directions. Hence, the location of a node should be defined by three indices such as (i, j, k) as seen from Figure 8.2. The radial neighbors of a node such as (i, j, k) are (i+1, j, k) and (i-1, j, k), the angular neighbors are (i, j+1, k) and (i, j-1, k) and finally axial neighbors are (i, j, k+1) and (i, j, k-1). Hence, the adsorbent bed is divided to (nn x mm x zz) number of grids. At the beginning of numerical procedure, this division should be performed and location of each node should be specified.

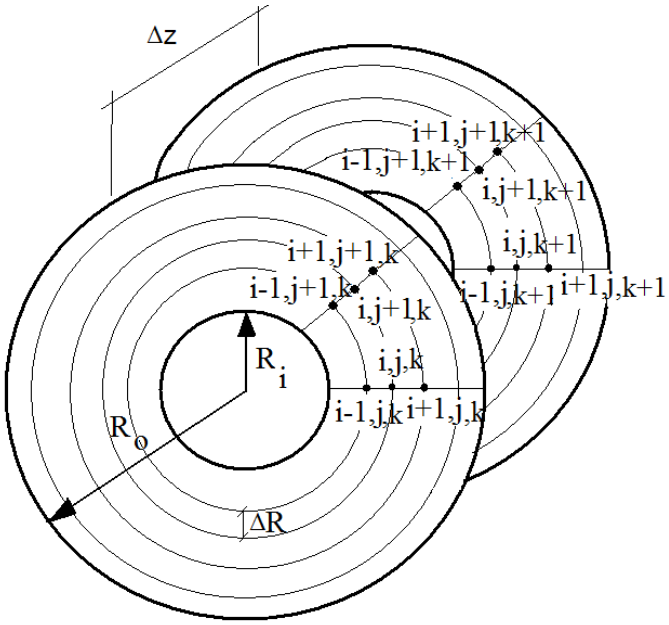


Figure 8.2. The location of the nodes for the considered adsorbent bed

## 8.3. Finite Difference Form of the Governing Equations for the Considered Adsorbent Bed

The considered heat and mass transfer problems are solved by both uniform and non-uniform pressure approaches as mentioned in Chapter 6. The governing equations for both approaches are given in the same chapter. In this subsection, the finite difference forms of the governing equations of both approaches are given. The finite difference forms of the equations are derived for a three dimensional space, and then they are reduced to two and/or one dimensional space.

### 8.3.1. Finite Difference Form of the Governing Equations of Uniform Pressure Approach

Energy equation for the adsorbent bed and the mass transfer equation for the adsorbent particle (LDF, solid diffusion model) are the governing equations for the uniform pressure approach. By using the finite difference method, the nodal equations of these equations are derived for both of the dimensional and dimensionless forms.

### 8.3.1.1. Energy Equation

The three dimensional heat transfer equation for the annular adsorbent bed in cylindrical coordinate can be written as:

$$\frac{\partial T}{\partial t} = \alpha_{eff}\ \frac{1}{R}\frac{\partial}{\partial R}\left(R\frac{\partial T}{\partial R}\right) + \frac{\alpha_{eff}}{R^2}\frac{\partial^2 T}{\partial \phi^2} + \alpha_{eff}\ \frac{\partial^2 T}{\partial z^2} + \frac{(1-\varphi\ )\rho_S}{(\rho C_p)_{eff}}\Delta H_{ads}\ \frac{\partial W}{\partial t} \qquad (8.5)$$

By using central difference for the first and second order derivatives in space (Eq. 8.3) and backward difference for the first order derivative in time (Eq.(8.2), the finite difference form of the Eq. (8.5) for a node with location of (i, j, k) can be written as:

$$\left[\frac{T^{n+1}(i,j,k) - T^{n}(i,j,k)}{\Delta t}\right] =$$

$$\alpha_{eff}\ \frac{1}{R(i)}\left[\frac{T^{n+1}(i+1,j,k) - T^{n+1}(i-1,j,k)}{2\Delta R} + R(i)\frac{T^{n+1}(i+1,j,k) - 2T^{n+1}(i,j,k) + T^{n+1}(i-1,j,k)}{\Delta R^2}\right] +$$

$$\alpha_{eff}\ \frac{1}{R(i)^2}\left[\frac{T^{n+1}(i,j+1,k) - 2T^{n+1}(i,j,k) + T^{n+1}(i,j-1,k)}{\Delta \phi^2}\right] +$$

$$\alpha_{eff}\left[\frac{T^{n+1}(i,j,k+1) - 2T^{n+1}(i,j,k) + T^{n+1}(i,j,k-1)}{\Delta z^2}\right]$$

$$+ \frac{(1-\varphi)\rho_S \Delta H_{ads}}{(\rho C_p)_{eff}}\left[\frac{\overline{W}^{n+1}(i,j,k) - \overline{W}^{n}(i,j,k)}{\Delta t}\right] \qquad (8.6)$$

The nodal equation of the above equation can be written as:

$$T^{n+1}(i,j,k) = \{BT^{n+1}(i+1,j,k) + CT^{n+1}(i-1,j,k) + DT^{n+1}(i,j+1,k) + DT^{n+1}(i,j-1,k) +$$

$$ET^{n+1}(i,j,k+1) + ET^{n+1}(i,j,k-1) + F + GT^{n}(i,j,k)\}/A \qquad (8.7)$$

where the constants from A to G can be written as:

$$A=\left[\frac{1}{\Delta t}+\frac{2\alpha_{eff}}{\Delta R^2}+\frac{2\alpha_{eff}}{R(i)^2\Delta\phi^2}+\frac{2\alpha_{eff}}{\Delta z^2}\right];B=\left[\frac{\alpha_{eff}}{\Delta R^2}+\frac{\alpha_{eff}}{2R(i)\Delta R}\right];C=\left[\frac{\alpha_{eff}}{\Delta R^2}-\frac{\alpha_{eff}}{2R(i)\Delta R}\right];$$

$$D=\left[\frac{\alpha_{eff}}{R(i)^2\Delta\phi^2}\right];E=\left[\frac{\alpha_{eff}}{\Delta z^2}\right];F=\frac{(1-\varphi)\rho_S\Delta H_{ads}}{\left(\rho C_p\right)_{eff}}\left[\frac{\overline{W}^{n+1}(i,j)-\overline{W}^{n}(i,j)}{\Delta t}\right];G=\left[\frac{1}{\Delta t}\right] \quad (8.8)$$

For a two dimensional problem in radial and axial directions, the energy equation can be reduced into the following form:

$$\frac{\partial T}{\partial t}=\alpha_{eff}\ \frac{1}{R}\frac{\partial}{\partial R}\left(R\frac{\partial T}{\partial R}\right)+\alpha_{eff}\ \frac{\partial^2 T}{\partial z^2}+\frac{(1-\varphi\ )\rho_S}{(\rho C_p)_{eff}}\Delta H_{ads}\ \frac{\partial W}{\partial t} \quad (8.9)$$

This equation is used to find temperature distribution in the bed where heat transfer occurs in R and z direction. Similarly, the nodal equation of Eq. (8.9) can be obtained as:

$$T^{n+1}(i,k)=\{BT^{n+1}(i+1,k)+CT^{n+1}(i-1,k)+DT^{n+1}(i,k+1)+DT^{n+1}(i,k-1)$$
$$+E+FT^{n}(i,k)\}/A \quad (8.10)$$

where the constants from A to F can be written as:

$$A=\left[\frac{1}{\Delta t}+\frac{2\alpha_{eff}}{\Delta R^2}+\frac{2\alpha_{eff}}{\Delta z^2}\right];B=\left[\frac{\alpha_{eff}}{\Delta R^2}+\frac{\alpha_{eff}}{2R(i)\Delta R}\right];C=\left[\frac{\alpha_{eff}}{\Delta R^2}-\frac{\alpha_{eff}}{2R(i)\Delta R}\right];$$

$$D=\left[\frac{\alpha_{eff}}{\Delta z^2}\right];E=\frac{(1-\varphi)\rho_S\Delta H_{ads}}{\left(\rho C_p\right)_{eff}}\left[\frac{\overline{W}^{n+1}(i,j)-\overline{W}^{n}(i,j)}{\Delta t}\right];F=\left[\frac{1}{\Delta t}\right] \quad (8.11)$$

If the heat transfer occurs only in the radial direction, the energy equation reduces to the equation as given in Eq. (6.1). The nodal equation of Eq. (6.1) can be obtained as:

$$T^{n+1}(i)=\{BT^{n+1}(i+1)+CT^{n+1}(i-1)+D+ET^{n}(i)\}/A \quad (8.12)$$

where the constants from A to E are:

$$A=\left[\frac{1}{\Delta t}+\frac{2\alpha_{eff}}{\Delta R^2}\right];B=\left[\frac{\alpha_{eff}}{\Delta R^2}+\frac{\alpha_{eff}}{2R(i)\Delta R}\right];C=\left[\frac{\alpha_{eff}}{\Delta R^2}-\frac{\alpha_{eff}}{2R(i)\Delta R}\right];$$

$$D=\frac{(1-\varphi)\rho_s\Delta H_{ads}}{\left(\rho C_p\right)_{eff}}\left[\frac{\overline{W}^{n+1}(i)-\overline{W}^{n}(i)}{\Delta t}\right];E=\left[\frac{1}{\Delta t}\right] \tag{8.13}$$

The energy equation which is written in R and $\phi$ direction can be non-dimensionalized by using dimensionless parameters as given in Eq. (6.9). The dimensionless energy equation is given in Eq. (6.33). The finite difference form of this equation for a node with location of (i, j) can be written as:

$$\left[\frac{\theta^{n+1}(i,j)-\theta^{n}(i,j)}{\Delta\tau}\right]=$$

$$\frac{1}{R(i)^*}\left[\frac{\theta^{n+1}(i+1,j)-\theta^{n+1}(i-1,j)}{2\Delta R^*}+R(i)^*\frac{\theta^{n+1}(i+1,j)-2\theta^{n+1}(i,j)+\theta^{n+1}(i-1,j)}{\Delta R^{*2}}\right]+$$

$$\frac{1}{R(i)^{*2}}\left[\frac{\theta^{n+1}(i,j+1)-2\theta^{n+1}(i,j)+\theta^{n+1}(i,j-1)}{\Delta\phi^2}\right]+$$

$$+Ku\left[\frac{\overline{W}^{*n+1}(i,j)-\overline{W}^{*n}(i,j)}{\Delta\tau}\right] \tag{8.14}$$

The nodal equation of Eq. (8.14) can be obtained as:

$$\theta^{n+1}(i,j)=\{B\theta^{n+1}(i+1,j)+C\theta^{n+1}(i-1,j)+D\theta^{n+1}(i,j+1)+D\theta^{n+1}(i,j-1)+$$

$$E+F\theta^{n}(i,j)\}/A \tag{8.15}$$

where the constants can be written as:

$$A=\left[\frac{1}{\Delta\tau}+\frac{2}{\Delta R^{*2}}+\frac{2}{R^{*}(i)^{2}\Delta\phi^{2}}\right];B=\left[\frac{1}{\Delta R^{*2}}+\frac{1}{2R^{*}(i)\Delta R^{*}}\right];C=\left[\frac{1}{\Delta R^{*2}}-\frac{1}{2R^{*}(i)\Delta R^{*}}\right];$$

$$D=\left[\frac{1}{R(i)^{2}\Delta\phi^{2}}\right];E=Ku\left[\frac{\overline{W}^{*n+1}(i,j)-\overline{W}^{*n}(i,j)}{\Delta\tau}\right];F=\left[\frac{1}{\Delta\tau}\right] \tag{8.16}$$

The energy equation which is written only in R direction can be non-dimensionalized by using dimensionless parameters as given in Eq. (6.10). The finite difference form of the Eq. (6.10) for a node with location of (i) can be written as:

$$\left[\frac{\theta^{n+1}(i)-\theta^{n}(i)}{\Delta\tau}\right]=$$

$$\frac{1}{R(i)^{*}}\left[\frac{\theta^{n+1}(i+1)-\theta^{n+1}(i-1)}{2\Delta R^{*}}+R(i)^{*}\,\frac{\theta^{n+1}(i+1)-2\theta^{n+1}(i)+\theta^{n+1}(i-1)}{\Delta R^{*2}}\right]+$$

$$+Ku\left[\frac{\overline{W}^{*n+1}(i)-\overline{W}^{*n}(i)}{\Delta\tau}\right] \tag{8.17}$$

The nodal equation of Eq. (8.17) can be obtained as:

$$\theta^{n+1}(i)=\{B\theta^{n+1}(i+1)+C\theta^{n+1}(i-1)+D+E\theta^{n}(i)\}/A \tag{8.18}$$

where the constants from A to E:

$$A=\left[\frac{1}{\Delta\tau}+\frac{2}{\Delta R^{*2}}\right];B=\left[\frac{1}{\Delta R^{*2}}+\frac{1}{2R^{*}(i)\Delta R^{*}}\right];C=\left[\frac{1}{\Delta R^{*2}}-\frac{1}{2R^{*}(i)\Delta R^{*}}\right];$$

$$D=Ku\left[\frac{\overline{W}^{*n+1}(i,j)-\overline{W}^{*n}(i,j)}{\Delta\tau}\right];E=\left[\frac{1}{\Delta\tau}\right] \tag{8.19}$$

### 8.3.1.2. LDF Model Equation

The adsorbate change with time in an adsorbent particle can be calculated by LDF model as given in Eq. (6.3). The finite difference method LDF model (Eq. (6.3)) can be written as:

$$\left[\frac{\overline{W}^{n+1}(i,j)-\overline{W}^{n}(i,j)}{\Delta t}\right]=\frac{15D_{eff}}{r_p^2}\left(\overline{W}_{\infty}^{n+1}(i,j)-\overline{W}^{n}(i,j)\right) \tag{8.20}$$

As seen, the Euler method is used to solve the first order ordinary differential equation. The nodal equation of Eq. (6.3) can be obtained as:

$$\overline{W}^{n+1}(i,j)=\frac{15D_{eff}}{r_p^2}\Delta t\left(\overline{W}_{\infty}^{n+1}(i,j)-\overline{W}^{n}(i,j)\right)+\overline{W}^{n}(i,j) \tag{8.21}$$

The finite difference form of the dimensionless form of the Eq. (6.12) can be written as:

$$\left[\frac{\overline{W}^{*n+1}(i,j)-\overline{W}^{*n}(i,j)}{\Delta \tau}\right]=\Gamma\left(\overline{W}^{*n+1}_{\infty}(i,j)-\overline{W}^{*n}(i,j)\right) \tag{8.22}$$

The nodal equation of Eq. (6.12) can be obtained as:

$$\overline{W}^{*n+1}(i,j)=\Gamma\Delta\tau\left(\overline{W}^{*n+1}_{\infty}(i,j)-\overline{W}^{*n}(i,j)\right)+\overline{W}^{*n}(i,j) \tag{8.23}$$

### 8.3.1.3. Solid Diffusion Model Equation

The local adsorbate change in an adsorbent particle with time can be also calculated by solid diffusion model. The solid diffusion equation is given by Eq. (6.4). The finite difference form of the Eq. (6.4) can be written as:

$$\left[\frac{W^{n+1}(i,j)-W^{n}(i,j)}{\Delta t}\right]=\frac{D_{eff}}{r(i)}\left(\frac{W^{n+1}(i+1,j)-W^{n+1}(i-1,j)}{\Delta r}\right)$$

$$+\frac{D_{eff}}{\Delta r^{2}}\left(W^{n+1}(i+1,j)-2W^{n+1}(i,j)+W^{n+1}(i-1,j)\right) \qquad (8.24)$$

The nodal equation for the solid diffusion equation can be obtained as:

$$W^{n+1}(i,j)=\{BW^{n+1}(i+1,j)+CW^{n+1}(i-1,j)+DW^{n}(i,j)\}/A \qquad (8.25)$$

where the constants from A to D can be written as:

$$A=\left(\frac{1}{\Delta t}+\frac{2D_{eff}}{\Delta r^{2}}\right);B=\left(\frac{D_{eff}}{r(i)}+\frac{D_{eff}}{\Delta r^{2}}\right);C=\left(-\frac{D_{eff}}{r(i)}+\frac{D_{eff}}{\Delta r^{2}}\right);D=\left[\frac{1}{\Delta t}\right] \qquad (8.26)$$

The dimensionless form of the solid diffusion model is presented by Eq. (6.13). The finite difference form of the Eq. (6.13) can be written as:

$$\left[\frac{W^{*n+1}(i,j)-W^{*n}(i,j)}{\Delta \tau}\right]=\frac{\Gamma}{r^{*}(i)}\left(\frac{W^{*n+1}(i+1,j)-W^{*n+1}(i-1,j)}{\Delta r^{*}}\right)$$

$$+\frac{\Gamma}{\Delta r^{*2}}\left(W^{*n+1}(i+1,j)-2W^{*n+1}(i,j)+W^{*n+1}(i-1,j)\right) \qquad (8.27)$$

The nodal equation for dimensionless solid diffusion equation can be obtained as:

$$W^{n+1}(i,j)=\{BW^{n+1}(i+1,j)+CW^{n+1}(i-1,j)+DW^{n}(i,j)\}/A \qquad (8.28)$$

where the constants are:

$$A=\left(\frac{1}{\Delta \tau}+\frac{2D_{eff}}{\Delta r^{*2}}\right);B=\left(\frac{\Gamma}{r^{*}(i)}+\frac{\Gamma}{\Delta r^{*2}}\right);C=\left(-\frac{\Gamma}{r^{*}(i)}+\frac{\Gamma}{\Delta r^{*2}}\right);D=\left[\frac{1}{\Delta \tau}\right] \qquad (8.29)$$

### 8.3.2. Finite Difference Form of the Governing Equations of Non-Uniform Pressure Approach

The nodal equations of the heat and mass transfer equations for the adsorbent bed and the Darcy equation for the non-uniform pressure approach are derived and given for both of the dimensional and dimensionless forms in this section.

#### 8.3.2.1. Energy Equation

The heat transfer equation for the adsorbent bed for non-uniform pressure approach along the radial direction of the bed is given in Eq. (6.17). By using central difference for the first and second order derivatives in space (Eq. 8.3) and backward difference for the first order derivative in time (Eq.(8.2), the finite difference form of the Eq. (6.17) for a node with location of (i) can be written as:

$$(\rho C_p)_{eff}\left[\frac{T^{n+1}(i)-T^{n}(i)}{\Delta t}\right]+\frac{1}{R(i)}\left[\rho_v^{n+1}(i)V_r^{n+1}(i)T^{n+1}(i)\right]+$$

$$\left[\frac{\rho_v^{n+1}(i+1)V_r^{n+1}(i+1)T^{n+1}(i+1)}{2\Delta R}-\frac{\rho_v^{n+1}(i-1)V_r^{n+1}(i-1)T^{n+1}(i-1)}{2\Delta R}\right]=$$

$$\lambda_{eff}\ \frac{1}{R(i)}\left[\frac{T^{n+1}(i+1)-T^{n+1}(i-1)}{2\Delta R}+R(i)\frac{T^{n+1}(i+1)-2T^{n+1}(i)+T^{n+1}(i-1)}{\Delta R^2}\right]+$$

$$+(1-\varphi)\rho_S\Delta H_{ads}\left[\frac{\overline{W}^{n+1}(i)-\overline{W}^{n}(i)}{\Delta t}\right] \qquad (8.30)$$

The nodal equation of the above equation is:

$$T^{n+1}(i)=\{BT^{n+1}(i+1)+CT^{n+1}(i-1)+D(1-\varphi)\rho_S\Delta H_{ads}+ET^{n}(i)\}/A \quad (8.31)$$

where the constants from A to E are:

$$A=\left[\frac{(\rho C_p)_{eff}}{\Delta t}+\frac{2\lambda_{eff}}{\Delta R^2}+\frac{\rho_v^{n+1}(i)V_r^{n+1}(i)}{R(i)}\right];B=\left[\frac{\lambda_{eff}}{\Delta R^2}+\frac{\lambda_{eff}}{2R(i)\Delta R}-\frac{\rho_v^{n+1}(i+1)V_r^{n+1}(i+1)}{2\Delta R}\right];$$

$$C=\left[\frac{\lambda_{eff}}{\Delta R^2}-\frac{\lambda_{eff}}{2R(i)\Delta R}-\frac{\rho_v^{n+1}(i-1)V_r^{n+1}(i-1)}{2\Delta R}\right];D=(\rho C_p)_{eff}\left[\frac{\overline{W}^{n+1}(i)-\overline{W}^{n}(i)}{\Delta t}\right];$$

$$E=\left[\frac{(\rho C_p)_{eff}}{\Delta t}\right] \tag{8.32}$$

Dimensionless heat transfer equation for the adsorbent bed is given in Eq. (6.26). The finite difference form of the dimensionless energy equation can be written as:

$$\left[\frac{\theta^{n+1}(i)-\theta^{n}(i)}{\Delta\tau}\right]+\frac{1}{R(i)}\left[\rho_v^{*n+1}(i)V_r^{*n+1}(i)\theta^{n+1}(i)\right]+$$

$$\left[\frac{\rho_v^{*n+1}(i+1)V_r^{*n+1}(i+1)\theta^{n+1}(i+1)}{2\Delta R^{*}}-\frac{\rho_v^{*n+1}(i-1)V_r^{*n+1}(i-1)\theta^{n+1}(i-1)}{2\Delta R^{*}}\right]=$$

$$\frac{1}{R(i)^{*}}\left[\frac{\theta^{n+1}(i+1)-\theta^{n+1}(i-1)}{2\Delta R^{*}}+R(i)^{*}\frac{\theta^{n+1}(i+1)-2\theta^{n+1}(i)+\theta^{n+1}(i-1)}{\Delta R^{*2}}\right]+$$

$$+Ku\left[\frac{\overline{W}^{*n+1}(i)-\overline{W}^{*n}(i)}{\Delta\tau}\right] \tag{8.33}$$

The nodal equation of the above equation can be written as:

$$T^{n+1}(i)=\{BT^{n+1}(i+1)+CT^{n+1}(i-1)+D+ET^{n}(i)\}/A \tag{8.34}$$

where the constants from A to E can be written as:

$$A=\left[\frac{1}{\Delta\tau}+\frac{2}{{\Delta R^*}^2}+\frac{{\rho_v}^{*n+1}(i){V_r}^{*n+1}(i)}{R^*(i)}\right];B=\left[\frac{1}{{\Delta R^*}^2}+\frac{1}{2R^*(i)\Delta R^*}-\frac{{\rho_v}^{*n+1}(i+1){V_r}^{*n+1}(i+1)}{2\Delta R^*}\right];$$

$$C=\left[\frac{1}{{\Delta R^*}^2}-\frac{1}{2R^*(i)\Delta R^*}-\frac{{\rho_v}^{*n+1}(i-1){V_r}^{*n+1}(i-1)}{2\Delta R^*}\right];D=Ku\left[\frac{{\overline{W}}^{*n+1}(i)-{\overline{W}}^{*n}(i)}{\Delta\tau}\right];$$

$$E=\left[\frac{1}{\Delta\tau}\right] \tag{8.35}$$

## 8.3.2.2. Continuity Equation

The continuity equation based on conservation of mass for water vapor flow through the adsorbent bed in radial direction is given in Eq. (6.16). By using central difference for the first and second order derivatives in space (Eq. 8.3) and backward difference for the first order derivative in time (Eq.(8.2), the finite difference form of the Eq. (6.16) for a node with location of (i) can be written as:

$$\varphi\left[\frac{{\rho_v}^{n+1}(i)-{\rho_v}^{n}(i)}{\Delta t}\right]=$$

$$\frac{1}{R(i)}\left\{\left[{\rho_v}^{n+1}(i){V_r}^{n+1}(i)\right]+\left[\frac{{\rho_v}^{n+1}(i+1){V_r}^{n+1}(i+1)-{\rho_v}^{n+1}(i-1){V_r}^{n+1}(i-1)}{2\Delta R}\right]\right\}$$

$$+(\varphi-1)\rho_S\left[\frac{{\overline{W}}^{n+1}(i)-{\overline{W}}^{n}(i)}{\Delta t}\right] \tag{8.36}$$

The nodal equation of the above equation can be written as:

$${\rho_v}^{n+1}(i)=\{B{\rho_v}^{n+1}(i+1)+C{\rho_v}^{n+1}(i-1)+D(\varphi-1)\rho_S+E{\rho_v}^{n}(i)\}/A \tag{8.37}$$

where the constants from A to E can be written as:

$$A=\left[\frac{\varphi}{\Delta t}-\frac{V_r^{n+1}(i)}{R(i)}\right];B=\left[\frac{V_r^{n+1}(i+1)}{2R(i)\Delta R}\right];C=\left[-\frac{V_r^{n+1}(i-1)}{2R(i)\Delta R}\right];$$

$$D=\left[\frac{\overline{W}^{n+1}(i)-\overline{W}^{n}(i)}{\Delta t}\right];E=\left[\frac{\varphi}{\Delta t}\right] \tag{8.38}$$

As given in Eq (6.25) the dimensionless continuity equation in radial direction of the adsorbent bed can be written by using central difference for the first and second order derivatives in space (Eq. 8.3) and backward difference for the first order derivative in time (Eq.(8.2). The finite difference form of the Eq. (6.25) for a node with location of (i) can be written as:

$$\varphi\left[\frac{{}^{*}\rho_V^{n+1}(i)-{}^{*}\rho_V^{n}(i)}{\Delta\tau}\right]=$$

$$\frac{1}{R(i)^{*}}\left\{\left[{}^{*}\rho_V^{n+1}(i){}^{*}V_r^{n+1}(i)\right]+\left[\frac{{}^{*}\rho_V^{n+1}(i+1){}^{*}V_r^{n+1}(i+1)-{}^{*}\rho_V^{n+1}(i-1){}^{*}V_r^{n+1}(i-1)}{2\Delta R^{*}}\right]\right\}$$

$$+(\varphi-1)G\left[\frac{{}^{*}\overline{W}^{n+1}(i)-{}^{*}\overline{W}^{n}(i)}{\Delta\tau}\right] \tag{8.39}$$

The nodal equation of the above equation can be written as:

$${}^{*}\rho_V^{n+1}(i)=\{B\,{}^{*}\rho_V^{n+1}(i+1)+C\,{}^{*}\rho_V^{n+1}(i-1)+D(\varphi-1)+E\,{}^{*}\rho_V^{n}(i)\}/A \tag{8.40}$$

where the constants are:

$$A=\left[\frac{\varphi}{\Delta\tau}-\frac{{}^{*}V_r^{n+1}(i)}{{}^{*}R(i)}\right];B=\left[\frac{{}^{*}V_r^{n+1}(i+1)}{2{}^{*}R(i)\Delta{}^{*}R}\right];C=\left[-\frac{{}^{*}V_r^{n+1}(i-1)}{2{}^{*}R(i)\Delta{}^{*}R}\right];$$

$$D = G\left[\frac{\overline{W}^{*n+1}(i) - \overline{W}^{*n}(i)}{\Delta\tau}\right]; E = \left[\frac{\varphi}{\Delta\tau}\right] \tag{8.41}$$

### 8.3.2.3. Darcy Equation

In the above equation, $V_r$ is facial water vapor velocity and it can be calculated by Darcy Law. Darcy's law equation is given I Eq.(6.18). By using central difference for the first order derivatives in space (Eq. 8.3) the finite difference form of the Eq. (6.18) for a node with location of (i) can be written as:

$$V_r{}^{n+1}(i) = -\frac{K_{app}}{\mu}\left[\frac{P^{n+1}(i+1) - P^{n+1}(i-1)}{2\Delta R}\right] \tag{8.42}$$

## 8.4. Finite Difference Form of the Governing Equations for the Single Particle

By using the finite difference method, the nodal equations of energy equation and the mass transfer equation for the adsorbent particle are given for both of the dimensional and dimensionless forms in this section.

### 8.4.1. Solid Diffusion Model Equation

The nodal equation of the dimensionless form of the adsorbate change in an adsorbent particle for solid diffusion model is given in Eq.(8.25) where the constants are given in Eq.(8.26). Same equations can be also used for a single particle problem.

### 8.4.2. Energy Equation

The dimensionless heat transfer equation for a single spherical adsorbent particle is given in Eq. (5.28). By using central difference for the first and second order

derivatives in space (Eq.(8.3)) and backward difference for the first order derivative in time (Eq.(8.2), the finite difference form of the Eq. (5.28) for a node with location of (i) can be written as:

$$\left[\frac{\theta^{n+1}(i)-\theta^{n}(i)}{\Delta\tau}\right]=Le\frac{1}{r^{*}}\left[\frac{\theta^{n+1}(i+1)-\theta^{n+1}(i-1)}{2\Delta r^{*}}+r^{*}\frac{\theta^{n+1}(i+1)-2\theta^{n+1}(i)+\theta^{n+1}(i-1)}{\Delta r^{*2}}\right]$$

$$+Ku\left[\frac{\overline{W}^{*n+1}(i)-\overline{W}^{*n}(i)}{\Delta\tau}\right] \tag{8.43}$$

The nodal equation of the above equation is:

$$\theta^{n+1}(i)=\{B\theta^{n+1}(i+1)+C\theta^{n+1}(i-1)+D+E\theta^{n}(i)\}/A \tag{8.44}$$

the constants from A to E are:

$$A=\left[\frac{1}{\Delta\tau}+\frac{2Le}{\Delta r^{*2}}\right];B=\left[\frac{Le}{\Delta r^{*2}}+\frac{Le}{2r^{*}(i)\Delta r^{*}}\right];C=\left[\frac{Le}{\Delta r^{*2}}-\frac{Le}{2r^{*}(i)\Delta r^{*}}\right];D=Ku\left[\frac{\overline{W}^{*n+1}(i)-\overline{W}^{*n}(i)}{\Delta\tau}\right];$$

$$E=\left[\frac{1}{\Delta\tau}\right] \tag{8.45}$$

## 8.5. Solution Procedure

The solution procedures for the problems of the uniform and non-uniform pressure approaches and the single particle problem are explained in this chapter. The convergence criterion used for the inner iterations and the equations used to determine the average value of the dependent variable are given.

### 8.5.1. Solution of the Uniform and Non-Uniform Pressure Approaches Problems

Finite difference method is used to solve the governing equations of both approaches. For the uniform pressure approach, the heat transfer equation (Eq. (6.1)) is solved to determine the local temperature in the adsorbent bed. Then, the obtained temperature values are used to solve the mass transfer equation of the silica gel particles (Eq. (6.2), (6.3) or (6.4)) and to calculate the water concentration in the silica gel particle. An inner iteration is used to obtain the simultaneous solution of the mass transfer equation for the silica gel particle and heat transfer equation for the adsorbent bed. After obtaining the simultaneous solution for a time step, the procedure is continued for the next time step. The same procedure is used for uniform pressure approach when dimensionless forms of heat transfer equation (Eq. (6.10)) and mass transfer equation for particle (Eq. (6.11), (6.12) or (6.13)) are solved.

For non-uniform pressure approach, firstly mass transfer equation for silica gel particle (Eq. (6.2), (6.3) or (6.4)), energy equation for the adsorbent bed (Eq.(6.17) and continuity equation for the water vapor (Eq.(6.16)) are solved to find the water concentration in the silica gel particle, distribution of temperature and water vapor density in the bed. Then, the pressure distribution of water vapor is obtained by using the temperature and adsorptive density distributions based on ideal gas relation. Finally, the water vapor velocity is obtained by using Darcy Law (Eq.(6.18)). Similar to the solution method employed in the uniform pressure approach, an inner iteration is used to obtain the simultaneous solution for temperature, water concentration in the silica gel particle, water vapor density and water vapor velocity in the bed. After obtaining a simultaneous solution for a time step, the procedure is continued for the next step. The same procedure is used for non-uniform pressure approach when dimensionless forms of continuity equation (Eq.(6.25)), the heat transfer equation (Eq. (6.26)) and mass transfer equation for particle ((6.12)) are solved.

The flow charts of both approaches are given in Appendix C. The following convergence criterion is used for the inner iterations in both approaches;

$$\left| \frac{\xi^{n+1} - \xi^{n}}{\Delta \tau} \right| < 10^{-5} \tag{8.46}$$

where $\xi$ represents $\overline{W}$ and T. The procedure is terminated when the adsorbate concentration and temperature reach the final values of $\overline{W} = 0.995\overline{W}_a$ and $T = 0.005T_a$. The following equation is used to determine the average value of a dependent variable in the bed.

$$\bar{\gamma}(t) = \frac{\int_{R_i}^{R_o} 2R\gamma(R,t)dR}{\left(R_o^2 - R_i^2\right)} \tag{8.47}$$

where $\gamma$ can be T, P, $\rho_V$ and $\overline{W}$. To save the computational time, the number of nodes inside of the bed was taken as 7 and it was sufficient to obtain accurate results. Figure 8.3 shows the variation of average bed temperature versus time for three different numbers of nodes of 5, 7 and 20 when the bed thickness is 10 mm. As seen, the variations of the average bed temperature with time for three different node numbers are close to each other. The time interval cannot be fixed due to different heat and mass transfer period for each problem. Time interval is checked for each obtained results to remove the effect of the value of time interval on the results. Based on the case and values of dimensionless parameter groups the time interval values are changed from 0.000001 to 0.0001.

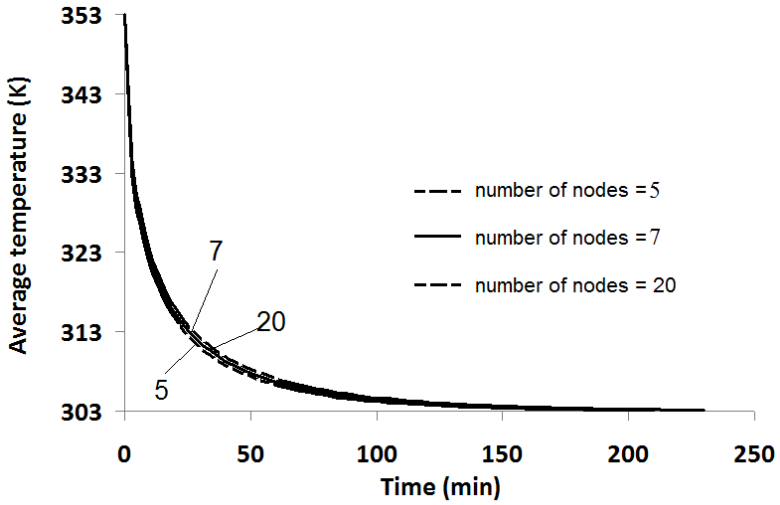


Figure 8.3. The variation of average dimensionless temperature versus dimensionless time for three different number of nodes for the bed with ΔR = 10 mm.

## 8.5.2. Solution of the Single Particle Problem

The solutions of the governing equations for single particle problems described in pervious section were found by finite difference method. By applying boundary conditions, the set of algebraic equations are solved by Gauss-Seidel iteration method. Following convergence criterion was used to terminate iteration;

$$\frac{\xi^{p+1}-\xi^{p}}{\left|\xi^{p}\right|_{\max}}<10^{-7} \tag{8.48}$$

where $\xi$ is dimensionless adsorbate concentration for mass transfer equation (Eq. (13)) and dimensionless temperature for heat transfer equation (Eq. (27)) and $p$ shows an iteration step. After finding solution for an instant, the time step was increased and solution for next instant was found. The outer iteration was terminated according to convergence of dimensionless average mass and temperature values.

$$\left|\xi^{n+1}-\xi^{n}\right|<10^{-3} \tag{8.49}$$

where n shows a time step. The nonlinear terms in heat and mass transfer equations or complexity in convective boundary conditions is overcome by using inner iterations. For example, for Case II, an inner iteration for each time step is performed to obtain the value of $\rho^{*}\Big|_{r^{*}=1}$ from Eq. (5.8). The following equation is used to determine the average value of a dependent variable in an adsorbent particle.

$$\bar{\gamma}(t)=\frac{3\int_{0}^{r_p} r^{2}\gamma(r,t)dr}{r_p^{3}} \tag{8.50}$$

where $\gamma$ can be $\theta$ and $\overline{W}$. The obtained results showed that 20 nodes are sufficient to obtain grid independent results for the four cases. Figure 8.4 shows the variation of

dimensionless average particle temperature versus time for Case 3 when Ku=1 and Le=1 for three different numbers of nodes of 5, 10 and 100. As seen, the variations of the dimensionless average particle temperature with time for three different node numbers come to close each other after 20 nodes.

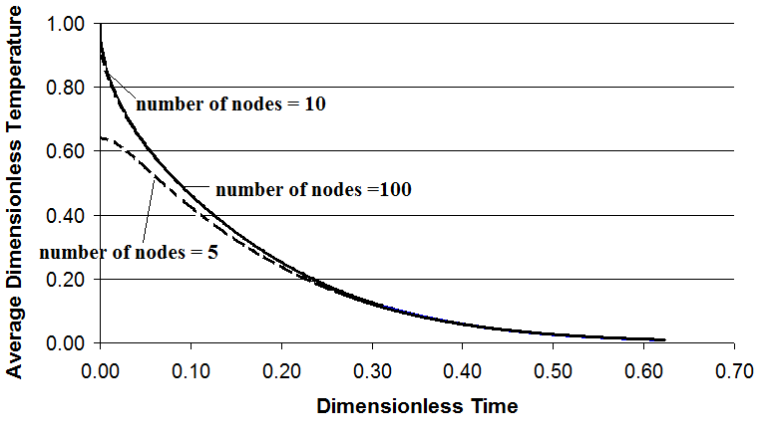


Figure 8.4. The variation of average dimensionless temperature versus dimensionless time for three different number of nodes for the single particle when Ku=1 and Le=1

A special attention was given to the number of nodes and time interval. Time interval cannot be fixed due to different heat and mass transfer period. However, time interval is checked for each obtained results to remove the effect of the value of time interval on the results. Based on the case and values of dimensionless parameter groups the time interval values are changed from 0.00001 to 1. The effect of time interval on dimensionless time is illustrated in Figure 8.5 for Case III when Ku=1 and Le=1.

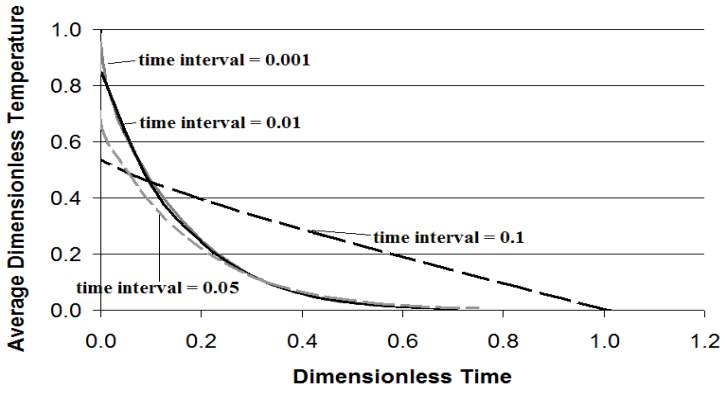


Figure 8.5. The variation of average dimensionless temperature versus dimensionless time for three different time intervals for the single particle when Ku=1 and Le=1

# CHAPTER 9

# RESULTS AND DISCUSSION ON THEORETICAL STUDIES

In this chapter, the results of the theoretical studies which were performed are discussed. Theoretical results of the studies for a single particle and for one and two dimensional studies on heat and mass transfer for an adsorbent bed, as well as dimensionless and dimensional forms of these problems, are summarized. Also, the effect of fin on heat transfer acceleration in an adsorbent bed, importance of dimensionless parameters, and effect of interparticle mass transfer resistance are discussed.

## 9.1. Results and Discussion on Theoretical Studies for a Single Particle

In this study, in order to understand the mechanism of the heat and mass transfer in an adsorbent bed of adsorption heat pump, the mechanism of the heat and mass transfer in a single particle is analyzed. The external heat and mass transfer resistances play important role on adsorbate transfer in an adsorbent particle. The aim of the present study is to perform a dimensionless analysis on heat and mass transfer in a single adsorbent particle located in an infinite adsorptive medium for isothermal and non-isothermal states. Four different combinations of external heat and mass transfer resistances are considered and given in Figure 5.1. The governing equations and corresponding initial and boundary conditions for four cases of adsorption in a single particle are given in Chapter 5. The results for each case (Case I-IV) obtained numerically were compared with each other to observe the effects of internal and external heat and mass transfer resistances. The assumptions used in this study were given in Chapter 5.1. The numerical results for the governing equation of four different cases were obtained and discussed in this section. The study is performed for Freundlich isotherm of silica gel and water pair (Eq. (5.1)). The ambient pressure is considered as 2 kPa.

### 9.1.1. Results of Case I

As is seen from the mass transfer equation, initial and boundary conditions for adsorbent particle without external mass transfer resistance under an isothermal process, the solution of Eq. (5.14) does not depend on any dimensionless parameter and dimensionless uptake curve for all adsorbent-adsorbate pairs is expected to be same. The solution of Eq. (5.14) was found and the dimensionless uptake curve is shown in Figure 9.1. After 0.48 dimensionless time, the dimensionless adsorbate concentration approaches to 1.

Since Eq. (5.14) and its initial and boundary conditions are linear, the analytical solution of them is possible. The analytical solution of Eq. (5.14) is reported in literature (Ruthven 1984, Suzuki 1990). Figure 9.1 also shows the comparison of analytical solution of Eq. (5.14) with present numerical results. A good agreement between the analytical and numerical results shows the accuracy of the present numerical study in somehow.

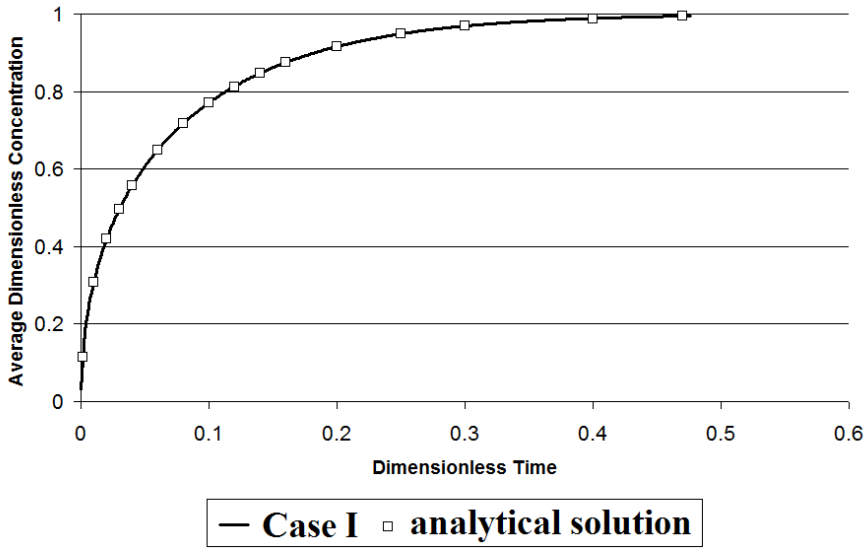


Figure 9.1. The comparison of analytical solution mass transfer equation with the numerical results of Case I

### 9.1.2. Results of Case II

Dimensionless mass transfer equation, boundary and initial conditions for adsorbent particle with considerable external mass transfer resistance show that the dimensionless uptake curve for this case not only depends on the modified mass Biot number but also depends on dimensionless adsorption isotherm of adsorbent-adsorbate pair. The dimensionless uptake curves of different adsorbent-adsorbate pairs for an identical modified mass transfer Biot number may be different. The numerical solution for the isothermal mass transfer equation with external mass transfer resistance for $\Gamma_i$ function represented by Eq. (5.7) is obtained and dimensionless uptake curves for modified mass transfer Biot number as 0.1, 0.3 and 5 are presented in Figure 9.2. The dimensionless uptake curve for adsorbent particle without external mass transfer resistance is also shown in the same figure. As is seen, for modified mass transfer Biot number as 20, all dimensionless uptake curves of Case II become closer to the dimensionless uptake curve of Case I. In this study, an attempt was performed to specify a value for modified mass transfer Biot number for deciding on importance of external mass transfer resistance for an isothermal adsorption. The obtained results shows that for modified mass transfer Biot number as 20, 90% of dimensionless uptake curves of Case I and II overlap each other and the relative difference between two uptakes becomes less than 5%. This shows that for large $Bi_m^{'}$ such as $Bi_m^{'} \geq 20$, the external mass transfer resistance is negligible, and the variations of dimensionless adsorbate concentration with dimensionless time for two isotherms are identical. For small $Bi_m^{'}$ such as $Bi_m^{'}=0.1$, the dimensionless uptake curves of two isotherms are separated from each other. This result shows that for the mass transfer in adsorbent particle with low modified mass transfer Biot number such as 0.1, the dimensionless uptake curve is affected from both external mass transfer resistance and the shape of isotherm of adsorbent-adsorbate pair.

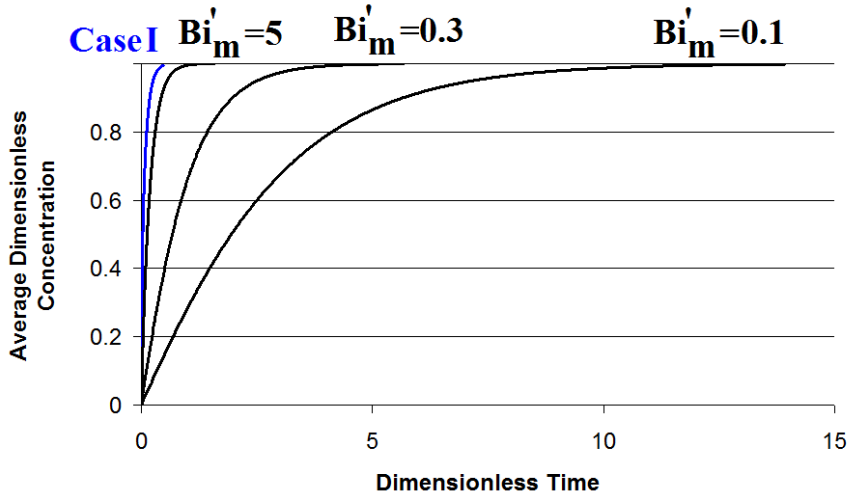


Figure 9.2. The dimensionless uptake curves for Case I and for Case II with different $Bi'_m$ as 0.1, 0.3, and 5

The variations of dimensionless adsorbate concentration at the surface of adsorbent particle ($r'_p$ =1) during adsorption process when modified mass transfer Biot number are 0.1, 0.3, and 5 are shown in Figure 9.3. As it is expected, the value of dimensionless adsorbate concentration at the surface of adsorbent particle is almost equals to 1 for $Bi'_m \geq 20$ which is identical with Case I. For $Bi'_m$ = 0.1, the variation of $W^*$ becomes different from that of $Bi'_m$ = 20.

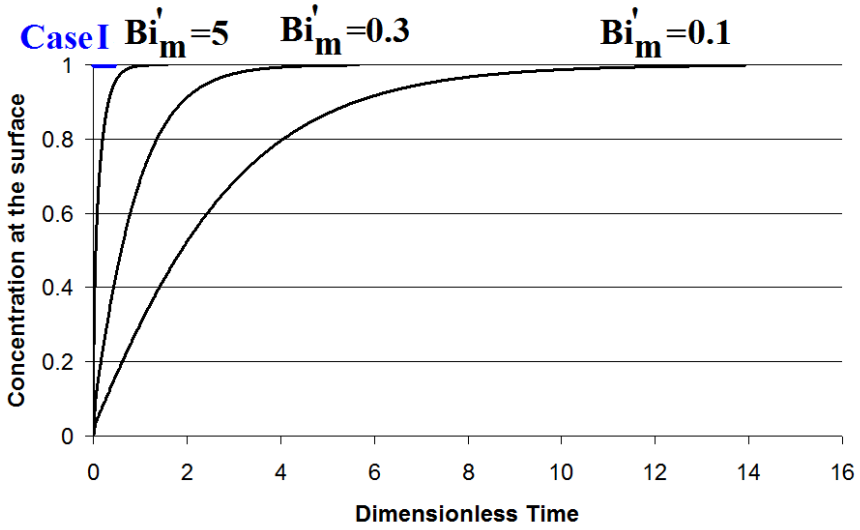


Figure 9.3. The concentration at the surface of the particle versus time for Case I and for Case II with different $Bi'_m$ as 0.1, 0.3 and 5

### 9.1.3. Results of Case III

The governing equations, initial and boundary conditions of Case III indicates that the results of Case III depends on two dimensionless parameter group as Ku and Le numbers. The results for Case III were obtained for Kutateladze number as Ku = 1 and 5 and Lewis number varies from Le = 1 to 50. Figure 9.4 shows the variation of average temperature and average adsorbate concentration for Ku = 1 when Le = from 1 to 50. As shown in Figure 9.4(a), the average of dimensionless temperature decreases with time while the average of adsorbate concentration increases when Ku=1 and Le=1. The total dimensionless time for the adsorption process for this case is around $\Delta\tau$=0.615. As seen, by increase of Le number (Le=3, 10, and 50), the dimensionless adsorption period decreases compared with Le=1. By increase of Le number (Le=3, 10 and 50), the total dimensionless time of adsorption process considerably decreases and attains to 0.412. Also, by increase of Le number, the average dimensionless temperature starts to fall faster. As seen clearly, for high values of Le number (i.e. Le=50) when Ku=1, the average of dimensionless temperature rapidly falls while adsorbate concentration increases slowly. The high value of Le number denotes the mass diffusion controls the adsorption in the particle. Figure 9.4(b) shows variation of $W^*$ and $\theta$ for Ku = 5 while Le is 1, 3, 10 and 50. Similar to the Figure 9.4(a), the increase of Lewis number causes lower heat transfer resistance in the particle and therefore the average dimensionless temperature rapidly falls. The increase of Ku number denotes the increase of heat of adsorption in the particle. The increase of average dimensionless temperature around 1.6 shows the effect of heat of adsorption in the particle for Ku=5 and Le=1. For Le=50 and Ku = 5, mass transfer controls transport of water in the particle and heat transfer is faster than mass transfer. Thus, the effect of heat of adsorption (i.e. the increase of temperature) does not observed with the increasing of Le number from 1 to 50. The comparison of Figure 9.4(a) and 9.4(b) shows that the increase of the Ku value from 1 to 5 extends adsorption period by 29%.

As seen from Figure 9.4, by the increase of Le number, the effect of mass transfer becomes important and it starts to control adsorption. The case can be considered as isothermal when Le > 50. Figure 9.5 shows that the change of Ku number does not have effect on the control mechanism, thus the Le>50 denotes that the case is isothermal and mass transfer controls the mechanism.

### 9.1.4. Results of Case IV

As can be seen from the governing equations of Case IV (Eqs.(5.14), (5.28)) and initial and boundary conditions (Eqs. (5.15), (5.16), (5.19), (5.29), (5.30), (5.35)), the results of Case IV depends on four dimensionless parameter group of *Ku, Le,* $Bi_h$, and $Bi_m^{'}$. The Figure 9.6(a) shows the variation of dimensionless temperature and concentration versus time for Ku=1 Le=1, $Bi_m^{'}$=1 but for variable heat transfer Biot numbers from 0.5 to 100. The increase of $Bi_h$ number from 0.5 to 10 decreases the adsorption period. By increasing of $Bi_h$ number from 0.5 to 10, the Case IV becomes closer to the Case III. However, further increase of $Bi_h$ number from 10 to 100 do not change the variations of average dimensionless temperature and concentration, and the same variation is observed for $Bi_h$=10 and 100.

The variation of average dimensionless temperature and concentration versus time for Ku=1 Le=1, $Bi_h$=1 but for variable $Bi_m^{'}$ numbers from 0.5 to 100 is given in Figure 9.6(b). The increase of $Bi_m^{'}$ from 0.5 to 10 does not change the dimensionless adsorption time significantly. Even, the adsorption period is not changed by increase of $Bi_m^{'}$ from 10 to 100, and the curves of $Bi_m^{'}$=10 and 100 overlap each other. The comparison of Figure 9.6(a) and 9.6(b) shows that the increase of $Bi_h$ number has more effect on the decrease of dimensionless adsorption period compared to $Bi_m^{'}$ number.

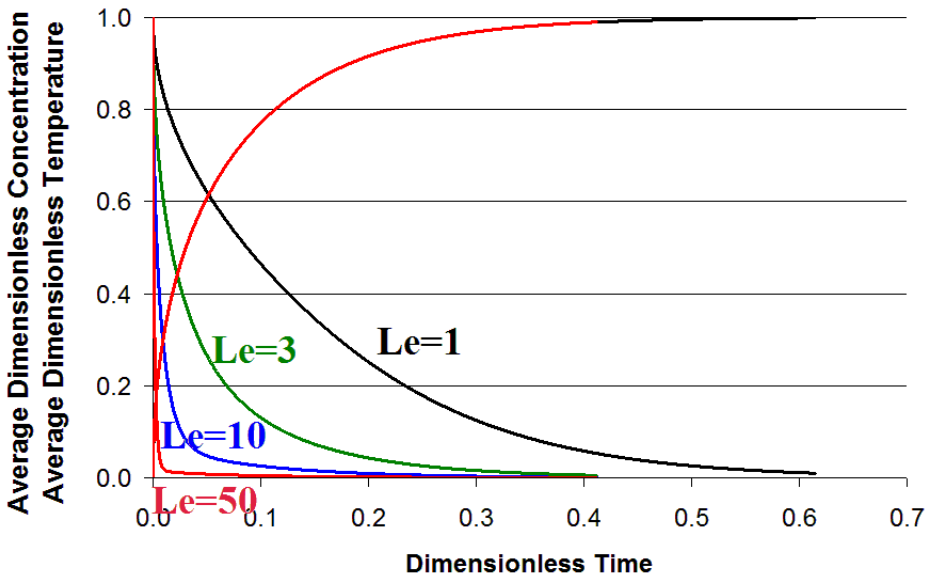


(a)

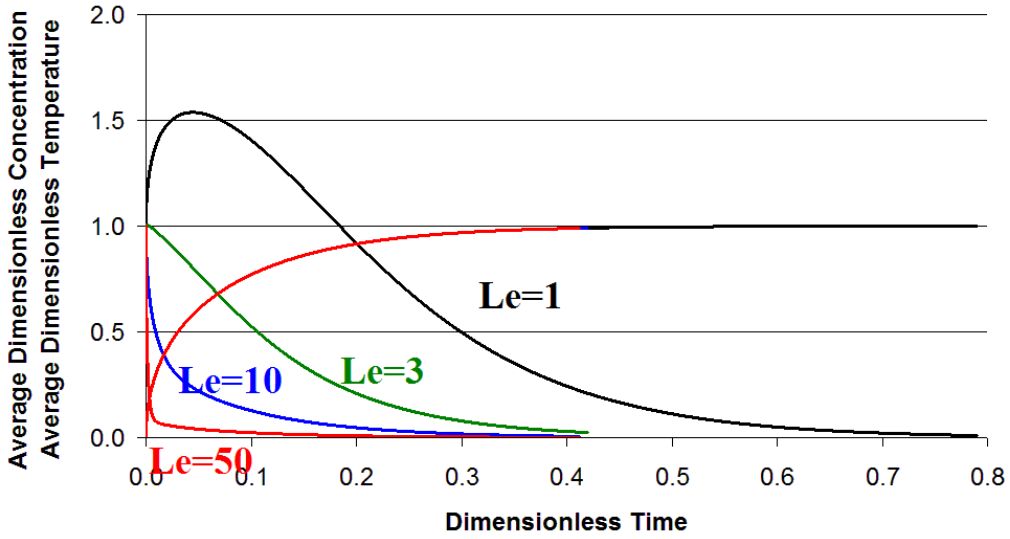


(b)

Figure 9.4. The variation of average dimensionless temperature and concentration versus time for Case III with different Lewis numbers (1, 3, 10, and 50) when (a) Ku=1, and (b) Ku=5

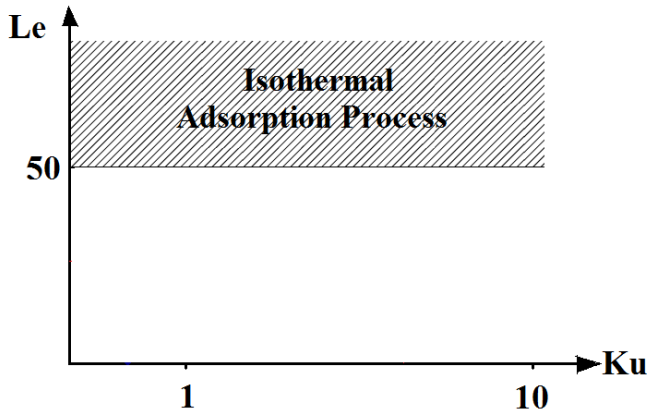


Figure 9.5. The isothermal adsorption process region for different Ku and Le numbers

The Figure 9.6(c) illustrates the variation of dimensionless temperature and concentration versus time for Ku = 1, Le = 1 and $Bi'_m$=100 but for variable $Bi_h$ numbers from 0.5 to 100. By increasing of $Bi_h$ from 0.5 to 10, the variations of temperature and concentration with time get closer to Case III. Further increase of $Bi_h$ causes the match of Case IV with Case III. Hence, for $Bi'_m$=100 and $Bi_h$ = 100, no external heat and mass transfer resistance exists.

Figure 9.6(d) illustrates the obtained results of dimensionless temperature and concentration versus dimensionless time Ku=1, Le=1, $Bi_h$=100 but for variable $Bi'_m$ numbers from 0.5 to 100. For small $Bi'_m$ numbers as 0.5, the dimensionless adsorption period is very long compared with the period of $Bi'_m$=10. By increase of $Bi'_m$, the external mass transfer resistances decreases and adsorption period becomes shorter. As expected, by increase of $Bi'_m$ form 10 to 100, the results of Case III overlaps the results of Case IV showing negligible external heat and mass transfer resistance. The Figure 9.6 clearly shows that, both $Bi_h$ and $Bi'_m$ numbers should be sufficiently high to have identical variations between Case IV and Case III, in which both the external heat and mass transfer resistances can be neglected.

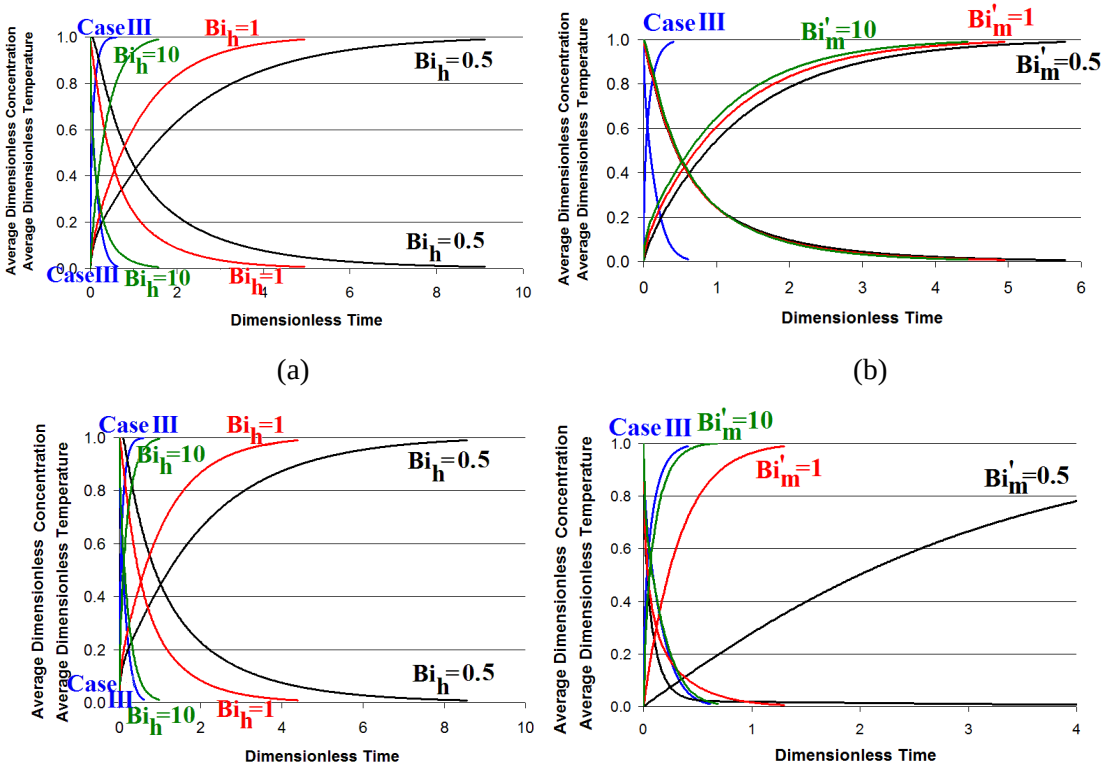


Figure 9.6. The variation of average dimensionless temperature and concentration versus time for Case IV when; (a) Ku=1 Le=1, $Bi_h$ =0.5, 1, and 10, $Bi'_m$ =1, (b) Ku=1 Le=1, $Bi'_m$ =0.5, 1, and 10, $Bi_h$ =1, (c) Ku=1 Le=1, $Bi_h$ =0.5, 1, and 10, $Bi'_m$ =100, (b) Ku=1 Le=1, $Bi'_m$ =0.5, 1, and 10, $Bi_h$ =100

Results for different values of $Bi_h$ and $Bi'_m$ when Ku = 1are obtained and presented in Table 9.1. The horizontal axis of Table 9.1 shows $Bi'_m$ while the vertical axis represents $Bi_h$. As seen from Tables from 9.1(a) to 9.1(d), both $Bi'_m$ and $Bi_h$ are changed from 0.01 to 1000. The gray area in these tables indicates region in which the obtained results of Case IV are different from Case III. However; the results of Case IV are almost identical with Case III for the white region. Hence, for the values of $Bi'_m$ and $Bi_h$ corresponding to the white region, the external heat and mass transfer can be neglected. Table 9.1(a) shows the obtained results for Le = 1. As seen, for high values of $Bi'_m$ and $Bi_h$ such as $Bi'_m$ =1000 and $Bi_h$ =1000, the external heat and mass transfer resistances can be neglected. Table 9.1(b) shows the comparisons of Case IV and Case III for Le = 3. The region in which the results of Case IV and Case III are identical is

expanded. In other words, for wide ranges of $Bi_m^{'}$ and $Bi_h$, the external heat and mass transfer resistances can be neglected. Table 9.1(c) and 9.1(d) are the same with Table 9.1(a) and 9.1(b), however it is obtained for Le = 50 and $10^6$, respectively. As seen from Table 9.1(c) and 9.1(d), by increasing the value of Le number, the results of Case III and Case IV become identical for wider ranges of $Bi_m^{'}$ and $Bi_h$. For instance, in Table 9.1(d), the white region can be achieved for wide ranges of $Bi_h$ from 0.01 to 1000. However, for the moderate values of $Bi_m^{'}$ (such as $Bi_m^{'}$=10), the results of Case III and Case IV does not match each other. Table 9.1 shows that the effect of external heat and mass transfer depend on not only $Bi_m^{'}$ and $Bi_h$ but also on Le number. The reason might be due to the competition between heat and mass transfer in the particle. For Le = 1, heat and mass are propagated with almost the same speed. That is why; the external heat and mass transfer resistances can be neglected only for high values of $Bi_m^{'}$ and $Bi_h$ (such as $Bi_m^{'}$=1000 and $Bi_h$=1000). By increasing of Le number value, the heat is propagated faster than the mass transfer inside the adsorbent particle, and the effect of internal heat transfer resistance become negligible. The adsorbate is transported slower than heat in the particle, and the effect of internal and external mass transfer resistances becomes dominant. That is why, even for low values of $Bi_h$ (such as $Bi_h$ = 0.01) the external heat transfer resistance can be neglected. The obtained results show that for Le = 50, adsorbent temperature drops immediately to the ambient temperature when $Bi_h$ > 10. However for Le = $10^6$, adsorbent particle is at ambient temperature when $Bi_h$ > 0.01 due to high value of Le number. The parameters of Table 9.2 is identical with Table 9.1(d), however the results are obtained for Ku = 8. No change is observed between the results of Tables 9.1(d) and 9.2.

Table 9.1. Case III zones for different values of $Bi_h$ and $Bi_m^{'}$ numbers when Ku = 1 for different Le numbers

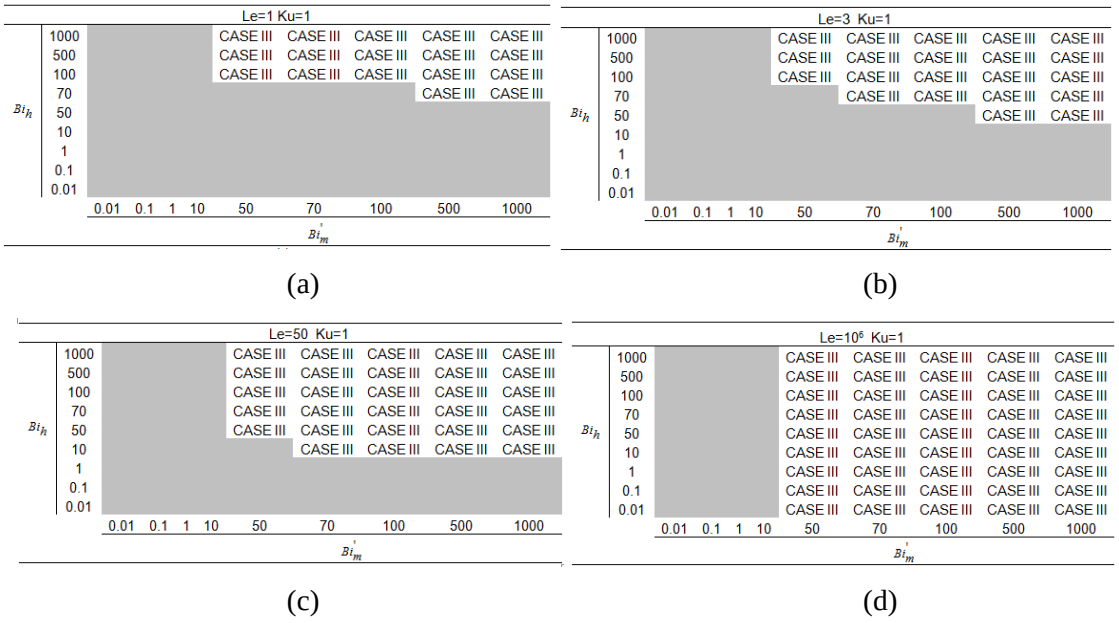


Table 9.2. Case III zones for different values of $Bi_h$ and $Bi_m^{'}$ numbers when Ku = 8 and Le = $10^6$

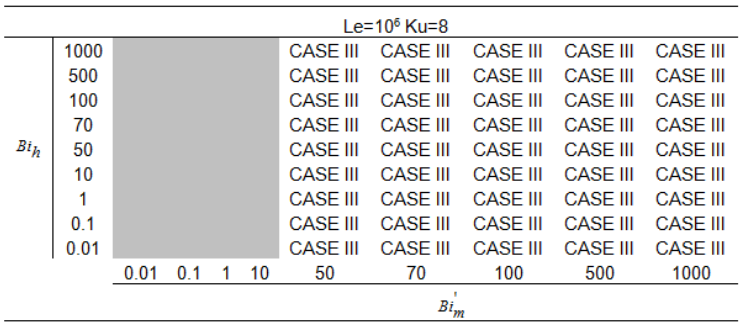


## 9.1.5. The Application of Results for Silica Gel Adsorbent Particle

In order to show the use of the above discussion in practice, a realistic case of adsorption in a single particle is considered. For the considered silica gel-water pair, an adsorption process started 363 K and ended at 303 K is assumed. The water vapor flows around the particle with 0.01 m/s at T = 278 K. The radius of the silica gel particle is 1.25 mm. The thermophysical properties of the considered silica gel-water pair are given in Table 9.3. The effective mass diffusivity is found for four different temperature values between 303 and 363 K and also given in Table 9.3. The heat of adsorption is taken as 2369 kJ/kg for silica gel/water. By using Table 9.3 the values of Ku, Le, heat

transfer Biot number for the considered silica gel/water pair are calculated and presented in Table 9.3. The effective mass diffusivity is found for four different temperature values between 303 and 363 K and presented in Table 9.3. The values of effective thermal capacitance $(\rho C_p)_{eff}$ and effective thermal diffusivity of silica gel are given in the same table (Table 4). These values are calculated by using Eqs (2) and (3), respectively. The heat transfer coefficient between particle and water vapor are calculated according to the equations given in Appendix D. The values of Ku number and heat transfer Biot number are found as 8.11 and 0.169. The Le number value varies from $10^5$ and $10^7$ for silica gel-water pair. Table 9.4 shows molecular diffusivity around the particle, Reynolds, Sherwood, Schmidt numbers, the mass transfer Biot number, G value, and modified mass transfer Biot number for different temperature of silica gel-water pair. These values are calculated according to the equations given in Appendix E. The modified mass transfer Biot numbers are calculated between 254 and 1766 for different temperature values.

According to the values of the Ku, Le, $Bi_h$, and $Bi_m^{'}$ numbers calculated and presented in Tables from 9.2 to 9.4 for the adsorption process from T = 303 to 363 K, these comments can be performed. For the obtained values of Le, Ku, $Bi_m^{'}$ and $Bi_h$ numbers, the effect of external heat and mass transfer resistances can be neglected. Furthermore, the silica gel particle can be assumed isothermal (at ambient temperature) during the adsorption process since the value of Lewis number is very high. There is no need to solve heat transfer equations (Eqs. (5.15-5.16, 5.19, 5.28-5.30, 5.35)) since the temperature in adsorbent particle is uniform and negligible external heat transfer resistance exists. Moreover, no need to consider external mass transfer resistance (Eq. (5.19)). The solution of mass transfer equation (Eq (5.14) of Case I is sufficient to simulate adsorption process in the considered adsorbent particle under mentioned conditions.

Table 9.3. The effective thermal capacity, Nusselt number, heat transfer coefficient, Kutateladze number, Heat transfer Biot number, the effective diffusivity, and Le numbers for different temperature values when u=0.01 m/s, $\Delta H_{ads}$=2369 kJ/kg, $\Delta W$=0.2 kg/kg, $\Delta T$=45$^{o}$C, $r_p$ = 1.25 mm

| Temp. (K) | $D_{eff}$ ($m^2/s$) | $(\rho C_p)_{eff}$ ($J/m^3K$) | $\alpha_{eff}$ ($m^2/s$) | $Nu_D$ | h ($W/m^2K$) | Le | Ku | $Bi_h$ |
|---|---|---|---|---|---|---|---|---|
| 303 | 1.46E-11 | 869.9 | 1.48E-04 | 2.03 | 17.4 | 1.01E+07 | 8.11 | 0.169 |
| 323 | 4.10E-11 | | | | | 3.60E+06 | | |
| 343 | 1.02E-10 | | | | | 1.45E+06 | | |
| 363 | 2.30E-10 | | | | | 6.43E+05 | | |

Table 9.4. The molecular diffusivity, Re, Sc, Sh, the mass transfer Biot numbers, the mass transfer Biot numbers, G values, and the modified mass transfer Biot numbers for different temperature values while $r_p$=1.25 mm when u=0.01 m/s

| Temp. (K) | $D_{molecular}$ ($m^2/s$) | Re | Sc | Sh | $Bi_m$ | G | $Bi'_m$ |
|---|---|---|---|---|---|---|---|
| 303 | 6.89E-05 | 8.13E-02 | 4.47 | 2.28 | 3.58E+06 | 8.55E-05 | 306 |
| 323 | 7.86E-05 | 2.05E-01 | 1.55 | 2.31 | 4.15E+06 | 2.44E-04 | 1010 |
| 343 | 8.85E-05 | 4.54E-01 | 0.622 | 2.35 | 4.73E+06 | 6.12E-04 | 2899 |
| 363 | 9.94E-05 | 9.03E-01 | 0.279 | 2.37 | 5.38E+06 | 1.39E-03 | 7451 |

## 9.2. Results and Discussion on Theoretical Studies for Adsorbent Bed

In this section, results and discussion on heat and mass transfer in adsorbent bed are presented. The governing equations and boundary conditions of the problems were presented in Chapter 6.

### 9.2.1. A Parametric Study on Heat and Mass Transfer in the Adsorbent Bed; Uniform Pressure Approach

In this study, heat and mass transfer in a granular adsorbent bed for an isobaric adsorption process is investigated numerically. The considered adsorbent bed is presented by Figure 6.2. As seen from Figure 6.2 and explained before, the shape of the bed is cylindrical and there is a hollow at the center of the bed provides motion of

adsorptive in the bed and then adsorptive moves in radial direction in the bed. The assumption of uniform pressure in the bed is accepted for this study. The isobaric adsorption process is illustrated in Figure 6.3. The dimensional governing equations, which are heat transfer equation for adsorbent bed and mass transfer equation for particle, and related boundary conditions are given by Table 6.1 in Section 6.2.1. The dimensionless for of these equations and boundary conditions are given by Table 6.2 in Section 6.2.2. The employed assumptions are also given in the Section 6.1.

As it is explained in the Section 6.2.2, nine independent variables which effect heat and mass transfer in the bed are combined only in two independent variables as Ku and Γ. The parameter Ku is the ratio of heat of adsorption generated in the adsorbent bed to the sensible thermal energy storage during adsorption process. Large values of Ku signify high heat of adsorption compared to the sensible thermal energy stored by adsorbent. The Γ parameter refers to the ratio of mass diffusion in radial direction of adsorbent particle to the diffusion of heat in radial direction of adsorbent bed. High value of Γ shows that the diffusion of mass in the radial direction of the adsorbent particle is faster than the transfer of heat in radial direction of the adsorbent bed. For the high values of Γ, the adsorptive can be adsorbed immediately in the adsorbent particle and the adsorbate concentration in the adsorbent particle may be expected be almost uniform. In this case, the mass transfer resistance in the particle can be neglected; therefore heat transfer resistance through the adsorbent bed controls the adsorption process. For low values of Γ, the propagation of heat in the adsorbent bed is faster than adsorptive transfer in the adsorbent particle. Hence, mass transfer resistance in the adsorbent particle is expected to control the adsorption process.

The aim of this study is to:

- investigate the effects of Ku and Γ parameters on local and average temperature and adsorbate concentration in the adsorbent bed for the adsorption process,
- compare three models used to simulate mass transfer through an adsorbent granule as instantaneous equilibrium, linear driving force (LDF), and solid diffusion models based on Ku and Γ parameters.

It should be mentioned that the results of present study is valid for adsorbent bed with $R_o/R_i = 2$. The constants of k and n in the isotherm equation which is given in Eq. (6.6) are 0.552 and 1.6, respectively for the silica gel-water pair. The thermophysical

properties of silica gel, for which the study is performed, are given in Table A.1 in Appendix A.

### 9.2.1.1. Determination of Rages of Ku and Γ

Ku and Γ numbers are numbers whose ranges are not known. The values of these dimensionless parameters highly depend on thermophysical properties of the adsorbent-adsorbate pair. Some values of Ku and Γ for silica gel-water, active carbon-methanol, and zeolite 13X-water pairs are shown in Table 9.5 by using the thermophysical properties of these pairs at 53.5$^{o}$C presented in Appendix A, Table A1 (Incropera and Dewitt 1996, Perry and Green 1984, Cheng and Kung 1994, Leong and Liu 2004, Wang et al. 2006, Ogueke and Anyanwu 2008).

As seen from Table 9.5, the particle radiuses are considered as 0.1, 0.5, and 1 mm, and consequently the values of Ku and Γ are changed. Based on this table, the values of Ku and Γ are changed from 1 to 100 and from $10^{-5}$ to 1, respectively.

### 9.2.1.2. Effect of Ku and Γ on Average Bed Temperature and Bed Adsorbate Concentration

Figure 9.7 shows the change of averages of dimensionless adsorbate concentration and temperature with dimensionless time for two different values of Ku and Γ. The results were obtained by LDF method. As shown in Figure 9.7(a), the average of dimensionless temperature decreases with time while the average of adsorbate concentration increases when Ku =1 and Γ=1. The total dimensionless time for the adsorption process for this case is around $\Delta\tau$ =6.95. For low values of Γ (i.e. Γ=$10^{-5}$) when Ku =1, the average of dimensionless temperature rapidly falls while adsorbate concentration increases slowly as seen from Figure 9.7(b). By decrease of Γ value to $10^{-5}$, the total dimensionless time of adsorption process considerably increases and attains to 52400.

Table 9.5. Values of Ku and Γ for an adsorbent bed filled with adsorbent particle when $\varphi$=0.35, $R_i$ = 10 mm, $T_{mean}$=53.5°C, $D_{eff}$ = 4.97x10$^{-11}$ m$^2$/s, $\overline{W}$ =0.1 and ΔT=10°C

| | $r_p$ (m) | $(\rho C_p)_{eff}$ (kJ/kgK) | $\lambda_{eff}$ (W/mK) | $\alpha_{eff}$ (m$^2$/s) | Ku | Γ |
|---|---|---|---|---|---|---|
| silica gel-water | 0.0001 | 565.475 | 0.136 | 0.000241 | 36.490 | 2.06E-03 |
| | 0.0005 | 565.475 | 0.136 | 0.000241 | 36.490 | 8.25E-05 |
| | 0.001 | 565.475 | 0.136 | 0.000241 | 36.490 | 2.06E-05 |
| activecarbon-methanol | 0.0001 | 278.249 | 0.078 | 0.000280 | 24.114 | 1.78E-03 |
| | 0.0005 | 278.249 | 0.078 | 0.000280 | 24.114 | 7.10E-05 |
| | 0.001 | 278.249 | 0.078 | 0.000280 | 24.114 | 1.78E-05 |
| zeolite13X-water | 0.0001 | 336.974 | 0.138 | 0.000408 | 56.664 | 1.22E-03 |
| | 0.0005 | 336.974 | 0.138 | 0.000408 | 56.664 | 4.87E-05 |
| | 0.001 | 336.974 | 0.138 | 0.000408 | 56.664 | 1.22E-03 |

The low value of Γ denotes the slow mass diffusion in the particle and that's why the adsorption time is highly increased. The changes of $\overline{W}^*$ and $\theta$ for Ku =100 and Γ=1 are similar to those of Figure 9.4(a), however the total dimensionless time of adsorption increases 61-folds due to the increase of Ku which is a source term in Eq. (6.10) and the increase of Ku value increases the period of adsorption process. Figure 9.7(d) shows variation of $\overline{W}^*$ and $\theta$ for Ku =100 while Γ= 10$^{-5}$. Similar to the Figure 9.7(b), the decrease of Γ signifies a lower heat transfer resistance in the adsorbent bed in radial direction and therefore the average dimensionless temperature rapidly falls. The comparison of Figure 9.7(b) and 9.7(d) shows that the increase of the Ku value from 1 to 100 extends adsorption period only by 0.4%.

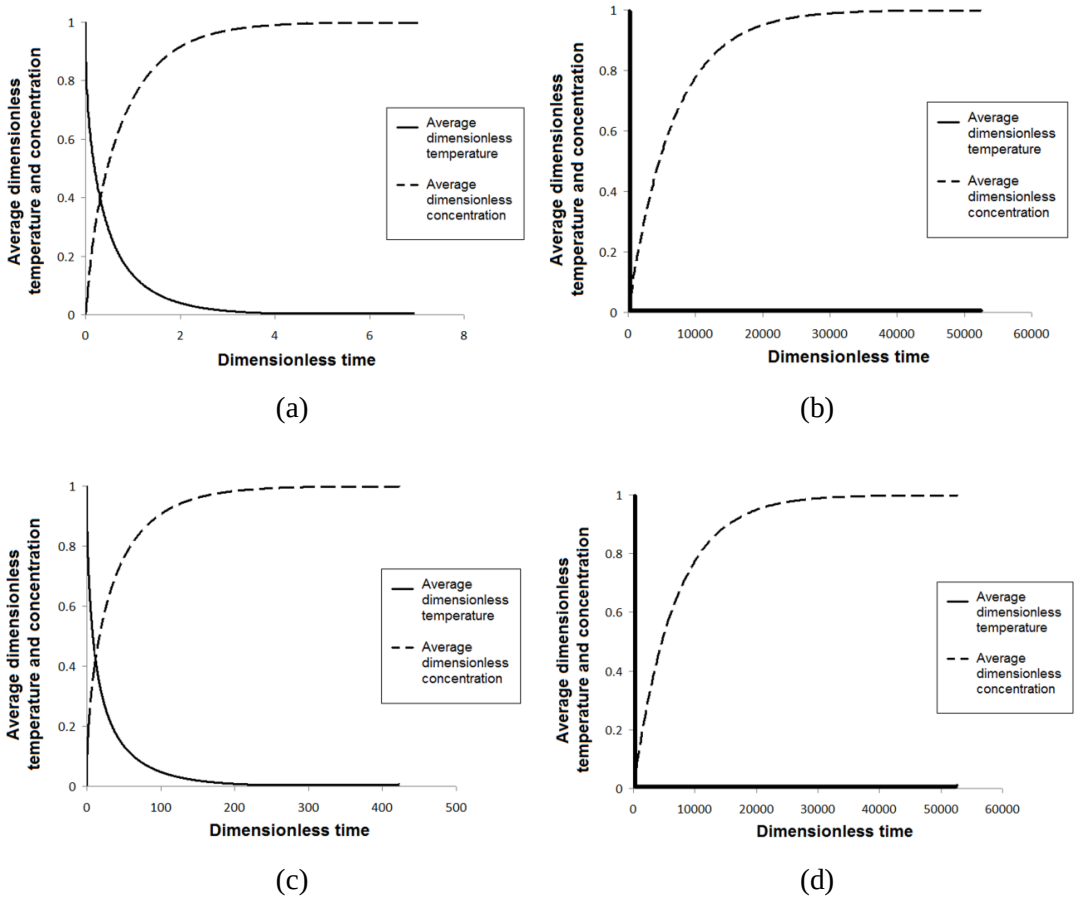


Figure 9.7. The variation of average dimensionless temperature and adsorbate concentration with dimensionless time, (a) Ku=1, Γ=1, (b) Ku=1, $\Gamma=10^{-5}$, (c) Ku=100, Γ=1, (d) Ku=100, $\Gamma=10^{-5}$

### 9.2.1.3. Effect of Ku and Γ on Local Temperature and Adsorbate Concentration

Figure 9.8 depicts the change of dimensionless adsorbate concentration and temperature profiles in the adsorbent bed for different dimensionless times for Ku =1 and 100, and $\Gamma=10^{-5}$ and 1. As is seen from Figure 9.8(a), for Ku =1 and Γ=1, both the diffusion of heat through the adsorbent bed and diffusion of adsorptive in the adsorbent particle reach the steady state after a short period τ = 6.95. Figure 9.8(b) shows the variations of $\overline{W}^{*}$ and $\theta$ when Ku =1 and $\Gamma=10^{-5}$. For small values of Γ (i.e. $\Gamma=10^{-5}$), the diffusion of heat through the adsorbent bed is faster than the diffusion of adsorptive in the adsorbent particle. After dimensionless time as τ =2, the distribution of temperature in the adsorbent bed becomes uniform and drops to around $\theta=0$ which overlaps the X axis. However, the adsorbate concentration attains to steady state after τ

= 52400 signifying that the low speed of adsorptive diffusion in the particle causes the increase of adsorption period. The distribution of local $\overline{W}^*$ and $\theta$ for Ku =100 and Γ=1 are shown in Figure 9.8(c). Similar to Figure 9.8(a), both the temperature and adsorbate concentration profiles in the adsorbent bed approaches to the steady state at the same time however the increase of Ku increases the period of adsorption process to τ = 422. The profiles of $\overline{W}^*$ and $\theta$ for the large value of Ku (i.e. Ku =100) but for small value of Γ (i.e. $\Gamma=10^{-5}$) are illustrated in Figure 9.8(d). Heat transfer through the adsorbent bed is faster than mass transfer in the particle and almost uniform mass transfer profile occurs during adsorption process.

### 9.2.1.4. Effect of Ku and Γ on Total Adsorption Period

The variation of total dimensionless period of adsorption process with Γ for Ku = 1 and 100 is presented in Figure 9.9. The mass transfer resistance through the particle becomes smaller by increase of Γ value from $10^{-5}$ to 1, and therefore total dimensionless period of adsorption process is decreased. The decrease of Γ from $10^{-5}$ to 1 reduces total dimensionless adsorption period by 753% when Ku=1. For large values of Γ, mass transfer resistance is negligible and heat transfer through the bed is the main transport resistance. The similar changes of total dimensionless period with Γ can also be observed when Ku=100. However; the rate of decrease of total dimensionless period is smaller compared with that of Γ=1. The increase of value of Ku increases the value of source term in Eq. (6.10) and consequently the cooling of the adsorbent bed becomes slower.

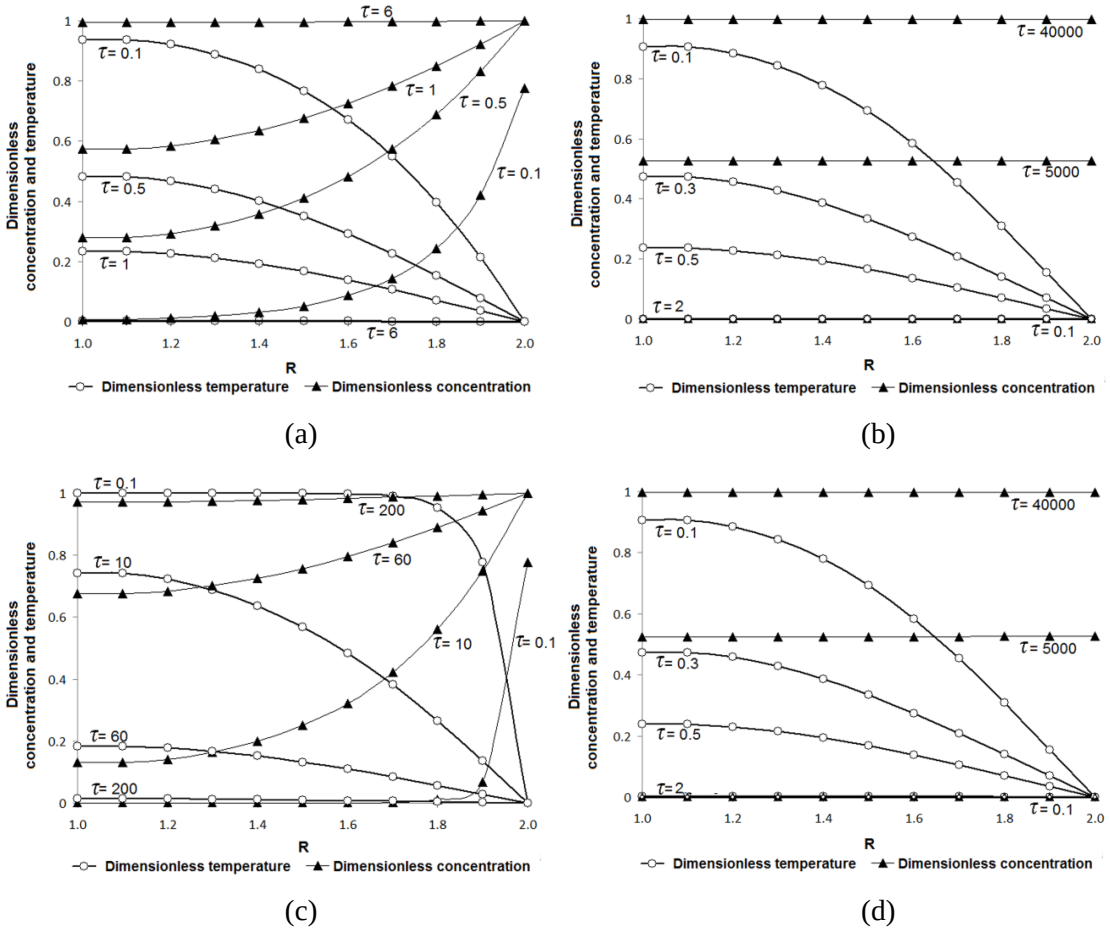


Figure 9.8. The change of dimensionless temperature and adsorbate concentration profiles along the radius of the adsorbent bed at different dimensionless time, (a) Ku=1, Γ=1, (b) Ku=1, $\Gamma=10^{-5}$, (c) Ku=100, Γ=1, (d) Ku=100, $\Gamma=10^{-5}$

### 9.2.1.5. Effect of Ku and Γ on Mass Transfer Model for Adsorbent Particle

Figure 9.10 shows the comparison of average of adsorbate concentration versus dimensionless time for three mass balance models for adsorbent particle as instantaneous equilibrium, LDF and solid diffusion models and for two different values of Γ as $10^{-5}$ and 1 when Ku= 1 . As shown in Figure 9.10(a), the changes of $\overline{W}^{*}$ for all three models are very close to each other when Γ = 1. Therefore, all three models can be used for high values of Γ when Ku=1.

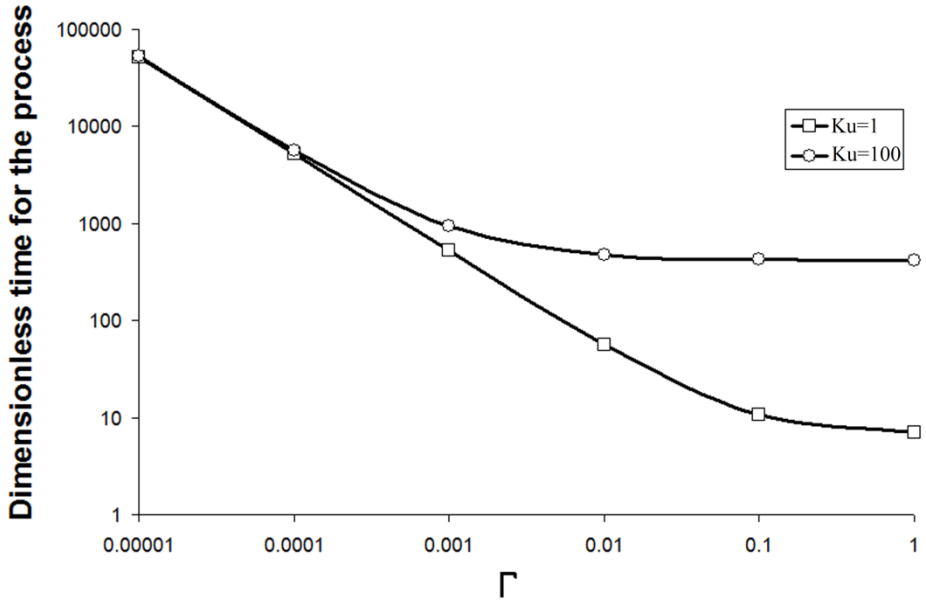


Figure 9.9. The variation of total dimensionless time of the adsorption process with Γ for Ku=1 and Ku=100

However, the variation of $\overline{W}^{*}$ with dimensionless time for instantaneous equilibrium model becomes very different than LDF and solid diffusion models when $\Gamma = 10^{-5}$ as seen from Figure 9.10(b). The adsorbate concentration rapidly attains to equilibrium condition for instantaneous equilibrium model and it overlaps Y axis. The changes of average of dimensionless concentration with time for LDF and solid diffusion models are similar to each other. This figure shows that the equilibrium model cannot be used for low values of Γ, but LDF and solid diffusion models provide similar results. Although the analytical solution of solid diffusion model provides exact solution for the changes of adsorbate concentration in the particle, the LDF model is more preferable due to saving of computational time. The obtained results show that the similar behavior observed for Ku=1 is valid when Ku=100.

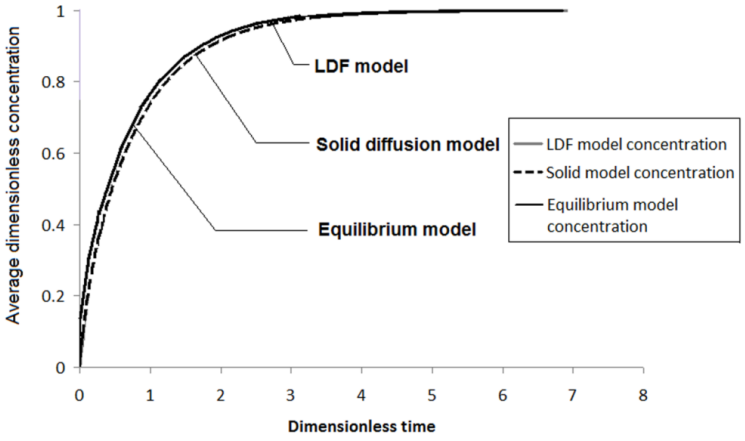


(a)

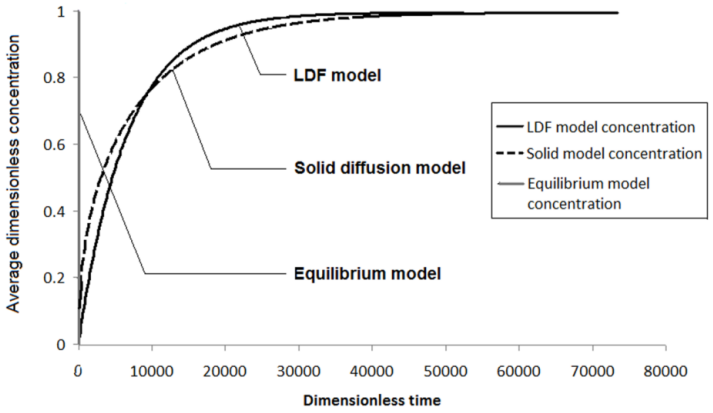


(b)

Figure 9.10. Comparison of average adsorbate concentration with dimensionless time for instantaneous equilibrium, LDF and solid diffusion models, (a) Ku=1, Γ=1, (b) Ku=1, $\Gamma=10^{-5}$

## 9.2.2. Effect of Fin on Heat Acceleration in an Adsorbent Bed

In this study, the analyzed adsorbent bed is an annular bed with inner fins in radial direction as shown in Figure 6.4. The silica gel-water pair is working pair and the silica gel particles located between fins. As mentioned in Section 6.4, it is assumed that the upper and lower surfaces of bed are well insulated and the adsorbent bed is enough long, so the end effects can be neglected. The heat and mass are transferred both in radial and angular directions of the bed. The uniform pressure approach is used for this study. Figure 6.3 illustrates the isobaric adsorption process. The governing equations of the considered problem (heat transfer equation for the bed and fin, mass transfer equation for a particle) are given in Chapter 6.4. The employed assumptions are also

given in the Section 6.1.The initial and boundary conditions of the problem are given in Table 6.5. The dimensionless forms of these equations and boundary conditions are given by Table 6.6 in Section 6.4.2.

As mentioned before, the non-dimensionalization of heat transfer equation for the adsorbent bed and mass balance equation for the adsorbent particle yields two dimensionless parameters as Kutateladze number and a dimensionless parameter denoted by $\Gamma$ which compares the rates of mass diffusion within the adsorbent particle and heat diffusion in the adsorbent bed. Moreover, the non-dimensionalization of conduction heat transfer equation of radial fin yields two dimensionless parameters as dimensionless fin coefficient parameter and thermal diffusivity ratio ($\Lambda$ and $\alpha^*$). Based on our knowledge, no dimensionless study on heat and mass transfer in an adsorbent bed with fins for an isobaric adsorption process has been conducted.

The aim of present study is;

- to perform a dimensionless study on heat and mass transfer in an adsorbent bed with fin
- to investigate the effect of the fin on acceleration of heat and mass transfer
- to use dimensionless parameter of Ku and $\Gamma$ for design of adsorbent bed with fins
- to understand effects of fin parameter such as thermal diffusivity ratio, thermal conductivity ratio, fin geometrical parameters on transfer of heat and mass in the bed.

Initially, the adsorbent bed is at $T_d$ temperature and adsorbate concentration in the bed is $W_d$ as shown in Figure 6.3(a). Suddenly, the temperature of the bed outer surface falls to $T_a$ and the valve between the adsorbent bed and the evaporator (V1 valve) is opened to allow the transfer of adsorptive (i.e., water vapor) to the bed (Figure 6.4). The adsorptive can flow easily between the silica gel particles; therefore the interparticle mass transfer resistance is neglected. The process is isobaric and the bed pressure is not changed during the adsorption process. The bed final temperature is $T_a$ and the corresponding adsorbate concentration is $W_a$. The inner and outer radiuses of the adsorbent bed are 50 and 110 mm, respectively. Number of fins in the adsorbent bed is 12. A schematic view of dimensionless adsorption equilibria is shown in Figure 6.3(b).

The values of the constants m and n used in the isotherm equation (Eq. (6.6)) are 0.552 and 1.6, respectively. Since the dimensionless forms of the governing equations are solved, the dimensionless adsorption equilibrium relation is required. By using dimensionless parameter groups represented by Eq. (6.9), an equation which yields the variation of $W_{\infty}^{*}$ in terms $\theta$ can be obtained:

$$W_{\infty}^{*} = -0.774\theta^{3} + 2.13\theta^{2} - 2.355\theta + 0.995 \qquad (9.1)$$

The above equation is valid for an adsorption process under a bed pressure of P = 2 kPa and the operation temperature ranges from 303 to 363 K (i.e., $T_a$= 303 K and $T_d$ = 363 K).

### 9.2.2.1. The Effect of Dimensionless Parameters Λ and α* on Dimensionless Temperature and Concentration in the Adsorbent Bed

The distributions of dimensionless temperature and adsorbate concentration in the half of the region between two fins at different steps of adsorption process are shown via contours. Figure 9.11 shows the distribution of dimensionless temperature in the half region between two fins at four time steps of adsorption period when Ku = 1, Γ= 1, $\Lambda$ = 100, and $\alpha^{*}$ = 0.01. As it was mentioned before, the bed initial temperature is 1 (i.e., $\theta$ = 1) and suddenly the bed outer surface temperature, and consequently the base temperature of fin, drops to $\theta$ = 0. After τ = 0.001, the distribution of dimensionless temperature in the adsorbent bed is shown in Figure 9.11(a). The temperature in the region close to the bed outer surface is smaller than the temperature of center region. Temperature gradient in radial direction of thin fin is very similar to the temperature gradient in the region between two fins. It seems that the thin fin does not have considerable effect on heat transfer in the bed since no remarkable temperature gradient is observed in angular direction of the bed. Although the fin thermal diffusivity is greater than bed effective thermal diffusivity, $\alpha_{fin} > \alpha_{eff}$ , heat flux from lateral surfaces of the thin fin is remarkably greater than the heat flux through the radial direction of the fin due to large value of dimensionless fin coefficient (i.e., $\Lambda$ = 100).

Therefore, no temperature gradient in the angular direction in the bed exits and temperatures of fin and the adsorbent region are almost identical. As seen from Figures 9.11(b) and 9.11(c), the temperature decreases by time in radial direction (i.e., from the outer to inner surface), and the temperature of center region drops to the surface temperature (i.e. $\theta = 0$) after $\tau = 3.77$ (Figure 9.11(d)).

The distribution of adsorbate concentration at the four time steps of adsorption process of Figure 9.11 is shown in Figure 9.12. The dimensionless adsorbate concentration in the adsorbent particles is zero at the beginning of the adsorption process. After opening V1 valve, shown in Figure 6.4, the adsorbate vapor uniformly enters to the bed from the inner surface. The adsorption rate in the adsorbent particle depends on equilibrium adsorbate concentration and consequently on the adsorbent particle temperature. As seen from Figures 9.12(a) and 9.12(b), the adsorption rate in the region with low temperature (i.e., region close to $R = R_o$) is higher than the concentration in region close to $R = R_i$. The particle temperature in the center region decreases over time, and consequently the adsorbate concentration increases (Figure 9.12(c)). The gradient of adsorbate concentration in angular direction is negligible due to the small angular gradient of temperature. The dimensionless adsorbate concentration in the bed is 1 at the end of adsorption period. No further adsorption almost occurs in the bed after $\tau = 3.77$.

Figure 9.13 shows the temperature distribution in the half region between two fins in the adsorbent bed when $Ku = 1$, $\Gamma = 1$, $\alpha^* = 0.01$, but $\Lambda = 0.01$. The decrease of $\Lambda$ signifies the increase of heat conduction in radial direction of fin. As seen from Figures 9.13(a), illustrating the distribution of dimensionless temperature at $\tau = 0.001$, fin temperature is lower than bed temperature. The temperature of entire fin is almost equal to the base temperature of fin at $\tau = 0.015$ (Figure 9.13(b)). The low value of $\Lambda$ (i.e., $\Lambda = 0.01$) causes a higher conduction heat transfer in radial direction of thin fin, and the fin temperature quickly drops to the base temperature (i.e., $\theta = 0$). That is why, a remarkable temperature gradient in angular direction is observed. The temperature in the region between two fins drops to the surface temperature (i.e., $\theta = 0$) after $\tau = 0.878$ as seen from Figure 9.13(d). The decrease in $\Lambda$ value from 100 to 0.01 reduces the adsorption period by 4.3-fold.

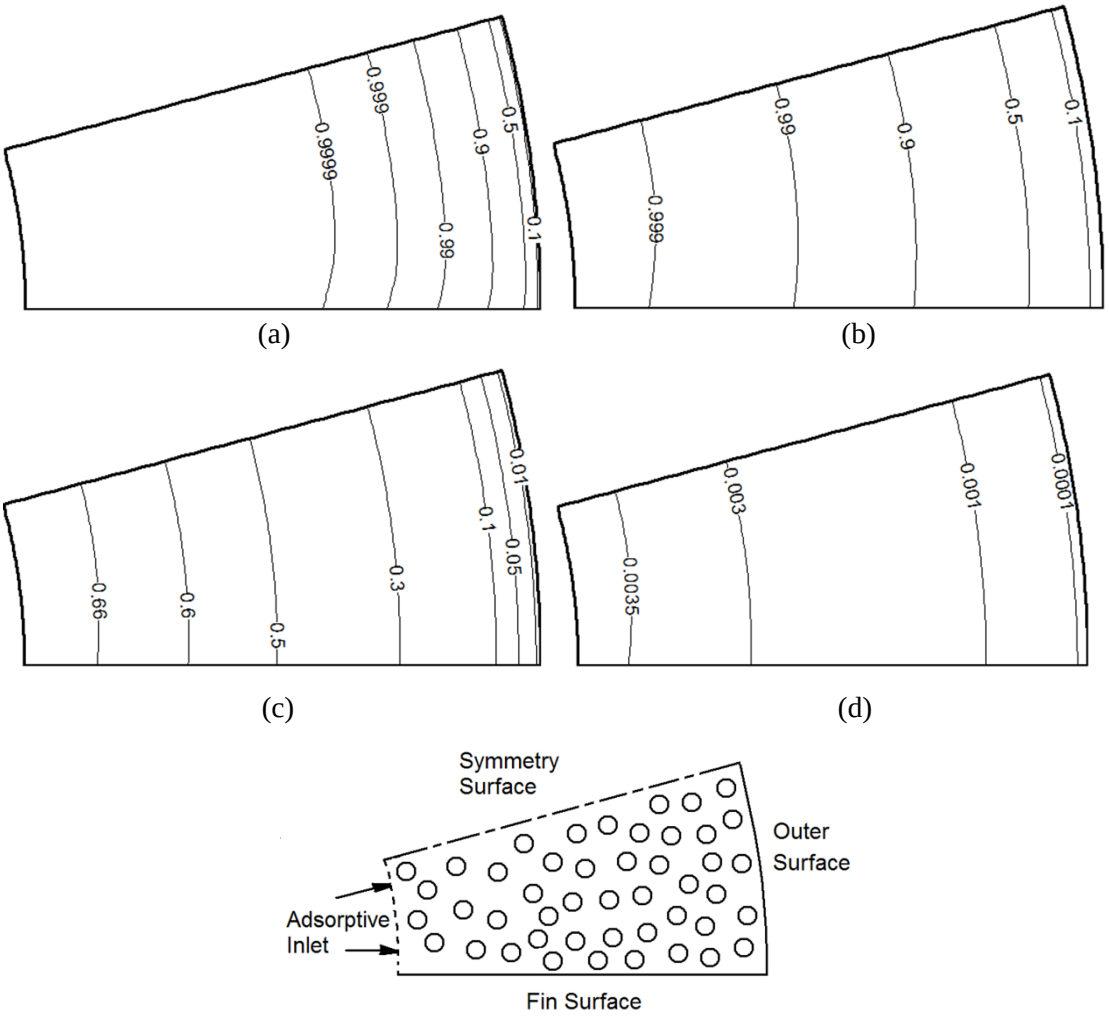


Figure 9.11. Dimensionless temperature distribution in the half region between two fins when Ku = 1, $\Gamma = 1$, $\Lambda = 100$, and $\alpha^* = 0.01$, a) $\tau = 0.001$, b) $\tau = 0.015$, c) $\tau = 0.2$, d) $\tau = 3.777$

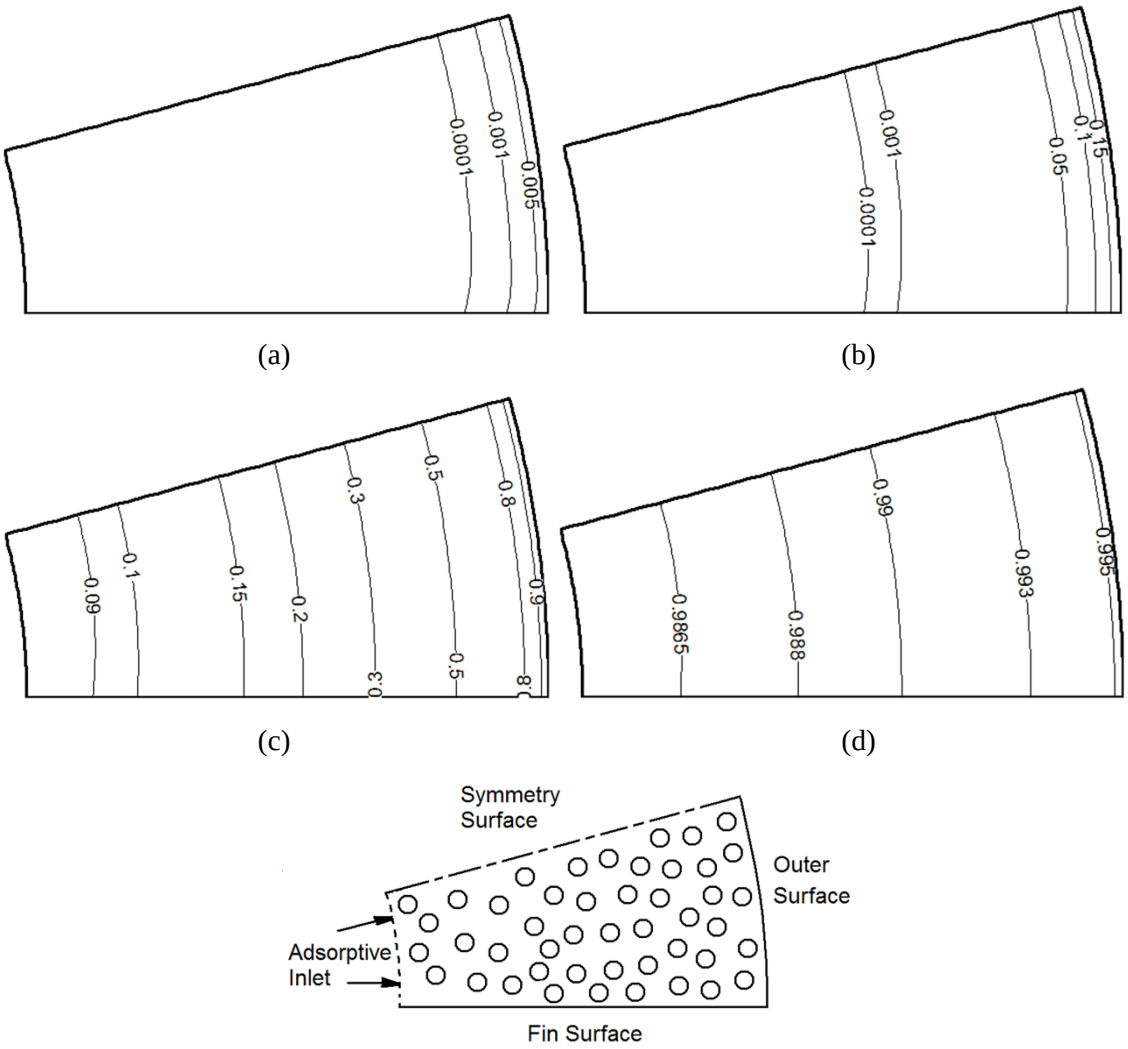


Figure 9.12. Dimensionless adsorbate concentration contours in the half region between two fins when Ku = 1, Γ = 1, Λ = 100, and α* = 0.01, a) τ = 0.001, b) τ = 0.015, c) τ = 0.2, d) τ = 3.77

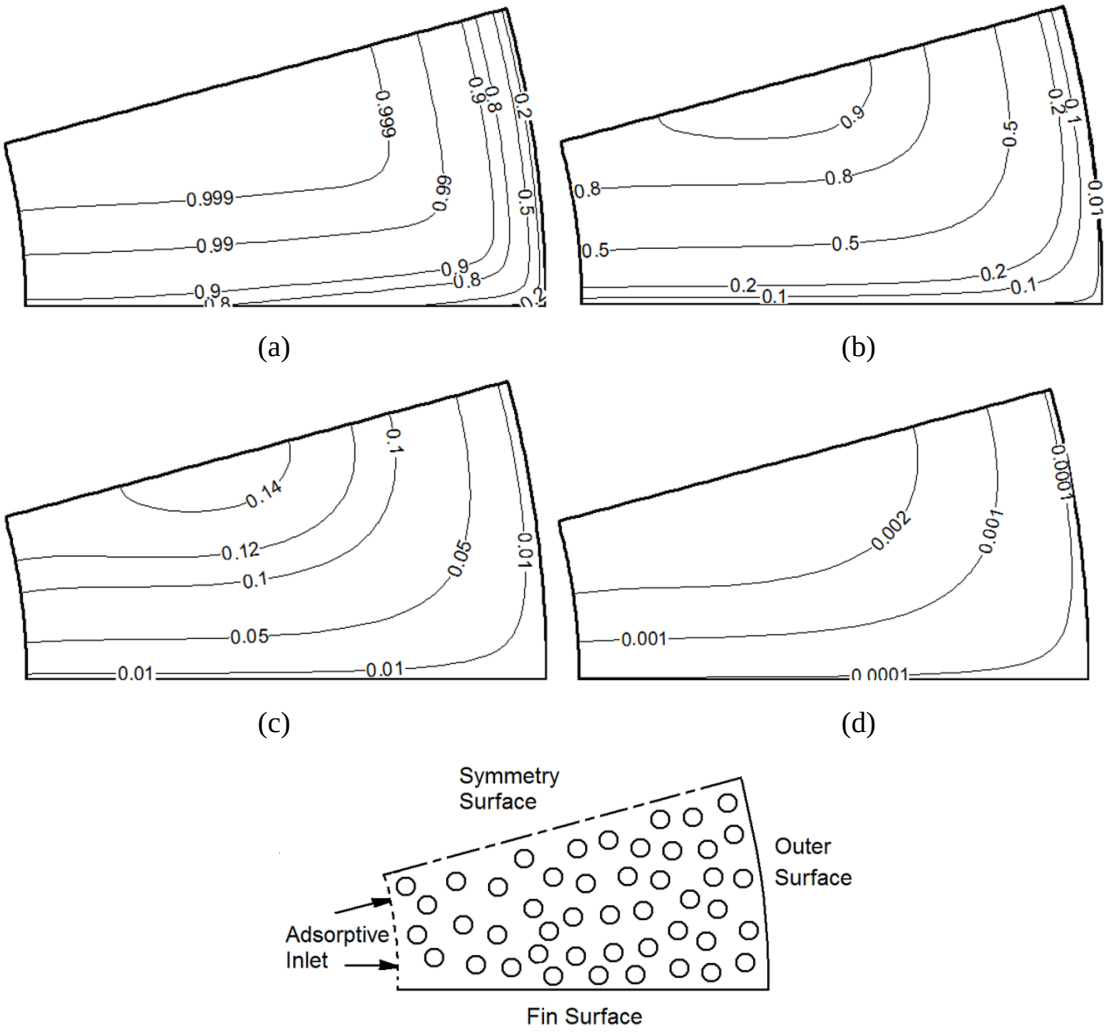


Figure 9.13. Distribution of dimensionless temperature in the half region between two fins when Ku = 1, Γ = 1, Λ = 0.01, and α* = 0.01, a) τ = 0.001, b) τ = 0.015, c) τ = 0.2, d) τ = 0.878

The temperature distribution in the bed at four time steps of adsorption process when Ku = 1, Γ= 1, Λ= 0.01, but for an extreme thermal diffusivity ratio as $\alpha^* = 100$ is shown in Figure 9.14. The temperature distribution in the bed is different than that presented in Figure 9.13, for which $\alpha^* = 0.01$. A high value of $\alpha^*$ (i.e., $\alpha^* > 1$) refers to the lower thermal diffusivity of fin compared to the bed effective thermal diffusivity. Therefore, the heat propagation in the bed is faster than the heat diffusion through the radial direction of fin. As clearly seen from Figure 9.14, the cooling rate in the region close to the fin is smaller than the cooling rate in the center, and consequently, the bed can not be cooled via fins for the cases with $\alpha^* = 100$. The increase of $\alpha^*$ value from 0.01 to 100 prolongs the adsorption period by 177-fold and the total period of adsorption increases from 0.878 to 156.03.

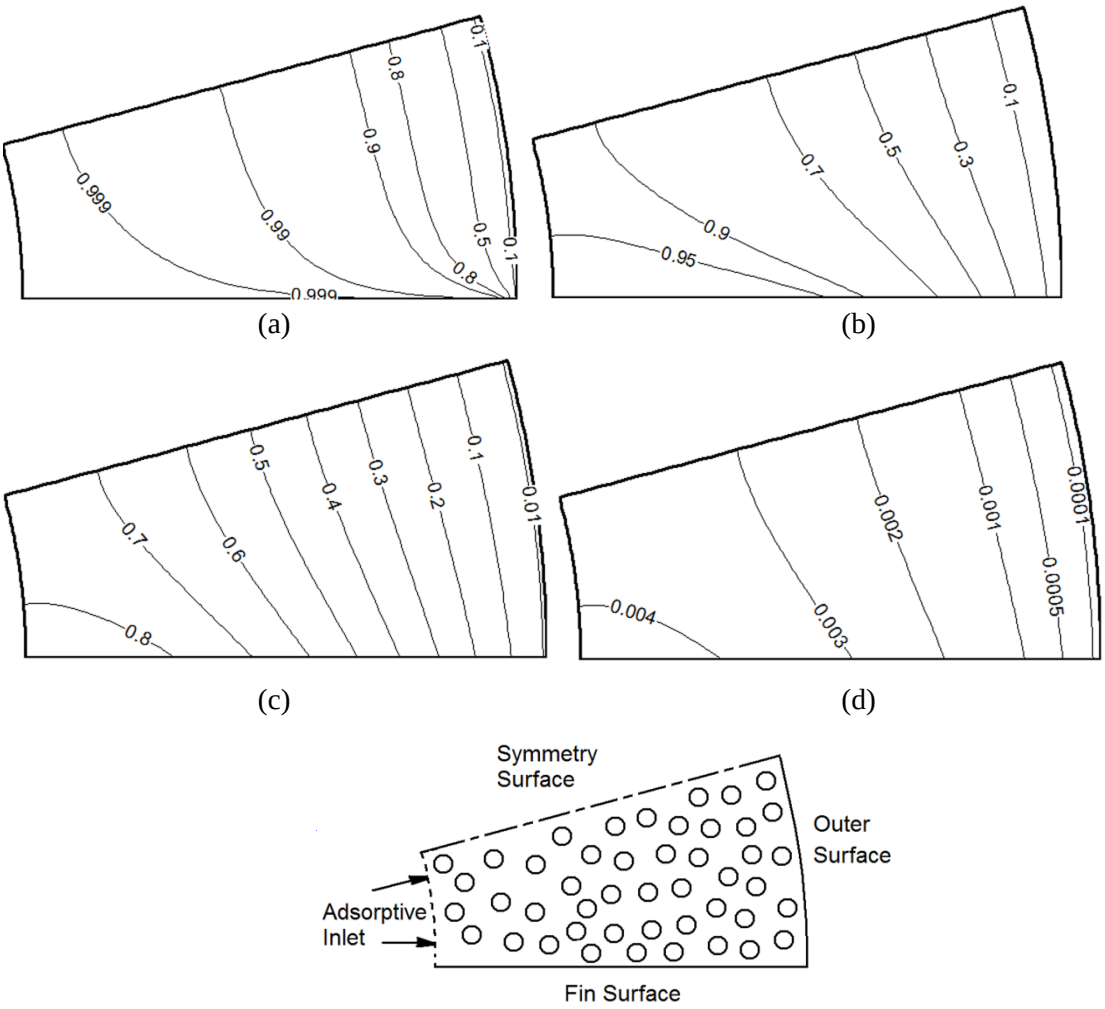


Figure 9.14. Dimensionless temperature distribution in the half region between two fins when Ku = 1, Γ = 1, Λ = 0.01, and α* =100, a) τ = 0.1, b) τ = 2, c) τ = 10, d) τ = 156.03

### 9.2.2.2. The Effect of Fin, Ku and Γ Numbers on Adsorption Period

Figure 9.15 depicts the changes in average temperature and adsorbate concentration of the bed during the adsorption process when Γ = 1, Λ = 0.01 and for two Kutateladze numbers of 1 and 100. The change in average temperature and adsorbate concentration when no fin exists in the adsorbent bed is also plotted in the same figure. As seen from Figure 9.15, the average dimensionless temperature decreases while the average adsorbate concentration increases during the adsorption process. The effect of fin on heat and mass transfer rate in the bed can be observed clearly. The duration of adsorption process in an adsorbent bed without fin when Ku = 1 and $\Gamma$ = 1 is $\tau_{total}$ = 3.86. The use of 12 fins with Λ = 0.01 and $\alpha^*$ = 0.01 reduces this

period to $\tau_{total}$ = 0.878. The use of fin reduces the dimensionless adsorption period by 439%. The increase of Ku value from 1 to 100 increases heat generation in the bed, and the adsorption period is increased (Figure 9.15 (b)). The use of 12 fins with $\Lambda$ = 0.01 and $\alpha^*$ = 0.01 reduces the adsorption period from 233.5 to 38.8 when Ku = 100. The percentage reduction of adsorption period for the adsorbent bed with Ku = 100 by using 12 fins is 601% which is higher than the reduction in the period of bed with Ku = 1. This result shows that for the adsorbent beds with high values of Ku number (i.e., Ku = 100), the role of fin on the reduction of adsorption period becomes more significant.

In order to present the effect of $\Gamma$ number on heat and mass transfer rate in an adsorbent bed, Figure 9.16 is presented. In this figure, the changes in average temperature and adsorbate concentration in a bed with $\Gamma = 10^{-5}$ for two values of Ku = 1 and 100 are illustrated while no fin exists in the adsorbent bed. The variation of average temperature and concentration for Ku = 1 and Ku = 100 is almost identical and temperature curves overlap. The bed average temperature rapidly falls to $\theta$ = 0, while the adsorbate concentration increases slowly over time. As it was mentioned before, $\Gamma$ parameter compares the mass diffusion in the radial direction of adsorbent particle to the diffusion of heat in the adsorbent bed. The low value of $\Gamma$ refers to higher heat transfer rate in the adsorbent bed and therefore the bed temperature rapidly falls to the outer surface temperature. Therefore, the mass diffusion in the adsorbent particle controls the adsorption period. The use of fin does not influence the period of adsorption process since heat transfer in the bed is quicker than mass diffusion in the adsorbent particle, considerably. For an adsorbent bed with a low value of $\Gamma$ (i.e., $\Gamma = 10^{-5}$), the period of the adsorption process can be shortened only by reducing mass transfer resistance in the adsorbent particle. A comparison between Figures 9.15(a) and 9.16 shows that, a decrease in the value of $\Gamma$ from 1 to $10^{-5}$ prolongs the adsorption period and it is increased from 0.878 to 35000. The increase of Ku from 1 to 100 does not influence the adsorption period.

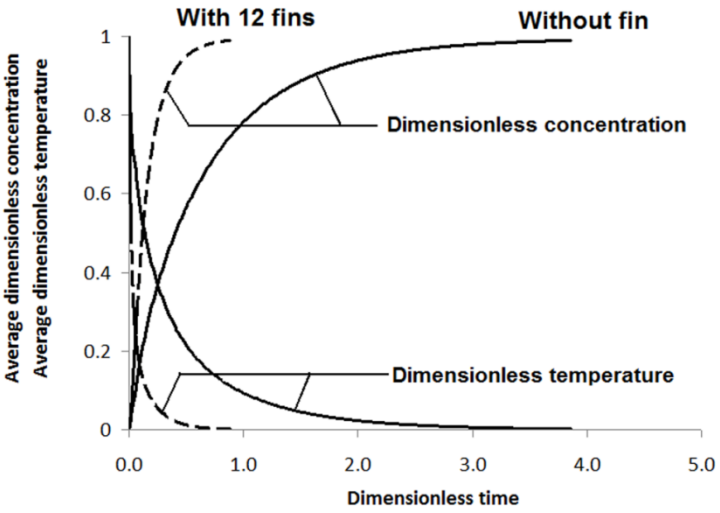


(a)

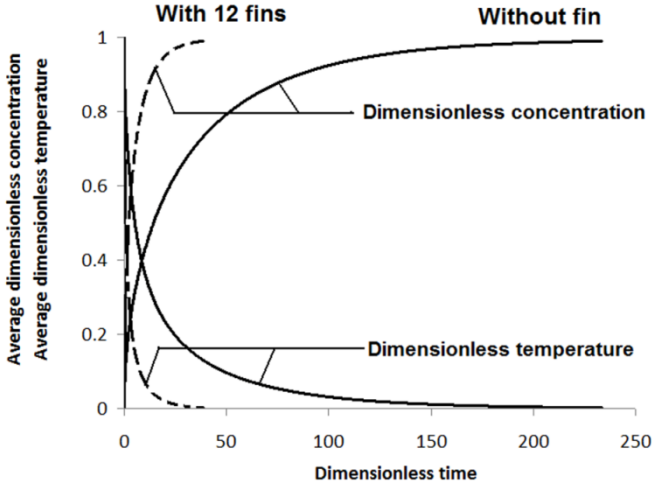


(b)

Figure 9.15. The changes in dimensionless average temperature and adsorbate concentration with dimensionless time for the adsorbent bed with 12 fins when $\Lambda = 0.01$, $\alpha^* = 0.01$ and for a bed without fin, a) $Ku = 1$ and $\Gamma = 1$, b) $Ku = 100$, $\Gamma = 1$

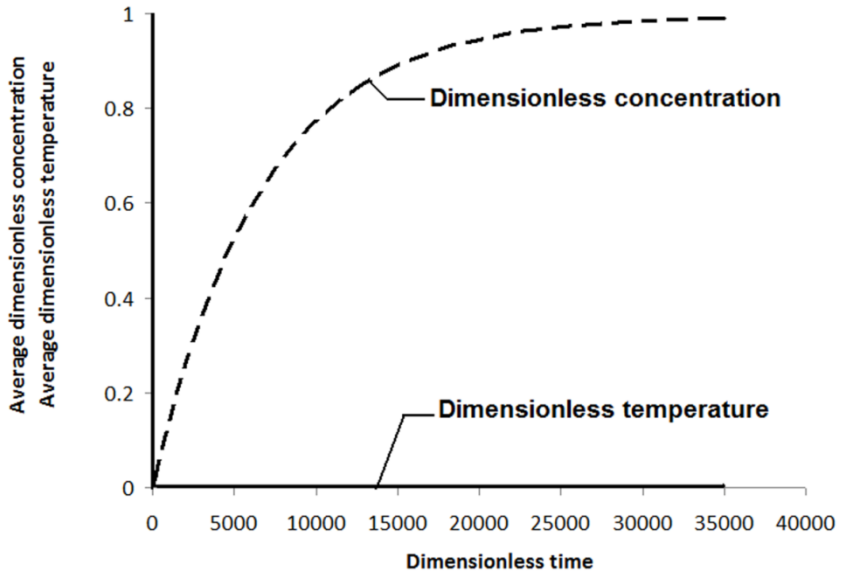


Figure 9.16. The variation in dimensionless average temperature and adsorbate concentration with dimensionless time for the adsorbent bed without fin when $\Gamma = 10^{-5}$ and Ku = 1 and 100

The change in total adsorption period with $\Gamma$ for an adsorbent bed with Ku = 1 and 100 and for the cases with and without fins are shown in Figure 9.17. As seen, the total dimensionless adsorption period for the adsorbent beds with low values of $\Gamma$ (i.e. $\Gamma = 10^{-5}$) are almost identical for both Ku = 1 and 100. For low values of $\Gamma$, the use of fin does not reduce the adsorption period since heat transfer is rapid and mass diffusion in the particle controls the process. An increase in value of $\Gamma$ reduces the adsorption period. The effect of fin on reduction of adsorption period in an adsorbent bed with high values of $\Gamma$ (i.e. $\Gamma = 1$) can be clearly seen from Figure 9.17. The use of fin reduces the adsorption period and this reduction particularly for the bed with Ku = 100 is greater than that of bed with Ku = 1.

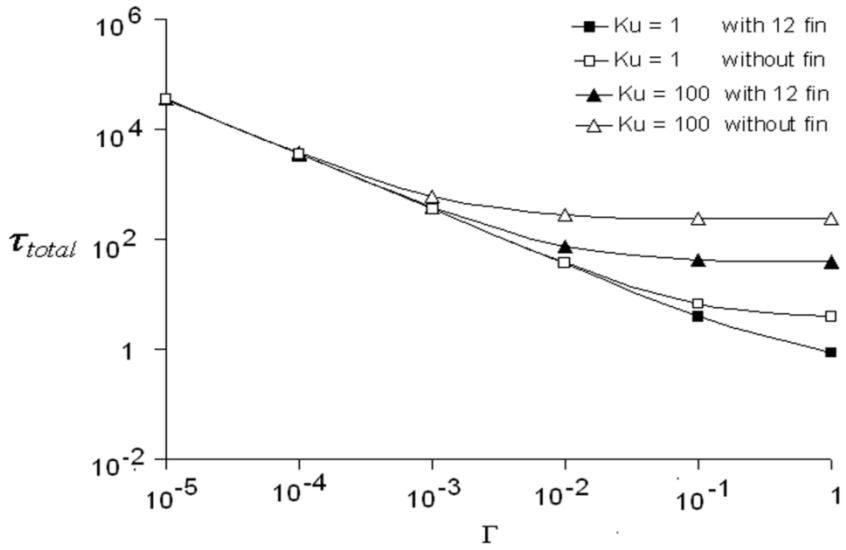


Figure 9.17. Variation in dimensionless total period of adsorption process with Γ for the adsorbent bed with 12 fins when Λ = 0.01 and α* = 0.01 and for the same bed without fin

For the silica gel/water pair (Appendix A), the Λ and α* values are calculated and give in Table 9.6. The half of the fin thickness is taken as 0.5 mm. The inner radius is changed from 10 to 100 mm. The fin is chosen stainless steel. The range of Λ and α* values is taken from 0.01 to 100 for both in this study for different fin materials and geometry of the bed.

Table 9.6. The Λ and α* values for the considered silica gel/water pair

| δ (m) | $R_i$ (m) | $\lambda_{eff}$ (W/mK) | $\lambda_{AISI\ 302}$ (W/mK) | $\Lambda_{AISI\ 302}$ (W/mK) | $\rho_{AISI\ 302}$ (kg/m$^3$) | $C_{p\ AISI\ 302}$ (kJ/kgK) | $\alpha^*$ |
|---|---|---|---|---|---|---|---|
| 0.0005 | 0.01 | | | 0.18 | | | |
| 0.0005 | 0.05 | 0.14 | 15.1 | 0.90 | 8055 | 480 | 61.67 |
| 0.0005 | 0.1 | | | 1.80 | | | |

## 9.2.3. Comparison of Uniform and Non-Uniform Pressure Approaches

The study is performed for silica gel-water pair and for two adsorbent beds with thickness of 10 and 40 mm which is illustrated in Figure 6.2. The inner radius for both adsorbent beds is $R_i$ = 10 mm. The assumptions taken into account for this study are given in Chapter 6.1. Both the uniform and non-uniform pressure approaches are used in this study. The governing equations of uniform and non-uniform pressure approaches

used in the analysis of the heat and mass transfer in the adsorbent bed are separately presented in the Chapter 6.2.1 and 6.3.1. As mentioned in these chapters, for the governing equations for uniform pressure approach are heat transfer equation for the adsorbent bed, and mass transfer equation for the adsorbent particle an these equations are given in Chapter 6.2. The continuity equation based on conservation of mass for water vapor flow through the adsorbent bed, the heat transfer equation for the adsorbent bed, Darcy law for adsorptive velocity, the ideal gas relation, and LDF relation for non-uniform approach are given in Chapter 6.3.

For all presented results, the adsorption process is started at $T_d$=353 K and ended at $T_a$=303 K as illustrated in Clapeyron diagram in Figure 6.3. For the uniform pressure approach, the water vapor pressure is assumed uniform as 2 kPa in the entire bed during the adsorption process. For the non-uniform pressure approach, the water vapor pressure inside the adsorbent bed is not uniform and it varies with the local adsorption rate and temperature. However, the water vapor pressure at the entrance of bed (R = $R_i$) is at 2 kPa. The initial and boundary conditions for the equations of both approaches are tabulated and given in Table 9.7. Two locations inside of the adsorbent bed are taken for presentation of local temperature, pressure, and concentration in this study. These locations at R = 16.7 and 43.3 mm for the bed thickness of 40 mm and two locations at R = 11.7 and 18.3 mm for the bed thickness of 10 mm is illustrated in Figure 9.19.

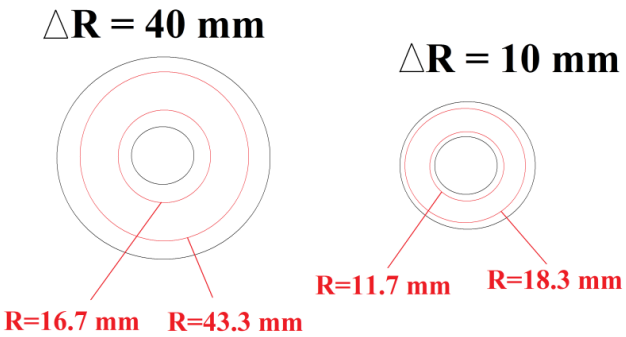


Figure 9.19. The detailed figure of the inner points taken inside of the adsorbent bed

The aim of the present study is to;

- analyze heat and mass transfer in a granular cylindrical adsorbent bed by using uniform and non-uniform pressure approaches and compare the obtained results,
- study the effect of particle size on the adsorption period and to determine a minimum adsorption period for an adsorption process.

Table 9.7. The initial and boundary conditions of the considered problem for the uniform and non-uniform pressure approach

| **Uniform Pressure Approach** | | | |
|---|---|---|---|
| **Dependent variable** | **B.C at R=$R_i$** | **B.C atR=$R_o$** | **Initial conditions** |
| Temperature (K) | $\partial T/\partial R = 0$ | $T = 303$ | $T = 353$ |
| Adsorptive pressure (kPa) | $P = 2$ | $P = 2$ | $P = 2$ |
| Amount of adsorbate ($kg_v\ kg_s^{-1}$) | $W = f(P,T)$ | $W = f(P,T)$ | $W$ = initial value @ 353K |
| | | | |
| **Non-uniform Pressure Approach** | | | |
| **Dependent variable** | **B.C at R=$R_i$** | **B.C atR=$R_o$** | **Initial conditions** |
| Temperature (K) | $\partial T/\partial R = 0$ | $T = 303$ | $T = 353$ |
| Adsorptive pressure (kPa) | $P = 2$ | $\partial P/\partial R = 0$ | $P = f(\rho,T)$ |
| Adsorptive density ($kg\ m^3$) | $\rho_v = f(P,T)$ | $\rho_v = f(P,T)$ | $\rho_v$ = initial value @ 353K |
| Amount of adsorbate ($kg_v\ kg_s^{-1}$) | $W = f(P,T)$ | $W = f(P,T)$ | $W$ = initial value @ 353K |
| Adsorptive velocity ($m\ s^{-1}$) | $V_r = f(\rho_v, K_{app})$ | $V_r = 0$ | $V_r = 0$ |

The study is performed only for adsorption process. The adsorbent particle is spherical and its radius is changed from 0.025 to 1 mm to find out the particle size effect on heat and mass transfer in the bed. The local and average adsorbate concentration, pressure, and temperature are calculated and plotted versus time. The changes of temperature, concentration, and pressure with time for these locations are obtained and drawn against time. The porosity of the adsorbent bed is assumed as 0.35. The thermophysical properties of the analyzed silica gel-water pair are given in Appendix A, Table A1. The reference diffusivity ($D_o$), the diffusion activation energy (E) which is used in LDF model equation (Eq.(6.3)) is given in Appendix A, Table A2. The constants k and n which are used in the isotherm equation Eq. (6.6) are taken as 0.552 and 1.6, respectively.

### 9.2.3.1. The Comparison of Temperature and Adsorbate Concentration for Uniform and Non-Uniform Pressure Approach; Effect of Adsorbent Particle Radius

Figure 9.20 shows the obtained numerical results for both uniform and non-uniform pressure approaches, and for an adsorbent bed with thickness of 40 mm and the silica gel particle radius of 1 mm. Figure 9.20(a) represents the change in average water concentration and temperature with time for both approaches. As it is seen, the average bed temperature decreases while the average of water concentration increases with time. The changes in $\overline{T}$ and $\overline{W}$ versus time for both approaches are very close to each other. The temperature change at R = 16.7 and 43.3 mm locations for both approaches are illustrated in Figure 9.20(b). As is seen from the figure, the local variations of temperature with time for both approaches are also close to each other. The temperature at both locations (R = 16.7 and 43.3 mm) decreases from 353 to 303 K. The temperature at R = 43.3 mm decreases faster than the temperature at R = 16.7 mm, since the bed is cooled from the outer surface. The change of local adsorbate concentration with time at the same points throughout the adsorption process is illustrated in Figure 9.20(c). As expected, the local adsorbate concentration at R = 43.3 mm increases faster compared to the local concentration of R = 16.7 mm since the bed is cooled from the outer surface. Figure 9.20(d) shows the pressure in the bed at the same locations for both approaches. The pressure at the entire bed does not vary with time and it is 2 kPa. The local pressure calculated by non-uniform pressure approach does not change with time and space, since the interparticle mass transfer resistance is negligible when $r_p$ = 1 mm. Hence, the uniform pressure approach, which is simpler than non-uniform approach, can be used to simulate the adsorption process in this bed.

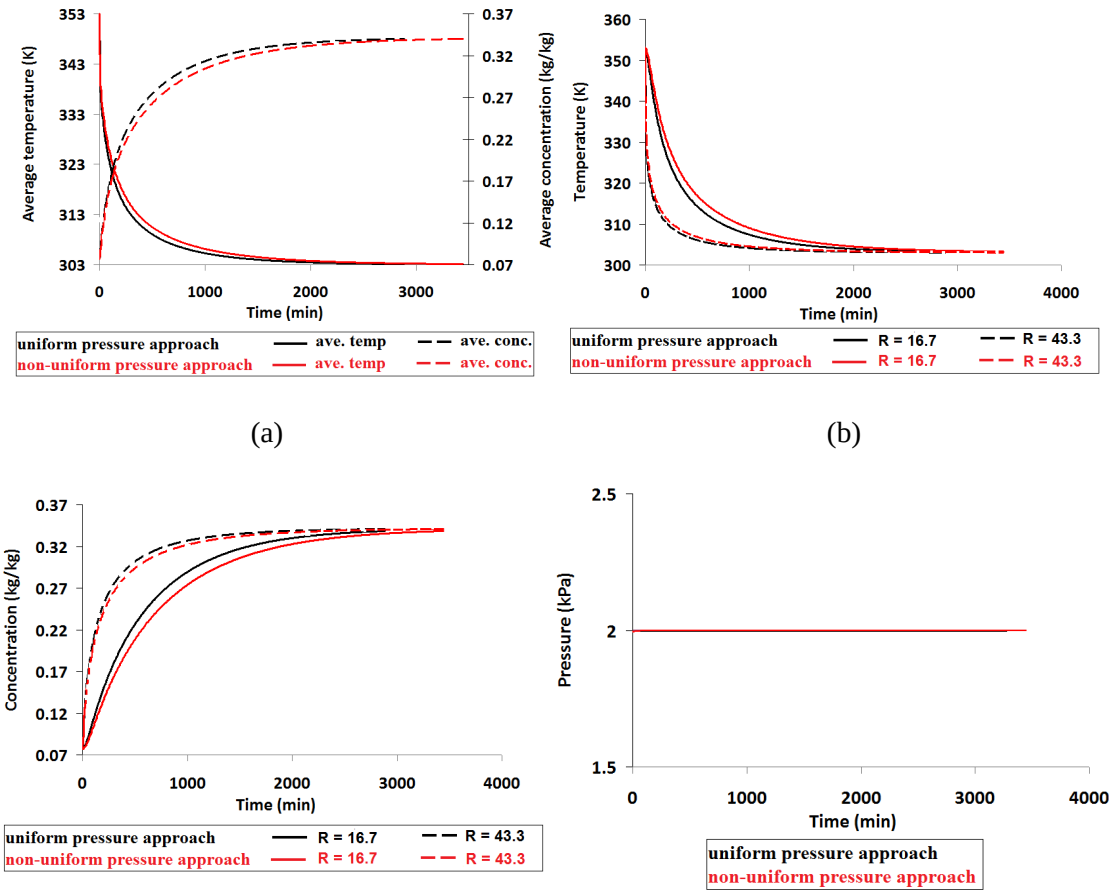


Figure 9.20. The numerical results of both uniform and non-uniform pressure approaches for an adsorbent bed with $R_i$ = 10 mm, $R_o$ = 50 mm, $r_p$ = 1 mm, (a) average adsorbate concentration and temperature, (b) the local adsorbate temperature at R =16.7 and 43.3 mm, (c) the local adsorbate concentration at R =16.7 and 43.3 mm, (d) the local pressure at R =16.7 and 43.3 mm

Figure 9.21 presents the results of the same bed discussed in Figure 9.20, but for the silica gel particle radius of $r_p$=0.025 mm. By comparison of Figures 9.20 and 9.21, the decrease of silica gel particle radius from 1 to 0.025 mm extends the adsorption process period. The reducing particle size increases the effect of interparticle mass transfer resistance and consequently, the water vapor flows slower in the voids between particles. As seen from Figure 9.21(a), the curves of the uniform and non-uniform pressure approaches are splitted from each other. If the uniform pressure approach is used to simulate the problem, the obtained period of adsorption become considerably shorter than the non-uniform pressure approach. The total adsorption time of the non-uniform pressure approach is longer than that of uniform pressure approach since the effect of interparticle mass transfer resistance is involved. The comparison of two

approaches indicates the invalidity of the uniform pressure approach for the considered bed with adsorbent particle radius of 0.025 mm. Figure 9.21(b) and 9.21(c) show the variation of temperature and adsorbate concentration in the bed at R = 16.7 and 43.3 mm locations. Both the variations of temperature and adsorbate concentration of uniform and non-uniform pressure approaches in these locations are different. The difference between the concentration variations of two approaches versus time is expected due to the significant of interparticle mass transfer resistance. Figure 9.21(d) indicates the variations of water vapor pressure at R = 16.7 and 43.3 mm locations during adsorption process for both approaches. For uniform pressure approach, the pressure does not change at both locations throughout the adsorption process, as expected. However, for the non-uniform pressure approach, the pressure at R = 43.3 mm drops from 2 to 0.4 kPa at the beginning of the adsorption process and then it slowly increases to 2 kPa. By decreasing temperature at the outer region of adsorbent bed, water vapor in this region is adsorbed by silica gel particles. The pressure in this region can be observed since water vapor does not easily flow from the inner to outer region due to interparticle mass transfer. Similar pressure change is seen for the location of R = 16.7 mm. The rate of pressure drop at the beginning of adsorption process at R = 16.7 mm location is less than that of R = 43.3 mm since it is closer to the water vapor inlet and its temperature decreases slowly.

In order to understand the effect of adsorbent bed thickness on the interparticle mass transfer resistance, Figures 9.22 and 9.23 are presented. Figure 9.22 and 9.23 depict the changes of temperature and adsorbate concentration for the bed with thickness of 10 mm filled with silica gel particle radius of $r_p$ = 1 and 0.025 mm, respectively. As seen from Figure 9.22, for the adsorbent bed with $r_p$ = 1 mm, the results of both uniform and non-uniform pressure approaches overlap each other, not only for the average bed temperature and concentration but also for local temperature, concentration and pressure at R = 11.7 and 18.3 mm. This indicates the validity of uniform pressure approach for the bed with silica gel particle size of $r_p$ = 1 mm. The comparison of Figure 9.20 and 9.22 shows that the

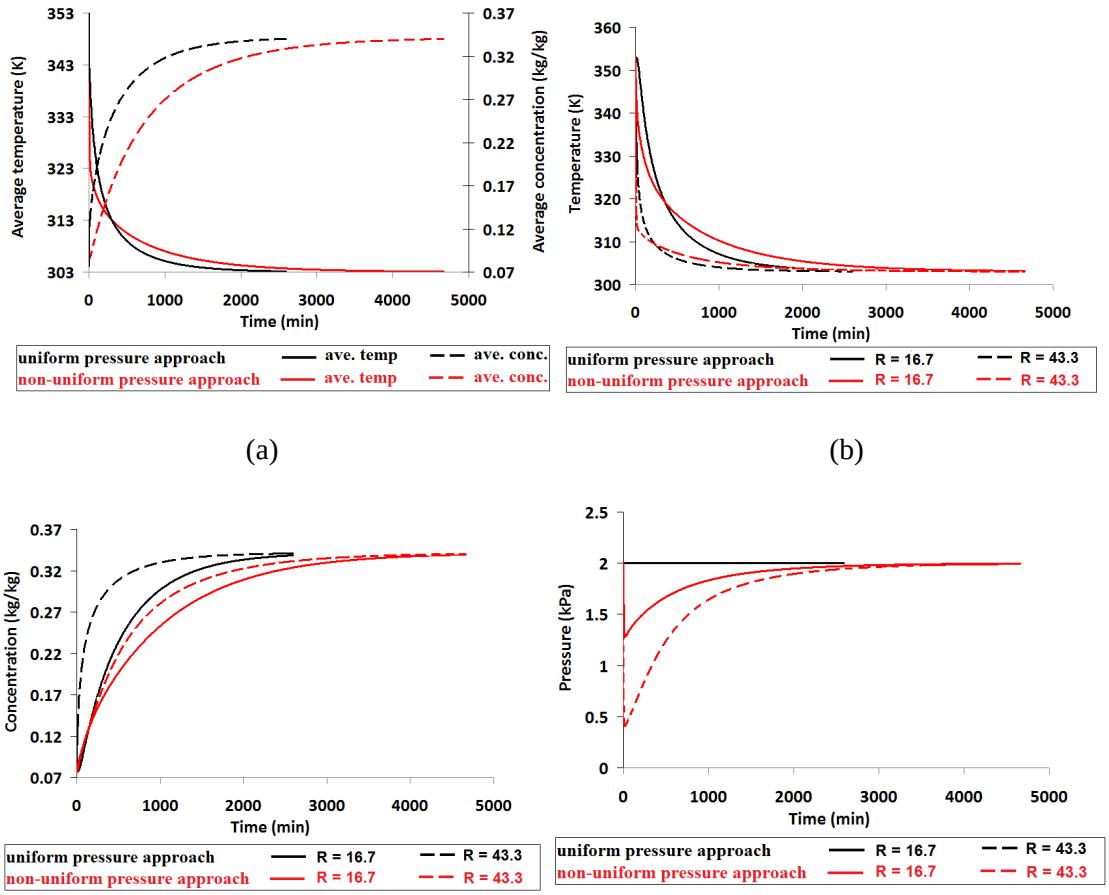


Figure 9.21. The numerical results of both uniform and non-uniform pressure approaches for an adsorbent bed with $R_i$ = 10 mm, $R_o$ = 50 mm, $r_p$ = 0.025 mm, (a) average adsorbate concentration and temperature, (b) the local adsorbate temperature at R =16.7 and 43.3 mm, (c) the local adsorbate concentration at R =16.7 and 43.3 mm, (d) the local pressure at R =16.7 and 43.3 mm

reducing bed thickness from 40 to 10 mm decreases adsorption period from 3440 to 588 min.. Although, the water vapor can easily move in the voids between adsorbent particles for the bed with the particles of $r_p$ = 1 mm, the decrease of bed thickness reduces bed thermal resistance in radial direction which results in the decrease of adsorption period. The decrease of adsorbent particle from 1 to 0.025 mm causes splitting of the curves due to the enhancement of the interparticle mass transfer resistance as seen from Figure 9.23. A pressure drop is observed at the outer region of the bed at the beginning of adsorption period due to the sudden decrease of temperature and slow transfer of water vapor in the radial direction of the bed. By reduction silica gel particle size, the interparticle mass transfer increases, hence the increase of adsorption period is expected. However, the comparison of the Figures 9.22 and 9.23

shows that the adsorption period is decreased by reducing silica gel particle size since the increase of interparticle mass transfer resistance my not be too much to affect the adsorption period. Hence, the decrease of particle size may have different effects on adsorption period and it depends on bed thickness.

### 9.2.3.2. Control Mechanism for Mass Transfer in the Bed

Figure 9.24 compares the changes in average temperature and adsorbate concentration of the bed with 10 mm thickness for three different silica gel particle radiuses of 0.7, 0.1, and 0.0075 mm. The non-uniform pressure approach is used to obtain these results. The adsorbate concentration increases from 0.077 to 0.3416 kg/kg while the temperature decreases from 353 to 303 K. The adsorption period decreases from 408 to 257 min. by reducing particle size from $r_p$ = 0.7 to 0.1 mm due to the reduction in intraparticle mass transfer resistance. However, further reduction of particle size from 0.1 to 0.0075 mm increases adsorption period from 257 to 497 min. due to the increase of interparticle mass transfer resistance. The reduction of particle size makes voids between particles smaller and enhances flow resistance through the bed. The result of this figure clearly shows that the neglecting interparticle mass transfer resistance in a granular bed with $r_p$ < 0.1 mm causes significant mistake in the results.

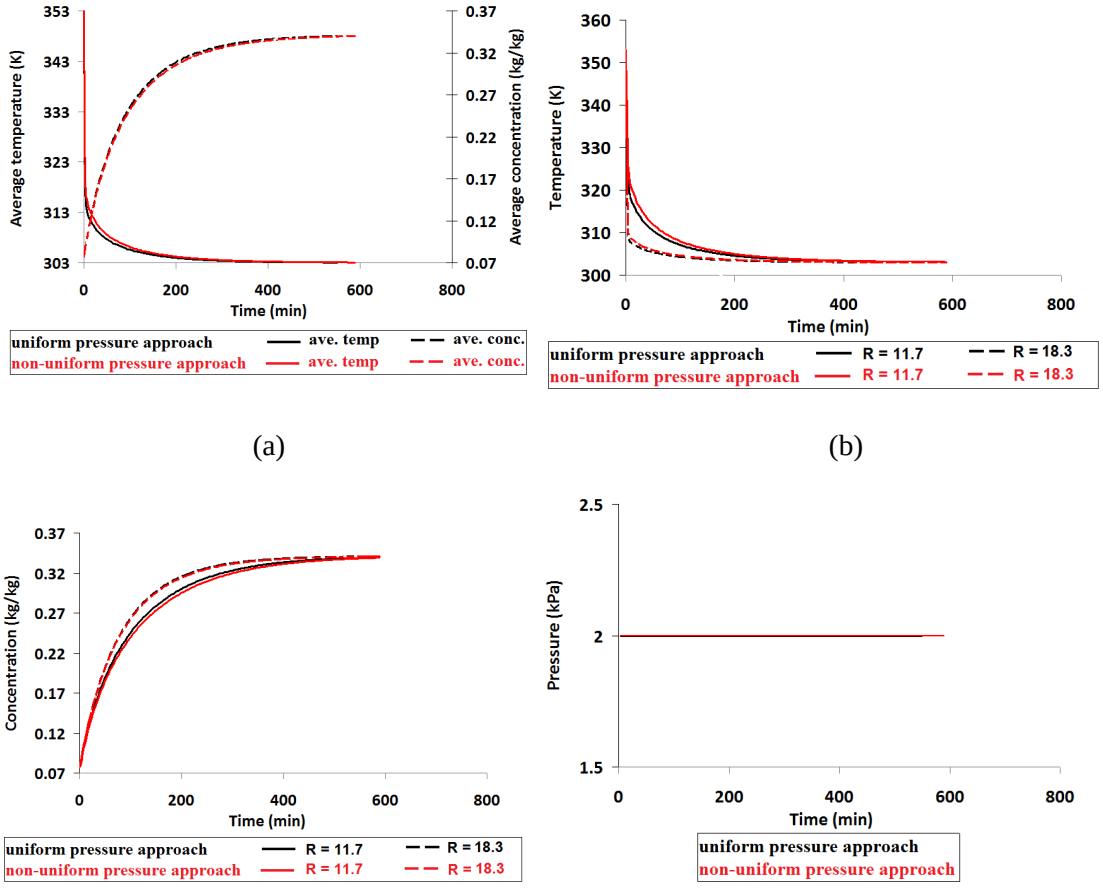


(a) (b)

(c) (d)

Figure 9.22. The numerical results of both uniform and non-uniform pressure approaches for an adsorbent bed with $R_i$ = 10 mm, $R_o$ = 20 mm, $r_p$ = 1 mm, (a) average adsorbate concentration and temperature, (b) the local adsorbate temperature at R =11.7 and 18.3 mm, (c) the local adsorbate concentration at R = 11.7 and 18.3 mm, (d) the local pressure at R =11.7 and 18.3 mm

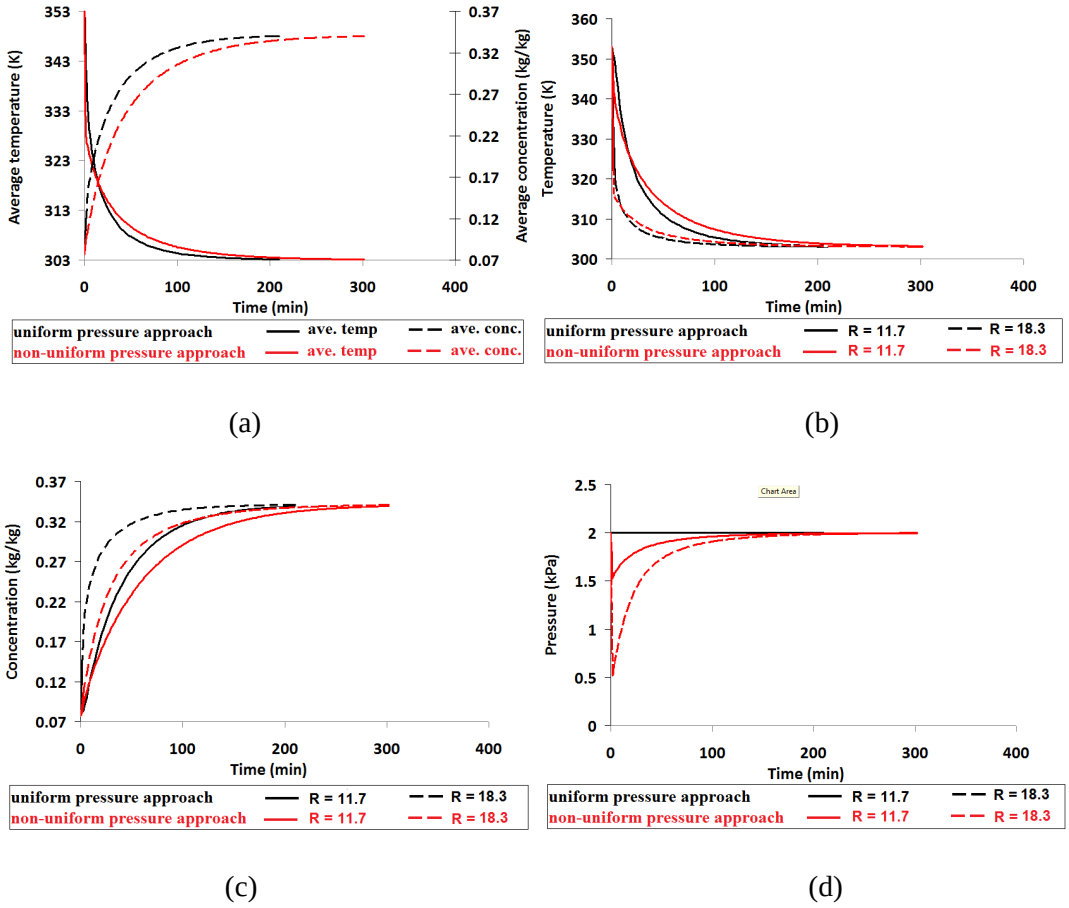


Figure 9.23. The numerical results of both uniform and non-uniform pressure approaches for an adsorbent bed with $R_i$ = 10 mm, $R_o$ = 20 mm, $r_p$ = 0.025 mm, (a) average adsorbate concentration and temperature, (b) the local adsorbate temperature at R =11.7 and 18.3 mm, (c) the local adsorbate concentration at R =11.7 and 18.3 mm, (d) the local pressure at R =11.7 and 18.3 mm

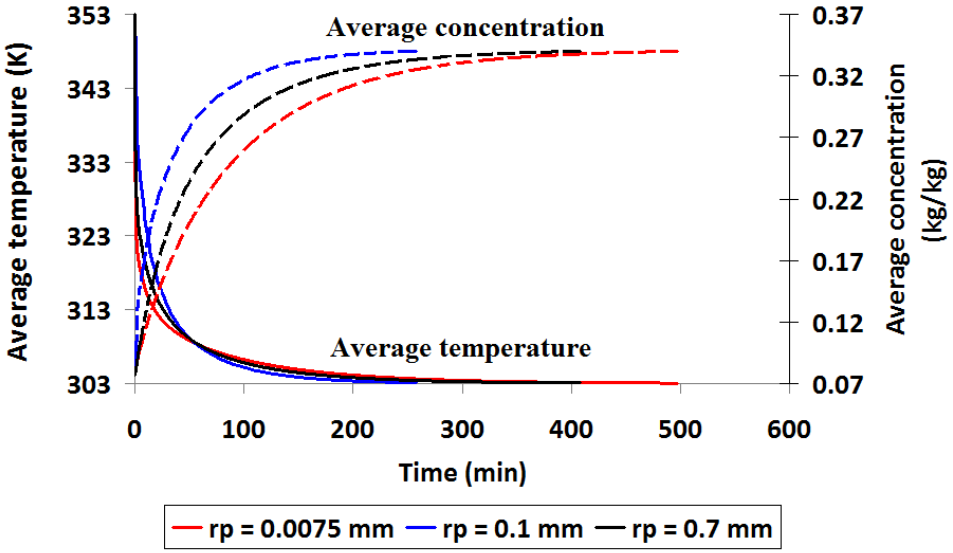


Figure 9.24. The comparison of the average adsorbate concentration and temperature for the bed with 10 mm thickness and different adsorbent particle size

The comments on Figure 9.24 can be improved by Figure 9.25 in which the total adsorption period versus adsorbent particle radius is plotted for the bed thickness of 40 and 10 mm. The adsorption period is defined when the average adsorbate concentration in the bed is reached 90% of final value (i.e. $\overline{W_a}$ = 0.3416 kg/kg). For the bed with thickness of 10 and 40 mm, the adsorption periods for $r_p$ = 1 mm are 205 and 1065 min., respectively. For both bed thickness, the adsorption period decreases by reducing the adsorbent particle size. This trend continues up to a specific particle size. After it, the adsorption period increases with decrease of silica gel particle size. For instance, for the adsorbent bed with thicknesses of 10 mm, the adsorption period decreases from 395.5 to 82 mm by reducing silica gel particle size from 1.5 to 0.1 mm. In this region of the particle size, the intraparticle mass transfer resistance is dominant and interparticle mass transfer resistance can be neglected. Hence, the reduction of the particle size reduces intraparticle mass transfer resistance and consequently the adsorption period decreases. The decrease of silica gel particle radius from 0.1 to 0.0075 mm increases the adsorption period from 82 to 185 min. since the interparticle mass transfer resistance becomes significant. Figure 10 shows that there should be a adsorbent particle size that provides minimum adsorption period for a granular adsorbent bed. For the adsorbent bed with 10 mm thickness, the adsorbent particle with $r_p$ = 0.1 mm provides the shortest adsorption period while for the bed with 40 mm thickness the minimum adsorption period can be achieved by using adsorbent particle size of 0.3 mm.

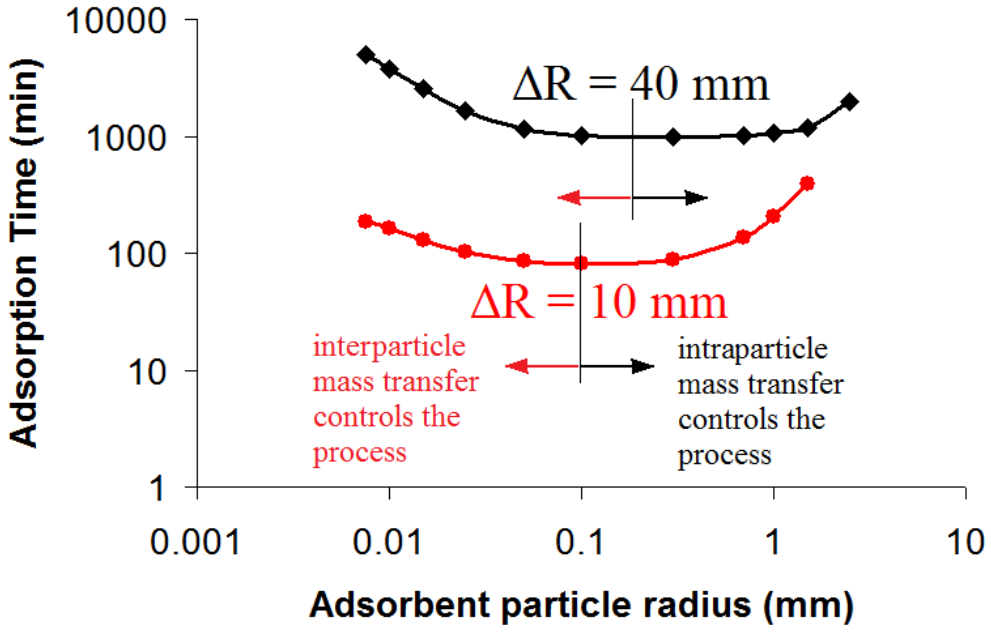


Figure 9.25. The change of adsorption period with adsorbent particle size for the bed thickness of 10 and 40 mm

### 9.2.4. A Study on Competition between Heat and Mass Transfer in an Adsorbent Bed

The adsorbent bed which is considered for the study, presented in this section, is given in Figure 6.2. The assumptions used for this study are also given in Chapter 6.1 in details. Both the uniform and non-uniform pressure approaches are used for this study. The results are obtained for silica gel-water pair whose thermophysical properties are given in Appendix A in Table A1. Figure 6.3 shows an isobaric adsorption process on Clapeyron diagram. The adsorption process is started when the adsorbate concentration in the adsorbent bed is $W_d$ and the bed temperature is at $T_d$. The process is terminated when the adsorbate concentration is attained to $W_a$ while the bed temperature is decreased to $T_a$. Moreover, for the analyzed process, the values of $T_a$, $T_d$, $W_a$, and $W_d$ are 303 K, 353 K, 0.3416 kg/kg, 0.077 kg/kg, respectively. For uniform pressure approach, the water vapor pressure is assumed uniform at 2 kPa in the entire bed during the adsorption process. For non-uniform pressure approach, the water vapor pressure inside the adsorbent bed is not uniform and it varies with the local adsorption rate and temperature. However, the water vapor pressure at the bed entrance is at 2 kPa.

The governing equations of uniform and non-uniform pressure approaches used in the analysis of the heat and mass transfer in the adsorbent bed are separately

presented in the Chapter 6.2 and 6.3. For uniform pressure approach the heat transfer equation for the bed and LDF model are written. The dimensionless form of these equations which are Eq.(6.10) and Eq.(6.12) are solved. For the non-uniform approach, the LDF relation (Eq. (6.3)) is also used to determine the change of mean water concentration in the silica gel particle at the given temperature and pressure. The initial and the boundary conditions of the both approaches with dimensional and dimensionless forms are given in Table 9.8. As given in Chapter 6.1, under the performed assumptions, independent variables which effect heat and mass transfer in the bed are combined only in five independent variables as Ku, G, Π, K and Γ. The heat transfer and mass transfer equations for the adsorbent bed, equation of the mass transfer for adsorbent granule, and the Darcy law are non-dimensionalized (Eq. (6.12), (6.25)-(6.27)). The corresponding initial and boundary conditions are also non-dimensionalized and solution for the set of governing equation is obtained. Finite difference method is employed to solve the governing equations.

The aim of the present study is to;

- analyze heat and mass transfer of an adsorption process in a granular cylindrical adsorbent bed by using dimensionless uniform and non-uniform approaches and to compare their results
- investigate the importance of the dimensionless parameters of Ku, G, Π, K and Γ
- use these dimensionless parameter for design of an adsorbent bed.

Table 9.8. The initial and boundary conditions of the considered problem with dimensional and dimensionless forms for the uniform and non-uniform pressure approaches

| **Uniform Pressure Approach** | | | |
|---|---|---|---|
| **Dependent variable** | **B.C at R=$R_i$** | **B.C atR=$R_o$** | **Initial conditions** |
| Temperature (K) | $\partial T/\partial R = 0$ | $T = 303$ | $T = 353$ |
| Adsorptive pressure (kPa) | $P = 2$ | $P = 2$ | $P = 2$ |
| Amount of adsorbate ($kg_v$ $kg_s^{-1}$) | $W = f(P,T)$ | $W = f(P,T)$ | $W$ = initial value @ 353K |
| Dimensionless Temperature | $\partial\theta/\partial R^* = 0$ | $\theta = 0$ | $\theta = 1$ |
| Dimensionless adsorptive pressure | $P^* = 0$ | $P^* = 0$ | $P^* = 0$ |
| Dimensionless amount of adsorbate | $W^* = f(P^*,\theta)$ | $W^* = f(P^*,\theta)$ | $W^* = 0$ |
| **Non-uniform Pressure Approach** | | | |
| **Dependent variable** | **B.C at R=$R_i$** | **B.C atR=$R_o$** | **Initial conditions** |
| Temperature (K) | $\partial T/\partial R = 0$ | $T = 303$ | $T = 353$ |
| Adsorptive pressure (kPa) | $P = 2$ | $\partial P/\partial R = 0$ | $P = f(\rho,T)$ |
| Adsorptive density (kg $m^3$) | $\rho_v = f(P,T)$ | $\rho_v = f(P,T)$ | $\rho_v$ = initial value @ 353K |
| Amount of adsorbate ($kg_v$ $kg_s^{-1}$) | $W = f(P,T)$ | $W = f(P,T)$ | $W$ = initial value @ 353K |
| Adsorptive velocity (m $s^{-1}$) | $V_r = f(\rho_v, K_{app})$ | $V_r = 0$ | $V_r = 0$ |
| Dimensionless Temperature | $\partial\theta/\partial R^* = 0$ | $\theta = 0$ | $\theta = 1$ |

**(cont. on next page)**

Table 9.8 (cont.).

| | | | |
|---|---|---|---|
| Dimensionless adsorptive pressure | $P^* = 0$ | $\partial P^* / \partial R^* = 0$ | $P^* = f(\rho^*, \theta)$ |
| Dimensionless adsorptive density | $\rho_v{}^* = f(P^*, \theta)$ | $\rho_v{}^* = f(P^*, \theta)$ | $\rho_v{}^* = 0$ |
| Dimensionless amount of adsorbate | $W^* = f(P^*, \theta)$ | $W^* = f(P^*, \theta)$ | $W^* = 0$ |
| Dimensionless adsorptive velocity | $V_r{}^* = f(\rho_v{}^*, K_{app}{}^*)$ | $V_r{}^* = 0$ | $V_r{}^* = 0$ |

The reference diffusivity ($D_o$), the diffusion activation energy (E) which is used in LDF model equation (Eq. (6.3)) is given in Appendix A, Table A2. The constants k and n which are used in the isotherm equation Eq.(6.6) are taken as 0.552 and 1.6, respectively. The ratio of the outer radius to inner radius of the adsorbent bed is taken as $R_o/R_i$=5 for this study. The values of dimensionless parameters Ku, G, Π, K and Γ are calculated for two different cases as Case A and Case B as shown in Table 9.9. The inner and outer radiuses of the considered adsorbent bed and the particle radius are given in Table 9.8 for both cases. The values of K and Γ will be change by changing the geometrical values of the adsorbent bed and the adsorbent particle radius. As a result, for this study, two Γ value are taken as $10^{-3}$ and 105.27 to understand the effect of the Γ value on the control mechanism. Also the effects of the K value on control mechanism are taken into consideration.

Table 9.9. The values of Ku, G, Π, K and Γ for two different cases

| | $R_i$ (m) | $R_o$ (m) | $r_p$ (m) | $R_o/R_i$ | Ku | Π | G | Γ | K |
|---|---|---|---|---|---|---|---|---|---|
| Case A | 0.01 | 0.05 | 0.001 | 5 | 7.14 | 5.05E-06 | 87582.06 | 0.029 | 1421408 |
| Case B | 0.06 | 0.3 | 0.001 | 5 | 7.14 | 5.05E-06 | 87582.06 | 0.029 | 1421408 |

### 9.2.4.1. Agreement of Dimensionless Results for Different Adsorbent Bed

Figure 9.26 depicts the change of dimensional adsorbate concentration and temperature profiles with time in two adsorbent beds with different inner and outer

radiuses when all dimensionless parameters are the same (Ku=7.14, Π=5.05x10$^{-6}$, Γ=0.029, G=87582.06, K=1,421,408). As is seen from Figure 9.26(a), for the bed with $R_i$=0.01 m and $R_o$=0.05 m (Case A), both the diffusion of heat through the adsorbent bed and diffusion of adsorptive in the adsorbent particle reach the steady state after a period t = 3000 min. Figure 9.26(b) shows the variation of temperature and adsorbate concentration when $R_i$=0.06 m and $R_o$=0.30 m (Case B). Both the variation of temperature and concentration in Figure 9.26(b) is different than the variation in Figure 9.26(a) due to the different inner radiuses and the thicknesses of the beds. As seen from Figure 4, the change of the dimensional temperature and adsorbate concentration profiles along the radius of the bed are different. The change of dimensionless temperature and adsorbate concentration profiles along the radiuses for these beds are given in Figure 9.27. As mentioned before, two different bed designs have the same dimensionless parameters as Ku=7.14, Π=5.05x 10$^{-6}$, Γ=0.029, G=87582.06, and K=1,421,408. When the local dimensional temperature and adsorbate concentration results are non-dimensionalized, the variations of dimensionless temperature and concentration profiles for both beds overlap each other. This clearly indicates that, for different beds with the same dimensionless parameters (Case A and Case B), identical dimensionless temperature and adsorbate concentration profiles are achieved.

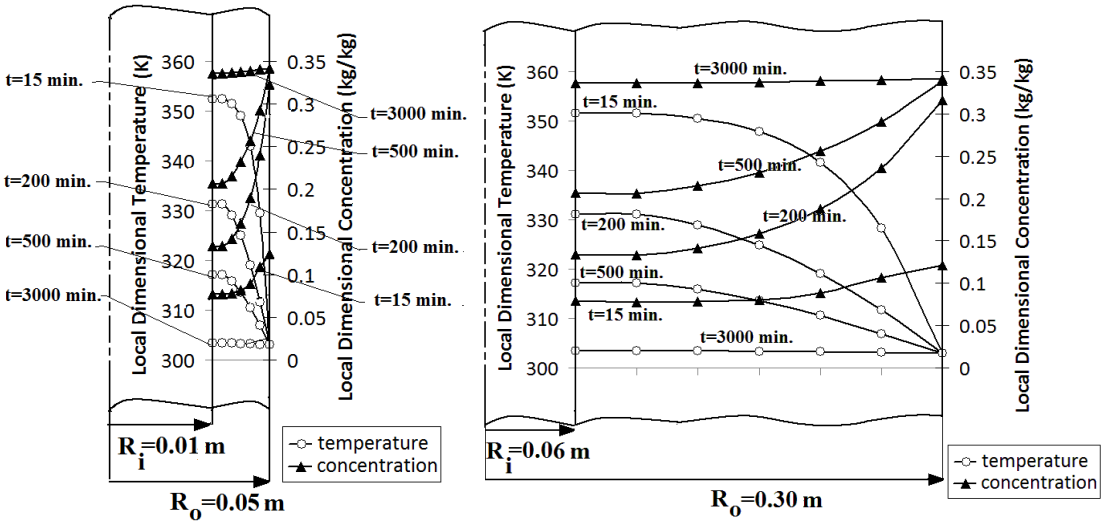


Case A (a) Case B (b)

Figure 9.25. The change of dimensional temperature and adsorbate concentration profiles along the radius of the adsorbent bed at different dimensional times when Ku=7.14, Π=5.05x10$^{-6}$, Γ=0.029, G=87582.06, and K=1,421,408, a)$R_i$=0.01 m and $R_o$=0.05 m, b)$R_i$=0.06 m and $R_o$=0.30 m

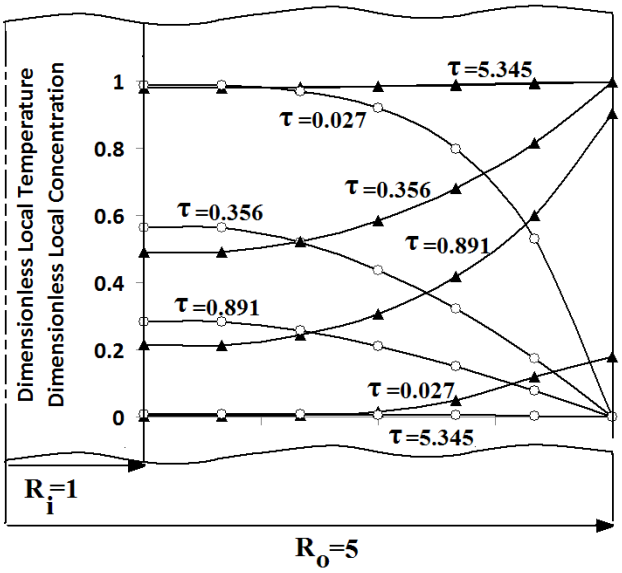


Figure 9.26. The change of dimensionless temperature and adsorbate concentration profile along the radius of the adsorbent beds ($R_i$=0.01 m and $R_o$=0.05 m, and $R_i$=0.06 m and $R_o$=0.30 m) at different dimensionless times when Ku=7.14, $\Pi=5.05\times10^{-6}$, $\Gamma$=0.029, G=87582.06, and K=1,421,408

### 9.2.4.2. The Effect of K and Γ Parameter on Adsorption Period; Decision on the Control Mechanism

Figure 9.27 shows the obtained numerical results of non-uniform pressure approach for adsorbent beds with the same Ku, Π, and G, when the Γ value is fixed to a high value as Γ=105.27 (Ku=7.14, $\Pi=5.05\times10^{-6}$, and G=87582.06). The results are obtained for two values of K as 142 and 222. The variation of temperature and concentration obtained by uniform pressure approach are also given for comparison of two approaches. The dimensionless average temperature decreases when the dimensionless average concentration increases during the adsorption process. For K as 142, the variation of dimensionless adsorbate concentration and temperature with time is highly different than the uniform pressure approach. Hence, the interparticle mass transfer resistance is considerable for K = 142. By the increase of K values, the profiles of the temperature and adsorbate concentration become closer to the uniform pressure approach profiles. This shows that the interparticle mass transfer resistance decreases by increase of K value. The increase of K value also decreases process time since interparticle mass transfer resistance is reduced. Also, it is clearly seen that, the heat transfer resistance is lower than the mass transfer resistance in the bed with K=142.

Thus, the uniform pressure approach can be used for analyzing of heat and mass transfer in adsorbent beds with high values of K.

The results for the high values of K as 1124 and 2530, and for the same dimensionless parameters of Figure 9.27 are presented in Figure 9.28. For high values of K as 1124 and 2530, the results for dimensionless average temperature and concentration profiles approach to the uniform pressure profiles since the interparticle mass transfer resistance decreases by increase of K value. The comparison of Figure 9.27 and 9.28 indicates that temperature decreases slower by further increase of K value, and the heat transfer resistance gets importance.

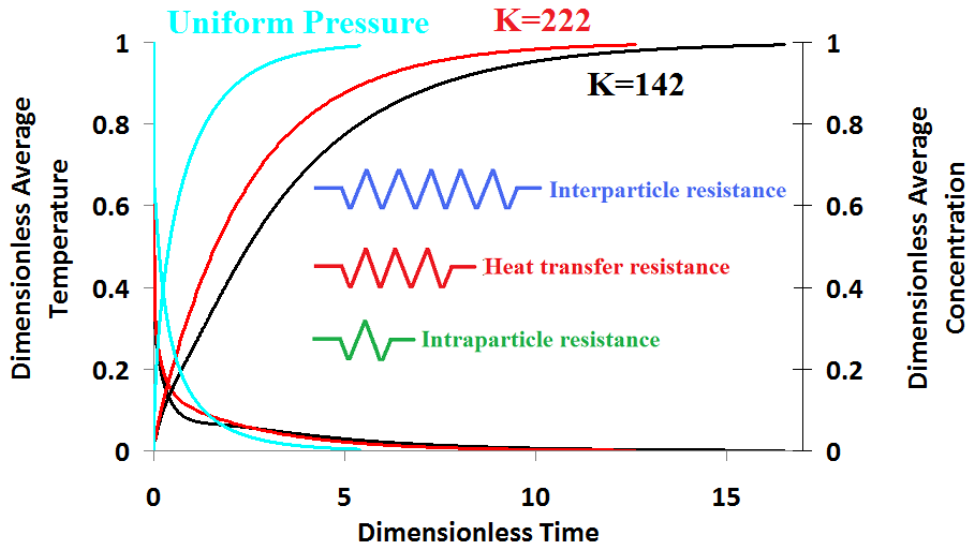


Figure 9.27. The comparison of the dimensionless average temperature and concentration of the bed during the dimensionless adsorption period for both uniform and non-uniform pressure approaches for low K values as 142 and 222 when $\Gamma$=105.27 (Ku=7.14, $\Pi$=5.05x$10^{-6}$, and G=87582.06)

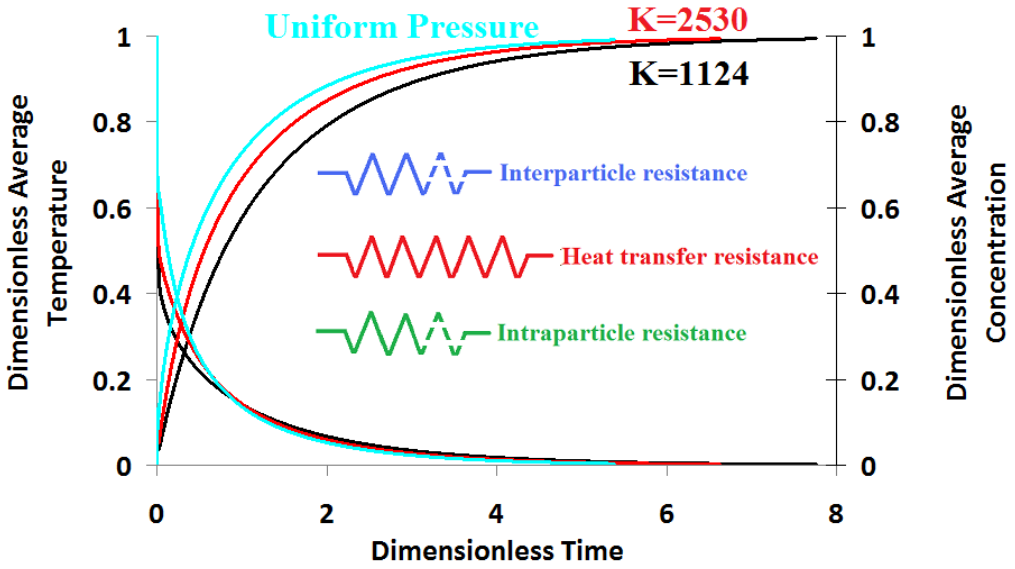


Figure 9.28. The comparison of the dimensionless average temperature and concentration of the bed during the dimensionless adsorption period for both uniform and non-uniform pressure approaches for high K values as 1124 and 2530 when Γ=105.27 (Ku=7.14, Π=5.05x$10^{-6}$, and G=87582.06)

The results of non-uniform pressure approaches for an adsorbent bed with the same Ku, Π, and G, and small value of Γ as Γ=$10^{-3}$ are illustrated in Figure 9.29. The results are plotted for the values of K as 142 and 500. Due to the low value of Γ, the dimensionless average temperature decreases rapidly when compared with the variation of the dimensionless average adsorbate concentration. In this case, the heat transfer is too fast (or the heat transfer resistance is too low), consequently the mass transfer resistance (interparticle or intraparticle resistance) controls the process. The concentration profile of K=142 is close to the profile of the uniform pressure approach, thus interparticle mass transfer resistance is not dominant and intraparticle mass transfer resistance controls the adsorption process. There is no doubt that, by further decrease of interparticle mass transfer resistance, the concentration profile becomes closer to the profile of uniform pressure approach.

This behavior can be seen also from Figure 9.30 in which the variation of temperature and concentration with time for K = 500 and 1124 are plotted. As seen from Figure 9.30, by increase of K value, the results approach further to the uniform pressure and the effect of interparticle mass transfer resistance decreases. Figure 9.30 shows that both heat transfer and interparticle mass transfer resistances are not dominant.

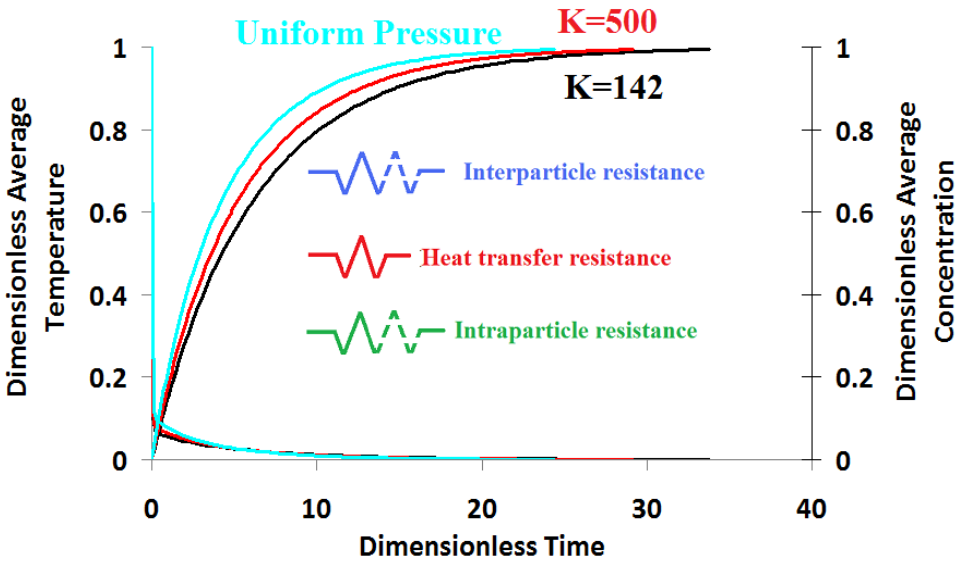


Figure 9.29. The comparison of the dimensionless average temperature and concentration of the bed during the dimensionless adsorption period for both uniform and non-uniform pressure approaches for low K values as 142 and 500 when $\Gamma=10^{-3}$

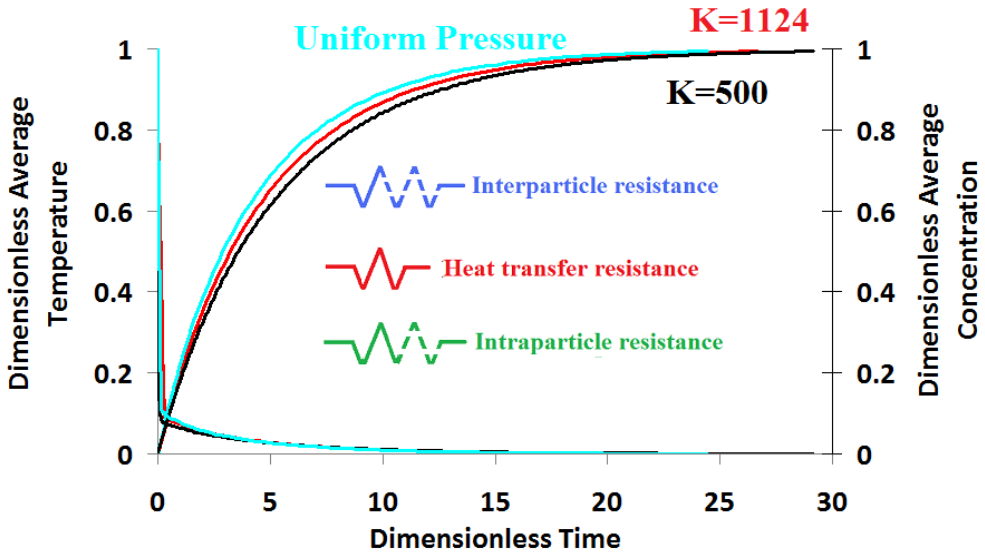


Figure 9.30. The comparison of the dimensionless average temperature and concentration of the bed during the dimensionless adsorption period for both uniform and non-uniform pressure approaches for high K values as 500 and 1124 when $\Gamma=10^{-3}$

### 9.2.4.3. The Adsorption Period by Changing of K and Γ Parameters

The total dimensionless period of adsorption versus Γ for different K values are presented in Figure 9.31. As seen from the figure, the process time increases by

decrease of Γ value. For low values of Γ, the intraparticle mass transfer resistance controls the process. By increase of Γ value, intraparticle mass transfer resistance decreases and therefore total process time decreases. Further increase of Γ value, the process time is not changed and the adsorbent particle reaches equilibrium condition instantaneously. The same behavior can be observed for the change of total adsorption time with K values. The total dimensionless adsorption period decreases by the increase of K value and the results become closer to the results of uniform pressure approach where the interparticle mass transfer resistance becomes negligible.

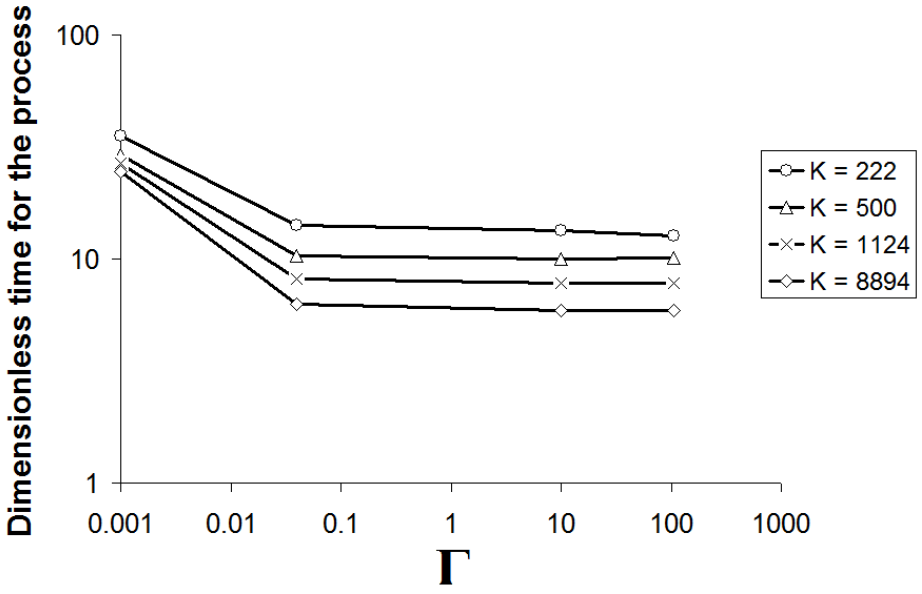


Figure 9.31. The change of dimensionless adsorption period with K values for different Γ values

# CHAPTER 10

# RESULTS AND DISCUSSION ON EXPERIMENTAL STUDY AND VALIDATION OF NUMERICAL RESULTS

In this chapter, the results of the experimental studies which were carried out in this thesis are given. The experiments were performed for different bed and evaporator temperatures. Based on the obtained experimental results, the variation of average and local bed temperatures, evaporator and bed pressure, and adsorption amount during the adsorption process are plotted and discussion are performed. Furthermore, the performed experiments were simulated by a uniform pressure approach explained in previous chapters. The comparisons of the numerical and experimental data for each experiment were done and good agreement between them is seen.

## 10.1. Experimental Results

The silica gel-water vapor adsorption experiments were performed in the constructed setup which was explained in details in Chapter 7. The measured temperature and pressures were logged by data loggers and software. The related diagrams were plotted and illustrated via diagrams.

The experiments which were done are reproducible. Even many experiments were done for the same conditions, the angular temperature variations are plotted only for two of them. The results from the experimental setup are taken for the points which are illustrated in Figure 7.7 in details. The average temperatures of the inner points, the averaged temperatures of the outer region points, the outer surface temperature of the bed, the evaporator temperature, the evaporator and bed pressures, the water uptake of the adsorbent during the experiments are collected and plotted.

### 10.1.1. Temperature and Pressure Variations

The results of two experiments which were done for the same conditions are illustrated in this section. The evaporator pressure was set to 40$^{o}$C while the adsorbent bed surface temperature was fixed to 63$^{o}$C during the experiment. As it was mentioned in Chapter 7, three points at 0, 120 and 240 degrees for two different radiuses of R = 105 mm and R = 130 mm are measured (Figure 7.7). The angular average of measured temperatures for at 0, 120, and 240 degrees are calculated for the two radiuses. The average angular temperatures of the inner and outer points and the surface temperature of the bed were plotted during the adsorption process and illustrated in Figure 10.1. As seen from Figure 10.1, for $T_{bedos}$ = 63 $^{o}$C, and $T_{eva}$ = 40 $^{o}$C, two experiments overlap each other and almost the same results were observed. At the beginning of the experiment, the water vapor adsorbed by the silica gel granules then the bed and surface temperatures increase due to the heat of adsorption. The angular averages of the inner and outer points' temperatures (temperatures at R = 105 mm and R = 130 mm) increase approximately to 104.2 and 104.7$^{o}$C. Then, heat is transferred from the bed outer surface, which is maintained at 63$^{o}$C, to the surrounding and the angular averaged temperatures of the inner and outer points decrease to 63$^{o}$C. The total adsorption period is 1440 min for this experiment. At the end of the adsorption process, the temperatures of the certain points inside of the bed reach to the bed surface temperature showing the bed is at the equilibrium condition. Figure 10.1 also shows that temperature at the outer region (R = 130 mm) decreases faster than inner region (R = 105 mm).

As mentioned in Chapter 7, there is a temperature variation along the z direction on the Teflon sheets located to the upper and bottom of the silica gel volume. The temperatures of the bottom and the upper surfaces of the silica gel volume and the outer surface bed temperature of the bed were collected during the adsorption process and illustrated in Figure 10.2. These variations were functionalized and used in the numerical code to functionalize the variation in z direction.

The temperatures at 0, 120, and 240 degrees for two different radiuses of R = 105 mm and R = 130 mm of the same experiment of Figure 10.1 were plotted and illustrated in Figure 10.3. Figure 10.3(a) illustrates the temperatures at different locations of R = 105 mm for the same experiments. The symbols filled with black represent the inner points' average temperature variation during the adsorption process

of the first experiment. The symbols filled with white represent the inner points' average temperature variation during the adsorption process of the second experiment. Similar to Figure 10.1, the temperatures at different angles of outer radius steeply increases at the beginning of adsorption process and attain to a maximum temperature and then starts to decrease due to heat transfer to the surroundings. The temperatures of different points are around 63$^{o}$C at the end of adsorption process. Figure 10.3(b) shows the temperatures at different angles of outer radius (R = 130 mm) of the same experiments. The same thermal behavior can be observed for the outer region. As can be seen from Figure 10.3(a) and 10.3(b), the temperature of different points in angular direction (on the same radius) are very close to each other showing that there is almost no temperature gradient in the angular direction for both performed experiments.

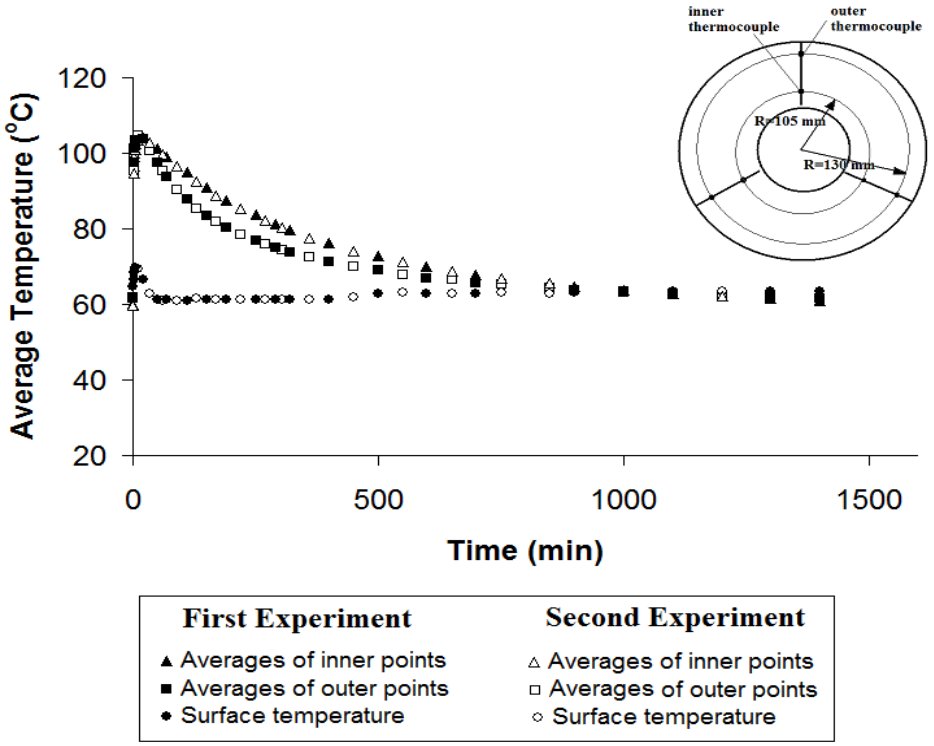


Figure 10.1. The variations of angular averaged temperature of the inner and outer points and the surface temperature during the adsorption process for the two different experiments for $T_{bedos}$ = 63$^{o}$C, and $T_{eva}$ = 40$^{o}$C

Also, the variation of the pressures of the bed and the evaporator, and the temperature of the evaporator during the adsorption process were plotted for both of the experiments of Figure 10.1. The experiment results for the first and the second experiments are illustrated by symbols filled with black and white, respectively. As seen

from Figure 10.3, the evaporator temperatures of the experiments were set to 40$^{o}$C and the same variations were obtained for the both experiments. The average evaporator pressure of the first and second experiments is 5 kPa, where the bed pressure is around 5.85 kPa.

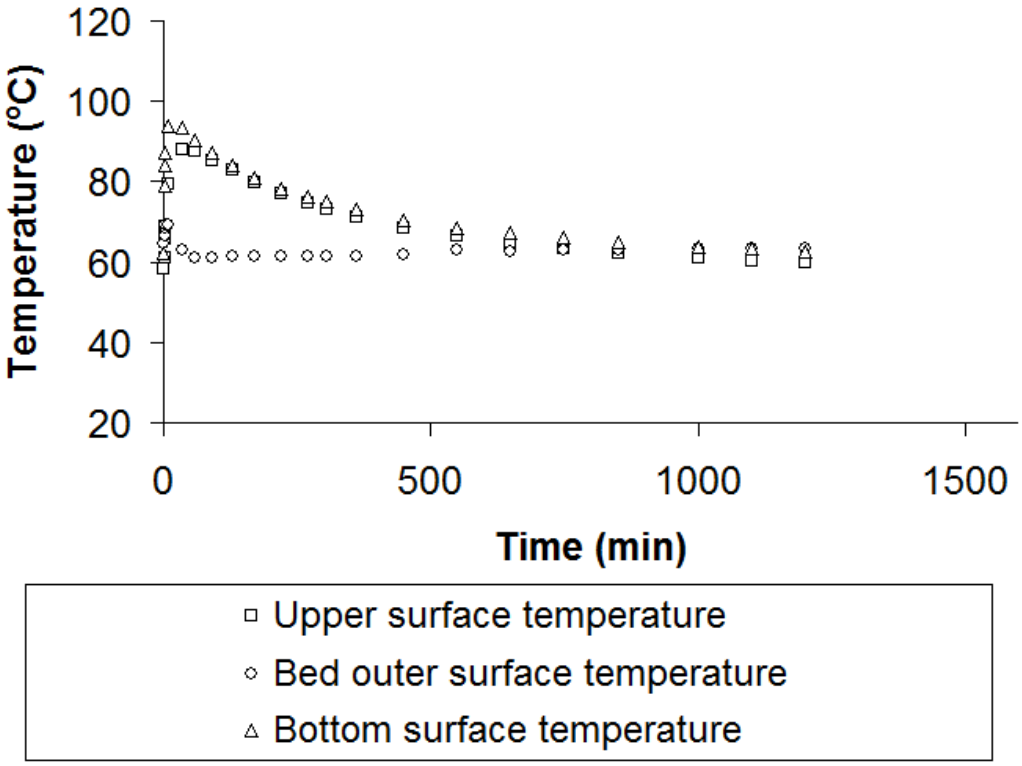


Figure 10.2. The variations of bottom and upper surface of the silica gel volume and outer surface temperature of the bed during the adsorption process for $T_{bedos}$ = 63$^{o}$C, and $T_{eva}$ = 40$^{o}$C

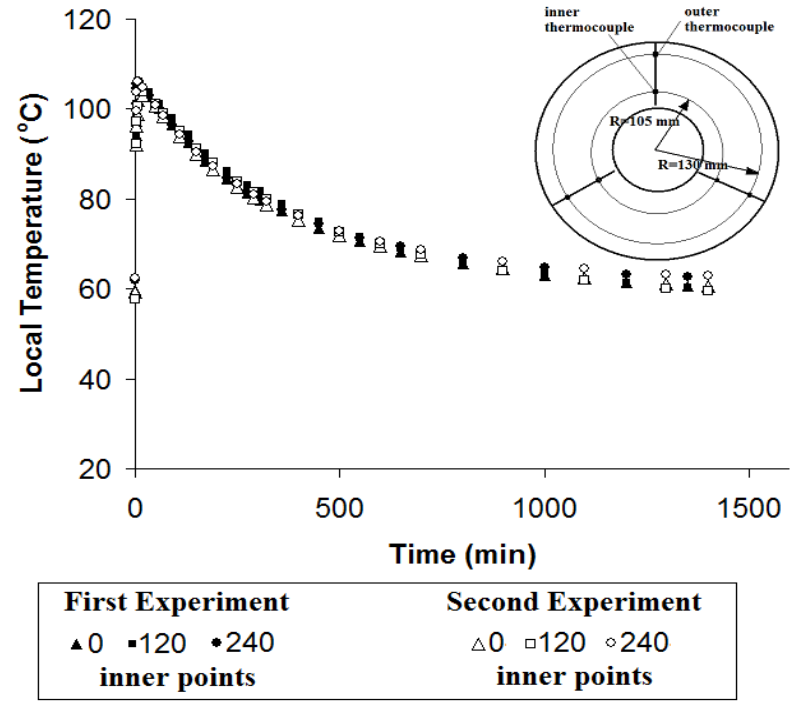


(a)

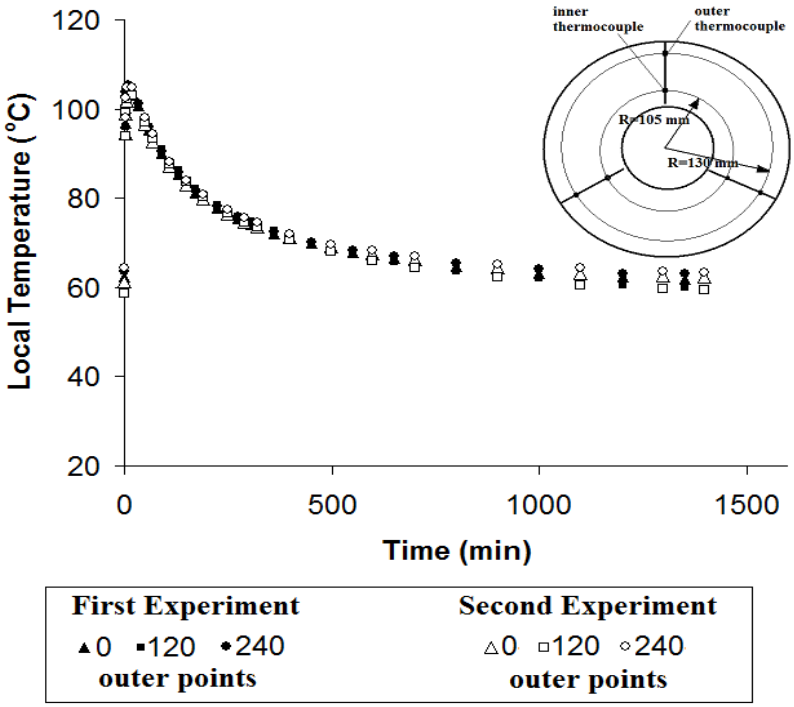


(b)

Figure 10.3. The temperature variations during the adsorption process for the two different experiments for $T_{bedos}$ = 63°C, and $T_{eva}$ = 40°C, a) inner points, b) outer points

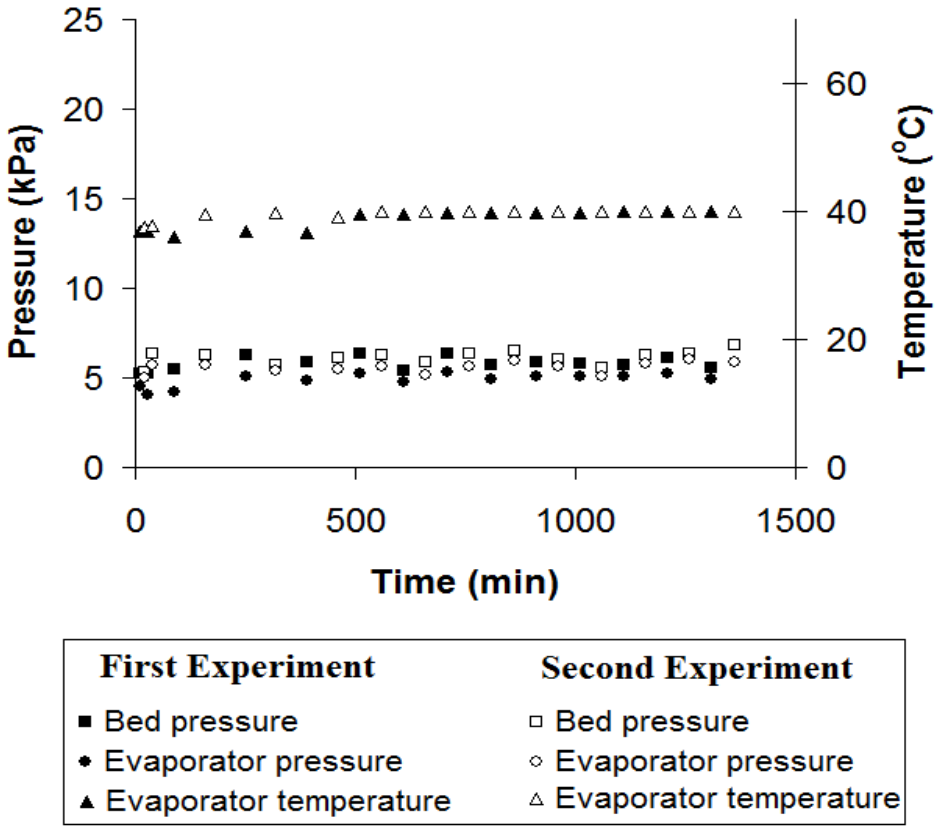


Figure 10.4. The variations of temperature and pressure in the evaporator, and bed pressure during the adsorption process for the two different experiments of $T_{bedos}$ = 63°C, and $T_{eva}$ = 40°C

Two experiments were done for the bed temperature of 73°C and evaporator temperature of 40°C. The results of the both experiments can be seen from Figures 10.5, 10.6 and 10.7. Figure 10.5 shows changes of the angular averaged temperature at R = 105 mm and R = 130 mm, and average bed surface temperature during the adsorption process. The temperature variations of this experiment is similar to the results of the previous experiment ($T_{bedos}$ = 63°C, and $T_{eva}$ = 40°C) by comparisons of Figure 10.1 and 10.5. The only difference between two experiments is outer bed surface temperature. In this experiment, the bed surface temperature was at 73°C. After starting of adsorption process, the inner and outer point average temperatures reach up to 109 and 110.3°C. Then, the averages of the temperatures of the certain points start to be decreased to 73°C. At the end of the adsorption process, all inner, outer, and surface temperatures reach to the bed surface temperature maintained at 73°C. The inner and outer point average temperatures decrease to 73°C in a shorter period compared with the previous experiments. Figure 10.6(a) and 10.6(b) show temperatures at 0,120 and $240^0$ for R = 105 mm and R = 130 mm, respectively. As expected, almost no temperature gradient

exists in angular direction. The evaporator pressure for the both experiment with $T_{bed}$ = 73 $^{o}$C is around 4.9 kPa, where the bed pressure is around 5.8 kPa.

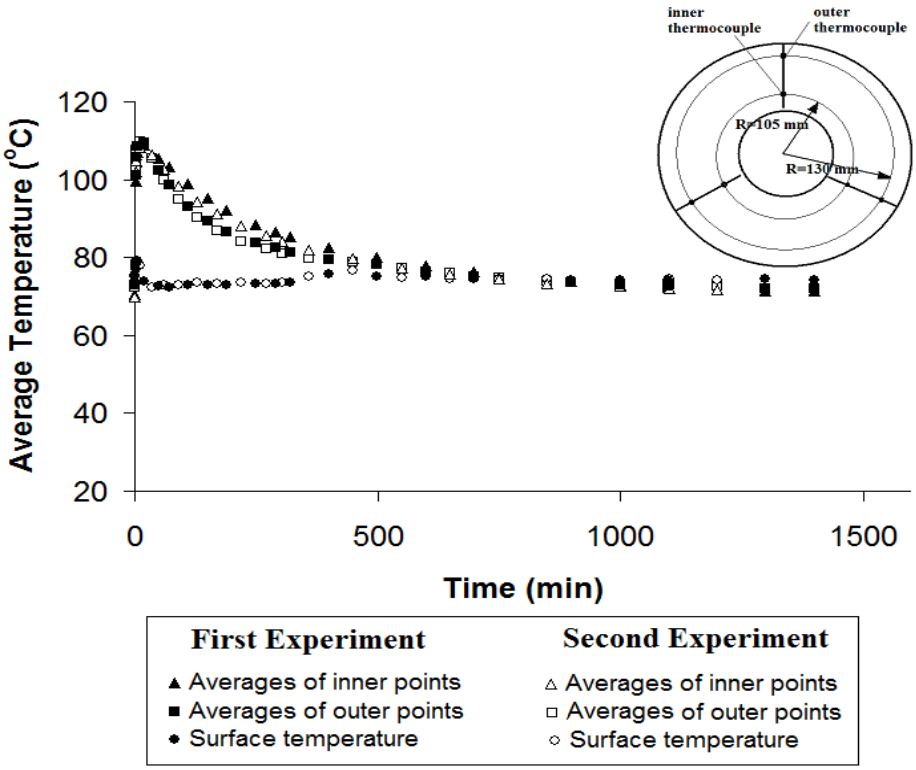


Figure 10.5. The variations of angular averaged temperature of the inner and outer points and the surface temperature during the adsorption process for the two different experiments for $T_{bedos}$ = 73$^{o}$C, and $T_{eva}$ = 40$^{o}$C

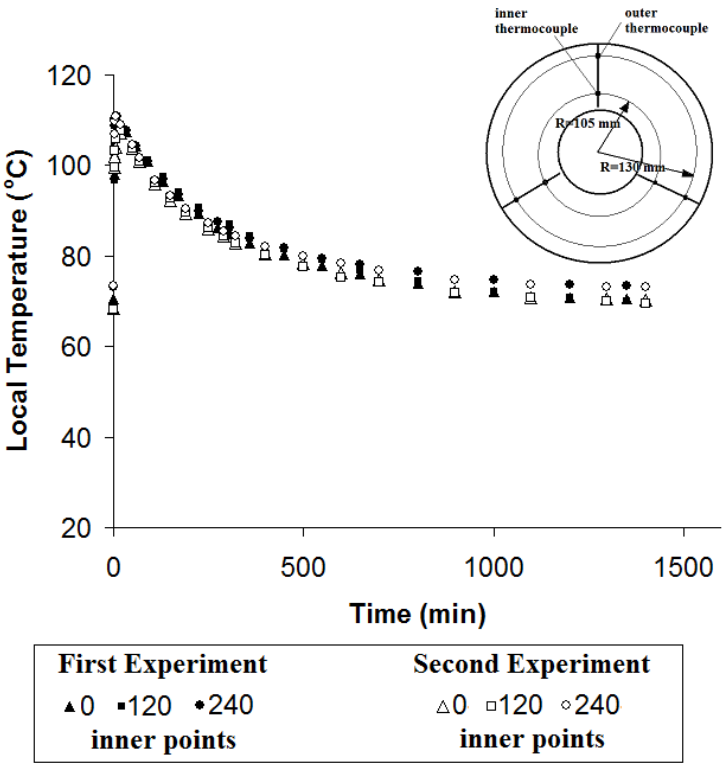


(a)

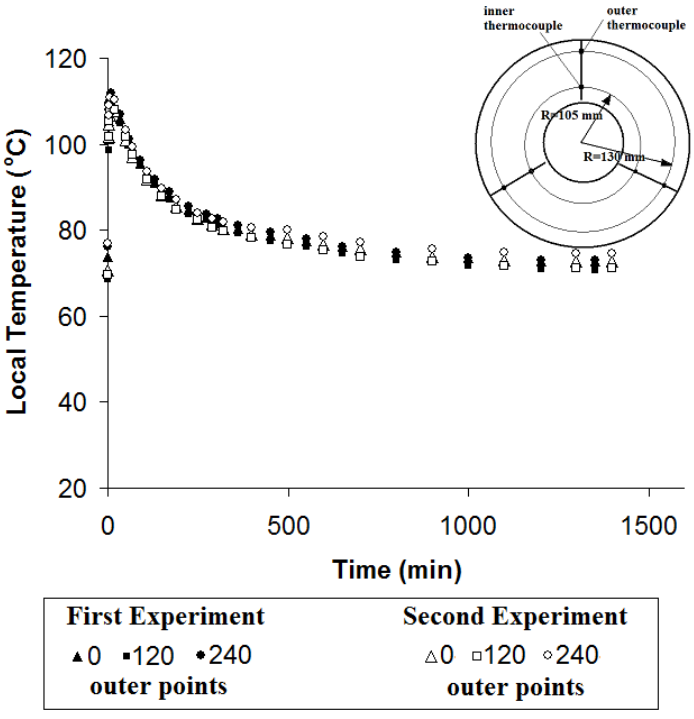


(b)

Figure 10.6. The temperature variations during the adsorption process for the two different experiments for $T_{bedos}$ = 73°C, and $T_{eva}$ = 40°C, a) inner points, b) outer points

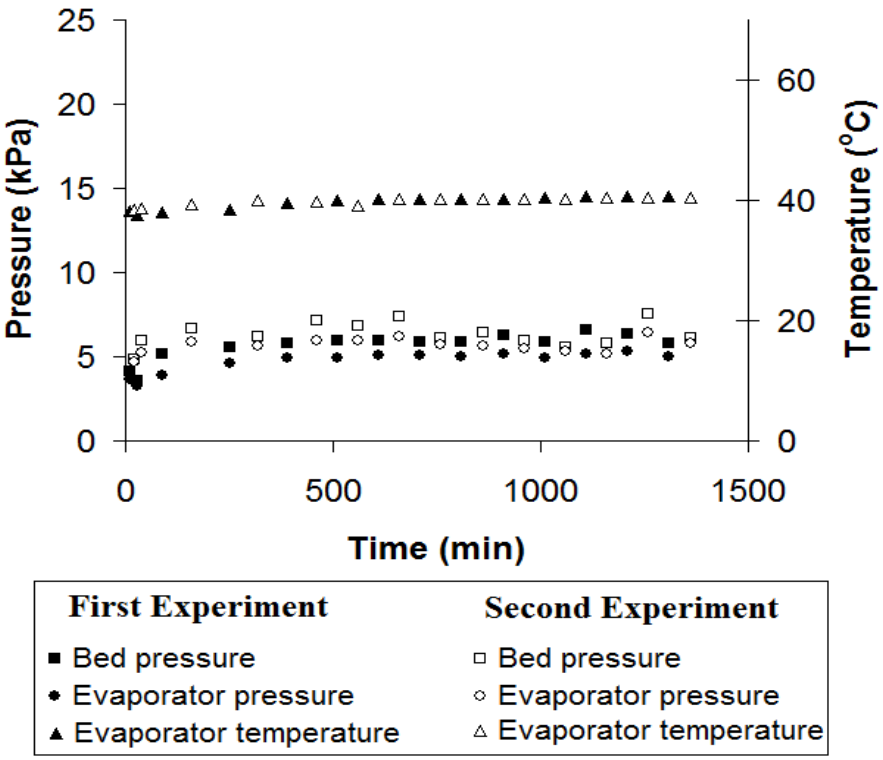


Figure 10.7. The variations of temperature and pressure in the evaporator, and bed pressure during the adsorption process for the two different experiments of $T_{bedos}$ = 73°C, and $T_{eva}$ = 40°C

The third experiment was performed for different initial temperature while the evaporator temperature and bed outer surface temperature were fixed to $T_{eva}$ = 40°C and $T_{bedos}$ = 60°C, respectively. The adsorption process was started when the bed temperature was at $T_{bedos}$ = 73°C and it is ended when the temperature of the adsorbent bed becomes equal to the bed outer surface temperature ($T_{bedos}$ = 60°C). Two experiments were performed for the same set temperatures of the bed outer surface and the evaporator. The angular averaged temperature variations of the inner and outer points and the surface temperature, the temperature variation of the evaporator and the pressures of the evaporator and the bed during the adsorption process for the two experiments can be seen from Figures 10.8 and 10.9. The inner and outer points' temperatures attain to 108.8 and 109.4°C, at the beginning of the process due to heat of adsorption. As seen from Figure 10.8 and 10.9, the results of both experiments are almost identical. The average evaporator pressure for this experiment is 5.4 kPa, where the bed pressure is around 6.1 kPa.

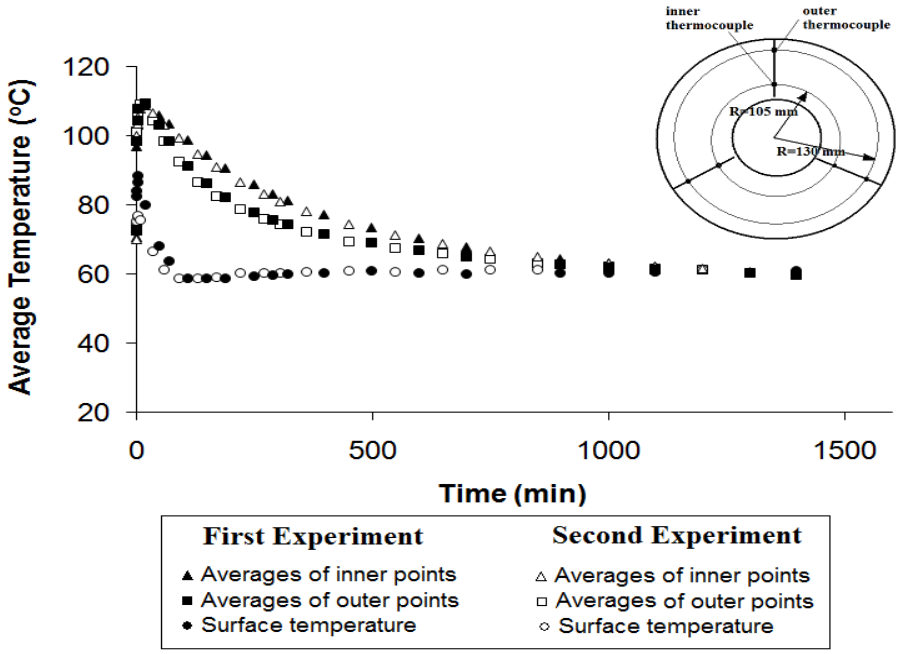


Figure 10.8. The variations of angular averaged temperature of the inner and outer points and the surface temperature during the adsorption process for the two different experiments for $T_{bedos}$ = 73-60°C, and $T_{eva}$ = 40°C

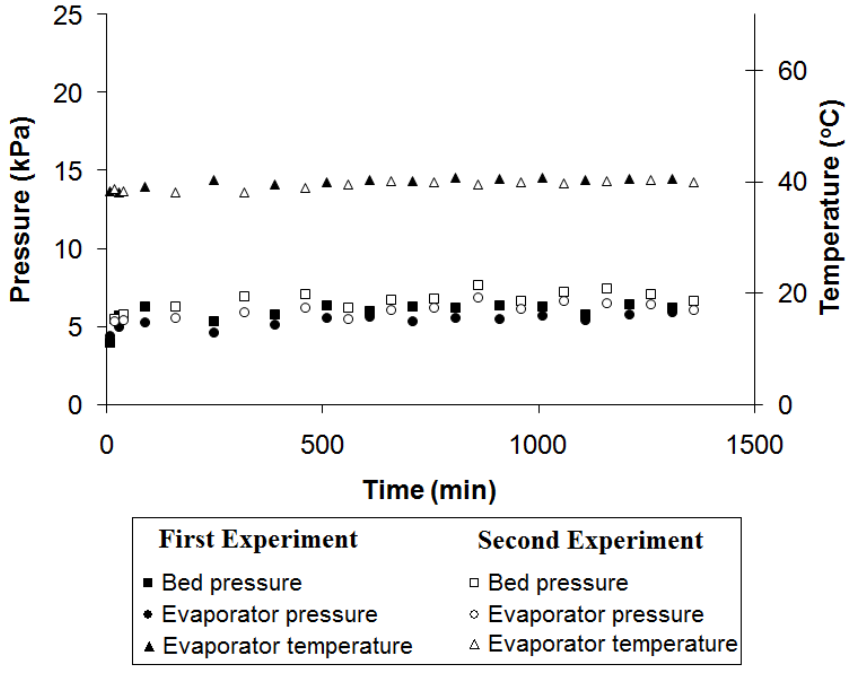


Figure 10.9. The variations of temperature and pressure in the evaporator, and bed pressure during the adsorption process for the two different experiments of $T_{bedos}$ = 73-60°C, and $T_{eva}$ = 40°C

The fourth experiment was performed with the same initial conditions with the third experiment. But this time, the adsorption process was started when the bed

temperature was at $T_{bedos}$ = 80°C and it is ended when the temperature of the adsorbent bed becomes equal to the bed outer surface temperature ($T_{bedos}$ = 60°C). The angular averaged temperature variations of the inner and outer points and the surface temperature, the temperature variation of the evaporator and the pressures of the evaporator and the bed during the adsorption process for the two experiments can be seen from Figures 10.10 and 10.11. The inner and outer points' average temperatures attain to 111.1 and 112.7°C, at the beginning of the process due to heat of adsorption. The average evaporator pressure for this experiment is 5.7 kPa, where the bed pressure is around 6.6 kPa.

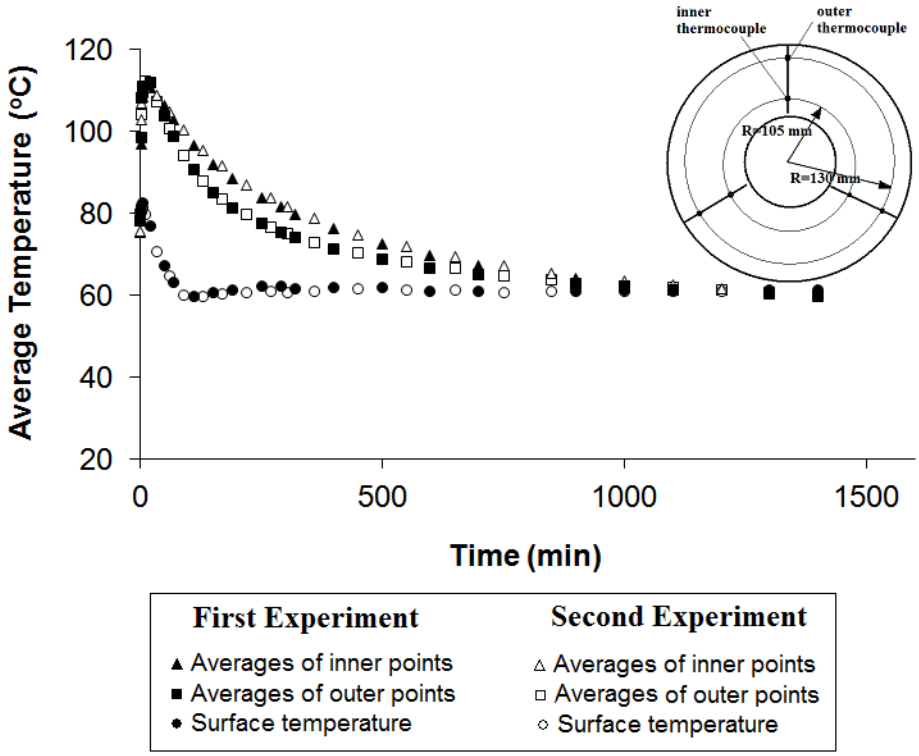


Figure 10.10. The variations of angular averaged temperature of the inner and outer points and the surface temperature during the adsorption process for the two different experiments for $T_{bedos}$ = 80-60°C, and $T_{eva}$ = 40°C

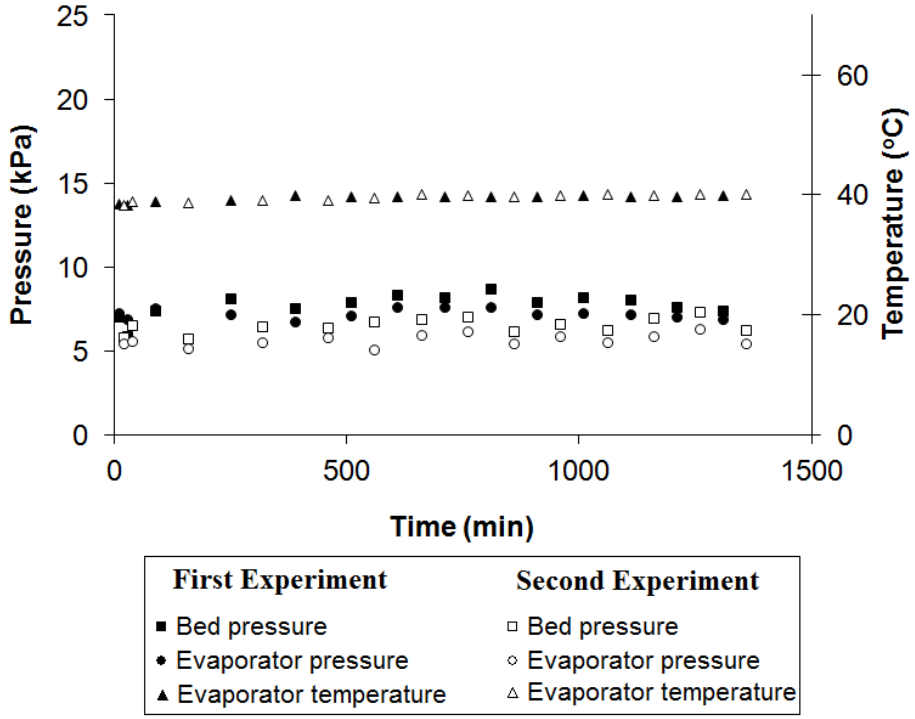


Figure 10.11. The variations of temperature and pressure in the evaporator, and bed pressure during the adsorption process for the two different experiments of $T_{bedos}$ = 80-60°C, and $T_{eva}$ = 40°C

The experiments under different initial and outer surface temperatures were also performed, and they are given in Appendix F. The same comments presented in this section are also valid for the given diagrams in Appendix F.

## 10.2. Comparison of Theoretical and Experimental Results

The numerical results were obtained for the experiments described in previous section. The comparison of numerical and experimental results is given in order to validate the numerical method explained in Chapter 8. The agreement between the numerical and experimental results also shows the accuracy of the performed experimental study.

### 10.2.1. The Validation of the Numerical Results

The uniform pressure approach was considered since the experimented adsorbent particles are large and there are sufficient space between the particles. Water vapor can easily moves between silica gel particles and no interparticle mass transfer resistance is considered. The governing equations should be solved to simulate heat and mass transfer in the experimented bed is given in Chapter 6.5. Both r and z directions are taken into account. A temperature gradient in z direction is observed, that is why z direction was taken. A cubic particle arrangement is assumed in the bed and the porosity value was 0.45 (Collins 1961, Heinemann 2005). The density and the specific heat of the silica gel were taken from the silica gel product manual as 750 kg/m$^3$ and 1 kJ/kg$^o$C, respectively. The heat of adsorption for the silica gel-water pair was taken as 2644 kJ/kg (Demir et al. 2011). The effective thermal conductivity was 0.106 W/mK (Demir et al. 2011). The average radius of the silica gel particles inside of the bed was measured as 1.6 mm. The evaporator pressure was the same with the evaporator pressure of the performed experiments. The water and water vapor specific heats were considered based on the average of the evaporator and maximum bed temperature. The effective mass diffusivity equations, given in Ref (Demir 2008), for the employed silica gel-water pair were used. Two mass diffusivity equations were presented in that study for the short and the long terms as

For short term
$$D_{eff} = 1.28x10^{-2} e^{(\frac{-57758}{RT})} \quad (10.1)$$

For long term
$$D_{eff} = 2.48x10^{-6} e^{(\frac{-29066}{RT})} \quad (10.2)$$

These equations were used in the present numerical study. The thermal resistance of the bed casing on the energy equation was taken into consideration. The stainless steel thermal conductivity and casing thickness were taken as 16.2 W/mK and 4 mm, respectively. The isoster equations for W = 0.5, 1, 3, 5, 10, 13% ($kg_l\ kg_s^{-1}$) suggested by Demir (Demir 2008) were used to find a generalized isothermal equation for determination of water concentration in silica gel at different pressure and temperatures.

Based on the suggested isoster, the Freundlich isotherms (presented by Equation 6.6) were found for different water concentration. When $P/P_{sat}$ ratio less than 0.1233, the values of k and n are found as 0.3092, 0.8565, respectively. For $P/P_{sat}$ greater than 0.1233, the values of k and n are 0.1543, 0.5384, respectively. Mathematical functions were obtained for determination of variation of the bed surface temperature, the bottom and upper part temperatures of the Teflon sheets by using the temperatures measured during the experiments. These temperature functions were used in the numerical program. The obtained mathematical functions were changed according to the experiment.

#### 10.2.1.1. Comparison of the Inner and Outer Region Points' Temperature

The obtained numerical results were compared with the experimental results through Figures 10.12 to 10.15. The comparison between the experimental and numerical results for the first experiment, when $T_{bedos}$ = 63 $^{o}$C, and $T_{eva}$ = 40 $^{o}$C, is illustrated in Figure 10.12. As mentioned before, the angular averaged temperatures for R = 105 mm and R = 130 mm through the adsorption process are represented with square and circle symbols, respectively. Numerical solutions are given by dashed and flat lines for the temperatures at R = 105 mm and R = 130 mm, respectively. As can be seen from Figure 10.12, there is good agreement between the experimental and numerical results showing correctness of the suggested method and accuracy of the performed experiment.

The comparison between the experimental results versus numerical solution for three experiments, a) $T_{bedos}$ = 73 $^{o}$C, and $T_{eva}$ = 40 $^{o}$C, b) $T_{bedos}$ = 73-60 $^{o}$C, and $T_{eva}$ = 40 $^{o}$C, c) $T_{bedos}$ = 80-60 $^{o}$C, and $T_{eva}$ = 40 $^{o}$C are illustrated in Figures 10.13, 10.14, 10.15, respectively. As mentioned before, the functions of the lower and upper surfaces of the Teflon sheets, which give the temperature difference in z direction of the bed, and the bed surface temperatures, were changed in the program based on the measured temperatures.

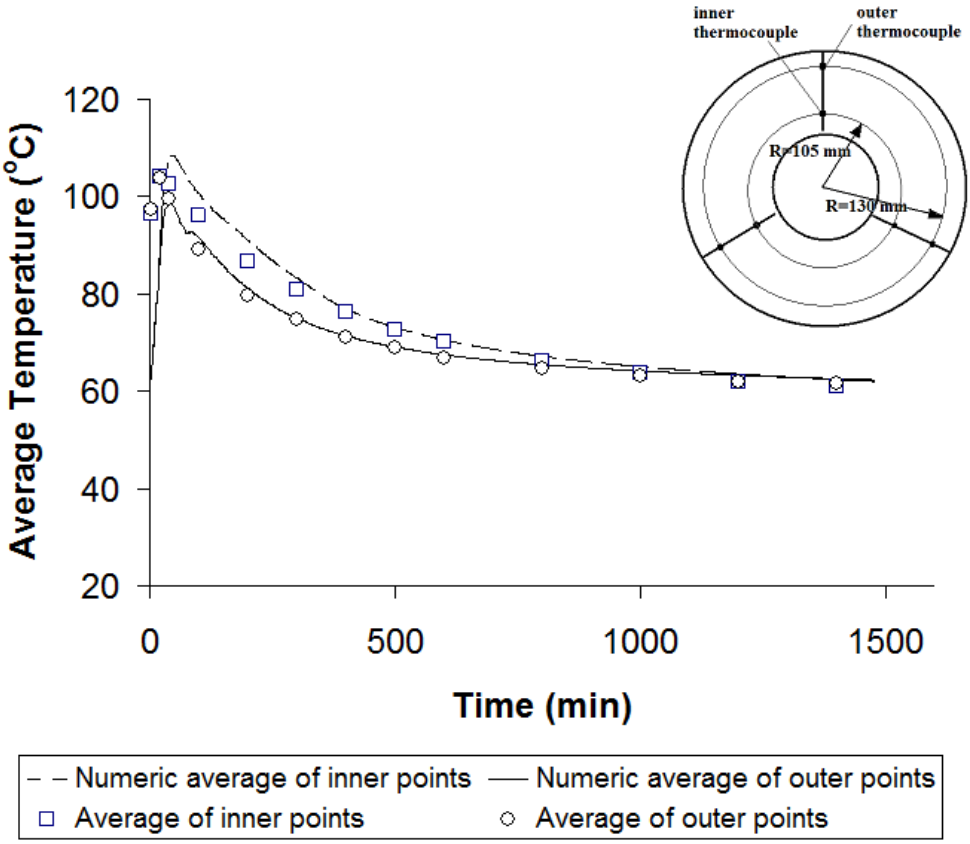


Figure 10.12. The comparison of numerical and experimental temperatures at the inner and outer points during the adsorption process for the experiment with $T_{bedos}$ = 63°C, and $T_{eva}$ = 40°C

The specific heats of the water and water vapor for the related temperatures were read from thermodynamics tables for the specified temperatures. As illustrated in these figures, the variation of temperature and concentration in the bed during adsorption process can be determined by solving the related heat and mass equations under uniform pressure approach, and the suggested method is appropriate to determine adsorption period.

The experimental and numerical temperatures of the both inner and outer points' are compared for the same time steps. The average difference of the results with experimentally and numerically for the temperatures of the certain points at the same time varies between 0.1% and 2.9% for each experimental set. As a result, a good agreement is seen with the numerical and experimental results.

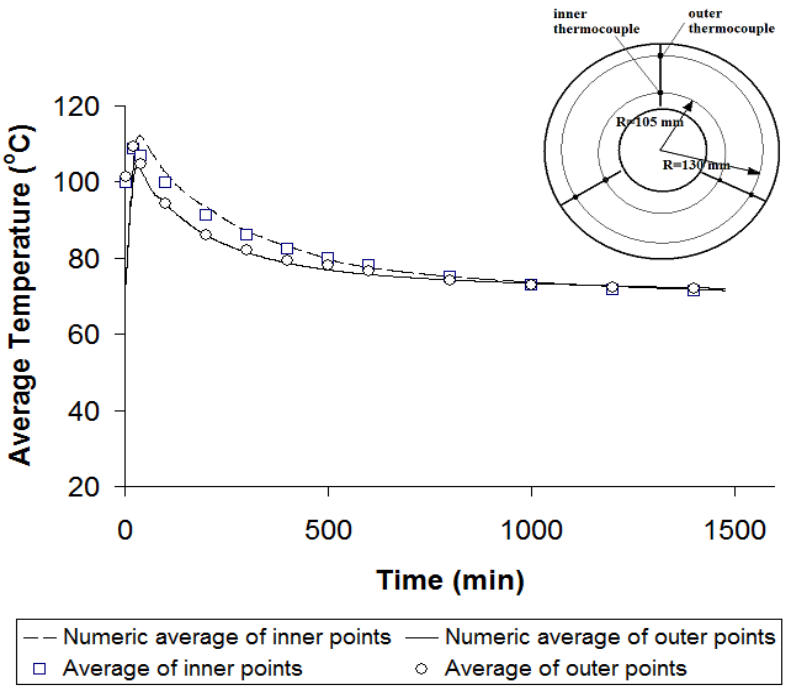


Figure 10.13. The comparison of numerical and experimental temperatures at the inner and outer points during the adsorption process for the experiment with $T_{bedos}$ = 73°C, and $T_{eva}$ = 40°C

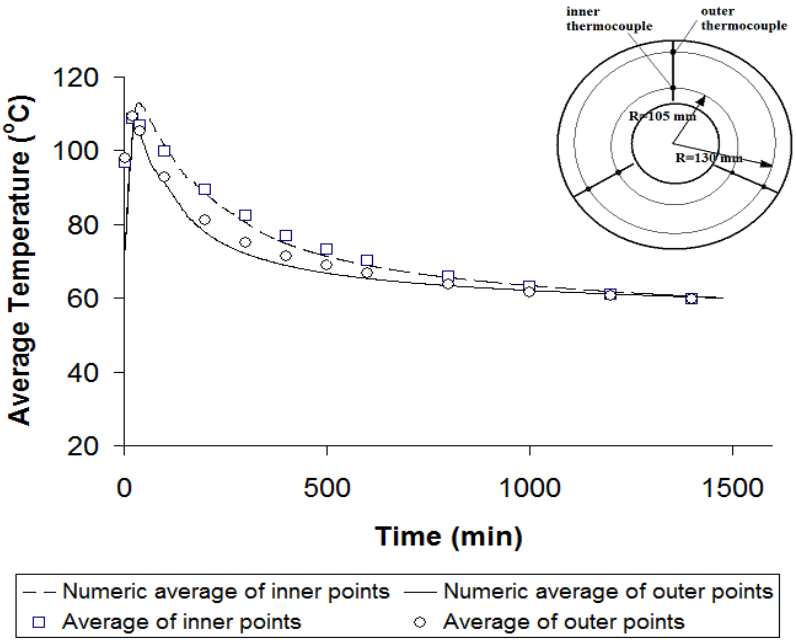


Figure 10.14. The comparison of numerical and experimental temperatures at the inner and outer points during the adsorption process for the experiment with $T_{bedos}$ = 73-60°C, and $T_{eva}$ = 40°C

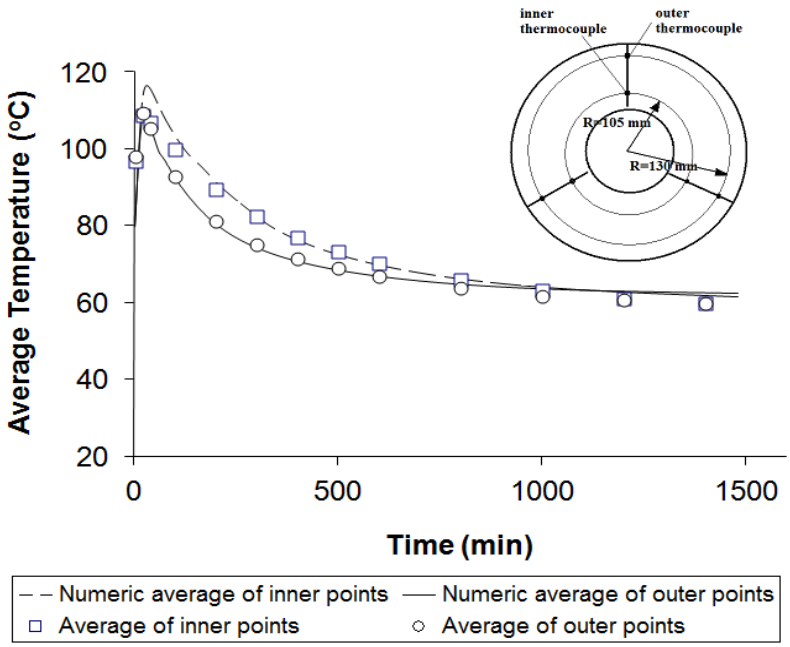


Figure 10.15. The comparison of numerical and experimental temperatures at the inner and outer points during the adsorption process for the experiment with $T_{bedos}$ = 80-60°C, and $T_{eva}$ = 40°C

### 10.2.1.2. Comparison of Water Adsorption

The water level inside of the evaporator was measured during the adsorption process from the glass on the evaporator surface. During reading the water level, measurement errors occurred since the water level was not stables. Our observation showed that an error with the range of ±1.5% occurred due to the measurement error. The comparisons of water concentration in the bed obtained by the experimental and numerical methods for different experiments are illustrated in the following figures. In Figure 10.16, the black vertical lines shows the range of the water concentration in the bed throughout the experiment for $T_{bedos}$ = 63 °C, and $T_{eva}$ = 40°C. The red line is also water concentration in the bed obtained by the numerical solutions. The water concentration in the bed for the experiments of three experiments as $T_{bedos}$ = 73 °C, $T_{eva}$ = 40 °C and $T_{bedos}$ = 73-60 °C, $T_{eva}$ = 40 °C, and $T_{bedos}$ = 80-60 °C, $T_{eva}$ = 40 °C, were plotted in Figure 10.17, 10.18, and 10.19, respectively. The achieved water concentration in the bed by numerical method is in the range of measured water concentration for the all presented results. The comparison of numerical and experimental water concentration in the bed for other experiments are plotted and given in Appendix F.

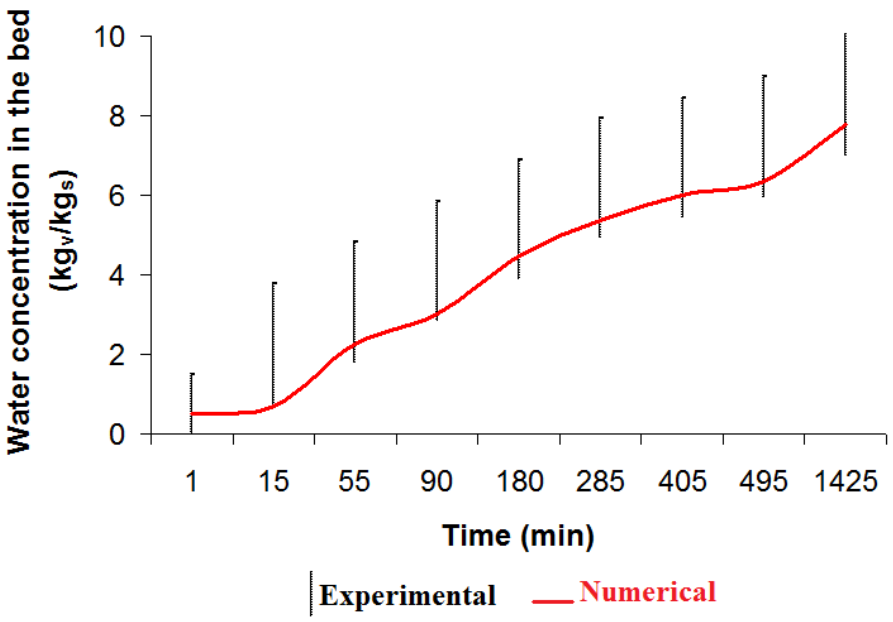


Figure 10.16. The comparison of water concentration in the bed obtained numerically and experimentally when $T_{bedos}$ = 63°C, and $T_{eva}$ = 40°C

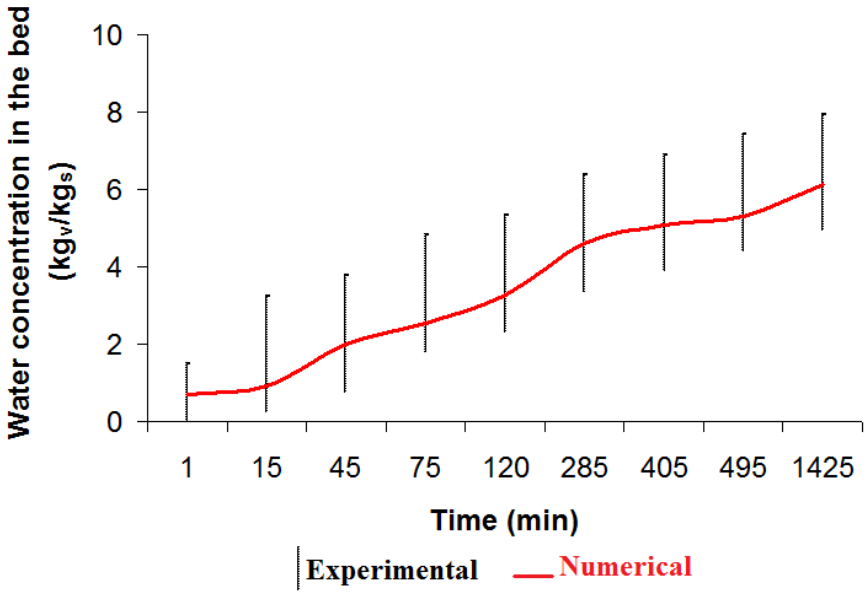


Figure 10.17. The comparison of water concentration in the bed obtained numerically and experimentally when $T_{bedos}$ = 73°C, and $T_{eva}$ = 40°C

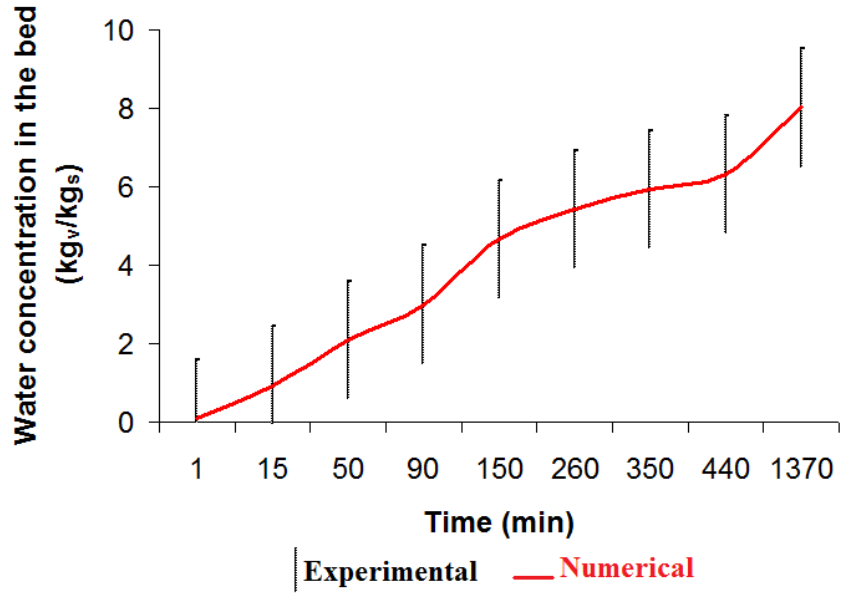


Figure 10.18. The comparison of water concentration in the bed obtained numerically and experimentally when $T_{bedos}$ = 73-60°C, and $T_{eva}$ = 40°C

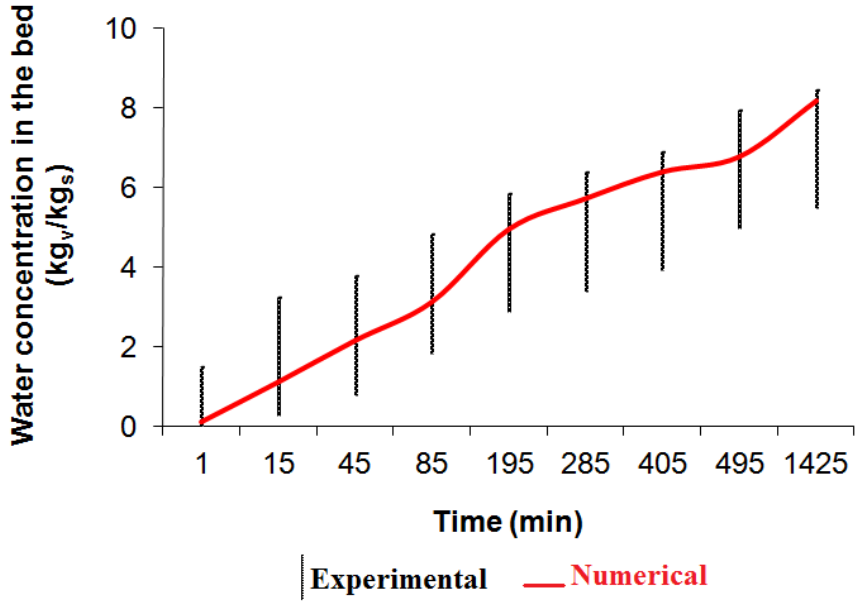


Figure 10.19. The comparison of water concentration in the bed obtained numerically and experimentally when $T_{bedos}$ = 80-60°C, and $T_{eva}$ = 40°C

## 10.3. Sensitivity Analysis

As mentioned in Chapter 10.2.1, many different parameters should be considered in order to simulate heat and mass transfer in the adsorbent bed. Some of these parameters proposed by silica gel manufacturer, or experimentally obtained in this study, or taken from a reference are;

- Density of the silica gel
- Specific heat of the silica gel
- Porosity
- Heat of adsorption
- Effective conductivity
- Diffusivity
- Conductivity of the bed material (steel)

Although, these parameters were taken from reliable sources such as the experimented silica gel manufacturer of Merck Co., a sensitivity study was performed to observe the effect of these parameters on the numerical results and to determine key parameters. Table 10.1 shows the aforementioned parameter values in the fourth column, these values are called as original value. The values of the same parameters increased or decreased by 25% are presented in the second and third columns.

Table 10.1. Sensitivity analysis decreased, increased, and original values of the parameters

| Parameter | Decreased Value (-25%) | Increased Value (+25%) | Original Value |
|---|---|---|---|
| $\rho_s$ [kg/m$^3$] | 562.5 | 937.5 | 750 |
| $C_{p_s}$ [kJ/kg$^o$C] | 0.75 | 1.25 | 1 |
| $\varphi$ [-] | 0.3375 | 0.5625 | 0.45 |
| $\Delta H_{ads}$ [kJ/kg] | 1983 | 3305 | 2644 |
| $\lambda_{eff}$ [W/mK] | 0.0795x10$^{-3}$ | 0.1325x10$^{-3}$ | 0.106x10$^{-3}$ |
| $\lambda_{steel}$ [W/mK] | 12.15x10$^{-3}$ | 20.25x10$^{-3}$ | 16.2x10$^{-3}$ |
| $D_{eff}$ [m$^2$/s] | Values found by using Eq.(10.1) and (10.2) *0.75 | Values found by using Eq.(10.1) and (10.2) *1.25 | Values found by using Eq.(10.1) and (10.2) |

In order to find out the effect of each parameter on heat and mass transfer in the bed, numerical results are obtained by changing one parameter to its increased value (or

decreased value) and fixing the other six parameters at original value. Temperature distribution is obtained for 15 cases. For each case, the angular averaged temperature at the inner and outer points' are calculated throughout the adsorption process. Then, they are compared with the angular averaged of temperature obtained by using the original values. The difference between temperatures of the original and increased/decreased values for each parameter is found by using Eq. (10.3) and illustrated from Figure 10.20 to 10.21.

$$Error(\%) = \frac{\begin{pmatrix} Decreased.or \\ Increased \\ temp. \\ value \end{pmatrix}_{@\,related.time} - \begin{pmatrix} Original \\ temp. \\ value \end{pmatrix}_{@\,related.time}}{\begin{pmatrix} Max. \\ temp. \\ value \\ during \\ adsorption \\ period \end{pmatrix} - \begin{pmatrix} Min. \\ temp. \\ value \\ during \\ adsorption \\ period \end{pmatrix}} x100 \tag{10.3}$$

As can be seen from Figure 10.20(a), the increase of specific heat of silica gel by +25%, the averaged temperature decreases by -18.4% from the original value when the adsorption time is smaller than 100 minute. On the contrary, the increase +25% of diffusivity and heat of adsorption values, the inner point temperature increases by +14.4% and +19.3%, respectively, when the adsorption time is smaller than 100 minutes. The increase of diffusivity and heat of adsorption increase temperature at the starting of the adsorption process. For this period (period<100 min.), the effective conductivity, porosity, and density of silica gel also effect the variations of the temperature inside of the adsorbent bed. Their effects are not comparable with the effects of specific heat, mass diffusivity, and heat of adsorption. For period greater than 100, the effects of specific heat, mass diffusivity, and heat of adsorption become smaller compared to the other parameters. The increase of density, porosity, and heat of adsorption by 25% increases temperature at the inner node, while the increase of effective conductivity reduces temperatures. This figure shows that if there is a difference between the numerical and experimental results at the beginning of the process (time less than 100), the reasons may be due to incorrect values of specific heat, mass diffusivity, and heat of adsorption. The values of these parameters should be

investigated and should be corrected. For the period greater than 100, the difference between the numerical and experimental studies may be caused due to incorrect values of porosity, density, heat of adsorption and effective conductivity. The important point of Figure 10.20(a) is that the increase of parameters listed in Table 10.1, does not have effect more than 20% on the results. The difference between temperatures of the original and increased values for each parameter for the outer points is illustrated by Figure 10.20(b). The same parameters as effective conductivity, porosity, and density of silica gel effect the variations of the temperature inside of the adsorbent bed for the short period (period<100 min.) when compared when compared with the inner points (Figure 10.20(a)).

The difference between temperatures of the original and decreased (-25% decreased) values for each parameter of inner and outer points is plotted in Figure 10.21. By the reduces of specific heat of silica gel by -25%, the averaged temperature increases by -25.5% from the original value when the adsorption time is smaller than 100 minute as seen from Figure 10.21(a). Also Figure 10.21(a) shows that, the -25% decreased function of diffusivity and heat of adsorption values, the averaged temperature decreases with the decreased value to -17.1% and -20.2% when the adsorption time is smaller than 100 min., respectively. The effect of conductivity of the steel can be neglected as can be seen from Figure 10.20 and 10.21, almost no change occurs by the increase of its value ±25%.

## 10.4. Uncertainty Analysis

The uncertainty in a measurement can be defined by the uncertainty analysis. The experimental results are affected by the errors of the instrumentation, experiment methodology etc. Uncertainty analysis is the procedure used to quantify data validity and accuracy. Device accuracy and precision of the measuring is related with the uncertainty of a measurement (JCGM, 2008).

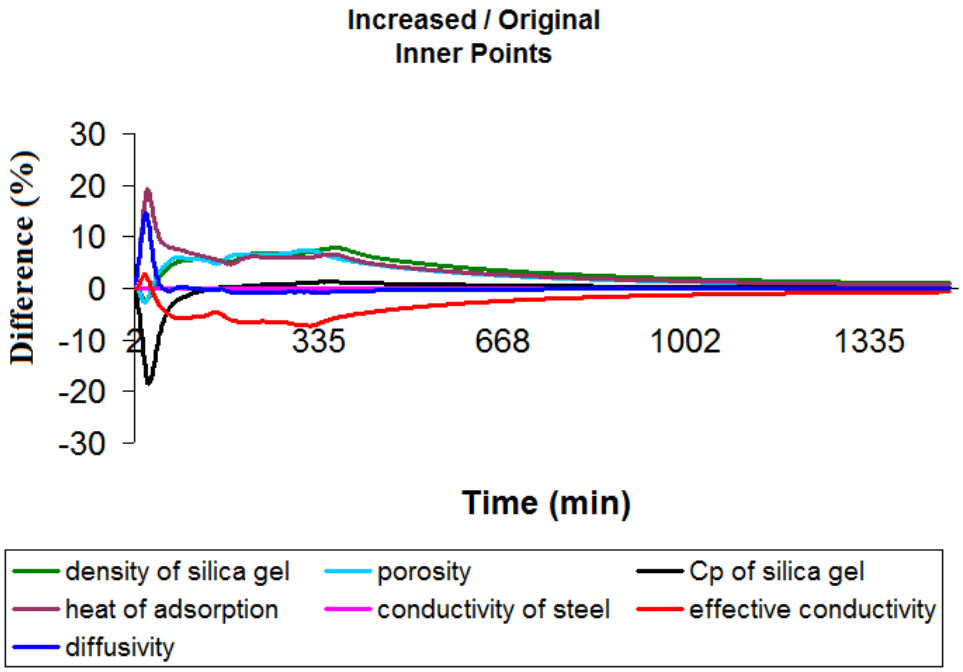


(a)

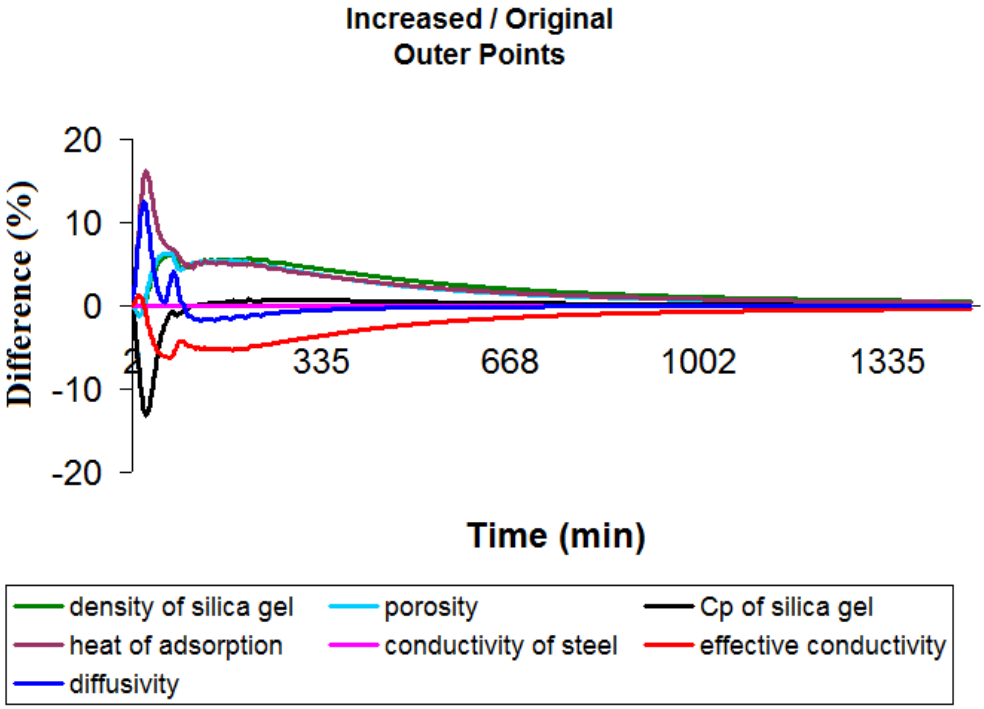


(b)

Figure 10.20. The error functions of each parameter during the adsorption process for increased values, a) inner points' temperature, b) outer points' temperature

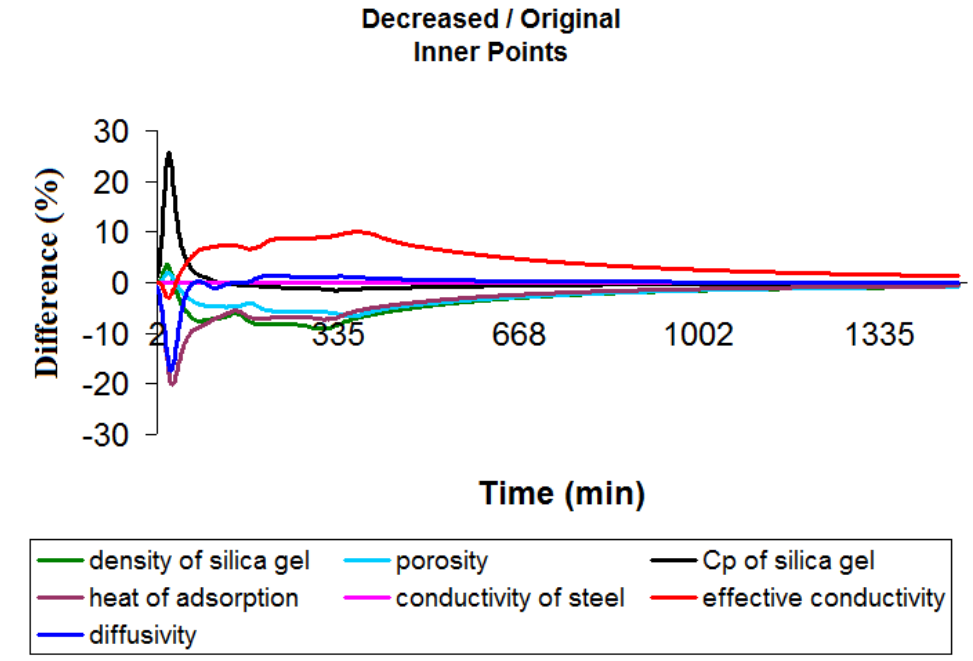


(a)

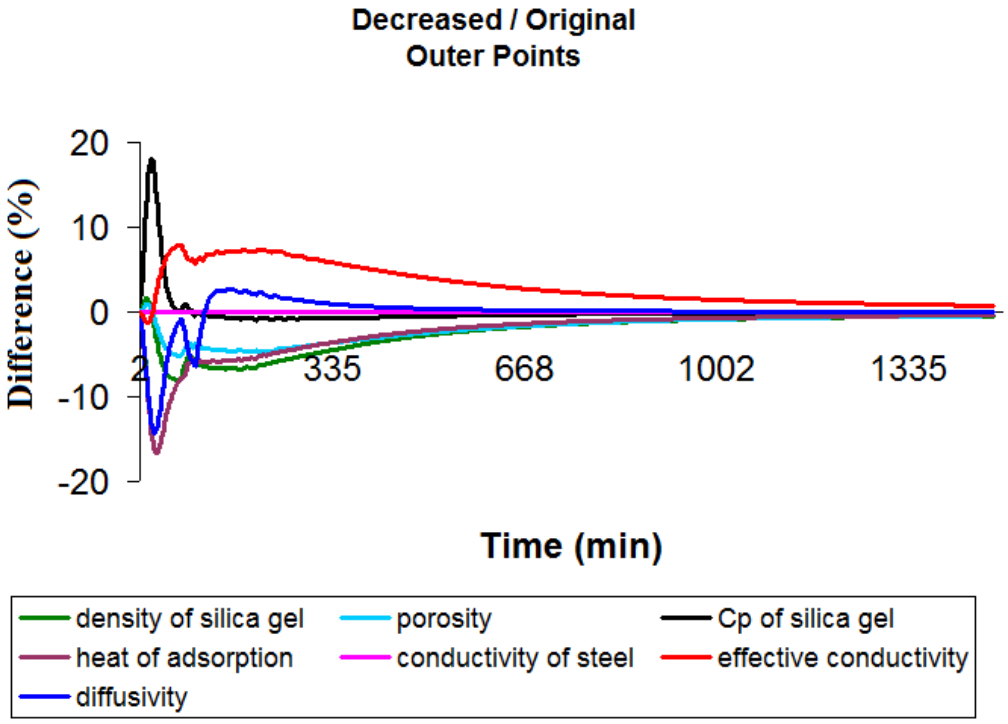


(b)

Figure 10.21. The error functions of each parameter during the adsorption process for decreased values, a) inner points' temperature, b) outer points' temperature

Let's assume q is a function of $x_1$, $x_2$, …, $x_n$ . The effect on q of an error measuring an individual $x_i$ may be estimated by analogy to the derivative of a function. A variation, $\delta x_i$ in $x_i$ would cause q to vary according to;

$$\delta q_i = \frac{\partial q}{\partial x_i}\delta x_i \tag{10.4}$$

If the equation is divided to q and multiplied with $x_i$;

$$\frac{\delta q_i}{q} = \frac{x_i}{q}\frac{\partial q}{\partial x_i}\frac{\partial x_i}{x_i} \tag{10.5}$$

$\partial x_i / x_i$ gives the uncertainty due to variations in $x_i$, where $\partial x_i$ is the accuracy of measurement. Uncertainty of the results can be calculated by the following equation:

$$u_q = \mp\left\{\left(\frac{x_1}{q}\frac{\partial q}{\partial x_1}u_1\right)^2 + \left(\frac{x_2}{q}\frac{\partial q}{\partial x_2}u_2\right)^2 + .....+\left(\frac{x_n}{q}\frac{\partial q}{\partial x_n}u_n\right)^2\right\}^{1/2} \tag{10.6}$$

In this study, the the isotherm equation is evaluated using pressure and temperature values of the adsorptive, and it can be written as;

$$q = k\left(\frac{P}{f(T)}\right)^{1/n} = k\left(\frac{P}{T}\right)^{1/n} \tag{10.7}$$

where n and k are constants.

The calculation depends on pressure and temperature parameters. So, the uncertainty analysis should be performed based on the accuracy of devices used to measure the quantities of these parameters. The measurement devices and accuracies of them are given in Table 10.2.

Table 10.2. Accuracies and uncertainties of measured parameters

| **Measurement** | **Device** | **Accuracy** | **Uncertainty** |
|---|---|---|---|
| Pressure | EW-07356-60 | 0.4% | ±0.004 |
| Mass | Kern-cb6k1 | 1% | ±0.01 |
| Temperature | K type | 0.3% | ±0.003 |
| Height | - | 1.5% | ±0.015 |

The uncertainty can be calculated from this equation:

$$u_q = \mp\left\{\left(\frac{P}{q}\frac{\partial q}{\partial P}u_P\right)^2 + \left(\frac{T}{q}\frac{\partial q}{\partial T}u_T\right)^2\right\}^{1/2} \tag{10.8}$$

$$u_q = \mp\left\{\left(\frac{PT^{\frac{1}{n}}}{p^{\frac{1}{n}}}\frac{P^{\left(\frac{1}{n}-1\right)}}{T^{\frac{1}{n}}}u_P\right)^2 + \left(\frac{TT^{\frac{1}{n}}}{P^{\frac{1}{n}}}(-T)\left(-\frac{1}{n}-1\right)P^{\frac{1}{n}}u_T\right)^2\right\}^{1/2} \tag{10.9}$$

$$u_q = \mp\left\{\left((1)\mp u_P\right)^2 + \left((-1)\mp u_T\right)^2\right\}^{1/2} \tag{10.10}$$

If the uncertainty is calculated:

$$u_q = \mp\left\{\left((1)\mp 0.004\right)^2 + \left((-1)\mp 0.003\right)^2\right\}^{1/2} \tag{10.11}$$

$$u_q = \mp 0.005 \tag{10.12}$$

The uncertainty of the experimental study on isotherm is found 0.005.

The concentration change in the bed is correlated with the data given in this equation.

$$q = \frac{\Delta m_v}{m_s} = \frac{\rho_v \Pi (R_o^2 - R_i^2)H}{m_s} \tag{10.13}$$

where H is the height water height in the evaporator. The uncertainty can be calculated from this equation:

$$u_q = \mp\left\{\left(\frac{H}{q}\frac{\partial q}{\partial H}u_H\right)^2 + \left(\frac{m_s}{q}\frac{\partial q}{\partial m_s}u_m\right)^2\right\}^{1/2} \tag{10.14}$$

$$u_q = \mp\left\{\left(\frac{Hm_s}{H}\frac{1}{m_s}u_H\right)^2 + \left(\frac{{m_s}^2}{H}\frac{-H}{{m_s}^2}u_m\right)^2\right\}^{1/2} \tag{10.15}$$

$$u_q = \mp\left\{\left((1)\mp u_H\right)^2 + \left((-1)\mp u_m\right)^2\right\}^{1/2} \tag{10.16}$$

If the uncertainty is calculated:

$$u_q = \mp\left\{\left((1)\mp 0.015\right)^2 + \left((-1)\mp 0.01\right)^2\right\}^{1/2} = \mp 0.018 \tag{10.17}$$

The achieved calculations and results should be evaluated considering this uncertainty quantity.

# CHAPTER 11

# HINTS FOR DESIGN OF A GRANULAR ADSORBENT BED

In this chapter, practical uses of the dimensionless parameters and discussions performed throughout this thesis for design of an adsorbent bed are given. Based on the numerical studies, four dimensionless parameters which are Ku, Γ, $R_o/R_i$, K are found very important on the design of an adsorbent bed and they should be calculated and considered. Based on our numerical and experimental observations, some significant points, which should be taken into account during design of an adsorbent bed, are presented in this section.

## 11.1. Clarifying Mechanism of Mass Transfer in the Space between Particles

Adsorptive pressure in an adsorbent bed can be uniform or non-uniform. The governing equations of uniform and non-uniform pressure approaches are very different from each other. The uniform pressure approach can simplify the problem and provide accurate results easier. During this thesis, studies show that for big size adsorbent particle (such as radius of 1 mm), the pressure distribution between particles can be uniform and hence interparticle mass transfer resistance can be neglected. For the small particle sizes (such as radius of 0.01 mm) a pressure gradient in space between particles can be observed. Designer should be careful on particle size. The intraparticle mass transfer resistance increases by increasing radius of adsorbent particle and consequently adsorption period increases. However, considerable decrease of adsorbent particle size may increase interparticle mass transfer resistance and this causes the extension of adsorption period. The adsorption period becomes minimum for an optimum adsorbent particle size. Designer should do computational calculations to determine the optimum particle size to achieve minimum adsorption period.

## 11.2. Determination of Γ Number to Compare Effects of Intraparticle and Heat Transfer Resistances for an Adsorption Process

As it was mentioned before, the Γ parameter refers to the ratio of mass diffusion in radial direction of adsorbent particle to the diffusion of heat in radial direction of adsorbent bed. A high value of Γ (such as Γ = 10) for an adsorbent bed indicates that the diffusion of mass transfer in the radial direction of the adsorbent particle is faster than the transfer of heat in radial direction of the adsorbent bed. Hence, the mass transfer resistance in the particle does not have a significant effect on adsorption period and heat transfer resistance through the adsorbent bed controls the adsorption process. For the adsorbent beds with high values of Γ, designer should enhance the heat transfer in the bed in order to reduce adsorption period by the methods such as using fins. For adsorbent beds with high values of Γ, the use of methods for decreasing of intraparticle mass transfer resistance is not a solution for reduction of adsorption period. For low values of Γ (such as $\Gamma = 10^{-5}$), the propagation of heat through the adsorbent bed is faster than the adsorbate diffusion in the adsorbent particle. Hence, the mass transfer resistance in the adsorbent particle controls the adsorption process. For an adsorbent bed with low value of Γ, the adsorption period can be shortened by the enhancement of mass transfer in the adsorbent particle by the methods such as improvement of mass diffusivity. The decrease of adsorbent particle size can also reduce intraparticle mass transfer resistance and reduce adsorption period.

## 11.3. Special Attention to the Bed Thickness

The bed thickness is also an important parameter for design of an adsorbent bed. The decrease of bed thickness can considerably reduce adsorption period. The decrease of bed thickness causes:

- the decrease of heat transfer resistance in radial direction of the adsorbent bed. Hence, heat transfer rate in radial direction increases. This causes the rapid decrease of temperature in the bed and it accelerates adsorption process.
- the decrease of interparticle mass transfer resistance. For thin beds, adsorptive can reach to the regions that are far from entrance in a short period, accordingly interparticle mass transfer reduces.

Our numerical observation shows that for an adsorbent bed filled with silica gel particles, the decrease of bed thickness from 40 mm to 10 mm, can reduce adsorption period from 1000 min to 80 min.. There is no doubt that the reduction of bed thickness reduces the amount of adsorbent particle inside the adsorbent bed. Hence, an optimization study should be performed to determine thickness of an adsorbent bed.

## 11.4. Determine Ku Number to Find Out Increase of Temperature Due to Heat of Adsorption

As it was mentioned, the Ku number compares the heat of adsorption generated in the bed due to the adsorbate concentration difference $(W_a - W_d)$ and the sensible stored heat in the bed due to temperature difference $(T_a - T_d)$. Hence, high values for Ku number refers to the high amount of heat generation in the bed compared to the sensible heat stored in the bed due to temperature difference. For an identical operation condition of an adsorption process, the values of Ku number for silica gel-water, zeolite 13X-water and active carbon-water are calculated and shown in Table 11.1. The thermophysical properties of these pairs are given in Appendix A. The adsorption process is started at 323 K and ended at 293 K. During this process, the change of adsorbate concentration for each pair is also given in Table 11.1. As seen from Table 11.1, zeolite 13 X-water pair has the maximum Ku number. This shows that the heat generation and increase of temperature in the bed during adsorption process may be higher with working pair zeolite-water than silica gel-water and active carbon–methanol pairs. Silica gel-water pair has the second value of Ku in Table 11.1, while active carbon-methanol has the minimum Ku number. Under the same operation conditions, the increase of temperature in the adsorbent bed of active carbon-methanol may be less than for silica gel–water and zeolite-water pairs. Our numerical experience shows that for an adsorption process with low values of Ku, the adsorption period is shorter compared to a process with high Ku number. Small value of Ku means small increase of temperature and consequently process can be finished in a shorter period. If $\Gamma$, $R_o/R_i$ and dimensionless isotherms are identical for the three aforementioned pair, the adsorption period for active carbon with Ku = 4.70 may be considerably shorter than the adsorption period of silica gel-water or zeolite-water pairs. As a result, the Ku number is one of the

other parameters that designers should be considered in the adsorbent bed designs. The smaller Ku number is the shorter adsorption period.

Table 11.1. The values of Ku for an adsorbent bed filled with adsorbent particle when φ=0.35 (Source: Incropera and Dewitt 1996, Perry and Green 1984, Cheng and Kung 1994, Leong and Liu. 2004, Wang et al. 2006, Ogueke and Anyanwu 2008)

| | $T_d$ (K) | $T_a$ (K) | $\overline{W}$ (kg/kg) | $\Delta\overline{W}$ (kJ/kg) | $(\rho C_p)_{eff}$ (kJ/kgK) | Ku |
|---|---|---|---|---|---|---|
| silica gel-water | 323 | 293 | 0.334 | 0.311 | 992 | 10.78 |
| Active carbon-methanol | | | 0.143 | 0.166 | 395 | 4.70 |
| Zeolite 13X-water | | | 0.209 | 0.311 | 689 | 14.36 |

## 11.5. Pay Attention on the Use of Fins

Many researchers use fins as an extended surfaces inside of an adsorbent bed. In some cases, the effect of the fins located between the adsorbent particles inside of the bed for enhancing heat transfer rate can be meaningless. In addition to Ku and Γ parameters, two parameters Λ and $\alpha^*$ get importance (as mentioned in Chapter 9.2.2), if a designer want to use fins to accelerate the heat transfer in the bed. Λ refers to the ratio of heat transfer from the fin lateral surface to the diffusion of heat in radial direction of the fin ($\Lambda = \frac{\lambda_{eff}}{\lambda_{fin}} \frac{R_i}{\delta}$) and $\alpha^*$ parameter is the ratio of effective thermal diffusivities of adsorbent medium and fin material ($\alpha^* = \frac{\alpha_{eff}}{\alpha_{fin}}$). The obtained results revealed that heat transfer rate in an adsorbent bed can be enhanced by using fin when the values of thermal diffusivity ratio and fin coefficient are low (i.e., $\alpha^*$ = 0.01, Λ = 0.01). Furthermore, the use of fin in an adsorbent bed with low values of Γ number (i.e. $\Gamma = 10^{-5}$) does not increase heat transfer rate, significantly.

The decrease of fin coefficient value Λ causes the increase of heat diffusion in the radial direction of fin and consequently heat and mass transfer in the adsorbent bed is enhanced. The decrease of α* signifies an increase in heat transfer in the fin and consequently the duration of adsorption process is reduced.

## 11.6. The Effect of Interparticle Mass Transfer Resistance

If the adsorptive pressure inside of the bed is non-uniform, the interparticle mass transfer resistance should be taken into account. The mass transfer equations for the adsorptive and Darcy law should be included to the set of equations. By non-dimensionalization of the governing equations, five dimensionless parameters as Ku, Π, G, Γ, and K are found. If all of these parameters are the same for two different beds, the dimensionless temperature and concentration profiles during the adsorption process will be unique. In addition to the Ku and Γ parameters, the K number gets importance which represents the ratio of the interparticle mass transfer to the heat diffusion in the bed. The increase of the K value reduces interparticle mass transfer resistance and consequently the adsorption period decreases for different Γ value. High values of K can be obtained by design of an adsorbent bed with high values of apparent permeability. Our numerical observation shows that both the values of K and Γ should be large to have short period of adsorption. Unfortunately, the aforementioned dimensionless parameters are coupled and it is difficult to define a range of K and Γ parameters for minimum adsorption period. Hence, the best method is to do computational calculation for each case.

# CHAPTER 12

# CONCLUSION

This study basically focuses on the adsorbent bed which is the most important components of the adsorption heat pump, and its design. A study on heat and mass transfer in an adsorbent particle is performed to understand the effect of external heat and mass transfer resistances. Discussions on the uniform and non-uniform approaches are performed. Based on the performed discussion, some hints are advised to the designers for the design of an adsorbent bed.

The following remarks can be concluded for a single particle located inside of an infinite adsorptive media;

- Number of dimensional governing parameters for a non-isothermal adsorption in a single adsorbent particle with considerable effect of internal and external heat and mass transfer resistances is reduced to four dimensionless groups; Ku (Kutateladze number), Le (Lewis number), $Bi_h$ (heat transfer Biot number), and $Bi_m^{'}$ (modified mass transfer Biot number). The $Bi_m^{'}$ is probably the first time mentioned in the literature.
- The obtained results show that for an isothermal adsorption with considerable effects of internal but negligible effect of external mass transfer resistances, the dimensionless adsorbate concentration does not depend on any parameter even isotherm equilibria. For isothermal adsorption case with considerable effects of internal and external mass transfer resistances, the results depend on modified mass transfer Biot number and the shape of isotherm if $Bi_m^{'} < 20$.
- For the non-isothermal adsorption process with considerable effects of internal but negligible external heat and mass transfer resistances (Case III), the mass transfer resistance controls the adsorption process and adsorption can be assumed as an isothermal process when Le value is high (i.e. Le =50). For the non-isothermal case with considerable internal and external heat and mass transfer resistances (Case IV), the external heat and mass transfer resistances are found according to values of $Bi_h$, $Bi_m^{'}$ and Le numbers. For low values of Le

number (i.e., Le = 50), the external heat and mass transfer resistances can be omitted when $Bi_h > 50$ and $Bi'_m > 50$. By increasing Le number, the range of $Bi_h$ for which external heat and mass transfer can be neglected is expanded. For Le = $10^6$, the external heat and mass transfer resistances can be neglected when $Bi_h > 0.01$ and $Bi'_m > 50$.

- The obtained results show that for evaluation of external heat and mass transfer resistance effect, Le number should also be taken into account.

The governing equations for a uniform adsorption process are mass transfer in an adsorbent particle and heat transfer for adsorbent bed. These equations are non-dimensionalized for a granular type adsorbent bed operating under an isobaric adsorption process. The non-dimensionalization of the governing equations successfully reduces number of governing parameters to three parameters as $R_o/R_i$, Ku, and Γ. Each parameter has a meaning, described below. Most probably, this is the first time Γ number is introduced to the literature. The following remarks can be concluded from the performed study:

- For a specified adsorption process, different adsorbent adsorbate pairs may have different Ku numbers. A high value of Kutateladze number indicates that the generated heat in the adsorbent during adsorption process is greater than the sensible thermal energy stored in the bed. Thus, for the adsorbent-adsorbate pairs with high values of Ku number, the temperature increase in the bed during adsorption process may be higher than for the pairs with low value of Ku number.
- For an adsorbent bed with a specified Ku value (such as 1 and 100), the decrease of Γ value (i.e. $10^{-5}$) causes the increase of mass transfer resistance in the particle compared to resistance of heat transfer through the adsorbent bed. Therefore, the total dimensionless period for adsorption process is increased.
- For low values of Γ (i.e. $10^{-5}$), heat transfer in the adsorbent bed is faster than the mass transfer in the adsorbent particle. For those cases, the enhancement of heat transfer through the bed may not reduce adsorption period since mass transfer resistance in the particle controls the adsorption process. The change of Ku does not highly influence total dimensionless period of the process but for high values

of Γ (i.e. Γ=1) the total dimensionless period of adsorption process considerably decreases with decrease of Ku value.

- For high values of Γ (i.e. Γ=1), heat transfer resistance through the adsorbent bed controls the adsorption process. Hence, the enhancement of heat transfer through the bed can reduce the adsorption period.
- For high values of Γ, the solutions of the governing equations for three models of mass transfer within a particle (instantaneous equilibrium, LDF, and solid diffusion models) are very close to each other. However, for low values of Γ (i.e. $\Gamma=10^{-5}$) the results of instantaneous equilibrium model becomes too different than those of LDF and solid diffusion models signifying instantaneous equilibrium model can not be used for problems with low values of Γ.
- The total adsorption period can be reduced by decrease of $R_o/R_i$ ratio.

The effect of fin on heat and mass transfer in an adsorbent bed with silica gel–water pair during an adsorption process is numerically studied. The governing equations (mass transfer equation for adsorbent particle, heat transfer equation for the adsorbent bed and conduction heat transfer equation for fin), initial and boundary conditions are non-dimensionalized and they yield four dimensionless parameters as Ku number, thermal diffusivity ratio (α*), dimensionless fin coefficient (Λ) and a dimensionless parameter as Γ. The literature survey showed that this is the first time that the dimensionless Λ number is introduced. Following remarks can be concluded from the performed study;

- The decrease of fin coefficient value causes the increase of heat diffusion in the radial direction of fin and consequently heat and mass transfer in the adsorbent bed is enhanced.
- The decrease of α* signifies an increase in heat transfer in the fin and consequently the duration of adsorption process is reduced.
- For low value of Γ (i.e. $10^{-5}$), the use of fin in the adsorbent bed is meaningless since heat transfer in the adsorbent bed is highly rapid compared to the mass transfer.

The heat and mass flow in a granular type adsorbent bed for a non-isothermal adsorption process are analyzed by uniform and non-uniform pressure approaches. The study is performed for silica gel-water pair. The present study is performed to show the effect of interparticle mass transfer resistance on the adsorption period in an adsorbent

bed. Based on the results obtained by two approaches, the following remarks can be concluded:

- The uniform pressure approach can be used to simulate the heat and mass transfer in a granular adsorbent bed when the voids between particles are sufficiently large (i.e., interparticle mass transfer is negligible). For the bed with small particle size, the results of uniform pressure approach may not be valid.
- A sudden pressure drop is observed at the outer region of adsorbent bed with small particle size ($r_p$ = 0.0075 mm). This change in local pressure cannot be observed if the uniform pressure approach is used.
- The interparticle mass transfer resistance is enhanced by decrease of particle size. After a specified adsorbent particle size, it becomes dominant and affects adsorption period.
- There is an optimum adsorbent particle size for which the minimum adsorption period is achieved.
- The adsorption period is highly affected by bed thickness. The increase of bed thickness enhances thermal resistance along the bed and consequently adsorption period increases.

The non-dimensionalization of the governing equations (mass transfer equation for the adsorbent particle, heat and mass transfer equation for the adsorbent bed, Darcy equation) for a granular type adsorbent bed and for non-uniform adsorption process reduces number of parameters and yields five dimensionless parameters as Ku, Π (not mentioned in the literature before), G (not mentioned in the literature before), Γ, and K. The non-dimensionless K (not mentioned in the literature before) and Γ parameters involve geometrical parameters such as inner and outer radiuses of the bed and the radius of adsorbent particle. In this study, the other three parameters are taken constant (Ku, Π, G) and the effects of the changes of two parameters (K and Γ) are analyzed. Under the made assumptions and based on the obtained results, the following remarks can be concluded:

- If the all five dimensionless parameters are the same for different adsorbent beds, the change of dimensionless temperature and adsorbate concentration profiles for these beds will be the same.
- For different Γ values, the increase of the K value reduces interparticle mass transfer resistance and consequently the adsorption period decreases. The results

of uniform and non-uniform pressure approaches are close to each other after a specified K value. After the specified K value, further increase in K value does not decreases adsorption period.

- For high values of K (such as K = 1000 when Γ = 105), the uniform pressure approach can be used as a valid approach.
- The total process time decreases by the increase of K value since the effect of interparticle mass transfer resistance becomes negligible.

In order to understand the mechanism of heat and mass transfer in the adsorbent bed, an experimental setup is constructed and the adsorption experiments for different bed and evaporator temperatures are performed. In addition, the experimental results are compared with the numerical results in order to validate the performed numerical solutions. Based on the performed experiments, following remarks can be concluded:

- A considerable increase of temperature is observed during the adsorption process. At the beginning the adsorption period, the temperature of the inner region increases due to heat of adsorption and it starts to decrease gradually.
- The validation of the experimental results with the numerical results showed that the adsorptive pressure inside of the adsorbent bed can be assumed as uniform.
- The numerical results showed good agreement with the experimental results. The heat and mass transfer in the adsorbent bed can be simulated with the described numerical method.
- The sensitivity analysis showed that the density and specific heat of the silica gel have important effect on heat and mass transfer in the bed, particularly at the beginning of the process. The heat of adsorption and the effective conductivity are also important and a special attention should be paid for determination of their values. The diffusivity values for the pair have importance at the beginning of the adsorption.

Based on the obtained experimental and numerical results, further studies can be performed on the following issues:

- The adsorbent particle size has important effect on the heat and mass transfer mechanism in the bed. The optimum adsorbent particle size should be found for the shortest adsorption period. Further studies on the favorable particle size should be performed on the experimental setup.

- The thermophysical properties of the adsorbent-adsorbate pair have significant importance on the simulation of the experimental results. The density and the specific heat of the silica gel, heat of adsorption, effective conductivity, and diffusivity values should be calculated and special attention should be paid on these values for the accuracy of the numerical results.
- The experimental and numerical results should be performed for different adsorbent-adsorbate pairs. The utilization of the adsorption heat pumps can be investigated by using an innovative adsorbent-adsorbate pair.

# REFERENCES


Abdallah K., Grenier Ph., Sun L.M., Meunier F.. 1988. Nonisothermal adsorption of water by synthetic NaX zeolite pellets. *Chemical Engineering Science*. 43: 2633-2643.

Afonso M. and Silveira V.. 2005. Characterization of equilibrium conditions of adsorbed silica gel - water bed according to Dubinin - Astakhov and Freundlich. *Thermal Engineering*. *4*: 3-7.

Ahn H., Moon J., Hyun S., Lee C.. 2004. Diffusion mechanism of carbon dioxide in zeolite 4A and CaX pellets. *Adsorption*. 10: 111–128.

Al-Sharqawi H. S. and Lior N.. 2004. Conjugate computation of transient flow and heat and mass transfer between humid air and desiccant plates and channels. *Numerical Heat Transfer, Part A*. 46: 525–548.

Alam K.C.A., Saha B.B., Kang Y.T., Akisawa A., Kashiwagi T.. 2000. Heat exchanger design effect on the system performance of silica gel adsorption refrigeration systems. *International Journal of Heat and Mass Transfer*. 43 4419-4431.

Bejan A.. 1984. *Convection Heat Transfer*. New York: John Wiley and Sons.

Ben Amar N., Sun L.M., Meunier F.. 1996. Numerical analysis of adsorptive temperature wave regenerative heat pump. *Applied Thermal Engineering*. 405–418.

Bird B.R., Stewart E.W., Lightfoot N.E.. 2002. *Transport Phenomena*. Second ed., John Wiley and Sons Inc., New York, pp. 189–191.

Bonaccorsi L., Freni A., Proverbio E., Restuccia G., Russo F.. 2006. Zeolite coated copper foams for heat pumping applications. *Microporous Mesoporous Mater*. 7–14.

Cacciola G., Hajji A., Maggio G., Restruccia G.. 1993. Dynamic simulation of a recuperative adsorption heat pump. *Energy*. 18: 1125-1137.

Cheng W. H. and Kung H. H.. 1994. Methanol production and use. Marcel Dekker Inc..

Chahbani H.M., Labidi J., Paris J.. 2002. Effect of mass transfer kinetics on the performance of adsorptive heat pump systems. *Applied Thermal Engineering*. 22: 23-40.

Chahbani H.M., Labidi J., Paris J.. 2004. Modeling of adsorption heat pumps with heat regeneration. *Applied Thermal Engineering*. 24: 431-447.

Chua H.T., Ng K.C., Malek A., Kashiwagi T., Akisawa A., Saha B.B.. 1999. Modeling the performance of two-bed, silica gel-water adsorption chillers. *International Journal of Refrigeration*. 22: 194–204.

Chua H.T., Ng K.C., Malek A., Kashiwagi T., Akisawa A., Saha B.B.. 2001. Multi-bed regenerative adsorption chiller-improving the utilization of waste heat and reducing the chilled water outlet temperature fluctuation. *International Journal of Refrigeration*. 24: 124-136.

Chua H.T., Ng K.C., Chakraborty N., Oo M., Othman A.. 2002. Adsorption characteristics of silica gel-water systems. *Journal of Chemical & Engineering Data*. 47: 1177-1181.

Chua H.T., Ng K.C., Wang W., Yap C., Wang X.L.. 2004. Transient modeling of a two-bed silica gel–water adsorption chiller. *Int J. Heat Mass Trans*.. 659–669.

Cerkvenik B., Poredos A., and Ziegler F.. 2001. Influence of adsorption cycle limitations on the system performance. *International Journal of Refrigeration.* 24: 475-485.

Collins R. E.. 1961. *Flow of fluids through porous material*. U.S, Litton Eduvational Publishing.

Critoph R.E., Telto T.Z., Davies L.N.G.. 2000. A prototype of a fast cycle adsorption refrigerator utilizing a novel carbon–aluminum laminate. *In: Proceedings of the institution of mechanical engineers*. 439-448.

Cussler E.L.. 1997. *Diffusion, mass transfer in fluid systems.* Cambridge, Cambridge Univ. Pr..

Demir H..2008. An experimental and theoretical study on the improvement of adsorption heat pump performance. *Chemical Engineering.* Izmir, Izmir Institute of Technology. **Doctor of philosophy**.

Demir H., Mobedi M., Ülkü S.. 2008. A review on adsorption heat pump: problems and solutions. *Renewable Sustainable Energy Rev.*. 12: 2381–2403.

Demir H., Mobedi M., Ülkü S.. 2008. An experimental study on silica gel-water intermittent adsorption heat pump. *International Sorption Heat Pump Conference.* Korea.

Demir H., Mobedi M., Ülkü S.. 2009. Effects of porosity on heat and mass transfer in a granular adsorbent bed, International Communications in Heat and Mass Transfer. 36: 372–377.

Demir H., Mobedi M., Ülkü S.. 2011. Microcalorimetric investigation of water vapor adsorption on silica gel, Journal of Thermal Analysis and Calorimetry. 105: 375–382.

Dellero T., Sarmeo D., Touzain Ph.. 1999. A chemical heat pump using carbon fibers as additive. Part I: enhancement of thermal conduction. *Appl. Therm. Eng.*. 19: 991-1000.

Douss N. and Meunier F.. 1989. Experimental study of cascading adsorption cycles. *Chemical Engineering Science*. 44: 225-235.

Fedorov A. and Viskanta R.. 1999. Scale analysis and parametric study of transient heat/mass transfer in the presence of nonporous solid adsorption. *Chemical Engineering Communications*. 171: 231-257.

Freni A., Maggio G., Vasta S., Santori G., Polonara F., Restuccia G.. 2008. Optimization of a solar-powered adsorptive ice-maker by a mathematical method, *Solar Energy*. 82: 965–976.

Georgiou A.. 2004. Asymptotically exact driving force approximation for intraparticle mass transfer rate in diffusion and adsorption processes: nonlinear isotherm systems with macropore diffusion control. *Chemical Engineering Science*. 59: 3591 – 3600.

Golubovic M. N. and Worek W. M.. 2004. Influence of elevated pressure on sorption in desiccant wheels. *Numerical Heat Transfer, Part A*. 45: 869–886.

Gui, Y.B., Wang R.Z., Wang W., Wu J.Y., and Xu Y.X.. 2002. Performance modeling and testing on a heat-regenerative adsorptive reversible heat pump. *Applied Thermal Engineering*. 22: 309-320.

Gurgel J.M., Andrade Filho L.S., Grenier Ph., et al. 2001. Thermal diffusivity and adsorption kinetics of silicagel/water. *Adsorption*. 121-32.

Haul R. and Stremming H.. 1984. Nonisothermal sorption kinetics in porous adsorbents. *Journal of Colloid and Interface Science*. 97: 348-355.

Heinemann Z.E.. 2005. *Textbook Series Volume 1 Fluid Flow In Porous Media*. Montanuniversität Leoben Petroleum Engineering Department. Leoben.

Ilis G. G., Mobedi M., Ülkü S.. 2010. A parametric study on isobaric adsorption process in a closed adsorbent bed. *International Communications in Heat and Mass Transfer*. 37: 540–547.

Ilis G. G., Mobedi M., Ülkü S.. 2011. A dimensionless analysis of heat and mass transport in an adsorber with thin fins; uniform pressure approach. *International Communications in Heat and Mass Transfer*. 38: 790–797.

Incropera F.P. and Dewitt D.P.. 1996. *Fundamentals of Heat and Mass Transfer*. 3rd Ed. New York, Wiley.

Ingman D.B. and Pop I.. 2002. *Transport Phenomena in Porous Media II*, Elsevier, UK. Part I, D.A. Nield, Modeling Fluid Flow in Saturated Porous Media and at Interfaces.

Joint Committee For Guides in Metrology. 2008. *Evaluation of measurement data - Guide to the expression of uncertainty in measurement*, JCGM.

Karger J. and Ruthven M.D.. 1992. *Diffusion in zeolites and other microporous solids*. A Wiley-Interscience Pubs., New York.

Kivrak Z..1987. Adsorpsiyonlu ısı pompaları. *Mechanical Engineering*. Izmir, Dokuz Eylül University. **Master of Science**.

Kodama A., Jin W., Goto M., Hirose T. and Pons M.. 2000. Entropic analysis of adsorption open cycles for air conditioning. Part 2: interpretation of experimental data. *International Journal of Energy Research*. 24: 263–278.

Kupiec K. and Georgiou A.. 2005. Analysis of thermal effects in a spherical adsorbent pellet. *International Journal of Heat and Mass Transfer*. 48: 5047–5057.

Lang R., Roth M., Sticker M., et al. 1999. Development of a modular zeolite, water heat pump. *Heat Mass Transfer/Waerme und Stoffuebertragung*. 229-34.

Leong K.C. and Liu Y.. 2004a. Numerical study of a combined heat and mass recovery adsorption cooling cycle. *International Journal of Heat and Mass Transfer*. 47: 4761–4770.

Leong K.C. and Liu Y.. 2004b. Numerical modeling of combined heat and mass transfer in the adsorbent bed of a zeolite/water cooling system. *Applied Thermal Engineering*. 2359–2374.

Leong K.C. and Liu Y.. 2006. System performance of a combined heat and mass recovery adsorption cooling cycle: A parametric study. *International Journal of Heat and Mass Transfer.* 49 2703–271.

Leong K.C. and Liu Y.. 2008. Numerical modeling of a zeolite/water adsorption cooling system with non-constant condensing pressure, *International Communications in Heat and Mass Transfer.* 35 618–622.

Li Yong and Sumathy K.. 2004. Comparison between heat transfer and heat mass transfer models for transportation process in an adsorbent bed. *International Communications in Heat and Mass Transfer*. 47: 1587–1598.

Liu Y. and Leong K.C.. 2005. The effect of operating conditions on the performance of zeolite/water adsorption cooling systems. *Applied Thermal Engineering*. 22: 1403–1418.

Liu Y. and Leong K.C.. 2006. Numerical study of a novel cascading adsorption cycle. *International Journal of Refrigeration*. 29: 250–259.

Maggio G., Freni A., Restuccia G.. 2006. A dynamic model of heat and mass transfer in a double-bed adsorption machine with internal heat recovery. *International Journal of Refrigeration*. 29: 589–600.

Maggio G., Gordeeva L.G., Freni A., Aristov Y.I., Santori G., Polonara F., Restuccia G.. 2009. Simulation of a solid sorption ice-maker based on the novel composite sorbent "lithium chloride in silica gel pores". *Applied Thermal Engineering*. 29: 1714-1720.

Marletta L., Maggio G., Freni A., Ingrasciotta M., Restuccia G.. 2002. A non-uniform temperature non-uniform pressure dynamic model of heat and mass transfer in compact adsorbent beds. *International Journal of heat and Mass Transfer*. 45: 3321–3330.

Meunier F.. 1985. Second law analysis of a solid adsorption heat pump operating on reversible cascade cycles: Application to the zeolite-water pair. *Journal of Heat Recovery Systems.* 5: 133-141.

Meunier F.. 2002. Adsorptive cooling: A clean technology. *Clean Products and Processes.* 3: 8-20.

Meunier F., Kaushik S.C., Neveu P. and Poyelle F.A.. 1996. A comparative thermodynamic study of sorption systems: second law analysis. *International Journal of Refrigeration*. 19: 414-421.

Meunier F., Poyelle F. and LeVan M.D.. 1997. Second-law analysis of adsorptive refrigeration cycles: The role of thermal coupling entropy production. *Applied Thermal Engineering*. 17: 43-55.

Mobedi M..1987. Adsorpsiyonlu ısı pompaları üzerine teorik ve deneysel bir çalışma. *Mechanical Engineering.* Izmir, Dokuz Eylül University. **Master of Science**.

Montastruc L., Floquet P., Mayer V., NikovI., Domenech S.. 2010. Kinetic modeling of isothermal or non-isothermal adsorption in a pellet: Application to adsorption heat pumps. *Chinese Journal of Chemical Engineering*. 18: 544-553.

Ng K., Chua H., Chung C.Y., Kashiwagi T., Akisawa A., Saha B.B.. 2001. Experimental investigation of the silica gel-water adsorption isotherm characteristics. *Applied Thermal Engineering.* 21: 1631-1642.

Nield D.A. and Bejan A. 2006. *Convection in Porous Media*. New York: Springer.

Pons M., Meunier F., Cacciola G., Critoph R.E., Groll M., Puigjaner L., Spinner B. and Ziegler F.. 1999. Thermodynamic based comparison of sorption systems for cooling and heat pumping. *International Journal of Refrigeration*. 22: 5-17.

Pons M. and Kodama A.. 2000. Entropic analysis of adsorption open cycles for air conditioning. Part 1: first and second law analyses. *International Journal of Energy Research*. 24: 251-262.

Pons M. and Szarzynski S.. 2000. Accounting for the real properties of the heat transfer fluid in heat-regenerative adsorption cycles for refrigeration. *International Journal of Refrigeration*. 23: 284-291.

Restruccia G., Freni A., Maggio G. 2002. A zeolite-coated bed for air conditioning adsorption systems: parametric study of heat and mass transfer by dynamic simulation. *Appl Therm Eng*.. 619–30.

Restuccia G., Freni A., Vasta S., Aristov Y.. 2004. Selective water sorbent for solid sorption chiller: experimental results and modeling. *International Journal of Refrigeration*. 27: 284–293.

Restuccia G., Vasta S., Freni A., Russo F., Aristov IY. 2005. An advanced solid sorption chiller using SWS-1L: performance analysis and hydrothermal cycling stability of the sorbent bed. *In: Proceedings of the international sorption heat pump conference*, Denver, USA.

Rouquerol F., Rouquerol J. and Sing K.. 1999. *Adsorption by powders and porous solids*. London: Academic Press.

Ruivo C. R., Costa J. J., Figueiredo A. R.. 2006. Analysis of simplifying assumptions for the numerical modeling of the heat and mass transfer in a porous desiccant medium. *Numerical Heat Transfer, Part A*. 49: 851–872.

Ruthven M.D.. 1984. *Principles of adsorption and adsorption processes*. New York: A Wiley-Interscience Pubs.

Saha B.B., Koyama S., Kashiwagi T., Akisawa A., Ng K.C., Chua H.T.. 2003. Waste heat driven dual-mode, multi-stage, multi-bed regenerative adsorption system. *International Journal of Refrigeration*. 26: 749–757.

Saha B.B., Koyama S., El-Sharkawy II., Kuwahara K., Kariya K., Ng KC. 2006. Experiments for measuring adsorption characteristics of an activated carbon fiber/ethanol pair using a plate–fin heat exchanger. *HVAC&R Res*. 767–82.

Saha B.B., Chakraborty A., Koyama S., Aristov Y.I.. 2009. A new generation cooling device employing $CaCl_2$ in silica gel water system. *International Journal of Heat and Mass Transfer*. 52: 516-524.

Sakoda A. and Suzuki M.. 1984. Fundamental study on solar powered adsorption cooling system. *Journal of Chemical Engineering of Japan*. 17: 52–57.

Sakoda A. and Suzuki M.. 1986. Simultaneous transport of heat and adsorbate in closed type adsorption cooling system utilizing solar heat. *Journal of Solar Energy Engineering-Transactions of ASME*. 108: 239–245.

Sing K.S.W., Everett D.H., Haul R.A.W., Moscou L., Pierrotti R.A., Rouqueroll J. and Siemieniewska T. 1985. Reporting physisorption data for gas/solid systems. *Pure and appl. Chem*.. 57: 603-619.

Sphaier L. A. and Worek W. M.. 2008 Numerical solution of periodic heat and mass transfer with adsorption in regenerators: analysis and optimization. *Numerical Heat Transfer, Part A*. 53: 1133–1155.

Sun L.M. and Meunier F.. 1987a. A detailed model for nonisothermal sorption in porous adsorbents. *Chemical Engineering Science*. 42: 1585-1593.

Sun L.M. and Meunier F.. 1987b. Non-isothermal adsorption in a bidisperse adsorbent pellet. *Chemical Engineering Science*. 42: 2899-2907.

Sun L.M., Ben Amar N., Meunier F.. 1995. Numerical study on coupled heat and mass transfers in an adsorber with external fluid heating. *Heat Recovery Systems*. 15: 19–29.

Suzuki M., 1990. Adsorption engineering. Amsterdam, *Elsevier Science Publisher*, Vol:25.

Suzuki M.. 1993. Application of adsorption cooling system to automobiles, *Heat Recovery Systems and CHP*. 13: 335–340.

Szarzynski S., Feng Y., and Pons M.. 1997. Study of different internal vapour transports for adsorption cycles with heat regeneration. *International Journal of Refrigeration.* 20: 390-401.

Ogueke N.V. and Anyanwu E.E.. 2008. Design improvements for a collector/generator/adsorber of a solid adsorption solar refrigerator, *Renewable Energy*. 33: 2428–2440.

Vafai K.. 2005. *Handbook of Porous Media*. New York: Taylor and Francis, Second Edition.

Vasta S., Maggio G., Santori G., Freni A., Polonara F., Restuccia G.. 2008. An adsorptive solar ice-maker dynamic simulation for north Mediterranean climate. *Energy Conversion and Management*. 49: 3025–3035.

Yong L. and Sumathy K.. 2004. Comparison between heat transfer and heat mass transfer models for transportation process in an adsorbent bed. *International Journal of Heat and Mass Transfer*. 47: 1587–1598.

Ülkü S. 1986. Adsorption heat pumps, *Heat Recovery Syst*. 277-284.

Ülkü S. 1987. Solar adsorption heat pumps, Solar Energy Utilization: Fundamentals and Applications, eds. Yüncü, H., Paykoç, E. and Y. Yener. The Netherlands: Martinus Nijkoff Publishers.

Ülkü S. 1991. *Heat and mass transfer in adsorbent beds, Convective heat and mass transfer in porous media*. Edited by S. Kakaç, B. Kılkış., A.F. Kulacki, F. Arınç, NATO Series, Kluwer Academic Pubs. pp. 695-724.

Ülkü A.S. and M. Mobedi. 1989. Adsorption in energy storage. In Proceedings of the NATO Advanced Study Institute on Energy Storage Systems. Series E. *Applied Science.* 167: 487-507.

Wang X. and Chua H.T.. 2007a. Two bed silica gel water adsorption chillers: An effectual lumped parameter model. *International Journal of Refrigeration*. 30: 1417-1426.

Wang X. and Chua H.T.. 2007b. A comparative evaluation of two different heat-recovery schemes as applied to a two-bed adsorption chiller. *International Journal of Heat and Mass Transfer*. 50: 433–443.

Wang S. and Zhu D., 2002. A novel type of coupling cycle for adsorption heat pumps. *Applied Thermal Engineering*. 22: 1083-1086.

Wang S.G., Wang R.Z., Li X.R. 2004. Research and development of consolidated adsorbent for adsorption system. *Renewable Energy*. 1-17.

Wang K., Wu J.Y., Wang R.Z., Wang L.W. 2006. Effective thermal conductivity of expanded graphite–CaCl2 composite adsorbent for chemical adsorption chillers. *Energy Conversion and Management*. 47: 1902–1912.

Wang L.W., Wang R.Z., Lu Z.S., Chen C.J., Wang K., Wu J.Y.. 2006. The performance of two adsorption ice making test units using activated carbon and a carbon composite as adsorbents. *Carbon.* 44: 2671–2680.

Whitaker S.. 1972. Forced convection heat-transfer correlations for flow in pipes, past flat plates, single cylinders, single spheres, and for flow in packed-beds and tube bundles. *AIChE J.*, 18: 361.

Xia Z.Z., Chen C.J., Kiplagat J.K., Wang R.Z., and Hu J.Q. 2008. Adsorption Equilibrium of Water on Silica Gel. *J. Chem. Eng. Data.* 53: 2462–2465.

Zhang L.Z. and Wang L.. 1999a. Effects of coupled heat and mass transfers in adsorbent on the performance of a waste heat adsorption cooling unit. *Applied Thermal Engineering*. 19: 195-215.

Zhang L.Z. and Wang L.. 1999b. Momentum and heat transfer in the adsorbent of a waste heat adsorption cooling system. *Energy*. 24: 605–624.

Zhang L.Z.. 2000. A three-dimensional non-equilibrium model for an intermittent adsorption cooling system. *Solar Energy*. 69: 27–35.

"Documenting Sources from the World Wide Web." 20 April 2012. iiarjournals.org 2011:http://ar.iiarjournals.org/content/29/1/27/F2.expansion, panoramio.com 2011:http://www.panoramio.com/photo/5197927, nashvillenaturalstone.com 2011: http://www.nashvillenaturalstone.com/limestone-products.html

# APPENDIX A

# PHYSICAL PROPERTIES OF MATERIALS

Table A.1. Thermophysical properties of three adsorbent - adsorbate pairs at $T_{mean}$=53.5$^{o}$C (Source: Incropera and Dewitt 1996, Perry and Green 1984, Cheng and Kung 1994, Leong and Liu 2004, Wang et al. 2006, Ogueke and Anyanwu 2008)

| | silica gel-water | active carbon-methanol | zeolite13X-water |
|---|---|---|---|
| density of adsorbent (s) (kg/m$^3$) | 670 | 460 | 620 |
| density of adsorptive (v) (kg/m$^3$) | 0.09838 | 0.78715 | 0.09838 |
| density of adsorbate (*l*) (kg/m$^3$) | 986.19 | 758.73 | 986.19 |
| Cp of adsorbent (s) (kJ/kgK) | 0.88 | 0.93 | 0.836 |
| Cp of adsorptive (v) (kJ/kgK) | 1.907 | 0.65 | 1.907 |
| Cp of adsorbate (*l*) (kJ/kgK) | 4.183 | 2.73 | 4.183 |
| thermal conductivity of adsorbent (s) (W/mK) | 0.198 | 0.11 | 0.2 |
| thermal conductivity of adsorptive (v) (W/mK) | 0.02146 | 0.01818 | 0.02146 |
| thermal conductivity of adsorbate (*l*) (W/mK) | 0.647 | 0.1944 | 0.647 |
| Heat of adsorption (kJ/kg) | 2369 | 1122 | 2369 |

Table A.2. Thermophysical properties and some important constants of the studied silica gel – water pair at Tmean=53.5oC (Source: Bird et al. 2002, Cussler 1997, Incropera and Dewitt 1996, Karger and Ruthven 1992)

| | **silica gel-water** |
|---|---|
| Molecular weight of water, (kg / mol) M | 18 |
| Reference diffusivity, ($m^2$/s) $D_o$ | $2.54x10^{-4}$ |
| Diffusion activation energy, (J / $mol^{-1}$) (Bird et al. 2002) E | $4.2\times10^{4}$ |
| Collision diameter for Lennard–Jones potential, (A) (Cussler 1997) σ | 2.641 |
| Collision integral (Cussler 1997) Ω | 2.236 |
| Boltzmann's constant (J /K molecule) (Incropera and Dewitt 1996) k | $1.38\times10^{-23}$ |
| Tortuosity (Karger and Ruthven 1992) τ | 3 |
| Viscosity of water vapor, (kNs/$m^2$ at 300K ) (Incropera and Dewitt 1996) μ | $10.29\times10^{-9}$ |

# APPENDIX B

# DERIVATION OF THE HEAT AND MASS TRANSFER EQUATIONS

In this appendix, heat and mass transfer equations for a cylindrical adsorbent bed are derived. When a non-uniform approach is used, the governing equations for the heat and mass transfer for a granular type adsorbent bed are the continuity, Darcy flow and energy equation for the adsorptive, mass transfer equation for the adsorbent particle and ideal gas equation. The heat and mass transfer equation for uniform pressure approach can be obtained by simplification of the non-uniform approach equations. The fin equation derivation which is written for the fins located inside of the adsorbent bed between adsorbent particles is also given. Furthermore, the heat and mass transfer equations for a single adsorbent particle are also derived and presented in this appendix.

## B.1. Derivation of Governing Equations of the Heat and Mass Transfer Problems for a Single Particle

### B.1.1. Solid Diffusion Equation

For unsteady flow, the net rate at which mass enters the control volume must equal to zero. A spherical control is taken where the thickness is dr. The mass flow inlet from the inner direction surface (i.e., r) is $\dot{m}_{in}$, the mass flow outlet from the outer r+dr direction surface is $\dot{m}_{out}$. The schematic view of the spherical particle and the control volume is given in Figure B1.

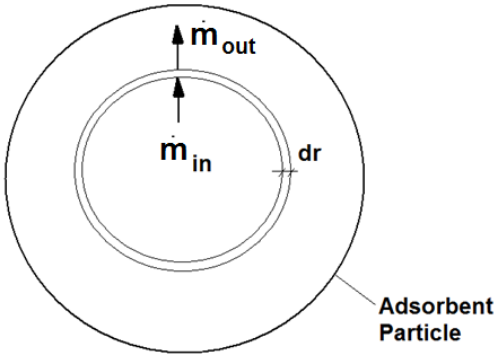


Figure B.1. The schematic view of the differential single particle for mass derivation

The conservation of mass for an unsteady process in a spherical particle can be derived as follows:
Mass balance of the control volume can be written as:

$$\dot{m}_{in} + \dot{m}_{generation} = \dot{m}_{out} + \dot{m}_{stored} \tag{B.1}$$

The mass flow inlet is:

$$\dot{m}_{in} = -D_{eff} r Sin\phi \, r dr d\phi \tag{B.2}$$

The mass flow outlet is:

$$\dot{m}_{out} = -D_{eff} r Sin\phi \, r dr d\phi + \frac{\partial}{\partial R}\left(-D_{eff} r Sin\phi \, r d\phi\right) dr \tag{B.3}$$

The mass generation in the control volume can be written as:

$$\dot{m}_{generation} = \frac{\partial \bar{W}}{\partial t} r Sin\phi \, r dr d\phi \tag{B.4}$$

If these equations from (B.2) to (B.4) are substituted into the mass balance equation (B.1) and solid diffusion model can be found as:

$$\frac{\partial \bar{W}}{\partial t} = \frac{1}{r^2}\frac{\partial}{\partial r}\left(D_{eff} r^2 \frac{\partial \bar{W}}{\partial r}\right) \tag{B.5}$$

## B.2.2. Energy Equation

A spherical control is taken where the thickness is dr. The energy inlet from the inner direction surface (i.e., r) is $\dot{q}_{in}$, the energyw outlet from the outer r+dr direction surface is $\dot{q}_{out}$. The schematic view of the spherical particle and the control volume is given in Figure B2.

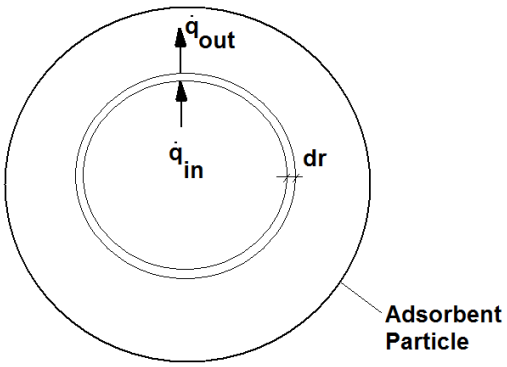


Figure B.2. The schematic view of the differential single particle, conservation of energy

For the considered particle, the conservation of energy for an unsteady process in spherical coordinates can be derived as follows:
Energy balance of the control volume can be written as:

$$\dot{q}_{in} + \dot{q}_{generation} = \dot{q}_{out} + \dot{q}_{stored} \tag{B.6}$$

The energy inlet from the inner surface is:

$$\dot{q}_{in} = -\lambda r Sin\phi \, r d\phi \, dr \frac{\partial T}{\partial r} \tag{B.7}$$

The energy outlet from the outer surface is:

$$\dot{q}_{out} = \dot{q}_{in} + \frac{\partial \dot{q}_{in}}{\partial R} dr = -\lambda r Sin\phi \, r d\phi \, dr \frac{\partial T}{\partial r} + \frac{\partial}{\partial r}\left(-\lambda r Sin\phi \, r d\phi \, \frac{\partial T}{\partial r}\right) dr \tag{B.8}$$

The energy generation can be written as:

$$\dot{q}_{generation} = \rho_s|\Delta H|\frac{\partial \bar{W}}{\partial t} rSin\phi\, r d\phi\, dr \quad \text{(B.9)}$$

The stored energy in the control volume can be written as:

$$\dot{q}_{stored} = (\rho_s C_s + \rho_s C_l \bar{W})\frac{\partial T}{\partial t} rSin\phi\, r d\phi\, dr \quad \text{(B.10)}$$

If these equations from (B.7) to (B.10) are substituted into the energy balance equations, energy balance equation (B.6) becomes as:

$$\rho_{eff} C_{eff}\frac{\partial T}{\partial t} = \frac{1}{\mathrm{r}^2}\frac{\partial}{\partial \mathrm{r}}\left(\lambda_{eff}\mathrm{r}^2\frac{\partial T}{\partial r}\right) + \rho_s|\Delta H|\frac{\partial \bar{W}}{\partial t} \quad \text{(B.11)}$$

where

$$\rho_{eff} C_{eff} = \rho_s C_s + \rho_s C_l \bar{W} \quad \text{(B.12)}$$

$$\lambda_{eff} = \lambda_s + \bar{W}\lambda_l \quad \text{(B.13)}$$

## B.2. Derivation of Heat and Mass Transfer Equations for the Annular Adsorbent Bed

### B.2.1. Continuity Equation

For unsteady flow, the net rate at which mass enters the control volume must equal to zero. A control volume filled with the adsorbent granules is taken where the inner radius is R and the outer radius is R+dR. The radial bed thickness is dR. The angle of surface control volume at the right side is $\phi$, while the surface angle of the left side is $\phi$ + d$\phi$, as seen from Figure B.3. The depth of the control volume is unit. The mass flow inlet from the inner radial direction surface (i.e., R) is $\dot{m}_{R,in}$ and the inner $\phi$ direction surface is $\dot{m}_{\phi,in}$, the mass flow outlet from the outer R+dR direction surface is $\dot{m}_{R,out}$ and the outer $\phi$ direction surface is $\dot{m}_{\phi,out}$.

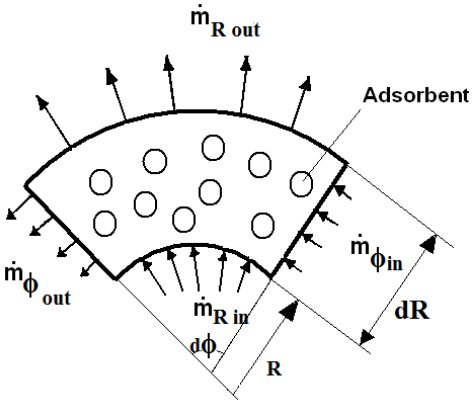


Figure B.3. The schematic view of control volume for derivation of mass conservation

As it was mentioned before, the size of adsorbent granules is assumed to be identical. Mass balance for the control volume can be written as:

$$\dot{m}_{R,in} + \dot{m}_{\phi,in} + \dot{m}_{generation} = \dot{m}_{R,out} + \dot{m}_{\phi,out} + \dot{m}_{stored} \tag{B.14}$$

The mass flow inlet from the inner R direction surface is:

$$\dot{m}_{R,in} = \rho_v v_R R d\phi \tag{B.15}$$

where $v_R$ is Darcy velocity in R direction. The mass flow outlet from the outer R direction surface (R+dR) is:

$$\dot{m}_{R,out} = \rho_v v_R R d\phi\, dR + \frac{\partial}{\partial R}(\rho_v v_R R d\phi)dR \tag{B.16}$$

The mass flow inlet from the inner $\phi$ direction surface is:

$$\dot{m}_{\phi,in} = \rho_v v_\phi dR \tag{B.17}$$

The mass flow outlet from the outer $\phi$ direction surface (teta+dteta) is:

$$\dot{m}_{\phi,out} = \rho_v v_\phi dR + \frac{\partial}{\partial \phi}\left(\rho_v v_\phi dR\right) d\phi \tag{B.18}$$

The mass generation in the control volume can be written as:

$$\dot{m}_{generation} = (1-\varphi)\rho_s \frac{\partial \bar{W}}{\partial t} RdRd\phi \tag{B.19}$$

The stored mass can be written as:

$$\dot{m}_{stored} = \varphi \frac{\partial \rho_v}{\partial t} RdRd\phi \tag{B.20}$$

If the equations from (B.15) to (B.20) are substituted into the mass balance equation (B.14), the following equation will be found:

$$R(1-\varphi)\rho_s \frac{\partial \bar{W}}{\partial t} = \frac{\partial}{\partial \phi}\left(\rho_v v_\phi\right) + \frac{\partial}{\partial R}(\rho_v v_R R) + \varphi \frac{\partial \rho_v}{\partial t} R \tag{B.21}$$

If all of the sides of the equation (6.8) are divided to φR then the continuity equation;

$$\frac{1-\varphi}{\varphi}\rho_s \frac{\partial \bar{W}}{\partial t} = \frac{\partial \rho_v}{\partial t} + \frac{1}{\varphi}\frac{1}{R}\frac{\partial}{\partial \phi}\left(\rho_v v_\phi\right) + \frac{1}{\varphi}\frac{1}{R}\frac{\partial}{\partial R}(\rho_v v_R R) \tag{B.22}$$

the above equation is the continuity equation for the annular adsorbent bed when mass transfer in radial and Θ direction is found where $\bar{W}$ is the mean adsorbed phase concentration within the particle.

## B.2.2. Darcy Flow

As mentioned in Chapter 2.3, in three dimensions the Darcy law is written as:

$$\mathrm{v} = -\mu \mathrm{K}_{\mathrm{app}} \nabla \mathrm{P} \tag{B.23}$$

where the $K_{app}$ is the apparent permeability and P is the pressure. The Equation (B.23) can be written for the annular bed in r and $\phi$ directions as (Bejan 1984):

$$\frac{\partial P}{\partial R} = -\frac{\mu}{K_{app}} v_r \tag{B.24}$$

$$\frac{\partial P}{\partial \phi} = -\frac{\mu}{K_{app}} v_\phi \tag{B.25}$$

## B.2.3. Energy Equation

A control volume filled with the adsorbent granules is taken where the inner radius is R and the outer radius is R+dR. The radial bed thickness is dR. The angle of surface control volume at the right side is $\phi$, while the surface angle of the left side is $\phi$ + d$\phi$, as seen from Figure B4.The depth of the control volume is unit. The energy inlet from the inner radial direction surface (i.e., R) is $\dot{q}_{R,in}$ and the inner $\phi$ direction surface is $\dot{q}_{\phi,in}$, the energy outlet from the outer R+dR direction surface is $\dot{q}_{R,out}$ and the outer $\phi$ direction surface is $\dot{q}_{\phi,out}$.

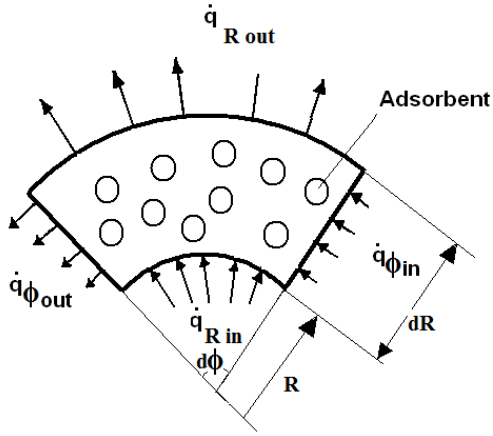


Figure B.4. The schematic view of control volume for derivation of energy equation

The conservation of energy for an unsteady process in cylindrical bed in two directions can be derived as follows:

Energy balance of the control volume can be written as:

$$\dot{q}_{R,in} + \dot{q}_{\phi,in} + \dot{q}_{generation} = \dot{q}_{R,out} + \dot{q}_{\phi,out} + \dot{q}_{stored} \tag{B.26}$$

The energy inlet from the inner R direction surface is:

$$\dot{q}_{R,in} = \dot{q}_{R,in\,conduction} + \dot{q}_{R,in\,convection} = -\lambda R d\phi\, dR \frac{\partial T}{\partial R} + \rho_v C_v (R d\phi\, dR) v_R T \quad \text{(B.27)}$$

The energy outlet from the outer R direction surface is:

$$\dot{q}_{R,out} = \dot{q}_{R,in} + \frac{\partial \dot{q}_{R,in}}{\partial R} dR = -\lambda R d\phi\, dR \frac{\partial T}{\partial R} + \rho_v C_v \left(R d\phi\, dR\right) v_R T + \frac{\partial}{\partial R}\left(-\lambda R d\phi\, dR \frac{\partial T}{\partial R} + \rho_v C_v \left(R d\phi\, dR\right) v_R T\right) dR \quad \text{(B.28)}$$

The energy inlet from the inner $\phi$ direction surface is:

$$\dot{q}_{\phi,in} = -\lambda dR \frac{\partial T}{\partial R} + \rho_v C_v v_\phi T dR \quad \text{(B.29)}$$

The energy outlet from the outer $\phi$ direction surface is:

$$\dot{q}_{\Phi,out} = -\lambda dR \frac{\partial T}{\partial R} + \rho_v C_v v_\phi T dR + \frac{1}{R^2}\frac{\partial}{\partial \phi}\left(-\lambda dR \frac{\partial T}{\partial R} + \rho_v C_v v_\phi R T dR\right) d\phi \quad \text{(B.30)}$$

The energy generation can be written as:

$$\dot{q}_{generation} = (1-\varphi)\rho_s |\Delta H| \frac{\partial \bar{W}}{\partial t} R dR d\phi \quad \text{(B.31)}$$

The stored energy in the control volume can be written as:

$$\dot{q}_{stored} = \left((1-\varphi)\rho_s C_s + \varphi \rho_v C_v + (1-\varphi)\rho_s C_l \bar{W}\right) \frac{\partial T}{\partial t} R dR d\phi \quad \text{(B.32)}$$

If these equations from (B.27) to (B.32) are substituted into the energy balance equations, energy balance equation (B.26) becomes as:

$$\rho_{eff} C_{eff} \frac{\partial T}{\partial t} + \frac{1}{\mathrm{R}}\frac{\partial}{\partial \mathrm{R}}\left(\rho_f C_f R v_R T\right) + \frac{v_\phi}{R}\frac{\partial}{\partial \phi}\left(\rho_v C_v v_\phi T\right) = \frac{1}{\mathrm{R}}\frac{\partial}{\partial \mathrm{R}}\left(\lambda_{eff} \mathrm{R} \frac{\partial T}{\partial R}\right) + \frac{1}{R^2}\frac{\partial}{\partial \phi}\left(\lambda_{eff} \frac{\partial T}{\partial \phi}\right) + (1-\varphi)\rho_s |\Delta H| \frac{\partial \bar{W}}{\partial t} \quad \text{(B.33)}$$

where

$$\rho_{eff}C_{eff} = (1-\varphi)\rho_s C_s + \varphi\rho_v C_v + (1-\varphi)\rho_s C_l \bar{W} \quad \text{(B.34)}$$

$$\lambda_{eff} = (1-\varphi)\lambda_s + \varphi\lambda_v \quad \text{(B.35)}$$

For one dimensional heat transfer in radial direction, Eq. (B.33) is reduced to the following for:

$$\rho_{eff}C_{eff}\frac{\partial T}{\partial t} + \frac{1}{\mathrm{R}}\frac{\partial}{\partial \mathrm{R}}\left(\rho_f C_f R v_R T\right) = \frac{1}{\mathrm{R}}\frac{\partial}{\partial \mathrm{R}}\left(\lambda_{eff}\mathrm{R}\frac{\partial T}{\partial R}\right) + (1-\varphi)\rho_s|\Delta H|\frac{\partial \bar{W}}{\partial t} \quad \text{(B36)}$$

For uniform pressure approach, the interparticle mass transfer resistance can be assumed as negligible due to the adsorptive pressure in the entire adsorbent bed is uniform. The convective transport term can be neglected in the heat transfer equation. The adsorptive velocity in the bed is dropped. Then the Eq. (B.33) reduces:

$$\rho_{eff}C_{eff}\frac{\partial T}{\partial t} = \frac{1}{\mathrm{R}}\frac{\partial}{\partial \mathrm{R}}\left(\lambda_{eff}\mathrm{R}\frac{\partial T}{\partial R}\right) + (1-\varphi)\rho_s|\Delta H|\frac{\partial \bar{W}}{\partial t} \quad \text{(B.37)}$$

## B.2.4. Energy Equation for the Fin Inside of the Bed

The same control volume is taken as represented in the previous figures. A fin is located between the adsorbent granules inside of the control volume with thickness of $\delta$. The energy inlet for the fin from the inner R direction surface is $\dot{q}_{fin,in}$, the energy outlet for the fin from the outer R direction surface and to the inner part of the bed is $\dot{q}_{fin,out}$. The schematic view of the control volume assisted with fin is given in Figure B5.

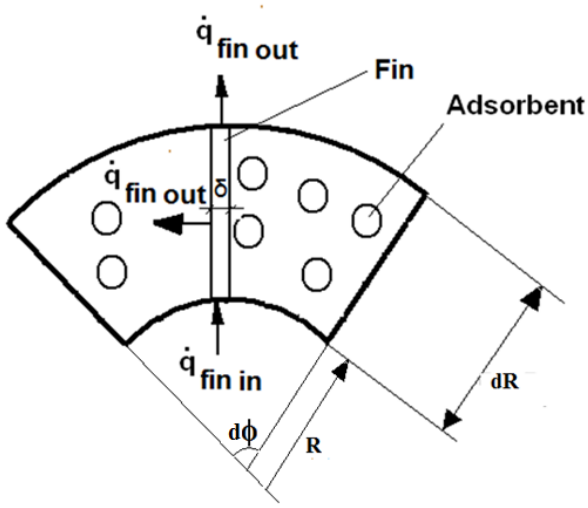


Figure B.5. The schematic view of the control volume for derivation of fin equation

The conservation of energy for an unsteady process in cylindrical bed assisted with fins can be derived as follows:

Energy balance of the control volume can be written as:

$$\dot{q}_{fin,in} = \dot{q}_{fin,out} + \dot{q}_{stored} \tag{B.38}$$

The energy inlet from the inner R direction surface is:

$$\dot{q}_{fin,in} = \dot{q}_{fin,in\,conduction} = -\lambda_{fin}\delta dR\frac{\partial T}{\partial R} \tag{B.39}$$

The energy outlet from the outer R direction surface is:

$$\dot{q}_{fin\,out} = \dot{q}_{fin\,in} + \frac{\partial \dot{q}_{fin\,in}}{\partial R}dR = -\lambda_{fin}\delta dR\frac{\partial T}{\partial R} + \frac{\partial}{\partial R}\left(-\lambda_{fin}\frac{\partial T}{\partial R}\right)\delta dR \tag{B.40}$$

The energy outlet from the outer $\phi$ direction surface of the fin is:

$$\dot{q}_{fin\ out} = -\lambda_{eff}\frac{1}{R}dR\frac{\partial T}{\partial \phi} \tag{B.41}$$

The stored energy can be written as:

$$\dot{q}_{generation} = \left(\rho C_p\right)_{fin} \delta \frac{\partial T}{\partial t} dR \tag{B.42}$$

If these equations from (B.39) to (B.42) are substituted into the energy balance equations, energy balance equation (B.38) becomes as:

$$\left(\rho C_p\right)_{fin} \delta \frac{\partial T}{\partial t} = \lambda_{eff} \frac{1}{\mathrm{R}} \frac{\partial \mathrm{T}}{\partial \phi} + \lambda_{fin} \delta \frac{\partial^2 T}{\partial R^2} \tag{B.43}$$

# APPENDIX C

# THE ALGORITM OF NUMERICAL SOLUTIONS

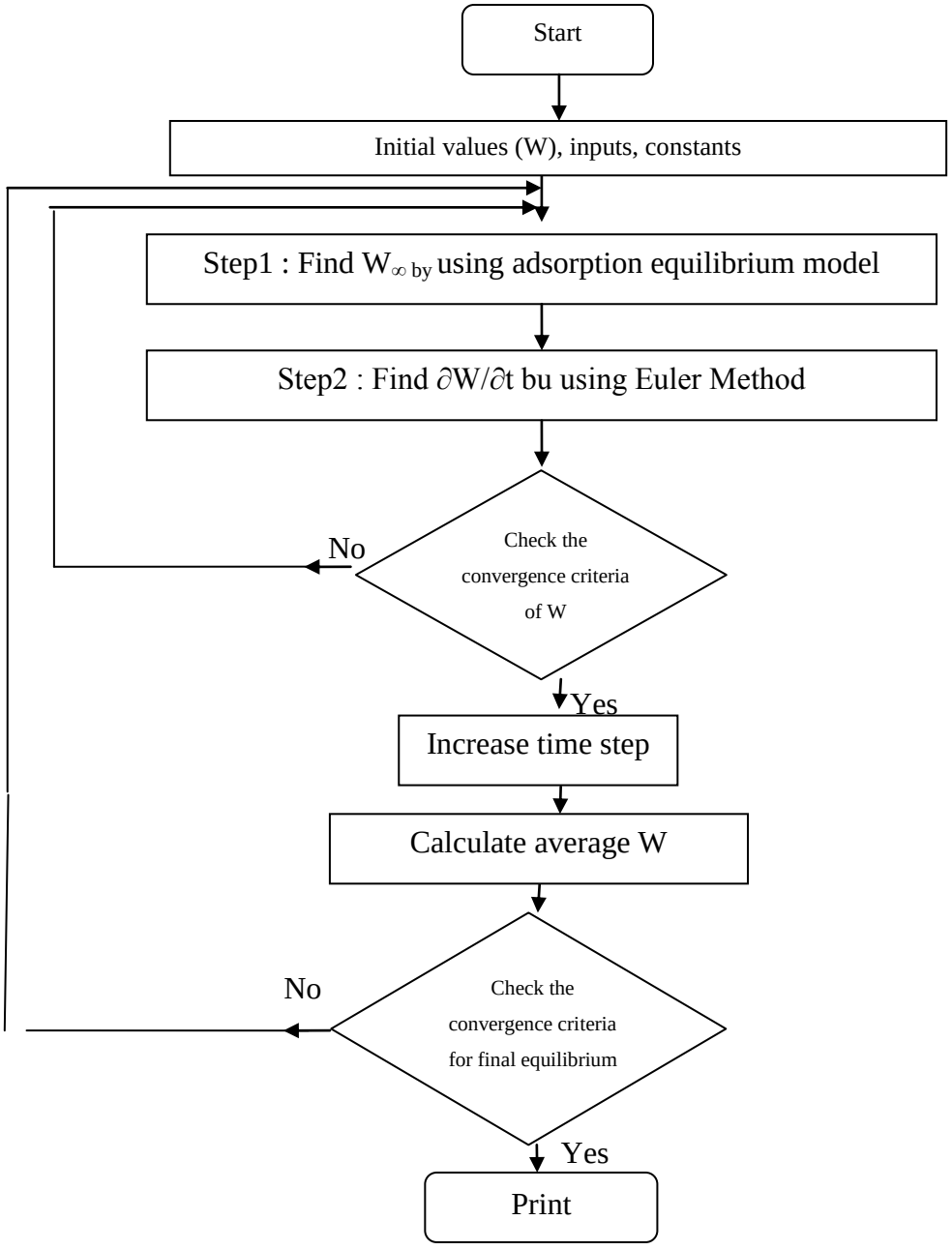


Figure C.1. The algorithm of the numerical solution of governing equations for adsorbent particle - Case I and II

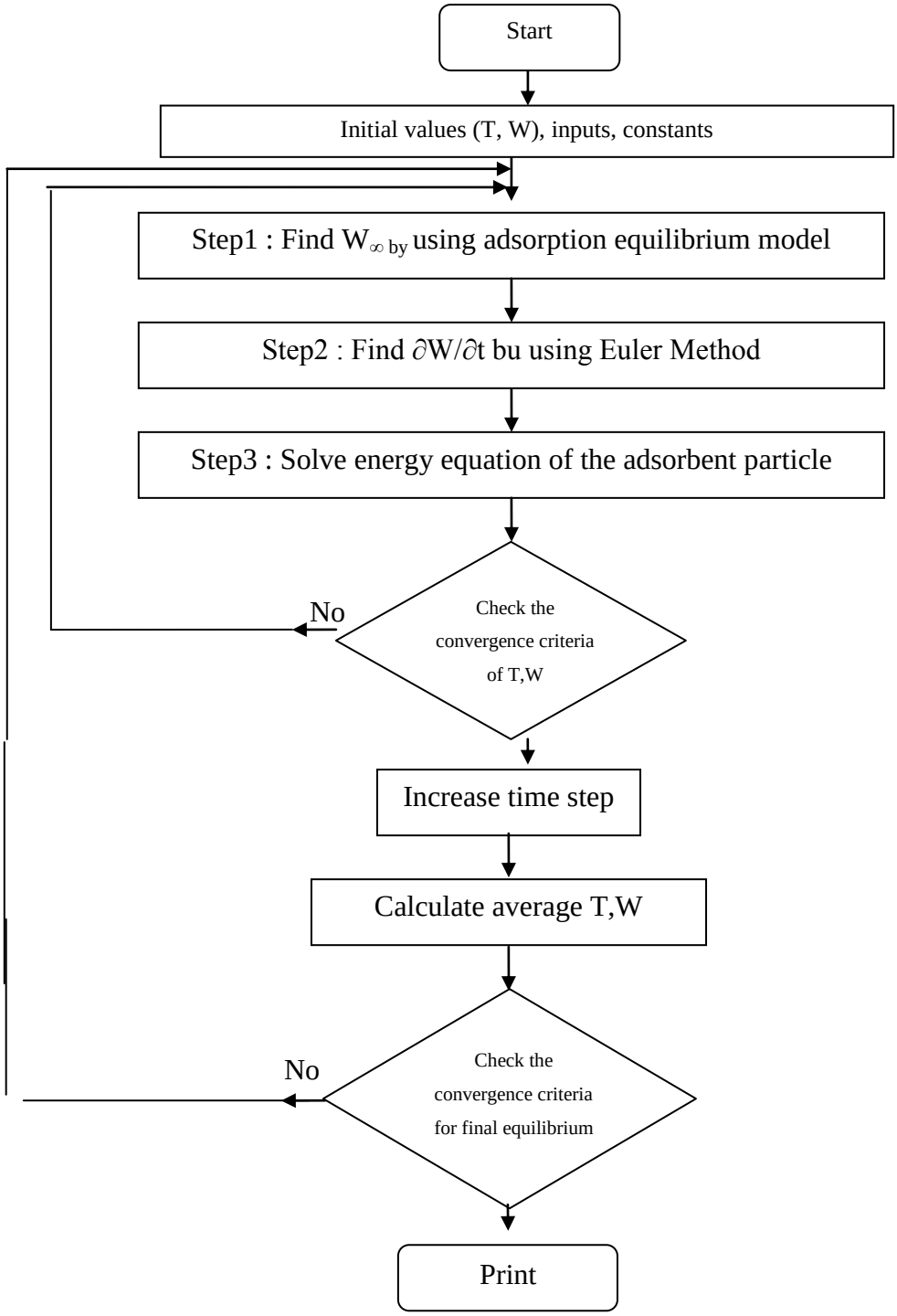


Figure C.2. The algorithm of the numerical solution of governing equations for adsorbent particle - Case III and Case IV

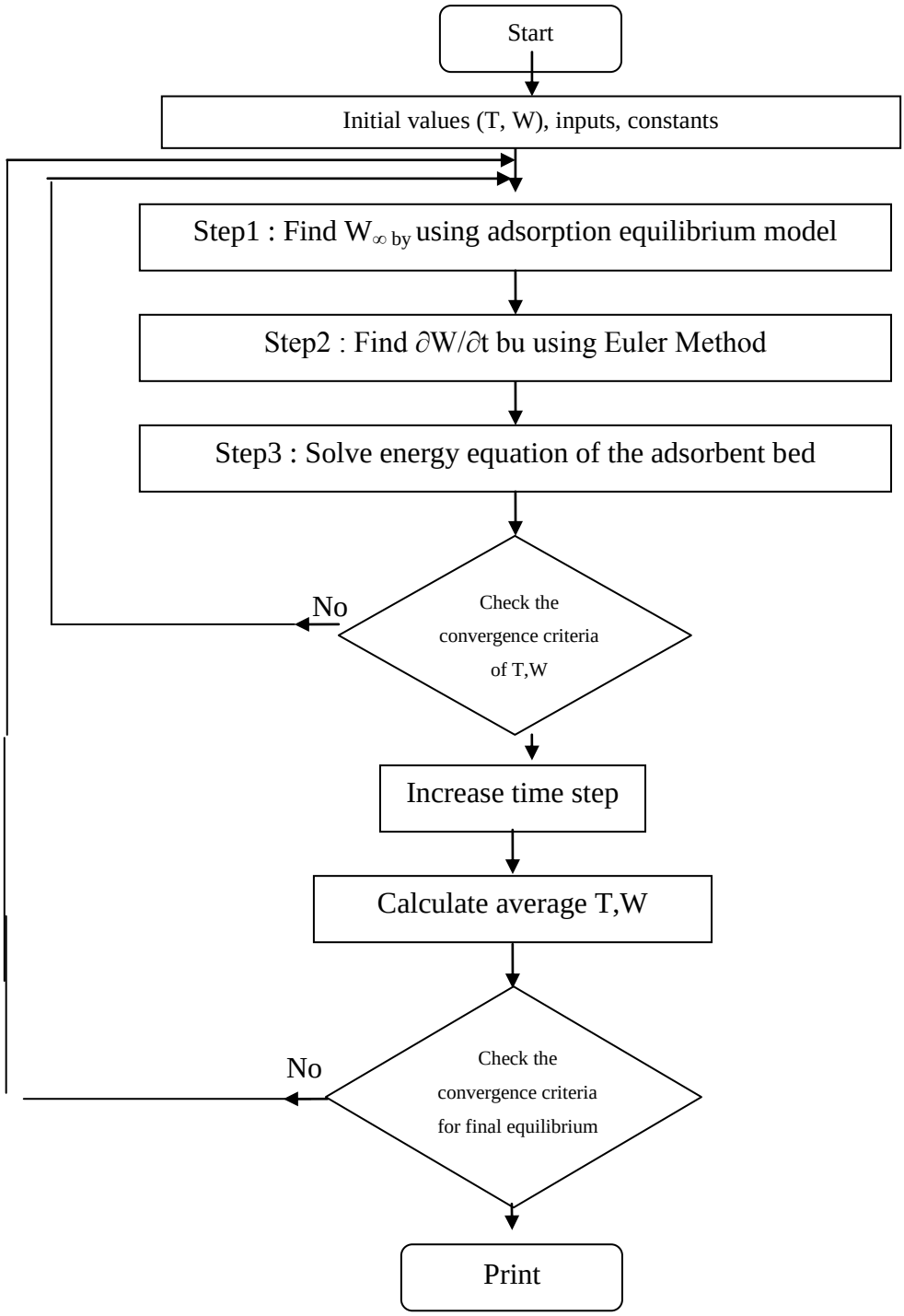


Figure C.3. The algorithm of the numerical solution of governing equations for adsorbent bed for uniform pressure approach

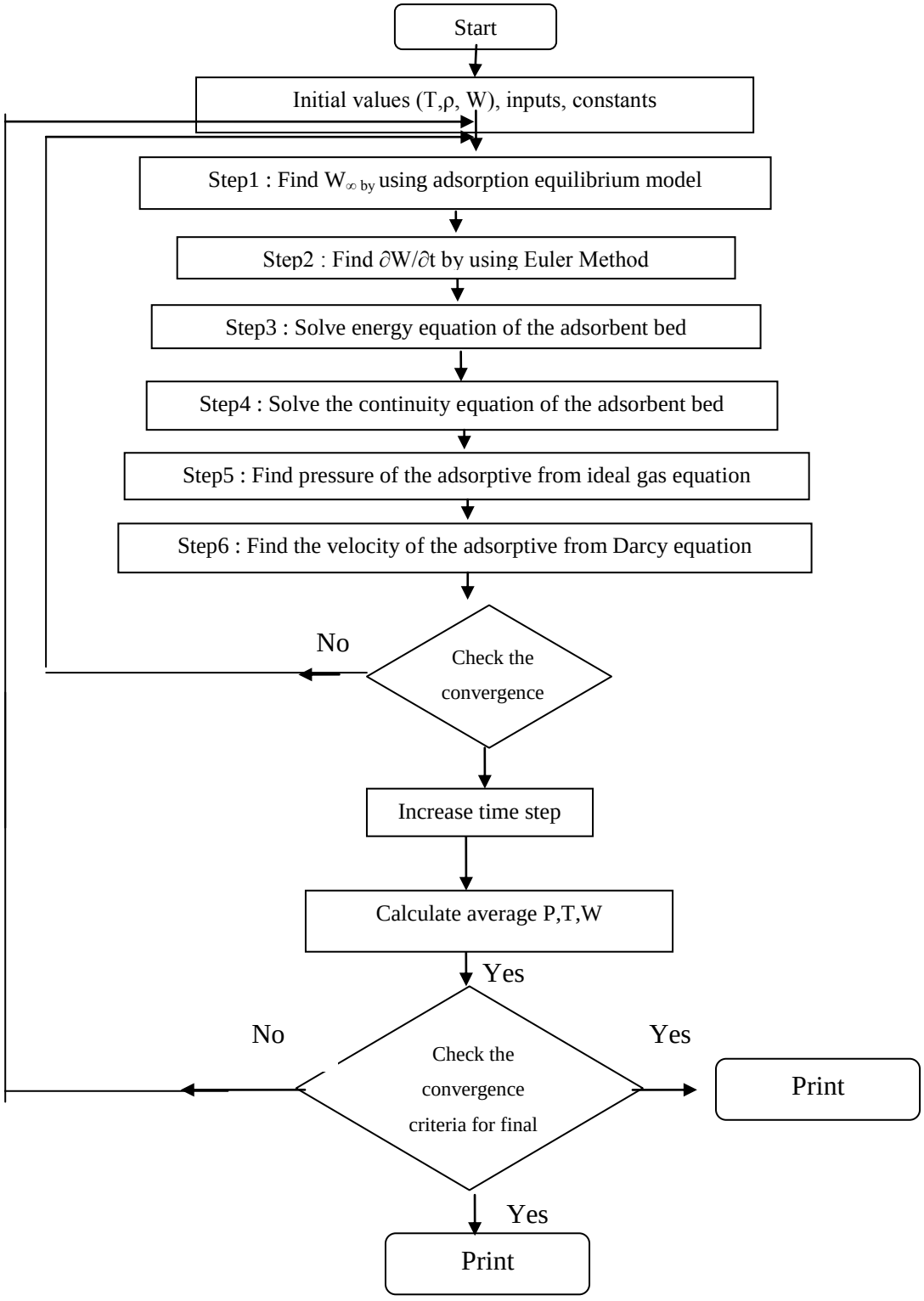


Figure C.4. The algorithm of the numerical solution of governing equations for adsorbent bed for non-uniform pressure approach

# APPENDIX D

# RESISTANCE EQUATIONS OF EXTERNAL HEAT TRANSFER

The heat transfer Biot number ($Bi_h$) is a dimensionless parameter and plays a fundamental role in conduction problems. The $Bi_h$ number is the ratio of the heat transfer resistances inside and at the surface of a body. Biot number measures the temperature drop in the solid relative to temperature difference between the surface and the fluid. For small Biot numbers (much smaller than 1) a uniform temperature distribution is expected across the solid. Biot numbers much larger than 1 refers non-uniformity of temperature fields within the object. Mathematically, Biot number can be defined as:

$$Bi_h = \frac{R_{conduction}}{R_{convection}} = \frac{L_c / k}{1/h} = \frac{h_h L_c}{k} \tag{D.1}$$

where k is the thermal conductivity of the solid, $h_h$ is the film or heat transfer coefficient at the surface of the body and $L_c$ represents the characteristic length. It is commonly defined as the volume of the body divided by the heat transfer surface area of the body.

As it was mentioned above, the distribution of temperature in a solid body contacts with a fluid depends on $Bi_h$ number. Two thermal resistances exists at the interface between solid and fluid. Biot number specifies which thermal resistance is dominant at the surface. For $Bi_h << 1$, the resistance of conduction within the solid is much less than the resistance of convection between solid and fluid. In this case, almost a uniform temperature distribution can be expected in the solid body and consequently temperature gradient in the solid is small. For $Bi_h >> 1$, conduction resistance inside the body is much greater than convection resistance. Hence, convection between solid and fluid controls heat transfer between solid and fluid. A high gradient temperature may be expected inside the fluid and temperature difference across the solid is much greater than that between the surface and the fluid.

## D.1. Lewis Number across a Silica gel Particle

The Lewis number is a dimensionless number defined as the ratio of thermal diffusivity to mass diffusivity.

$$Le = \frac{\alpha_{eff}}{D_{eff}} \tag{D.2}$$

The effective thermal capacity can be calculated by using the following relations:

$$(\rho C_p)_{eff} = (\rho C_p)_s + \rho_s C_{pl} \overline{W} \tag{D.3}$$

The thermo physical properties of silica gel particle and water is given in Table A1.

## D.2. Kutateladze Number

The dimensionless parameter Ku represents the ratio of heat of adsorption to the sensible heat storage (Federov and Viskanta 1991):

$$Ku = \frac{\rho_s \Delta H_{ads} \Delta W}{(\rho C_p)_{eff} \Delta T} \tag{D.4}$$

## D.3. Nusselt Number

The heat transfer coefficient between particle and fluid with forced convection can be calculated by following relations for a sphere in fluids for 0.71<Pr<380 and $3.5<Re_D<7.6x10^4$ (Whitaker 1972).

$$\overline{Nu_D} = 2 + \left(0.4\,\mathrm{Re}_D^{1/2} + 0.06\,\mathrm{Re}_D^{2/3}\right)\mathrm{Pr}^{0.4}\left(\frac{\mu}{\mu_s}\right)^{1/4} \tag{D.5}$$

The problem of the present study can be is illustrated in Figure D1.

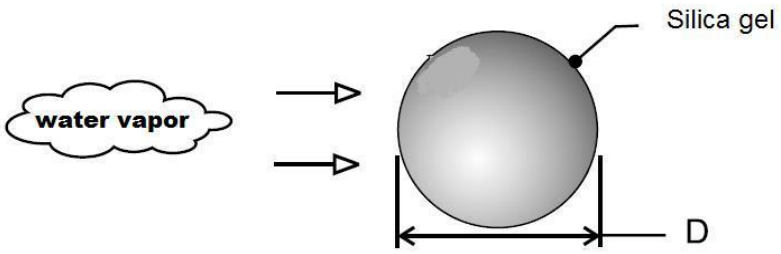


Figure D.1. Water vapor across a silica gel particle

There is a silica gel particle with diameter of D inside and infinite water vapor medium. Considering a classical adsorption heat pump cycle, for the realistic case of silica gel-water pair adsorption period in an adsorbent bed, the initial adsorption temperature is taken as 80$^{o}$C and the adsorption is assumed to be ended at 35$^{o}$C. The diameter is assumed as D=0.0025 m. The effect or radiation heat transfer between silica gel and surroundings is neglected.

For the related problem, the effective mass diffusivity, and Lewis numbers are calculated for different temperature values as 303, 323, 343, and 363 K, the effective thermal diffusivity, Nu number, the heat transfer coefficient between particle and water vapor, Kutateladze number and heat transfer Biot number are calculated and given in Table 9.3.

# APPENDIX E

# RESISTANCE EQUATIONS OF EXTERNAL MASS TRANSFER

## E.1. Mass Transfer Biot Number

The amount of transferred is proportional to concentration difference and mass transfer area where this proportionality is summarized as the mass transfer coefficient:

$$n_A = h_m(A\Delta C) \tag{E.1}$$

where $h_m$ is the mass transfer coefficient [mol/(s·m$^2$)/(mol/m$^3$), or m/s], $n_A$ is the mass transfer rate [mol/s], $A$ is the effective mass transfer area [m$^2$], and $\Delta C$ is the driving force concentration difference [mol/m$^3$].

The mass transfer Biot number (Bi$_m$) should be considered for the importance of external mass transfer resistance relative to the internal mass transfer resistance. The mass transfer Biot number is a dimensionless parameter giving information about the concentration distribution inside the adsorbent. The mass transfer Biot number can be represented as:

$$Bi_m = \frac{h_m 2r_p}{D_{eff}} \tag{E.2}$$

## E.2. Molecular Diffusivity

To determine the concentration distribution in the particle, the diffusion of water molecules should be defined. The diffusion of water molecules for the external stagnant fluid film can be calculated by using molecular diffusivity equation:

$$D_m = \frac{1.86x10^{-3}\sqrt{T^3/M}}{P\sigma^2\Omega} \quad \text{(E.3)}$$

where the σ is collision diameter (A), k refers to Boltzmann constant (J $K^{-1}$molecule$^{-1}$), and M is molecular mass (kg/mole) . The molecular diffusivity depends on pressure and temperature (Karger and Ruthven 1992).

## E.3. Sherwood and Schmidt Numbers

The concentration gradient can be defined by a dimensionless number, Sh. The Sherwood number represents the ratio of convective to diffusive mass transport. Sherwood number is a function of Reynolds and Schmidt numbers. The relevant dimensionless numbers also characterize the hydrodynamics of boundary layer.

$$Sh = \frac{2h_m r_p}{D_m} = f(\mathrm{Re}, Sc) \quad \text{(E.4)}$$

Ranz and Marshall proposed a correlation for fluid to spherical particle for forced convection (0 < Pr < 250 and 0 < Re < 200) (Cussler, 1997):

$$Sh = 2 + 0.6\,\mathrm{Re}^{1/2}\,Sc^{1/3} \quad \text{(E.5)}$$

## E.4. Mass Transfer Biot Number across a Silica gel Particle

The dominant mode of mass transfer between silica gel particle and fluid can be specified by determination of $Bi_m$ number. The problem of the present study can be is illustrated in Figure D1. There is a silica gel particle with diameter of D inside and infinite water vapor medium. The diameter of the particle is taken as 0.0025 m. It is assumed that a forced convection mass transfer exists between silica gel particle and water vapor.

For the problem illustrated in Figure D1, $Bi_m$ number according to the Sherwood and Schmidt numbers is given in Table E1.

Table E.1. The molecular diffusivity, Re, Sc, Sh, mass transfer Biot numbers for different temperature values while $r_p$=1.25 mm when u=0.01 m/s

| **Temp. (K)** | **$D_{molecular}$ ($m^2$/s)** | **Re** | **Sc** | **Sh** | **Bi'$_m$** |
|---|---|---|---|---|---|
| 303 | 6.89E-05 | 8.13E-02 | 4.47 | 2.28 | 306 |
| 323 | 7.86E-05 | 2.05E-01 | 1.55 | 2.31 | 1010 |
| 343 | 8.85E-05 | 4.54E-01 | 0.622 | 2.35 | 2899 |
| 363 | 9.94E-05 | 9.03E-01 | 0.279 | 2.37 | 7451 |

As given in the study, the dimensionless boundary condition at the sphere surface is written as;

$$r^* = 1; \qquad \frac{\partial W^*}{\partial r^*} = Bi'_m\left(1-\rho^*\Big|_{r=r_p}\right) \tag{E.6}$$

where modified Biot mass number ($Bi'_m$) is defined as $Bi'_m = Bi_m G$ and G can be defined as:

$$G = \frac{\rho_{ev}}{\rho_s W_{ev}} \tag{E.7}$$

The modified mass transfer Biot number ($Bi'_m$) defined the external mass transfer resistance. According to the different temperatures, the G values and modified mass Biot numbers for Freundlich isotherm are given in Table 9.4.

The increase of $Bi'_m$ denotes that no external mass transfer resistance can be applied to the system otherwise the external mass transfer resistance should be considered. For this case, the modified Biot number is very large. This denotes that the external mass transfer resistance can be neglected for this problem.

# APPENDIX F

# FURTHER EXPERIMENTAL RESULTS

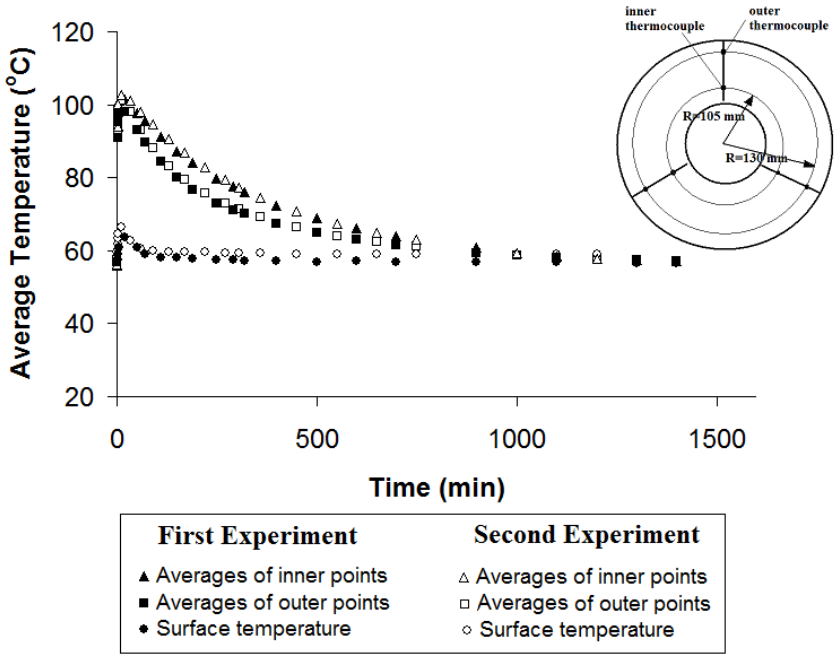


Figure F.1. The variations of angular averaged temperature of the inner and outer points and the surface temperature during the adsorption process for the two different experiments for $T_{bedos}$ = 57°C, and $T_{eva}$ = 40°C

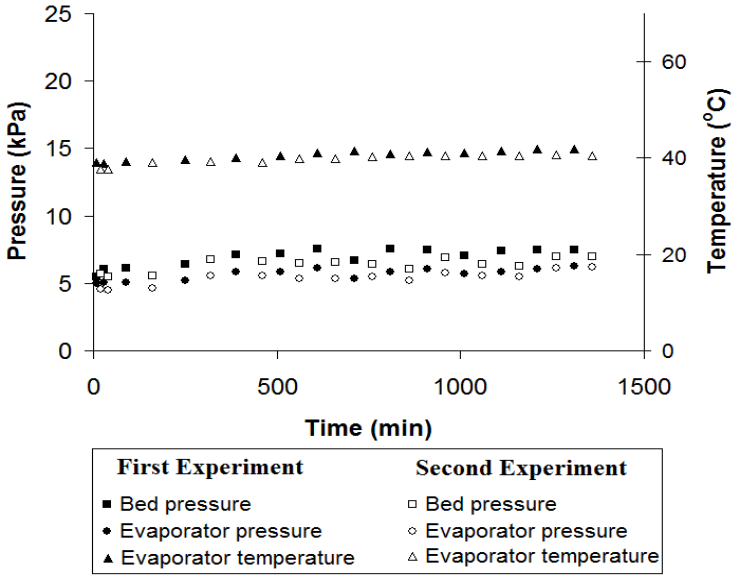


Figure F.2. The variations of temperature and pressure in the evaporator, and bed pressure during the adsorption process for the two different experiments of Tbedos = 57°C, and Teva = 40°C

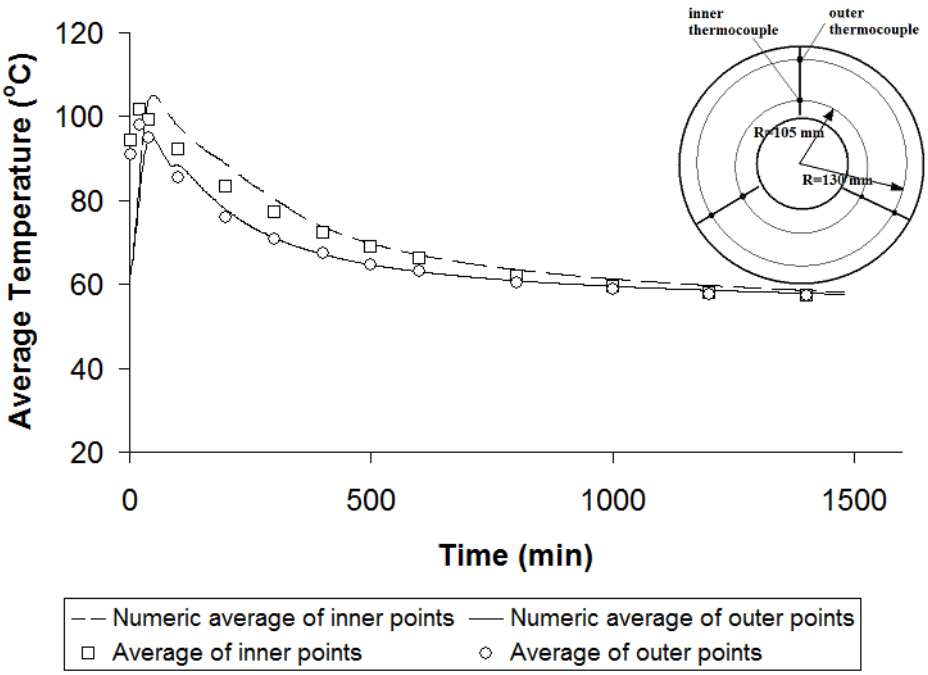


Figure F.3. The comparison of numerical and experimental temperatures at the inner and outer points during the adsorption process for the experiment with $T_{bedos}$ = 57°C, and $T_{eva}$ = 40°C

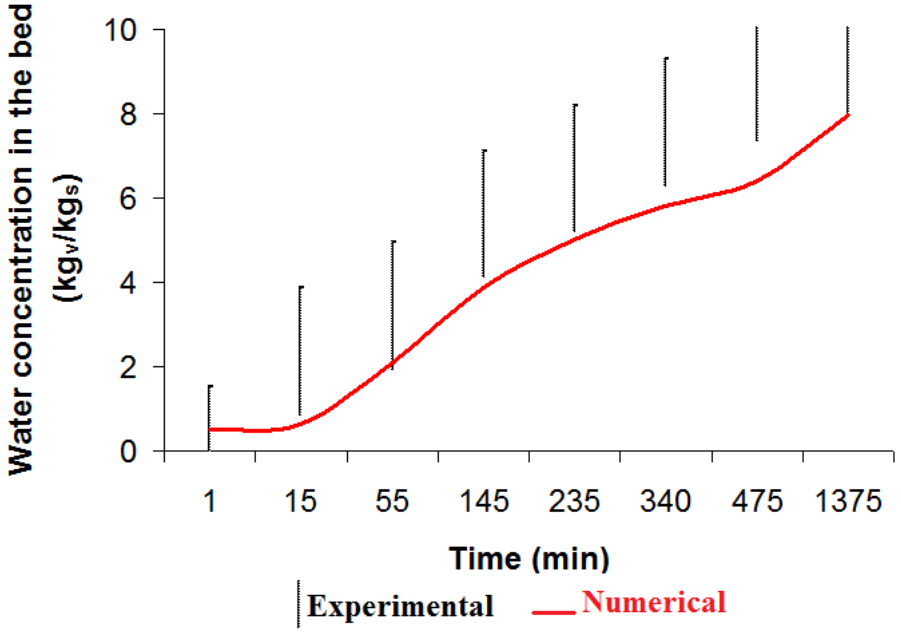


Figure F.4. The comparison of water concentration in the bed obtained numerically and experimentally when $T_{bedos}$ = 57°C, and $T_{eva}$ = 40°C

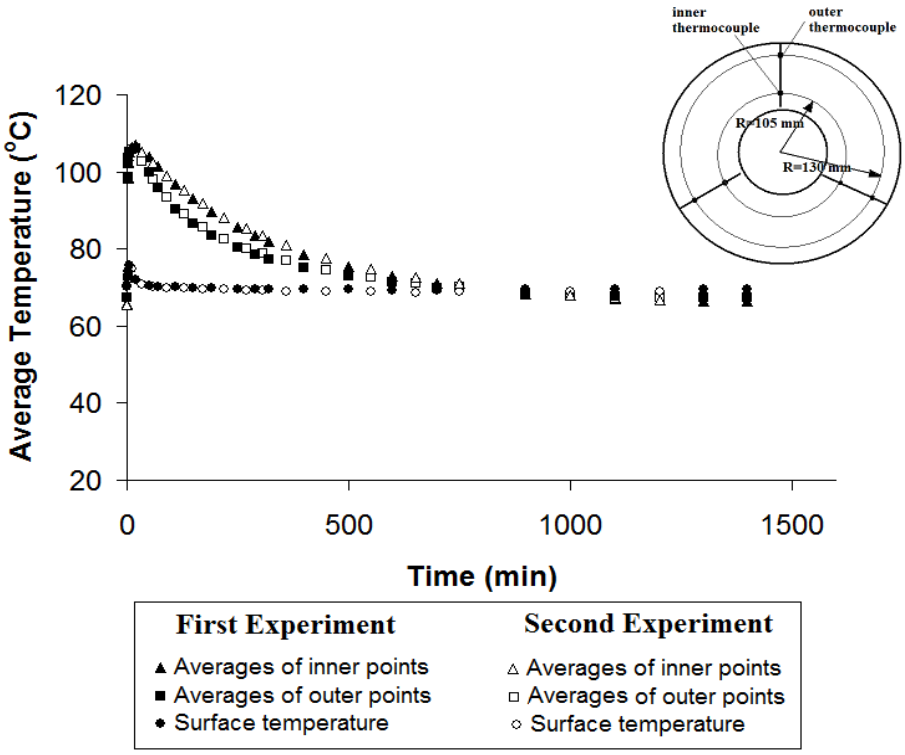


Figure F.5. The variations of angular averaged temperature of the inner and outer points and the surface temperature during the adsorption process for the two different experiments for $T_{bedos}$ = 67°C, and $T_{eva}$ = 40°C

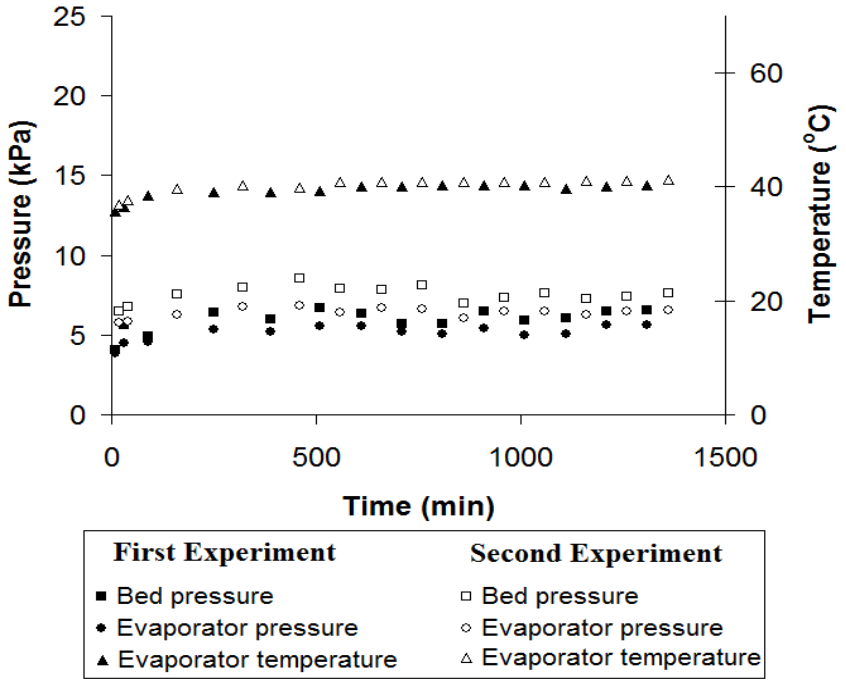


Figure F.6. The variations of temperature and pressure in the evaporator, and bed pressure during the adsorption process for the two different experiments of $T_{bedos}$ = 67°C, and $T_{eva}$ = 40°C

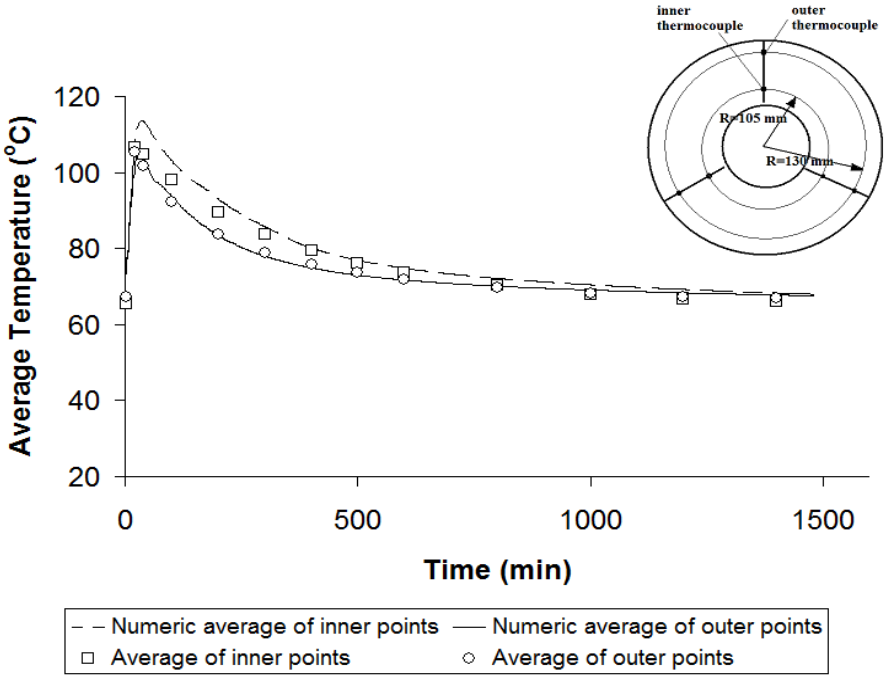


Figure F.7. The comparison of numerical and experimental temperatures at the inner and outer points during the adsorption process for the experiment with $T_{bedos}$ = 67°C, and $T_{eva}$ = 40°C

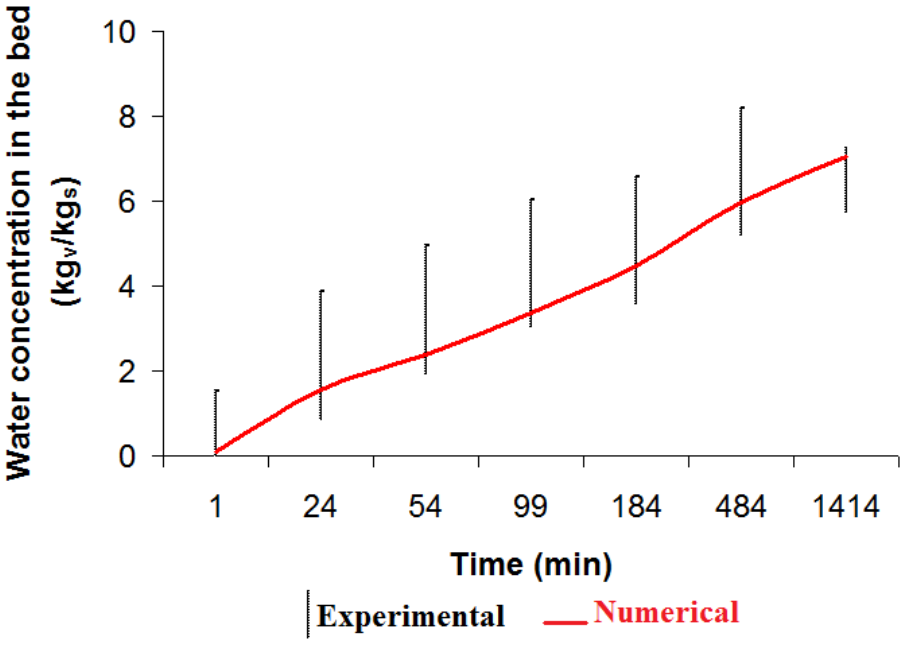


Figure F.8. The comparison of water concentration in the bed obtained numerically and experimentally when $T_{bedos}$ = 67°C, and $T_{eva}$ = 40°C

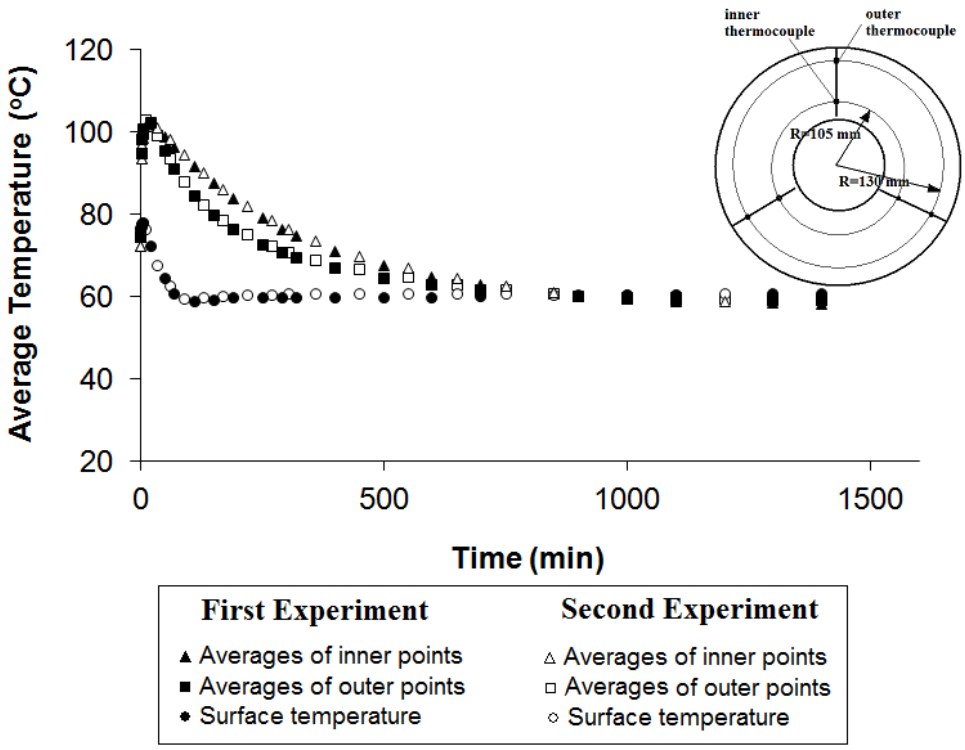


Figure F.9. The variations of angular averaged temperature of the inner and outer points and the surface temperature during the adsorption process for the two different experiments for $T_{bedos}$ = 75-60°C, and $T_{eva}$ = 29°C

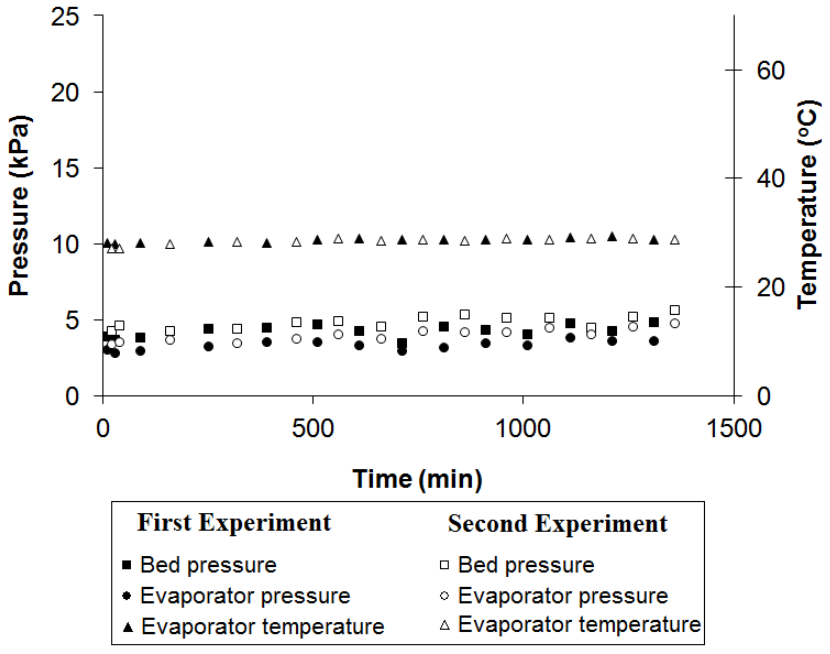


Figure F.10. The variations of temperature and pressure in the evaporator, and bed pressure during the adsorption process for the two different experiments of $T_{bedos}$ = 75-60°C, and $T_{eva}$ = 29°C

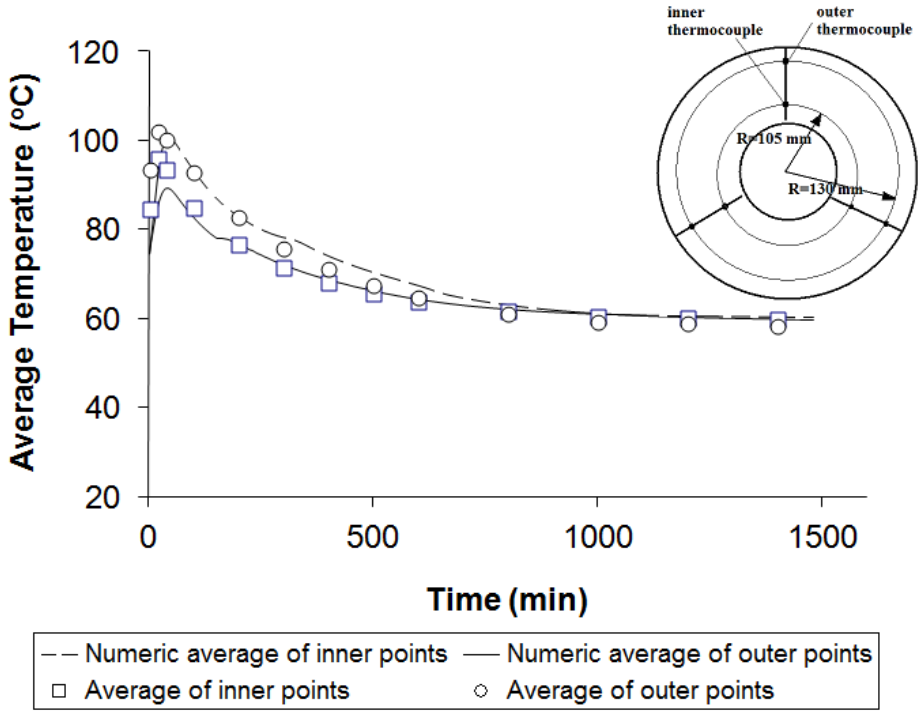


Figure F.11. The comparison of numerical and experimental temperatures at the inner and outer points during the adsorption process for the experiment with $T_{bedos}$ = 75-60°C, and $T_{eva}$ = 29°C

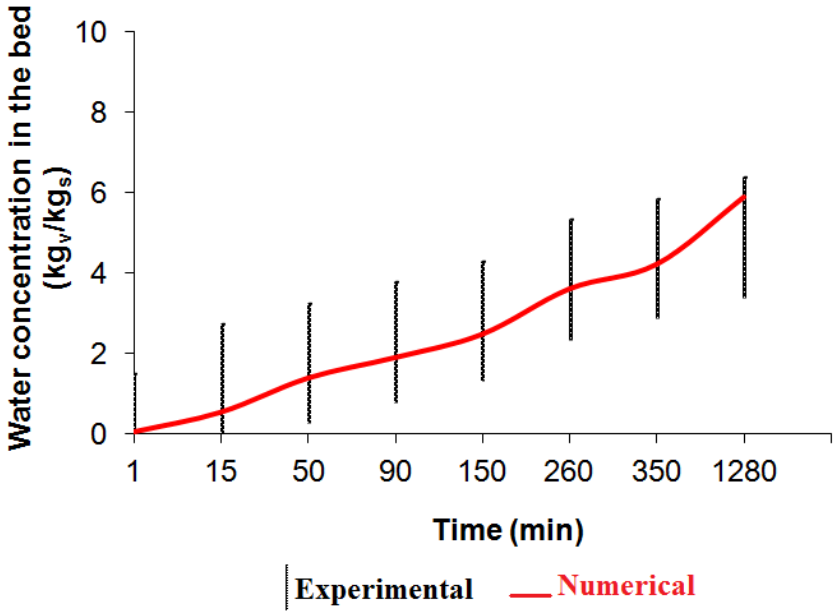


Figure F.12. The comparison of water concentration in the bed obtained numerically and experimentally when $T_{bedos}$ = 75-60°C, and $T_{eva}$ = 29°C

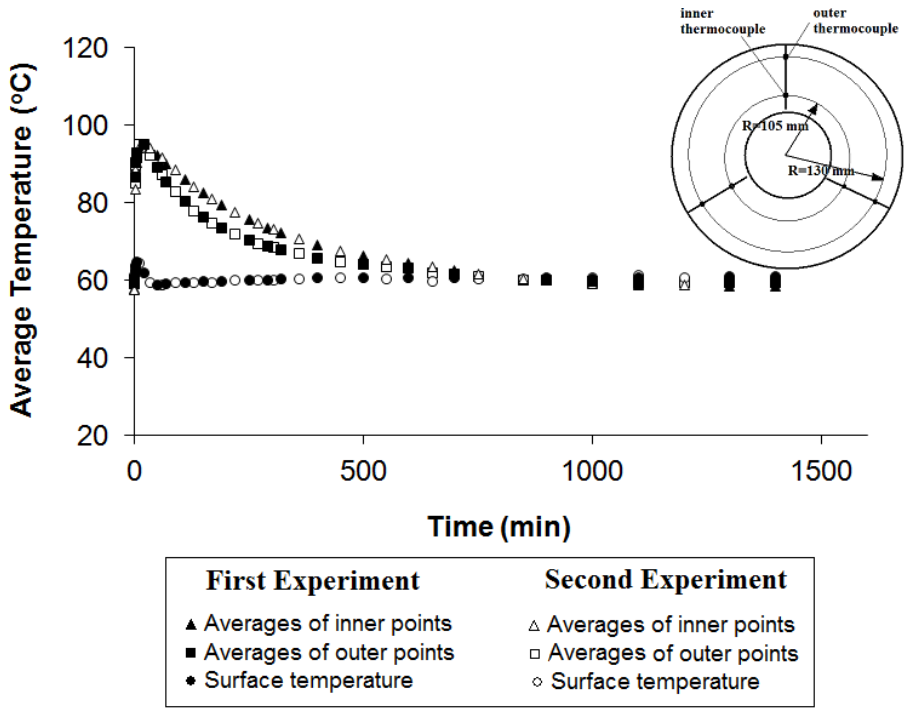


Figure F.13. The variations of angular averaged temperature of the inner and outer points and the surface temperature during the adsorption process for the two different experiments for $T_{bedos}$ = 60°C, and $T_{eva}$ = 29°C

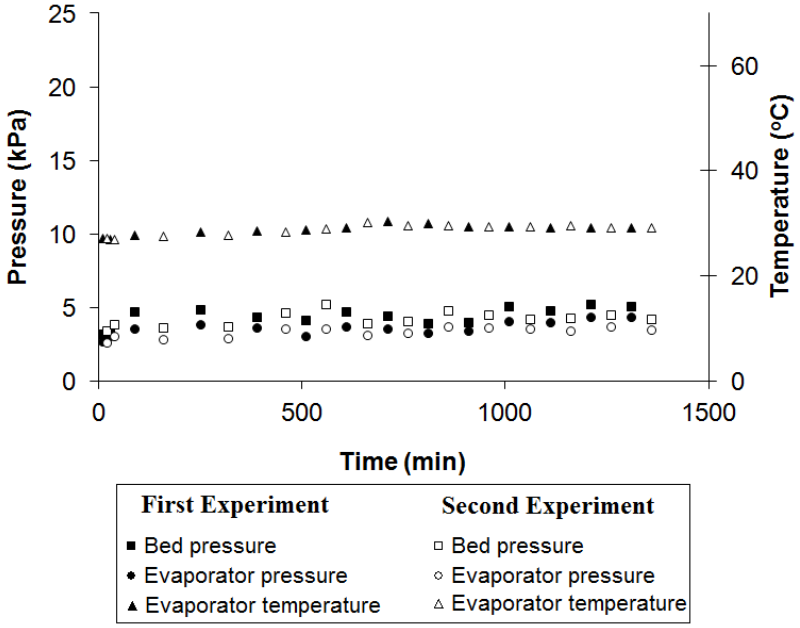


Figure F.14. The variations of temperature and pressure in the evaporator, and bed pressure during the adsorption process for the two different experiments of $T_{bedos}$ = 60°C, and $T_{eva}$ = 29°C

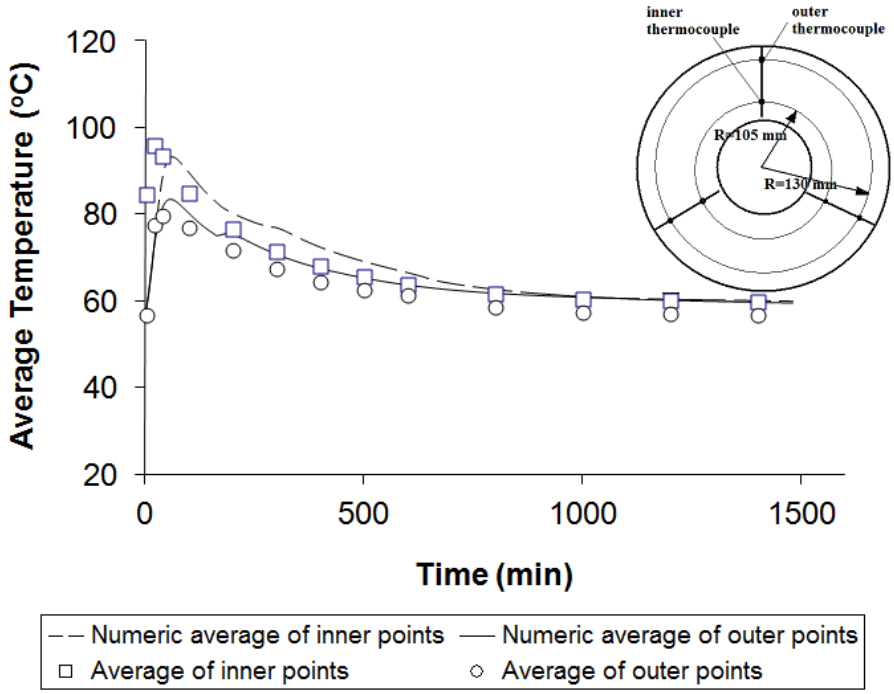


Figure F.15. The comparison of numerical and experimental temperatures at the inner and outer points during the adsorption process for the experiment with $T_{bedos}$ = 60°C, and $T_{eva}$ = 29°C

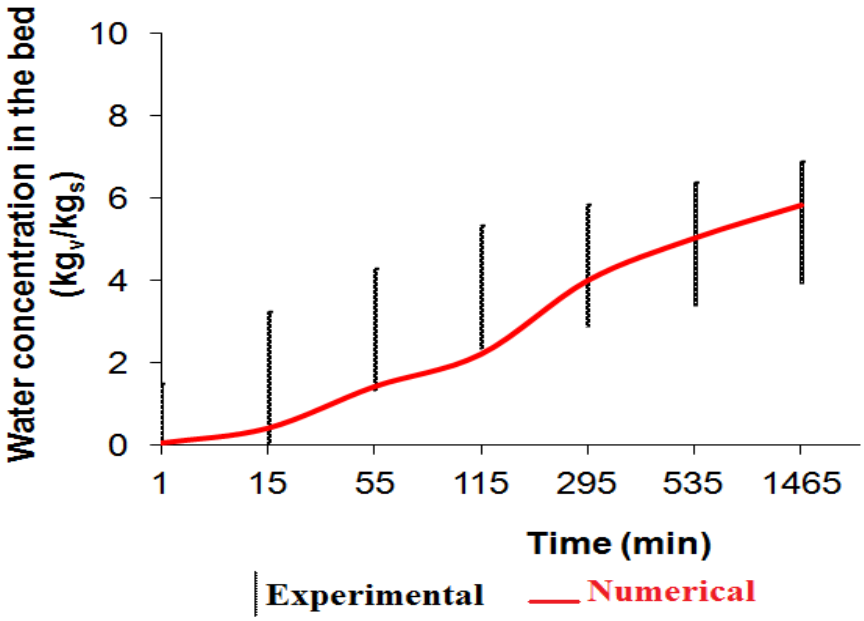


Figure F.16. The comparison of water concentration in the bed obtained numerically and experimentally when $T_{bedos}$ = 60°C, and $T_{eva}$ = 29°C

# VITA

## PERSONALITY

**Date of Birth :** 13-07-1978
**Place of Birth :** Izmir

### EDUCATION

**2012** **Philosophy of Doctorate (PhD)** Izmir Institute of Technology, Department of Mechanical Engineering
**2006** **Master of Science (MSci.)** Izmir Institute of Technology, Department of Engineering Management
**2004** **Master of Science (MSci.)** Izmir Institute of Technology, Department of Mechanical Engineering
**2001** **Bachelor of Science (BS)** Dokuz Eylul University, Department of Mechanical Engineering

### PUBLICATIONS

- A parametric study on isobaric adsorption process in a closed adsorbent bed, **Gediz Ilis G.**, Mobedi M., Ülkü S., *International Communications in Heat and Mass Transfer,* 37 (2010) 540–547.
- A dimensionless analysis of heat and mass transport in an adsorber with thin fins;uniform pressure approach, **Gediz Ilis G.**, Mobedi M., Ülkü S., *International Communications in Heat and Mass Transfer,* 38 (2011) 790–797.
- Effect of Isotherm Shape on Mass Transfer in an Adsorbent Particle; An Isothermal Adsorption Process, Yildirim Z. E., **Gediz Ilis G.**, Mobedi M., Ülkü S., *The Open Transport Phenomena Journal*, 3 (2011) 40–48.
- Comparison of uniform and non-uniform pressure approaches used to analyze an adsorption process in a closed type adsorbent bed, **Gediz Ilis G.**, Mobedi M., Ülkü S., *Numerical Heat Transfer, Part A, Under Review.*

### PRESENTATIONS

- An experimental study on heat and mass transfer in a closed adsorbent bed of an adsorption heat pump, **Gediz Ilis G.**, Mobedi M., Ülkü S., *HEFAT2010*, July 2010, Antalya, Turkey.
- Discussion on the use of dimensionless parameters in design of adsorbent beds, **Gediz Ilis G.**, Mobedi M., Ülkü S., *ISHPC11*, April 2011, Padua, Italy.
- Dimensionless analysis of heat and mass transfer in a single adsorbent particle; isothermal and non-isothermal cases, **Gediz Ilis G.**, Mobedi M., Ülkü S., *7th International Conference on Computational Heat and Mass Transfer*, July 2011, Istanbul, Turkey.